The Effects of Feedstock Pre-treatment on the Fluidized Bed Gasification of Biomass

BENJAMIN BRONSON

B.A.Sc., University of Ottawa 2011

Thesis submitted to the Faculty of Graduate and Postdoctoral Studies in partial fulfillment of the requirements for:

M.A.Sc. in Chemical Engineering

Department of Chemical and Biological Engineering
Faculty of Engineering, University of Ottawa

Abstract

Gasification is a promising technique for transforming solid biomass into a gas that can be used to produce renewable heat, power, fuels or chemicals. Biomass materials, such as forestry residues, can be high moisture, heterogeneous mixtures with low bulk density - properties that make them difficult to handle and convert. Consequently, this means that feedstock pre-treatment is usually necessary in order to facilitate its conversion by gasification. Pre-treatments methods, which include comminution, drying, pelletization, torrefaction, or carbonization will affect the properties of the biomass which will affect their gasification in a fluidized bed. The objective of this thesis was to determine how biomass pre-treatment can influence gasification in a fluidized bed. A single forestry residue was processed using five pre-treatment process levels: sieving (as a surrogate for comminution), drying (moisture content), pelletization, torrefaction, and carbonization. The fractions derived from these processes were gasified in a small pilot-scale air blown bubbling fluidized bed gasifier (feed rate 8 – 25 kg/h). The particle size and form had an impact on the gas composition, tar content, and cold gas efficiency of the gasification. Over the conditions tested, the finest fraction produced a gas with a H_2/CO ratio of 0.36 – 0.47 containing 7 – 59 g/m^3 tar (gravimetric) at a cold gas efficiency of 30 - 41%. The pellets on the other hand yielded a gas with a H_2/CO ratio of 0.89 - 1.14, containing 3 – 37 g/m^3 tar (gravimetric) at a cold gas efficiency of 41 – 60%. Drying, torrefaction and carbonization also had an impact on the gasification performance. Carbonization was able to reduce the yield of tar (as measured by gas chromatography) by more than 95% relative to the parent material. Finally, four different forestry residues were gasified in a large pilot-scale bubbling fluidized bed with air and steam-oxygen mixtures (feed rate 200 – 245 kg/h) in order to assess whether the comminution effect could be observed at the large scale. One feedstock with a significant portion of small particles showed the expected effects compared to the feed materials with large feed particles: lower H_2/CO ratio, greater tar yield, lower cold gas efficiency while the other feed material containing a substantial amount of small particles did not show these effects.

Résumé

La gazéification est une technique prometteuse pour transformer la biomasse solide en gaz qui peut être utilisé pour produire de la chaleur, de l'électricité, des carburants ou des produits chimiques. Les matériaux de la biomasse, comme les résidus forestiers, sont humides, hétérogènes et de faible densité - propriétés qui les rendent difficiles à manipuler et à convertir. Donc, le prétraitement est souvent nécessaire, afin de faciliter la conversion de la biomasse par la gazéification. Les méthodes de prétraitement, comme le broyage, le séchage, la granulation, la torréfaction et la carbonisation, auront un impact sur les propriétés physiques et chimiques de la biomasse. L'objectif de cette thèse était de déterminer comment le prétraitement de la biomasse peut influencer la gazéification en lit fluidisé, puisque l'impact de ces propriétés modifiées sur leur conversion par la gazéification n'est pas toujours évident. Un résidu forestier a été prétraité à cinq niveaux de prétraitement: tamisage (un substitut pour le broyage), séchage, granulation, torréfaction et carbonisation. Les fractions prétraitées ont été gazéifiées à l'air dans un lit fluidisé à l'échelle pilote (taux de biomasse: 8-25 kg/h). La taille des particules et la forme des particules ont un impact sur la composition du gaz produit, sur la quantité de goudron et sur l'efficacité de la gazéification. Sur la gamme de conditions d'essai, la fraction la plus fine a produit un gaz avec une proportion H_2/CO de 0,36 à 0,47 contenant 7 à 59 g/m^3 de goudron (gravimétrique) avec une efficacité (gaz froid) de 30 à 41 %. De l'autre côté, les granules ont produit un gaz avec une proportion H_2/CO de 0,89 à 1,14, contenant de 3 à 37 g/m^3 de goudron (gravimétrique) avec une efficacité (gaz froid) de 41 à 60 %. Le séchage, la torréfaction et la carbonisation ont également eu un impact sur la performance de gazéification. La carbonisation a été capable de réduire la quantité de goudron (mesurée par chromatographie en phase gazeuse) de plus de 95 % par rapport aux matériaux sources. Enfin, quatre résidus forestiers différents ont été gazéifiés dans une lit fluidisé bouillonnant (échelle pilote-grande) avec de l'air et des mélanges de vapeur d'eau et d'oxygène (taux de biomasse: 200 à 245 kg / h) afin d'évaluer si l'effet du broyage pourrait être observé à une échelle plus grande. L'un des résidus forestiers avec de nombreuses particules fines a montré les effets attendus par rapport aux deux résidus forestiers sans beaucoup de particules fines: rapport inférieur H_2/CO, plus de goudron et une efficacité moindre de gaz

froid. L’autre résidu forestier avec de nombreuses particules fines n'a pas montré les mêmes résultats.

Table of Contents

List of Figures

List of Tables

Nomenclature

SYMBOL	DESCRIPTION	UNITS (unless otherwise stated)
a	Measured / calculated value	context dependent
A_c	Column cross-sectional area	m^2
c	Concentration	g/m^3 (at 0°C, 1 atm, dry basis)
CGE	Cold gas efficiency	MJ/MJ
d_r	Relative difference	
$\hat{E}$	Specific energy	MJ/kg
ER	Equivalence ratio	mol/mol
g	Gravitational constant	m/s^2
h	Height	m
$\dot{m}$	Mass flow rate	kg/s
MW	Molecular weight	kg/mol
$\dot{n}$	Molar flow rate	mol/s
P	Pressure	Pa
r	Reaction rate	arbitrary
R	Gas constant	J/mol-K
R_c	Mass balance recovery / closure	kg/kg
SB	Steam-to-Biomass ratio	kg/kg
T	Temperature	K
u_s	Superficial gas velocity	m/s
$\dot{V}$	Volumetric flow rate	sLpm
x	Mass fraction	kg/kg
y	Mole fraction	mol/mol
ρ	Density	kg/m^3
χ	Conversion	kg/kg

Υ	Yield	kg/kg

ABBREVIATION / SUBSCRIPT	**DESCRIPTION**
abs	absolute (in reference to pressure)
ar	as received
b	biomass
C to gas	Carbon to gas
C to gas+tar	Carbon to gas and tar
daf (or DAF)	dry, ash-free basis
db	dry basis
grav	gravimetric
GC	Gas chromatography
GC/MS	Gas chromatography / mass spectroscopy
gt	gas and tar
in	input
Nm^3	Normal cubic meter (0°C, 1 atm)
NPS	nominal pipe size
out	output
sat	saturation
sLpm	standard liters per minute
std dev	standard deviation
T	total
th	thermal input
wb	wet basis

Acknowledgements

I would like to express my thanks and appreciation to my supervisors, Dr. Poupak Mehrani and Dr. Fernando Preto, for their guidance and assistance from formulating a thesis topic, to planning experiments, co-authoring publications based on this work, and reviewing this thesis. I would also like to thank Dr. Peter Gogolek for his advice and guidance.

There were many people who contributed to the operation and successful completion of the experimental work on the small pilot-scale air blown gasifier. Firstly, I would like to thank Dave Wambolt for starting the warm-up of the gasifier early in the morning on experimental days so that the system was ready for operation when everyone else showed up. Thanks to Jéremie Fournier for assistance in the set-up of the sample gas conditioning and analysis system in addition to attentively monitoring the feed system during operation. Thanks to Guy Tourigny and Travis Robinson for their assistance in dealing with frustrations and intricacies of tar sampling. Thanks to Patrick Charlebois for helping with the maintenance of the feed system. Thanks to Bart Young for assisting in the operations of the gasifier and managing the preparation and storage of the feed materials.

Operating the large pilot-scale gasifier was quite an experience and it took a lot of coordinated effort to get the system operation-ready and to carry out successful experiments. Thanks to Alex Johnson for assisting with all the cleaning and maintenance of the laboratory and diligent operation of the boiler. Thanks again to Guy Tourigny and Patrick Charlebois for all their hard work completing the gas and tar sampling. Thanks to Bart Young and David Oberholzer for all their hard work ensuring the smooth operation of the feed system, assisting me in monitoring the operation and providing extra hands as problems arose during the operation.

All of this work was only possible with complimentary analytical services, capabilities and guidance that were provided by the characterization laboratory located at the Bell's Corners Complex of CanmetENERGY in Ottawa, Canada. Thanks are given to FPInnovations and their pulp and paper company members who supplied the feed materials (forestry residues) that were used for the experimental work.

Funding for the experimental work has been provided through the Clean Energy Fund and Eco Innovation Initiative from the Office of Energy Research and Development of Natural Resources Canada.

Chapter 1. Introduction

Over the past century the majority of energy consumed has originated from fossil sources, primarily coal, oil, and natural gas. However, the geographic distribution of the fossil sources, concerns of their depletion, and the environmental implications of their use have sparked considerable interest in finding cleaner, renewable alternatives for energy production. The most promising short term replacement for fossil energy sources is biomass.

In Canada there exists significant potential to better utilize biomass resources to displace fossil energy sources and create economic activity based on renewable resources. For example, it is estimated that there are $500x10^{15}$ J/y of available urban and roadside wood waste in Canada (Paré et al., 2011). The use of these residues could roughly double the contribution of bioenergy to Canada's primary energy mix. In order to access the full potential of these wood waste resources, and other residual biomass resources in Canada including agricultural residues, further development is required for biomass conversion technologies that efficiently convert biomass into wide variety of products to replace products and services currently provided by fossil resources.

1.1 Significance of the Work

Biomass gasification is a conversion process that represents significant potential for the utilization of residual and low value fuels such as forestry and agricultural residues for the creation of renewable energy, fuels, and "green" chemicals. Biomass gasification has already seen significant development in Canada and abroad. Gasification is well-established for generating heat and steam, has a few successful commercial combined heat and power applications, and there currently are demonstrations for the production of chemicals and fuels from biomass using gasification.

For large scale applications (10-100 MW_{th}), fluidized beds are the likely choice for the gasification of biomass. Fluidized bed gasifiers do not have the scale limitations of downdraft gasifiers, they do not have the same magnitude of tar problem as updraft gasifiers, and do not have the strict requirements on the fuel size and ash characteristics

like entrained flow gasifiers. For these reasons, fluidized bed gasifiers are one of the most important types to study.

The unfavorable fuel characteristics while using residual biomass feedstocks are one of the main constraints to the proliferation of biomass conversion techniques. Raw biomass is low energy density, diffuse resources which makes it costly to transport, store, and convey into conversion process. Residual fuels often have high moisture content leading to biodegradation of the fuel and their inefficient conversion. Every low cost residual biomass fuel will need some level of pre-treatment before it is transportable as a commodity or being useable in a biomass gasification conversion process.

Some type of pre-treatment must be performed on biomass feedstock in order to meet the criteria of the handling and conversion equipment. Comminution is required in order to move biomass in traditional conveying system and for it to be easily fed into a fluidized bed gasifier. Drying must be completed to prevent biodegradation and spontaneous combustion of fuel piles. An under appreciation of the importance of drying has led to countless operational issues on biomass combustion equipment. Other pre-treatments are not strictly required but are part of fuel beneficiation strategies. Densification, such as pelletizing or briquetting can greatly increase the transportability and handling characteristics of residual biomass fuels. Canada exported about 1.37 million tonnes of pellets to Europe in 2012 (Statistics Canada, 2013) because the pelletization transforms the material into a uniform, higher density fuel. Torrefaction offers the possibility to improve and commoditize residual biomass fuels even further than conventional pelletization. There are at least four Canadian companies who are actively developing pilot torrefaction technologies (Torrefuels, Airex Energy, Allied Blower, and Diacarbon) in addition to many international players.

The importance of pre-treatment has already been well established for the biochemical conversion of biomass as it is necessary for the efficient conversion of the material into desired products (Lipinsky, 1985) and as such, pre-treatment for biochemical conversion is still an active research field. The same understanding of the linkage between pre-treatment and thermochemical conversion has never been achieved. The particle size, porosity, surface area and anisotropy are all examples of particle properties that are affected by the pre-treatment processes, they will have consequences on the thermochemical conversion.

Thermochemical conversion processes, fluidized bed gasifiers especially, are often praised for their "fuel flexibility". This is often misinterpreted to mean that the products from a fluidized bed gasifier have no dependency on the physical and chemical characteristics of the input biomass. This is not the case, the physical and chemical characteristics of biomass will have an impact on the performance of fluidized bed gasification. An understanding of how these pre-treatment processes affect the gasification performance is absolutely necessary so that product gas yields meet design expectations, so that acceptable conversion efficiency is achieved and so that the product gas composition meets end use specifications.

1.2 **Thesis Objectives**

The evaluation of specific parameters, such as the effect of particle size or the effect of moisture on the performance of the fluidized bed gasification, has been individually completed in a few studies. The results of these studies are discussed in section 2.3. Despite this, a holistic study which determines how multiple pre-treatment levels affect, or can potentially be used to optimize a fluidized bed gasifier performance has never been completed. This work is necessary in order to establish the limits of fuel flexibility, improve gasifier designs to address specific fuel property driven issues, and build appropriate business cases for biomass fuel beneficiation strategies such as pelletization and torrefaction that respect its effect on thermochemical conversion processes.

The overall goal of this thesis is to experimentally determine the impact of different pre-treatments for forestry residues on the performance of fluidized bed gasification.

The feed materials selected have been purposefully chosen to be reflective of low cost residual biomass fuels that are available at single locations in substantial quantities. In the thesis, the materials chosen were hog fuels and chipped wood products. The scale of the systems utilized in this thesis ensures that fuels can be used in forms that are reflective of the form that would be found at a pulp mill.

The specific objectives of this research were to study the following pre-treatments:

- Comminution level:

In order to understand the impact of comminution, forestry residues of different particle size distribution were tested in a fluidized bed at the 1 – 2 MW_{th} (hereafter called "large pilot-scale") range with steam-oxygen and air as the gasification medium. A single forestry residue was separated into different size fractions and tested in an air-blown gasifier at the 50 – 100 kW_{th} range (hereafter called "small-pilot-scale").

- Drying:
  In order to understand the impact of drying, a single forestry residue fuel was tested at different moisture levels in a small pilot-scale gasifier.
- Pelletization:
  In order to understand the impact of pelletization, a single forestry residue fuel was pelletized and the results were compared to the parent material in a small pilot-scale gasifier.
- Torrefaction:
  In order to understand the impact of torrefaction, a single forestry residue was torrefied at two levels (torrefaction and carbonization). The materials, including the parent material, were then gasified in a small pilot-scale gasifier.

A wide variety of parameters will contribute to the overall desirability of a gasification process. Some of these parameters will be more relevant for producer gas aimed at different applications. For example, the yield of carbon monoxide and hydrogen will be very important parameters for chemical synthesis whereas the heating value may be more essential to study if the producer gas is to be used as a fuel. This work focused on the following measures of gasifier performance:

- Tar content of the producer gas
- Carbon conversion of the feed material to gaseous product
- Composition of major gaseous species such as CO, H_2, CO_2, CH_4, and other light hydrocarbons

- Cold gas efficiency (Energy contained in the producer gas at room temperature compared to the input energy to the gasifier)

There are other measures of gasifier performance which are important and will be discussed where relevant but will not be given as much attention as aforementioned measures.

1.3 **Thesis Outline**

- The second chapter of this thesis reviews the status of bioenergy, the issues with biomass gasification, and reviews the literature pertinent to the effect of various pre-treatment methods on the gasification of biomass in fluidized beds.
- The third chapter examines the results from air blown gasification of a forestry residue that was sorted into different sizes, different moisture levels, and from which pellets were made in order to ascertain the effect of physical pre-treatment on gasifier performance. The chapter also provides a description of the small pilot-scale experimental equipment used, procedures followed, data analysis techniques utilized, and discusses operational observations with the small pilot-scale system.
- The fourth chapter examines how thermal pre-treatments (torrefaction) were observed to affect results of the air-blown fluidized bed gasifier.
- The fifth chapter discusses the results from large pilot-scale steam-oxygen and air blown gasification of various forestry residues. The results are examined to determine how well the large pilot-scale results compare with the smaller scale results, whether there are differences that can be attributed to different size distributions of the fuels and whether or not the feed position in a fluidized bed interacts with the effects of particle size.
- The sixth chapter reviews the data and synthesizes generalizations about the impact of pre-treatments on the fluidized bed gasification of biomass. In addition, it provides recommendations for future work.

References

Lipinsky, E.S. “Pretreatment of Biomass for Thermochemical Biomass Conversion,” in “Fundamentals in Thermochemical Biomass Conversion,” R.P. Overend, T.A. Milne and L.K. Mudge, Eds. Elsevier Applied Science (1985), pp. 77-87

Paré, D., P. Bernier, E. Thiffault and B.D. Titus, "The potential of forest biomass as an energy supply for Canada," The Forestry Chronicle. **87**, 71-78 (2011).

Statistics Canada, "Canadian International Merchandise Trade Database," **2013**. http://www5.statcan.gc.ca/cimt-cicm/searches-cherchers?lang=eng&searchStr=4401&refYr=2012&refMonth=7&freq=6&countryId=999&provId=1

Chapter 2. Literature Review

This chapter highlights some of the issues with using biomass for energy and establishes why biomass pre-treatment is so important for the development of processes to use biomass for energy. The chapter reviews the process of biomass gasification from a fundamental perspective but also includes a discussion of the practical limitations of gasification platforms. The chapter describes the pre-treatment processes that were evaluated in this thesis and summarizes the existing results in literature which investigated the effect of a pre-treatment on the fluidized bed gasification of biomass.

2.1 Biomass for Energy

Biomass is any organic material which is produced on a renewable basis from living or recently living organisms. Given the broad definition of biomass, a wide variety of fuels are considered to be biomass, such as wood products & residues, agriculture products & residues, waste water sludge, and algae. Using energy produced from biomass ("bioenergy") can have several advantages over energy produced from fossil sources.

Bioenergy is considered to be a carbon neutral energy source. As a carbon neutral energy source, its usage has the ability to mitigate anthropogenic carbon dioxide emissions which are a contributor to the phenomena of global warming. Bioenergy, given its vast geographic distribution, can reduce dependency on imported energy sources. Increased usage of bioenergy is also suggested as a measure to the revitalize rural communities by providing jobs close to large biomass supplies. Most importantly, when harvested responsibly biomass represents a sustainable energy source.

Biomass currently contributes approximately 50×10^{18} J/year (representing over 10% of the total) to the world's primary energy consumption (International Energy Agency, 2008). This makes biomass the 4^{th} largest contributor to the world's primary energy consumption behind only coal, oil, and natural gas. The majority of biomass currently used for energy is used in traditional technologies for the purposes of heating and cooking, largely concentrated in the undeveloped world (Bauen et al., 2009). It is widely recognized that

there is substantial room for the growth for the sustainable use of biomass as an energy source (Berndes et al., 2003; Smeets et al., 2007).

There are many barriers to the increased use of biomass as an energy source in developed nations:

- Biomass is widely dispersed, low energy density resource. Thus, biomass must be harvested across large areas to collect significant volumes leading to costly transportation and complex logistics (Richard, 2010).
- Biomass is a highly variable resource. Different species of biomass can have vastly different attributes and require vastly different conversion technologies.
- Many types of biomass experience large annual variations in supply. This can magnify storage issues related to biomass since large inventories need to be maintained in order to provide a regular annual supply (Caputo et al., 2005).
- There are concerns about the potential competition for agricultural land between bioenergy and food production.
- There is a lack of confidence and commercial demonstration of many biomass conversion technologies.

One of the greatest barriers to increased usage of biomass is the cost of transport, storage, and handling systems. Many strategies exist so that biomass can be densified and protected against biodegradation which reduces transport, storage and handling costs. Upgrading biomass to conventional fuels such as liquid hydrocarbons or synthetic natural gas can take advantage of existing transport and storage infrastructure to deliver bioenergy to consumers.

The combustion of biomass is the most common conversion technology for producing energy from biomass and will likely continue to produce energy where space heating is required, emission standards are lenient, and where conventional steam cycle power generation is economically attractive (Stevens, 2001). For bioenergy to penetrate other energy markets, such as where emission standards are stricter, distributed power generation is preferred, or to enter the transport fuel market, other conversion technologies are required in order to upgrade raw biomass into a more convenient, cleaner fuel.

Currently, ethanol produced from the fermentation of agricultural crops (corn and sugarcane) and biodiesel produced from oil seeds represent a large portion of the biofuels production. Conventional fermentation and biodiesel production is limited to a narrow range of feedstocks (corn, sugarcane, oilseeds, etc.). Other conversion routes are currently being investigated which overcome some of these limitations. These include anaerobic digestion, lignocellulosic fermentation, gasification, and pyrolysis.

Biomass gasification is one of the conversion routes of biomass to energy that is receiving substantial attention. Biomass gasification has already seen some commercial application in Combined Heat & Power (CHP) generation and shows promise for Integrated Gasification Combined Cycle (IGCC), for the use in distributed generation technologies like fuel cells, and the production of synthetic fuels (Bridgwater et al., 2002). Gasification significantly increases the opportunities for using biomass as an energy source as compared to direct combustion since the gasification product can be used for a much greater range of purposes (Stevens, 2001) allowing much wider application.

2.2 **Biomass Gasification**

2.2.1 Overview

Biomass gasification is the thermochemical conversion of biomass into a gaseous product via the reaction of the biomass with a gasifying medium (such as air, oxygen, steam, or carbon dioxide) at elevated temperatures (typically above 600°C and often much hotter). The gaseous product is often called producer gas, or synthesis gas (syngas) which is a mixture of a number of components[1]. The major gaseous components are H_2, CO, CO_2, and H_2O. Depending on the process, CH_4 and other gaseous hydrocarbons can be present in the producer gas. The objective of gasification will typically be to produce a gas which is rich in CO and/or H_2.

[1] Some authors elect to distinguish between *synthesis gas* and *producer gas* (van der Drift and Boerrigter, 2006) such that *synthesis gas* refers to a gas that contains H_2 and CO **exclusively** as combustible components (generally produced from gasification at >1200°C) whereas *producer gas* refers to combustible gas mixtures from gasification which also contains hydrocarbons such as methane as combustible components in addition to H_2 and CO (generally produced from gasification at <1000°C).

After the evaporation of water moisture from biomass particles, the gasification of biomass can be attributed to three processes: pyrolysis (or devolatilization) of biomass, subsequent cracking and reforming of pyrolysis vapours, and conversion of solid char to gaseous products.

As the temperature of the biomass particle increases, pyrolysis of the biomass begins to take place. The temperature at which pyrolysis occurs varies with the composition of the biomass. Typically, the first component to begin pyrolysis is hemicellulose which begins to thermally decompose at below 200°C (Raveendran et al., 1996). In pyrolysis, the volatile components of the biomass are released as a mixture of permanent gases (such as methane, carbon dioxide, carbon monoxide, etc.), water vapour, and primary tars which leave behind a solid char. During the devolatilization, fuel particles can be affected by either shrinkage or swelling and potentially primary fragmentation as a consequence of the internal pressures and thermal stresses created by the release of the volatiles (Gómez-Barea and Leckner, 2010). The primary tars can undergo further cracking or condensation reactions depending on the conditions to yield secondary or tertiary tars, char or permanent gases. Evans and Milne (1987) proposed a pyrolytic pathway from biomass to tertiary products which is shown in Figure 2.1.

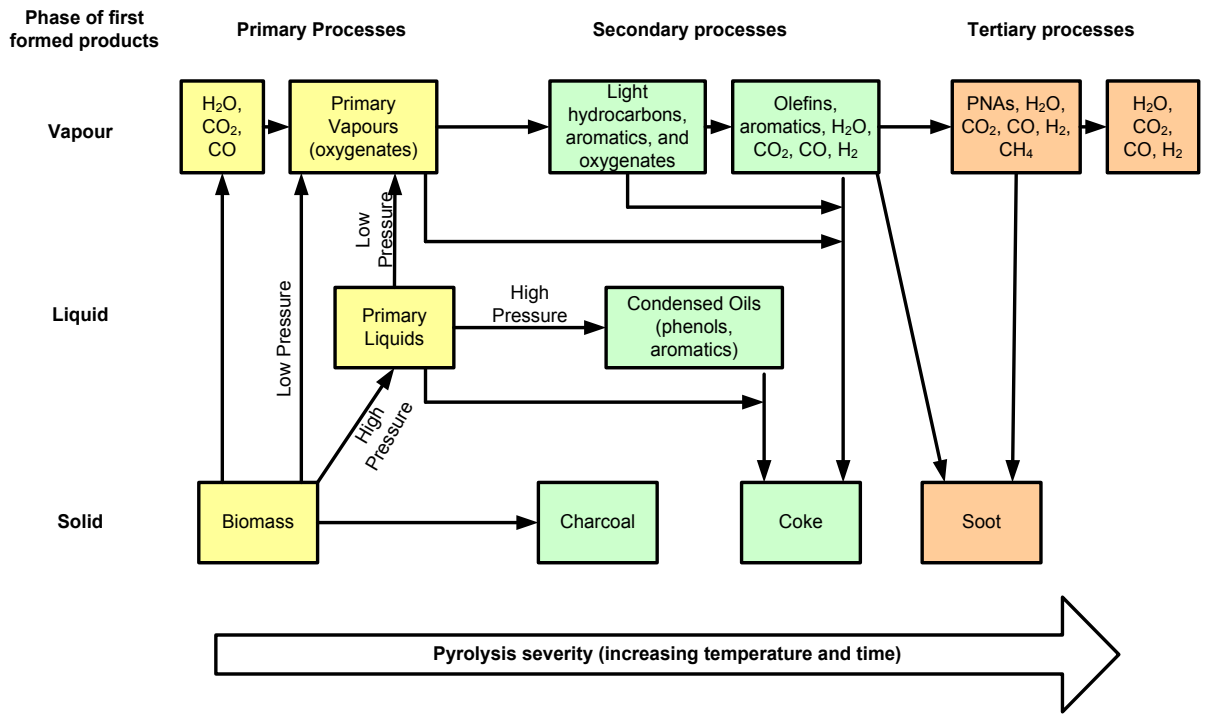

Figure 2.1: Pyrolytic decomposition of biomass and its pathways (Reproduced from Evans and Milne, 1987)

The char that is formed from the pyrolytic reaction is subsequently gasified via oxidation (if oxygen is available) or by reaction with other gaseous species such as steam, carbon dioxide, and hydrogen. The gaseous species which perform the gasification of the char are important in determining the rate of char gasification. An approximate order of magnitude relationship exists between the rates of char gasification, where the rate of oxidation of the char is much faster than the steam gasification of char, which is faster than the rate of carbon dioxide gasification of char, which is much faster than the hydrogasification of char (Basu, 2010).

$$-r_{C+O_2} \gg -r_{C+H_2O} > -r_{C+CO_2} \gg -r_{C+H_2} \qquad \text{Eq. 2.1}$$

The result of this is that in an oxygen based gasifier, the oxygen will be rapidly consumed owing to its high rate of reaction with the char (or available volatiles). This will create two distinct zones: one near the injection of air or oxygen where molecular oxygen is available and one for the rest of the gasifier where the oxygen concentration is close to zero. In addition to the difference in char gasification rates due to the concentrations of gasifying

species, the morphology and intrinsic reactivity of the char will depend on the biomass species and the pyrolysis conditions such as pressure and heating rate (Cetin et al., 2004). Thus, the pyrolysis conditions that formed the char are also important in determining the rate of char conversion. Additionally, since the char gasification reactions are solid-gas reactions, the physical characteristics of the char such as size, porosity, pore size, and others will also determine the rate of char gasification. Char gasification is the rate limiting step of biomass gasification and will determine many of the reactor parameters such as throughput.

Homogenous reactions in the gas phase also adjust the gaseous compositions. If any oxygen is available, it is assumed that oxidation reactions of combustible gas species will occur in the gas phase in parallel competing with char oxidation reactions. At gasification temperatures, many of the other gas species are reactive leading to alterations of the gaseous product distributions. Some of the key reactions which play a role in the gasification of biomass are summarized in Table 2.1.

Gasification occurs through a complex set of reactions, and can be very difficult to predict. Although many important reactions have been omitted, Table 2.1 illustrates the importance of equilibrium reactions in the gasification process which places thermodynamic limits on the gaseous composition of the producer gas.

Table 2.1: Homogeneous and heterogeneous reactions important for gasification

Reaction	Name	ΔH^{a}_{rxn} (kJ/mol)
Biomass → tars + char + gases	Pyrolytic decomposition	-
$C + 1/2O_2 \rightarrow CO$	Char oxidation	-111
$C + O_2 \rightarrow CO_2$	Char oxidation	-394
$C + H_2O \rightleftharpoons CO + H_2$	Heterogeneous water-gas equilibrium	131
$C + CO_2 \rightleftharpoons 2CO$	Boudouard equilibrium	173
$C + 2H_2 \rightleftharpoons CH_4$	Hydrogasification equilibrium	-75
$CO + H_2O \rightleftharpoons CO_2 + H_2$	Water-gas shift	-41
$C_xH_y + xCO_2 \rightleftharpoons 2xCO + \frac{y}{2}H_2$	Dry reforming	Endothermic, 247 for x=1,y=4 (methane)
$C_xH_y + 2xH_2O \rightleftharpoons xCO + (x + \frac{y}{2})H_2$	Steam reforming	Endothermic, 206 for x=1,y=4 (methane)

[a] at 273K, 1 bar

2.2.2 Contaminants in Producer Gas

The producer gas of gasification also contains substantial amounts of "contaminants", of which some of the major ones are:

- Particulate
- Tars
- Sulphur
- Nitrogen
- Chlorine
- Alkalis
- Hydrocarbon gases

Particulate is present in producer gas due to entrainment of ash, char (incompletely gasified carbon from the biomass), and attrition material from the gasifier bed. Significant quantities of char in the particulate represent incomplete gasification of the feedstock and represent a loss of carbon conversion efficiency. Particulate matter in gas streams can lead to plugging of downstream equipment, as well as abrading turbines and engine components (Stevens, 2001). In addition, particulate emission levels can also be regulated, often requiring the removal of particulate from producer gas directed at combustion applications.

Tars are formed to some degree in a gasification process. Tars are arguably the most critical contaminant in producer gas from gasifiers operating below 1000°C. The cost of gas cleaning systems needs to be substantially reduced in order for biomass gasification technologies to be widely implemented. Tars are often defined as any organic component produced from gasification which has a molecular weight greater than benzene (Stevens, 2001). Tars represent incomplete gasification of the biomass feedstock and hence result in lowered carbon conversion efficiency to gases. Tars also cause severe operational issues in downstream equipment due to plugging and fouling resulting in high maintenance requirements and low reliability (El-Rub et al., 2004). The range of tar concentration in the producer gas is greatly affected by the gasifier design, the gasifying agent and the operating conditions (Carpenter et al., 2010; Gil et al., 1999; Milne et al., 1998; Qin et al., 2010; van Paasen and Kiel, 2004). For example, increased operating temperatures in the gasifier have been well reported to substantially reduce tar content of producer gas.

Hydrocarbon gases such as methane, ethane, ethylene, and propane are not strictly a contaminant. In some situations, such as when the producer gas is to be used in combustion processes, hydrocarbon gases may be harmless or even beneficial (Stevens, 2001). If the producer gas is to be directed at methane synthesis, high methane content producer gas can actually lead to an overall boost in process efficiency because the loss caused by the exothermic synthesis of CH_4 from CO and H_2 is minimized (van der Meijden et al., 2010). However, when the synthesis gas is directed at other synthesis routes, hydrocarbon gases often go through the fuel synthesis unconverted and thus represent a loss of yield potential from biomass to final product.

Hydrogen sulphide, organic sulphur species, hydrogen chloride, ammonia, hydrogen cyanide and many others are also very important contaminant in producer gas and will be affected by many aspects of the gasification process including the feedstock characteristics. However, this thesis will not address those contaminants in detail.

Being able to reliably produce a clean synthesis gas at low cost is the main obstacle to biomass gasification processes that must be overcome before the technology can be widely adopted (Maniatis, 2001).

2.2.3 End-use of Producer Gas

Producer gas, which consists of a large fraction of carbon monoxide and hydrogen, is very useful as either a gaseous fuel or as a feedstock for the large scale synthesis of conventional fuels and chemicals. Hence, producer gas from biomass gasification is normally directed at one of two overall purposes:

1. A fuel for a combustion process or a fuel cell in order to produce electricity, mechanical energy, or heat.
2. A feedstock for chemical synthesis in order to produce a value-added fuel or chemical.

In order to satisfy these purposes, the producer gas often needs to be purified and conditioned to an appropriate level. The synthesis gas purification operations can represent higher capital investments than the gasification plant (Rauch, 2002). Thus, there is a large interest in the investigation of producing producer gas from biomass which contains lower contaminants levels.

For conversion to synthetic fuels or chemicals, the producer gas composition may need to be adjusted to meet the stoichiometric requirements of the synthesis reaction. One of the most important parameters is the ratio of H_2/CO. In order to adjust this parameter the water-gas shift reaction may be used prior to a fuel synthesis reactor.

Some of the chemicals that can be manufactured from producer gas are methane (synthetic natural gas), Fischer-Tropsch liquids, methanol, dimethyl ether, mixed alcohols, and hydrogen (van der Drift and Boerrigter, 2006).

2.2.4 Gasifier Designs

There are three main types of gasifier technologies which are shown in Figure 2.2: fixed bed, fluidized bed, and entrained flow.

Fixed bed gasifiers, such as the downdraft, updraft, and crossdraft designs, are well suited to small scale (up to approximately 10 MW_{feed}) applications due to their simplicity. Significant differences exist between design sub-types in terms of their tar production. For example downdraft gasifiers generally produce low tar level gas (on the order of 1 g_{tar}/Nm^3), while updraft gasifiers are generally regarded to produce much higher tar concentrations in the producer gas (on the order of 50 g_{tar}/Nm^3) (Milne et al., 1998). The difference in the tar content of the producer gas between these two designs is attributed to the differences in flow patterns between solid feed and gasifying medium. In the downdraft design pyrolysis vapours are forced through a hot char oxidation zone leading to the cracking of many tars, whereas in the updraft design pyrolysis vapours are carried out of the gasifier without contacting the hot char oxidation zone.

Fluidized bed gasifiers, which are usually subdivided into bubbling and circulating types, are generally preferred for mid- to large-scale applications because they are relatively flexible in terms of fuel quality, minimize tar problems associated with updraft gasifiers, and have more potential for scale-up than downdraft gasifiers (Bacon et al., 1985). Fluid bed gasifier designs use an inert or catalytic bed media which is fluidized by the flow of a gaseous medium. The result is a turbulent bed region that carries significant thermal inertia and promotes very high heat transfer and mass transfer rates to the rapidly mixing solids. High temperatures (>950°C) are normally avoided in these designs in order to avoid the ash softening temperature of biomass which can cause agglomeration of bed materials causing defluidization. These designs can handle a variety of biomass fuels but the producer gas normally contains significant amounts of char, tar, and hydrocarbon gases due to their operating temperatures.

Entrained flow gasifiers are the most complex design type relying on thorough biomass size reduction and require pure oxygen to operate at very high temperature (>1200°C). Due to their complexity they are generally only suited for the very large scale implementation (>100 MW_{feed}). Entrained flow gasifiers can produce a producer gas which is essentially free

of tar and hydrocarbon gases since the temperature is high enough that the producer gas approaches thermodynamic equilibrium. Due to the difficulties in size reduction of biomass to meet entrained flow requirements, aggressive nature of biomass slag, and inherent limitations to the quantities of biomass that can be delivered to a plant, it appears that in the short-term, fluidized bed gasifiers will be the predominant design type for larger scale operation (Higman and van der Burgt, 2008).

A number of reviews can be found which feature comparisons between different gasifier designs (Bridgwater, 1995; Maniatis, 2001; Zhang et al., 2010; Zhang, 2010).

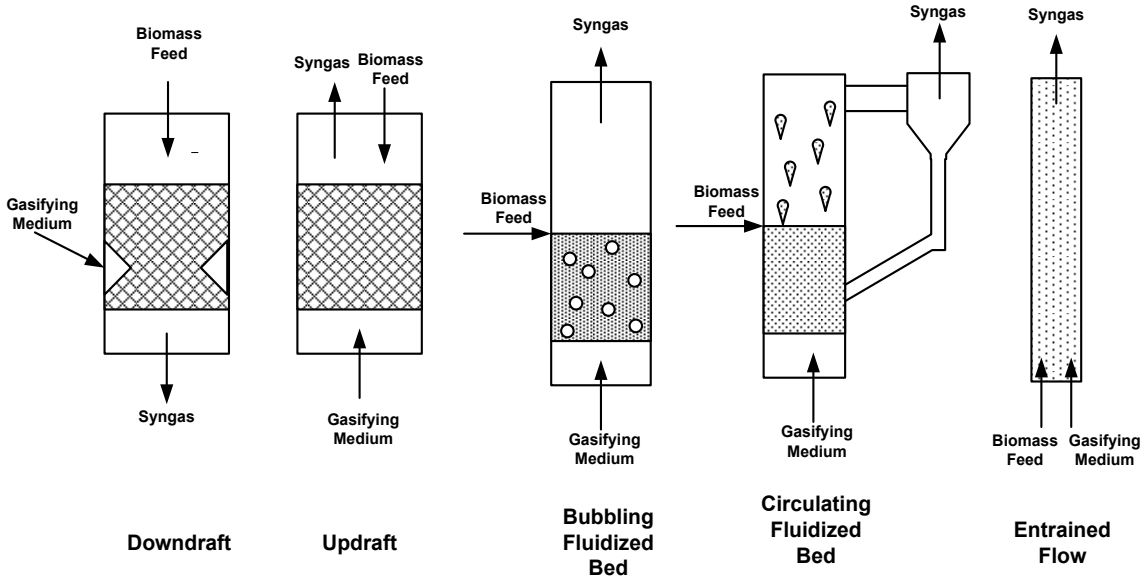

Figure 2.2: Overview of the major gasifier designs

2.2.5 Gasification Medium

Air, oxygen, steam, or some mixture of those is normally used as the medium for the gasification of biomass.

Air is the simplest option as a gasification medium since it is readily available. Using air for gasification can be unsuitable for many processes since the producer gas will contain large amounts of nitrogen which dilutes the producer gas. For gas cleaning operations and synthesis reactions, the large volume of resulting gas can result in unacceptably large

downstream processing equipment. The nitrogen content also dilutes the heating value of the producer gas which reduces its value as a fuel gas.

In order to produce a nitrogen-free gas, pure oxygen can be used as a gasification medium. Producing pure oxygen often comes at a significant cost both in terms of the energy efficiency of the process and the economics of the process. Oxygen plants are expensive installations which often rely on economy of scale benefits that are only realizable at the very large scales (Mozaffarian et al., 2004).

Steam gasification produces a nitrogen-free, high hydrogen content gas. However, in steam gasification, the absence of partial oxidation reactions means that the heat for the endothermic gasification reactions needs to be provided by alternate means. This can be accomplished by mixing in small amounts of air or oxygen into the steam in order to provide heat through partial oxidation reactions (autothermal gasification). Depending on the application, this can negate the advantages of using steam as a gasification medium. Heat for the gasification reaction can also be provided indirectly via the use of solids circulation or via the use of heat transfer surfaces. Hot solids circulation requires the use of a closely coupled gasifier and combustor. Char and inert solids are circulated from the gasifier to a combustor where the char is burned to heat the inert solids which are then recirculated back to the gasifier. If heat transfer surfaces are used, a small portion of producer gas combusted through heat exchange surfaces immersed in the gasifier bed. Heat transfer can be a challenge in these designs, special designs such as pulse-enhanced heat exchange systems need to be used to meet the heat transfer requirements.

For air and steam gasification there are normally two important quantities which are introduced to describe the amount of gasification medium that is provided for gasification. For air and oxygen as a gasification medium, the equivalence ratio (ER) is generally reported. The ER relates the amount of oxygen provided to the gasifier relative to the amount required for stoichiometric combustion.

$$ER = \frac{\dot{n}_{O2,actual}}{\dot{n}_{O2,stoichiometric}} \qquad \text{Eq. 2.2}$$

For steam based gasification systems the steam to biomass ratio (SB) is normally reported. The SB reflects the mass of steam provided relative to the amount of biomass being gasified.

$$SB = \frac{\dot{m}_{steam}}{\dot{m}_{biomass}} \qquad \text{Eq. 2.3}$$

2.2.6 Physical Considerations

In order to understand how the physical characteristics of biomass can affect the gasification performance, an in-depth discussion of the phenomena regulating gasification should be made. Consider the model shown in Figure 2.3. For a large enough particle, the progression of the gasification depends on the time and location within the particle. At the center of the particle where the temperatures stay cool the longest, drying will still be taking place, while closer to the outside of particle devolatilization is occurring. The surface of the particle, which will have reached the reactor temperatures the quickest, may have already converted to char while the devolatilization and drying processes are still taking place internally. The evolution of moisture and volatiles from the particle can also create a plume enveloping the particle which increases the effective diffusional resistance to gasifying medium transport from the bulk medium to the surface of the particle.

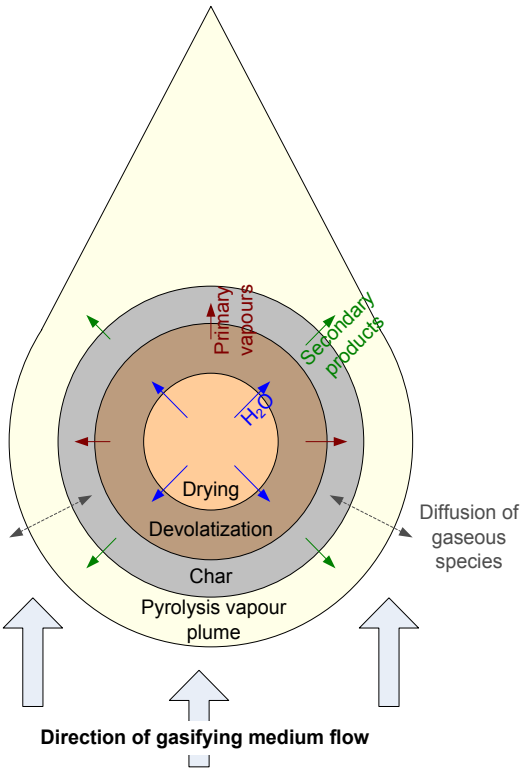

Figure 2.3: Gasification of a single biomass particle in the thermally thick regime

Three regimes for the devolatilization of a biomass particle have been identified (Di Blasi, 1996):

1. Pure kinetic control, where the rate of devolatilization is determined by kinetic limitations of conversion of cellulose, hemicelluloses, and lignin to active forms.

2. Thermally thin regime, where the rate of devolatilization is determined by the external heat transfer from the bulk medium to the particle surface.

3. Thermally thick regime, where the rate of devolatilization is determined by the heat transfer through the interior of the particle.

Although it is hard to demarcate the division between these regimes since these regimes will be affected by reactor conditions and biomass properties, some representative values can be found. At particle sizes below 0.2 mm, kinetic effects are the main contributor to the devolatilization process (Simmons and Gentry, 1986). At particle sizes below 1 mm, external heat transfer effects can dominate the rate of devolatilization (depending on

reactor conditions) while for sizes greater than 1 mm internal heat transfer effects dominate the rate of devolatilization (Koufopanos et al., 1991). Figure 2.3 assumes that the biomass particle is large enough to be affected by heat transfer limitations such that there is a significant temperature gradient within the particle.

In the thermally regulated regimes, differences in the progression of devolatilization are also expected to be influenced by physical properties of the biomass, such as the density, thermal conductivity, and permeability of both the virgin biomass material and the resultant char. Simulations performed by Di Blasi (1997) indicate for thermally thick particles, low permeability and thermal conductivity should encourage secondary cracking of tars due to the increased residence time of primary vapours in the particle.

Another important observation from the model presented in Figure 2.3, is that a mixture of steam and primary vapours may pass through the char layer of a thermally thick particle during gasification. Many authors have noted the catalytic ability of char generated from wood to crack both oxygenated and aromatic tars. At 500 – 600°C char has been observed to catalyze the conversion of oxygenated tars such as saccharides, furans, and guaiacols (Sun et al., 2011). Char is also found to be highly effective at converting more stable tar products such as phenol (at 700°C) and naphthalene (at 900°C) into gaseous products in the presence of carbon dioxide or steam (Abu El-Rub et al., 2008). Based on the work by El-Rub, char produced at 500°C has a catalytic activity for naphthalene conversion at 900°C somewhere between dolomite and commercial nickel catalysts (Abu El-Rub et al., 2008). At appropriate char thicknesses and mass fluxes of pyrolysis vapours through the outer surface of a particle, the char could assist in the catalytic conversion of heavier components to more stable lighter gases. When estimating the time scales for the processes during wood devolatization, Chan et al. (1985) proposed that the fluid residence time within cm-thick particles is sufficient for the secondary reactions of the primary vapours.

Using small particles it was shown that the heating rate of biomass has a strong influence on the yield of tars, chars, and gas products during devolatilization. The heating rate also influences the gasification reactivity of char. The gasification reactivity of char can be increased by a factor of three when the char is formed under high heating rate conditions (1000 – 10000 K/s) as opposed to lower heating rates (20 K/s) (Cetin et al., 2004). Other

research has confirmed that an increase in the heating rate of lignin increases the steam reactivity of the resultant char, which was attributed to the formation of macropores at higher heating rates (Fushimi et al., 2003).

When considering the model presented in Figure 2.3, the heat of reaction effects must also be considered in determining the temperature profile of a given particle undergoing devolatilization and gasification. Koufopanos et al. (1991) proposed that the initial reactions taking place during pyrolysis of wood are slightly endothermic while exothermicity is experienced at higher conversion of wood to pyrolysis products. When tracking the temperature history of large wood particles (diameter = 20 mm) they found that internal temperature of the wood particle exceeded the temperature of the surrounding atmosphere at certain times.

Since the present study focuses on fluidized bed gasification, it is also important to realize that the physical properties of the feed material will also influence the distribution of biomass particles in the fluidized bed through mixing and segregation phenomena which in turn will affect heat and mass transfer parameters. Some of the primary factors in the mixing and segregation in fluid beds are particle sizes involved, particle densities, shape, and fluidizing gas velocities (Cui and Grace, 2007; Zhang et al., 2009). It has been documented that for a large wood particle (relative to the bed media) with low particle density (relative to the bed media), the wood preferentially locates to the top of the bed (Shen et al., 2007).

2.2.7 Chemical Considerations

It should be respected that the term biomass can be used to represent a wide variety of potential fuels with a variety of different compositions. However, many biomass sources, such as wood products or agricultural crops, are composed of similar constituent materials, namely hemicellulose, cellulose, lignin, extractives, and ash. Each of these components shows unique characteristics in terms of its pyrolysis behaviour.

Hemicellulose is a polymer constructed from different sugar monomers (mainly xylose for hardwoods and mannose for softwoods (Shafizadeh, 1982)) which functions in binding cellulose in the cell wall. Hemicellulose normally represents 20 – 40% of the total weight of

a biomass sample (McKendry, 2002). Hemicellulose is the least thermally stable of major biomass components (hemicellulose, cellulose, and lignin). Hemicellulose can start to dehydrate at temperatures as low as 90°C, and reaches a maximum decomposition rate at around 300°C (Raveendran et al., 1996). Hemicellulose has an empirical formula somewhere between $C_5H_8O_4$ and $C_6H_{10}O_5$ depending on the amount of five and six carbon sugars present.

Cellulose is a polymer constructed from glucose monomers and represents the main component of cell walls. Cellulose normally represents 40 – 50% of the total weight of a biomass sample (McKendry, 2002). Cellulose begins to thermally decompose after hemicellulose and reaches a maximum decomposition rate at approximately 400°C (Raveendran et al., 1996). Cellulose can be modeled by the empirical formula $C_6H_{10}O_5$.

Lignin is a polymer consisting of hydroxy and methoxy substituted propyl phenol groups (Alén et al., 1996) which bind the cellulosic fibers together helping to impart strength to the plant matter. Lignin is normally more abundant in woody biomass, up to 30 wt% in softwoods (McKendry, 2002). Lignin has a slightly more complex structure than hemicellulose or cellulose and as such it decomposes over a much broader range of temperatures. Lignin can begin to thermally decompose at lower temperatures, but generally the bulk of the thermal decomposition occurs between 300 to 600°C (Raveendran et al., 1996). Lignin has a significantly reduced amount of oxygen relative to the amount of carbon and hydrogen compared to hemicellulose and cellulose.

Extractives and ash also make up a portion of biomass which in most cases does not exceed 10 wt%[2]. Extractives cover a wide variety of resins, waxes, fats, and oils that the biomass may contain. Ash is also a very important component consisting of the mineral matter contained within the organic structure of the biomass. Biomass also consists of small amounts of other elements such as sulfur, nitrogen, and chlorine which are accrued through the life cycle of the biomass. The amount of these elements can be highly variable depending on species and location (Demirbas, 2004a).

[2] wt% as used in the document refers the dry basis weight percent except for moisture results which are presented on an as received basis unless otherwise noted.

Much of the work done to understand the behaviour of the main constituents of biomass in gasification has been completed using high temperature pyrolysis conditions. These conditions may be reflective of the gas composition produced from an individual biomass particle during devolatilization and will have a strong influence on the gaseous environment for further reactions, such as the vapor phase reforming and char reduction. For example, the primary gas composition for each component of biomass has been found to be different. Hemicellulose devolatilization in a packed bed yields large amounts of CO_2, whereas the cellulose yields comparatively more CO, compared to lignin which yields large amounts of H_2 and CH_4 (Yang et al., 2007).

By inserting cellulose, glucomannan, xylan, and milled wood lignin in a furnace preheated to 800°C, Hosoya et al. (2007) were able to study the pyrolysis products of the main constituents of biomass at high heating rates and gasification temperatures. In this case, cellulose yielded the high amount of tar and the least amount of char. Despite the fact that lignin is the most structurally similar to tar typically found in biomass gasifiers (lignin is composed of aromatic structures), the lignin yielded the smallest amount of tar and highest level of char. One distinction that needs to be made is that the tar from the lignin and the cellulose were substantially different in character, whereas a substantial portion of the cellulose tar was water soluble, the lignin tar contained very few water soluble compounds. Due to secondary reactions in a gasifier, such as further cracking, oxidation, or reforming, the character of the tar will have a strong influence on the persistence of the tar.

In the fixed bed, air-steam gasification of cellulose, xylan, and lignin Hanaoka et al. (2005) found that good carbon conversion (>90%) of cellulose and xylan to gas at 900°C. The lignin on the other hand, produced a substantial amount of char (20%) and about 10 times more tar than the cellulose and the xylan.

In addition to the yield and composition of primary products from the thermal decomposition of the constituent polymers of wood, other differences in their reaction are expected to play an influence in the fluidized bed gasification of these materials. Materials with high rates of devolatilization will influence the hydrodynamics of a fluidized bed differently than a material that reacts slowly. The resulting char reactivity and mechanical strength of the char will determine how much char is retained in the bed of the gasification.

Van Paasen and Kiel (2004) evaluated the air gasification performance of beech (24% lignin), willow (18 wt% lignin) and pure cellulose (0% lignin) in a fluidized bed gasifier in order to evaluate the impact of the biochemical composition of biomass. Due to the altered C/H/O ratio of cellulose versus the woody materials, a higher ER was required in order to attain similar gasification temperature. The gas composition was fairly similar between the different fuels but the cellulose gave a producer gas with a tar content (as measured by solid phase adsorption - SPA) 2 to 3 times lower than the woody materials. Despite this, the dewpoint of the gas (the temperature at which the tar first starts to condense) was similar between the woody materials and the cellulose. Since gravimetric tar measurements were not determined it could be speculated that this means that the predominant composition of the tar from the cellulose gasification was heavily weighted towards materials that are not amenable to the SPA technique of tar measurement.

It cannot be said for certain that the contribution of lignin, cellulose, and hemicellulose are independent. Rather there may be interactive effects between the lignin, cellulose, and hemicelluloses.

By comparing the gas composition, gasifier efficiency, and tar content in producer gas from biomass, peat and coal, an appreciation can be obtained of the impact of the chemical composition of the feed material. The compositional differences between biomass, peat, and coal are reflected by the difference in the ratio of carbon to hydrogen to oxygen. Often times this difference is shown in a Van Krevelen diagram. Prins et al. (2006) show a comparison between the C/H/O distribution in biomass, peat, and coal which is reproduced in Figure 2.4.

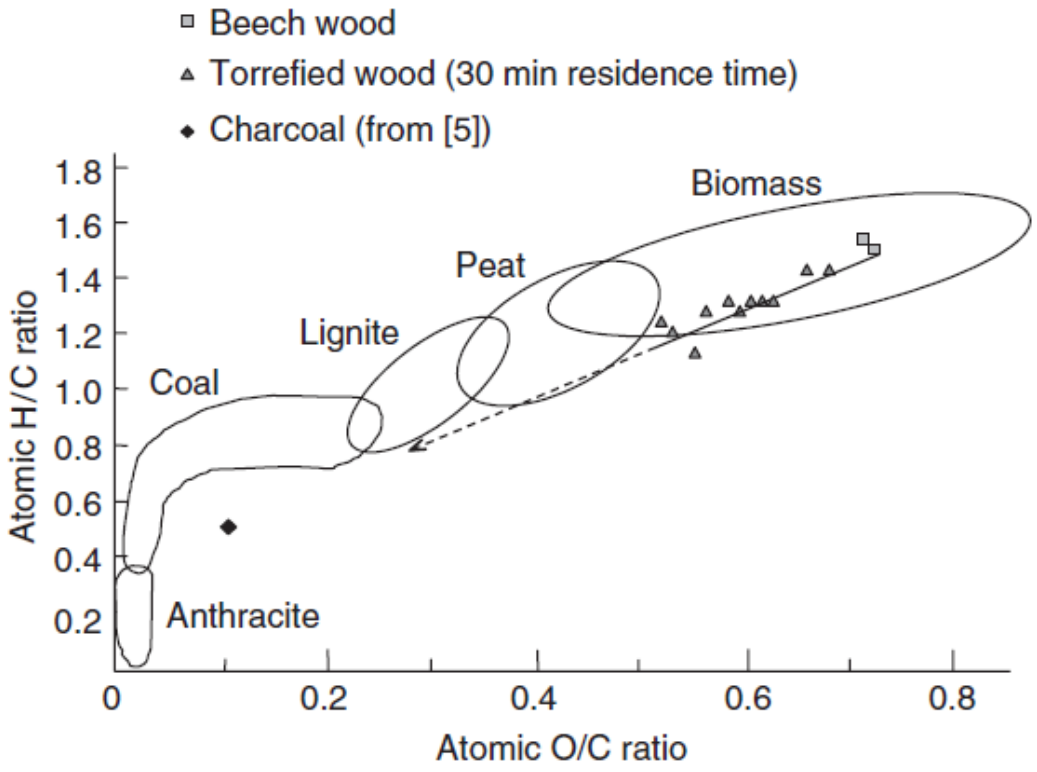

Figure 2.4: Van Krevelen diagram comparing coal, peat, torrefied wood, and wood (Copied from Prins et al., 2006)

The differences in fuel composition between coal, peat, and biomass also lead to very distinct gasification characteristics. Kurkela and Ståhlberg (1992) show the tar content measured in the producer gas from sawdust, peat, and brown coal gasification which is reproduced in Figure 2.5.

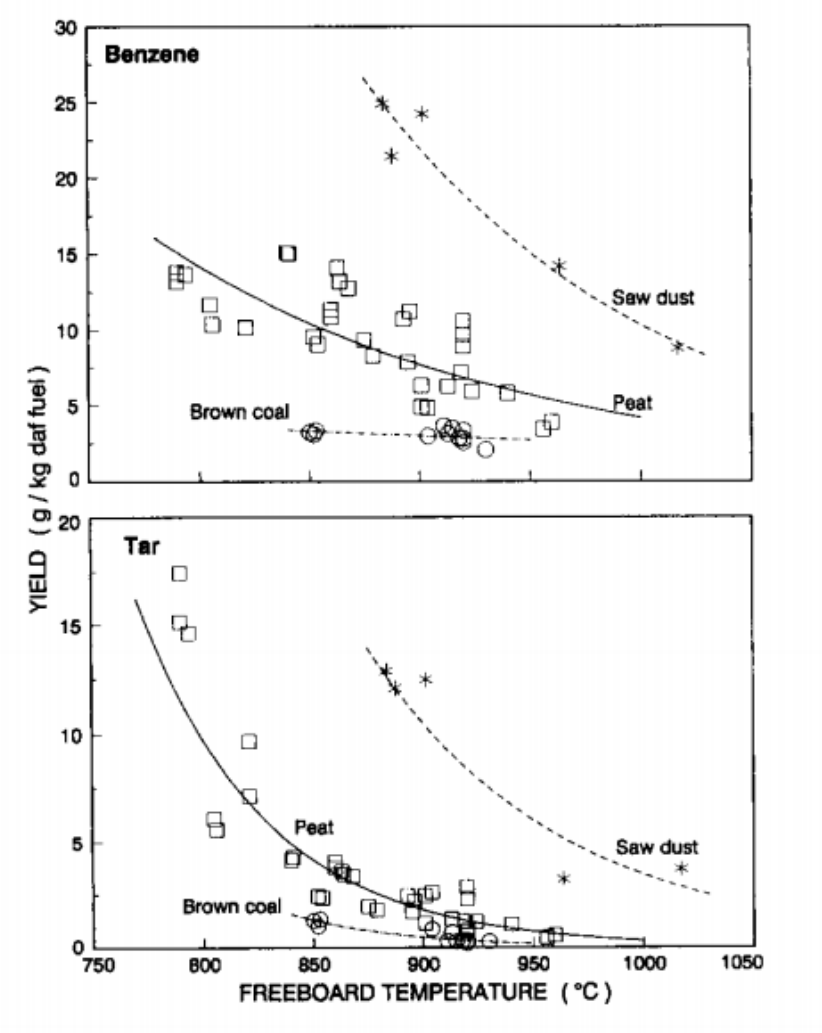

Figure 2.5: Benzene and tar yield from pressurized bubbling fluidized bed gasification of sawdust, peat, and coal (Copied from Kurkela and Ståhlberg, 1992)

The observation that the fluidized bed gasification of peat and coal to lead to much lower tar content producer gas compared to fluidized bed gasification of biomass is not unique to the source referenced in Figure 2.5. This difference is also recognized elsewhere (Bridgwater, 1995; Pan et al., 1999). This difference could be attributed to many factors. There are significant ash differences between coal, peat, and biomass. However, if the ash was contributing to the observed difference it would be expected to see a large range of tar content within biomass gasification that correlates strongly to the differences in the ash composition of the biomass. Chars from coal are normally less reactive than those from peat which are normally less reactive than those from biomass. The longer residence time of

char in the bed could be contributing to the catalytic elimination of tar. Differences in the amount of volatile matter could also be expected to be contributing to higher tar concentration. Although this may be true to some degree, brown coal and peat would be expected to produce much similar tar content if the tar level was only dependent on the volatile content of the fuel.

Over the C/H/O ratio differences present between wood, thistle, and wheat straw Herguido et al. (1992) found differences in the gas composition and the gas / tar / char yields between the fuels tested that they attributed to compositional differences at 650 – 700°C in steam gasification in a fluidized bed. The differences seemed to disappear at higher temperatures (750-800°C).

2.3 **Biomass Pre-treatment**

Biomass pre-treatment is the physical or chemical manipulation of raw biomass feedstock in a manner intended to improve its qualities or characteristics prior to its conversion in bioenergy processes (US Department of Energy - Energy Efficiency and Renewable Energy, 2010). The pre-treatment and the conversion of the biomass source often take place at different points along the supply chain. Often times, pre-treatment processes are undertaken as a means to improve the storage, handling, and transport properties of the biomass such as increasing the flowability, energy density, or resistance to biodegradation. The consequences of these pre-treatment processes on the conversion processes, such as gasification, are not always clear. Ideally, pre-treatment processes should be optimized with respect to both the feedstock handling and conversion performance.

Particle size, size distribution, porosity, surface area, and bulk density are physical properties of biomass that can be affected by pre-treatment processes. These physical properties will affect the heat conduction through the particle, the surface area for heterogeneous reactions, mass transfer of gaseous species to and from internal pores, fragmentation rates of the particles, and segregation of particles in fluidized beds. These changes then lead to differences in gasification kinetics, particulate levels, carbon conversion, and tar concentrations.

Chemical characteristics can also be affected by pre-treatment processes. This is especially true for thermal pre-treatment processes like torrefaction and carbonization. The chemical alterations change the O/C and H/C ratios in the gasifier fuel which affect product distribution and chemical efficiency. As well, the chemical changes alter the reactivity of the char that is produced.

Table 2.2 shows a comparison of some of the characteristics of typical raw, pelletized and torrefied biomass.

Table 2.2: Comparison of some of the main characteristics of biomass pre-treated in different manners

	Raw Biomass	Pelletized Biomass	Torrefied Biomass
Moisture Content (wt% ar)	up to 60	Less than 10	Less than 5
Carbon (wt% db)	45-55	45-55	50-65
Oxygen (wt% db)	35-45	35-45	25-40
Hydrogen (wt% db)	5-7	5-7	4-6
Calorific Value (MJ/kg db)	18-22	18-22	20-25
Bulk Density (kg/m^3 ar)	200 – 350	500 – 800	Depends on processing (whether it is pelletized or not)
Form	Heterogeneous mixture of a variety of sizes and particle shapes based on prior processing	Uniform cylindrical particles	Depends on processing (whether it is pelletized or not)

2.3.1 Drying

The goal of drying is to remove water from biomass without causing significant chemical change. The moisture content of freshly harvested or collected material can depend heavily on the source of biomass. Freshly harvested biomass can often have a moisture content of approximately 60 wt%, whereas for proper operation of feed handling equipment such as

augers and conveyors, moisture content of between 10 and 20 wt% is often desired (Cummer and Brown, 2002).

Drying is generally accomplished by raising the temperature of biomass such that free moisture and loosely-bound water evaporates from the surface and interior of the biomass particle. When drying biomass, it is often desirable to keep the particle temperature below or close to 100°C in order to minimize the emissions of volatiles from the biomass; at particle temperatures above 150°C chemical changes can start to be observed in the material due to the devolatilization of hemicellulose (Fagernäs et al., 2010).

By removing water by drying, the mass of the biomass fuel is significantly reduced without reducing the calorific value of the fuel. Drying improves the resistance of biomass to biological degradation which increases the ease of storage. The storage of overly wet biomass material may lead to odour issues and may represent a risk for spontaneous combustion in storage. Drying will have effects on other biomass parameters, such as the energy required for comminution or its flowability. Drier biomass feedstocks can reduce the energy requirements for comminution for some biomass feeds (Igathinathane et al., 2008; Miao et al., 2011) while other biomass feeds show no change (Igathinathane et al., 2009).

In relation to other feed characteristics, moisture can often have a dominant effect on gasification performance. High moisture content biomass is typically detrimental to the performance of a gasifier (Schuster et al., 2001) since heat from a high temperature source is used for water desorption and evaporation. Using the heat from the bed of the reactor to evaporate moisture from the biomass represents an inefficient use of heat from a high temperature source as compared to drying biomass by using waste heat rejected at a lower temperature. In order to satisfy the energy balance, high moisture fuels either result in a lower gasification temperature or require that additional heat be provided to the gasifier to maintain the same temperature relative to drier fuels. Lower gasification temperatures are well known to increase the tar content of the producer gas and reduce the carbon conversion and gas yield (Carpenter et al., 2010; Rapagnà and Latif, 1997; Schoeters et al., 1989; van der Drift and van Doorn, 2000). In order to provide additional heat to the gasifier, additional air or oxygen can be provided which has been found to lead to depressed heating values of the producer gas and lower cold-gas efficiencies (van der Drift et al., 2001).

Some research suggests that there are differences between steam injection and an equivalent amount of fuel-bound moisture. Li et al. (2004) found that injected steam showed better reactivity than an equal amount of fuel moisture. Some possible explanations for this include the location of steam injection versus the feed position and the local temperature effects of moisture evaporation on the biomass particle.

Experiments were also performed in a bubbling fluidized bed gasifier in which the effect of feed moisture on tar production was decoupled from the bed temperature and ER by means of maintaining the bed temperature and ER constant with heat tracing to supply the additional heat required to evaporate the additional moisture. These experiments demonstrated that when the effect of the moisture on the bed temperature can be eliminated, the tar content decreases from 14 to 8 g/m^3 with increasing feed moisture from 10 to 45wt% at 800-825°C and an ER of 0.24 – 0.26 (van Paasen and Kiel, 2004).

Due to the high latent heat of evaporation of water, it can be expected that the moisture within the biomass particle has the ability to significantly affect the internal heating rate of a particle relative to the dry case. Models and experiments show that high moisture content does in fact delay the devolatilization process (Bharadwaj et al., 2004; Chan et al., 1985) and that the moisture content of a particle also affects the distribution of char, tars, and gases formed during devolatilization (Demirbas, 2004b). Based on this work it is possible to explain why injecting water (or steam) into a gasifier will not produce the same results as an equivalent feed rate of moisture in the solid biomass.

The interaction between particle size and moisture may also be important to consider. Since for thermally thick particles, there may be a regime where the core of the particle is drying while the outer layers are devolatilizing. The high flux of water vapour mixing with pyrolysis products may lead to effective reforming as they travel across the hot char outer layer.

Table 2.3 shows the results of previous experimental work that is published on the effect of moisture content on the performance of fluidized bed gasifiers.

Table 2.3: Previous experimental fluid bed work where moisture level was varied

Authors and Year	Experimental Apparatus and Conditions	Range of Results	Effect of Moisture on the Producer gas	Ref.
A. van der Drift; J. van Doorn; J.W. Vermeulen 2001	• Circulating Fluidized Bed: 0.2 m ID x 6 m high • Air blown gasification • Temperature and superficial velocities held constant at approximately 850°C and 6 m/s • Biomass feedstock: ten different residual biomass fuels tested including: Demolition wood, chip board materials, verge grass, paper residues sludge, cacao shells, railroad ties, among others • Particle size: varied with fuel type generally <40 mm • Biomass feed rate: 50 – 100 kg/h • Bed material: Silica sand 0.4 – 0.6 mm • Moisture range: between 3.5 – 17.5 wt%	• H_2 content of gas: 1.8 – 9.02 % • HHV of gas: 2.05 – 5.13 % • Heavy tars: 20 – 658 mg/m^3	Moisture was found to have a dominant effect on carbon conversion, efficiency, and heating value of the gas. As the moisture level of the fuel increased, the ER increased in order to maintain constant temperature resulting in a large drop in higher heating value of the gas. The authors note that the important parameter to consider is not the as received moisture content, but the amount of moisture present relative to the amount of organic material (ash-free moisture content)	(van der Drift et al., 2001)
Sommas Kaewluan and Sunreerat Pipatmanomai 2011	• 100 kW(th) bubbling fluidized bed, ID 0.3m, 2.5 m high, air blown gasification Silica sand used • Feed inserted at 0.5 m above distributor (based on the diagram it appears this will be into the splash zone or just below the surface of the bed) • Bed temperature: 699-761°C • Biomass feedstock: rubber-tree wood	Results presented on a N_2-free basis • H_2: 13.9 – 15.5 vol% • CO: 27.0-31.6 vol% • CO_2: 38.1 – 43.8 vol% • CH_4: 8.3 – 8.7 vol%	The gas composition did not show any large shifts in the H_2/CO with the higher moisture fuels. With increasing fuel moisture, a lower bed temperature was achieved at a constant ER. As moisture increased (and consequently bed	(Kaewluan and Pipatmanomai, 2011)

	chips • Particle size: approximate size 10 x 10 x 5 mm • Biomass feed rate: approximately between 32 -54 kg/h • Fuel moisture range: 9.5 – 25.5%	• HHV gas: 4.04 – 4.71 MJ/m^3	temperature dropped) HHV of the gas decreased, the carbon conversion decreased, and the cold gas efficiency decreased.	
C. Pfeifer; S. Koppatz; H. Hofbauer 2011	• Dual fluidized bed, 100 kW Steam gasification • Bed material: Olive sand, 500 micron • Biomass feedstock: Wood chips, • Particle size: <20 mm • Gasifier temperature: 810 – 850°C • Steam fuel ratios between 0.75 – 1.6 kg/kg • Fuel moisture range: between 6 – 40%	• H_2: 34.1-37.2 vol% • CO: 16.8-24.4 vol% • CO_2: 21.7-28.1 vol% • CH_4: 10.6 -11.6 vol% • Tar: 4 – 9 g/m^3 (d.b.)	With increased fuel moisture, a slight increase in the hydrogen content of the gas was observed, with a decrease in carbon monoxide and methane concentration. Tar content appeared to hit a minimum at 19 % moisture (6% fuel moisture led to approx. 8 g/m^3 compared to approx. 5 g/m^3 at 19% fuel moisture).	(Pfeifer et al., 2009)
S.V.B. van Paasen; J.H.A. Kiel 2004	• Bubbling fluidized bed: 0.074 m ID (at bed) X 0.5 m tall • Air blown gasification • 1 kg/h feed rate • For moisture experiments: • Temperature range in bed 808 – 826°C • Bed electrically heated to allow for constant temperature and ER to be achieved for different moisture levels • Biomass feedstock: Willow • Particle size: 0.7 – 2.0 mm	(For moisture variation experiments only, after cyclone) • H_2 content of gas: 8.9 – 14.9 % • ER: 0.24-0.26 • Tar yield (by SPA): 8.5 – 14.2 g/m^3.	For these experiments, the effect of moisture on the temperature and / or ER was eliminated by using heaters to maintain constant temperature and ER at different moisture levels. Under these conditions, the increase in moisture from 10 to 43 wt% led to an increase in H_2 gas content from 8.9 to 14.9% at the expense of CO while the tar content dropped	(van Paasen and Kiel, 2004)

	• Fuel moisture level: 10 – 45%		from 14.2 to 8.5 g/m^3.	
X.T. Li; J.R. Grace; C.J. Lim; A.P. Watkinson; H.P. Chen; J.R. Kim 2004	• Circulating Fluidized Bed: 0.1 m ID X 6.5 m tall • Air blown gasification • Temperature range 700-850°C • Feedstock: Sawdust feed, variety of woody biomasses tested including Cypress, Hemlock, Cedar, Spruce, Pine, and Fir. • Particle size: between 0.38 and 1.49 mm • Moisture range: 4-22.0 wt%. • Sawdust feed rate between 16 – 45 kg/h with superficial velocities between 4 and 10 m/s	• H_2 content of gas: 3.0 – 7.3 %, dry basis • ER: 0.218 – 0.536 gas heating value: 2.43 – 6.13 MJ/m^3 • Tar yield: 0.04 – 15.13 g/m^3 (catalyst used for some tests)	Injected steam caused greater changes in the product ratios and had better reactivity than an equivalent feed rate of fuel moisture	(Li et al., 2004)

Table 2.3 shows that for works that did not adjust the equivalence ratio of the gasifier in order to achieve the same bed temperature, the addition of moisture depressed gas yields and carbon conversion and led to high tar loadings in the producer gas. Other work shows that there may in fact be an optimal moisture level to operate at since elevated fuel moisture can help with the reforming of tars and increases in the hydrogen content of the producer gas.

2.3.2 Comminution

Some degree of size reduction is often necessary in order to accommodate the handling and feeding the biomass into the gasifier, for the proper operation of the gasifier, or for further pre-treatment levels that are pursued. Biomass end-users often demand a flowable, relatively uniform feed which for most biomass sources requires that size reduction to take place somewhere along the supply chain.

Biomass can be delivered in a variety of sizes which depend largely on the source of biomass and the harvesting method used. Two of the most common devices for comminuting biomass appropriate for gasification are knife chippers and hammermills although auxiliary crushers may also be used for initial size reduction (Cummer and Brown, 2002).

Besides altering particle size and size distribution, mechanical size reduction may also have other effects on biomass such as opening hidden pores and altering the geometry of the particles which are relevant to conversion processes.

For any process consuming a residual biomass fuel, it is always advantageous if the material can be used in an as received particle form. The cost of milling equipment and the energy requirements can be significant. Tremel et al. (2013) show some representative energy requirements for comminuting woody materials, torrefied materials, and coal as shown in Figure 2.6.

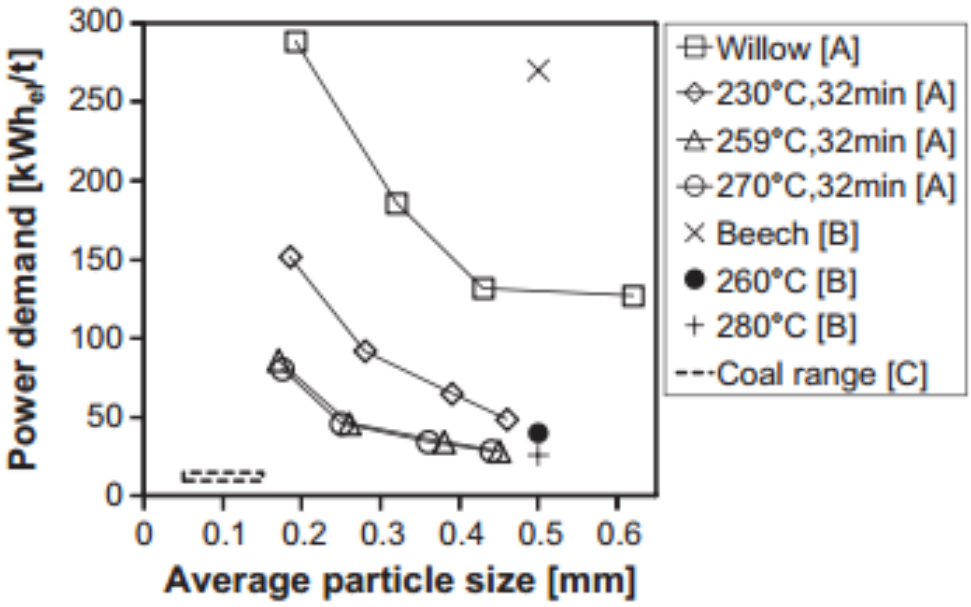

Figure 2.6: Power consumption for the milling of woody materials, torrefied materials, and coal (Copied from Tremel et al., 2013)

As Figure 2.6 shows, as the required particle size of biomass drops below 0.5 mm, the energy requirements start to exceed 100 $kWh_{electric}$/ton. This represents about 2 GJ of electrical energy for every 100 GJ of biomass processed.

Although the primary fragmentation of a biomass particle in a fluidized bed will result in the initial size reduction of the particles, the size of the original biomass particle still strongly influences the size distribution of the resulting char (Sudhakar et al., 2008).

Particle size can also be related to segregation phenomena in a fluidized bed reactor. It has been observed that biomass particles have a tendency to segregate to the top of a fluid bed. In addition to the "floatation" of biomass char due to its low density relative to bulk density of bed media, biomass particles tend to propelled to the top of the bed during devolatilization due to the formation of endogenous bubbles (Fiorentino et al., 1997). This phenomenon is affected by particle size and bed temperature. Small particles are less likely to be carried to be propelled to the top by endogenous bubble formation, especially at low temperatures. Large particles are generally quickly propelled to the top of the bed.

Work by Asadullah et al. (2010) has demonstrated the effect of particle size on the character of the resulting char. During the release of volatiles from a biomass particle there appears to be competition between escaping volatiles and recombination of volatiles on to the char surface. At high heating rates in fluid bed conditions, an increase in particle size from 0.3 to 5.18 mm led to the increase of the retention of alkali and alkaline earth metals and the reactivity of the char (Asadullah et al., 2010).

Some reviews suggest that a smaller particle size is always superior for biomass gasification but this factor must be balanced with the additional cost associated with biomass size reduction (Alauddin et al., 2010). However the full scope of the issue is often underappreciated as the problem is either related to range of particle sizes that are extremely small or rely on batch studies of material. For the data on particle size to be applicable to large, commercial-scale fluidized bed gasifiers, there is a need to cover a wide range of sizes, up to particle sizes that exceed the capabilities of most laboratory and bench-scale apparatuses.

Feed location may have a strong interaction with the effect of particle size. Feed locations in fluidized bed gasifiers can be divided into two categories: in-bed and over-bed positions. For an over-bed feed position, the feed material is injected into the gasifier above the surface of the bed and must fall on to the top of the bed. In an over-bed feed position, some of the feed material may begin to devolatilize above the bed and some of the finest material may be entrained and never reach the bed. For an in-bed feed position, the feed material is injected below the surface of the bed. For an in-bed feed position, all the feed material, or their vapors, must initially pass through the bed. It has been shown that feed location also has important effects on product distribution, tar production, and ammonia production from fluidized bed systems (Corella et al., 1988; Vriesman et al., 2000). Di Felice et al. (1999) looked into the devolatilization behaviour of biomass fed from in-bed and over-bed feed positions. They found that for a low density bed of alumina catalysts, where the biomass particles were denser than the bed material, preferring to sink into the bed, feeding location made no difference. However, in a sand bed, which had higher bulk density, the devolatilization time of the biomass was increased for the over-bed feed position relative to the under-bed feed system (Di Felice et al., 1999).

In an over-bed feed position, fines from the feed biomass can be entrained in the upward gas flow before reaching the bed region. These particles spend a reduced residence time in the gasifier relative to particles which are large enough to make it into the bed and devolatilize as they travel up the riser. As they devolatilize, the entrained particles produce tars which do not have sufficient residence time to crack into permanent gases. Since these tars are formed outside of the bed, they avoid any catalytic enhancement which may be provided by the bed media. In addition, they do not benefit from enhanced convective mass transfer provided in the bed region which provides gasifying medium to help convert the tars and chars to gaseous products. Due to the reduced heat transfer coefficient in the freeboard region, it can be reasonably assumed that for a biomass particle in the thermally thin regime, the devolatilization rates will be reduced. The char from the particle will be take longer to be formed, the char may be less reactive, and have less residence time to gasify which will lead to more unconverted carbon escaping as char.

When fed from an in-bed feed position, all particles travel through the bed region regardless of size. In this situation, the faster (and thus closer to the bottom of the bed) the particle devolatilizes, the more interaction the pyrolysis vapours have with the bed media and gasifying medium. High particle temperature (which can be expected to be achieved rapidly for a small particle in the bed) also favours light gas production at the expense of tar and char (Scott et al., 1988). The increased heating rate of a small particle should also lead to the production of more reactive char and the smaller the original particle, the smaller the resultant char. These effects should lead to the enhanced conversion of the char.

Considering the fundamental works performed on single particle devolatilization and previous experience with fluidized bed gasification, it is hypothesized that from an in-bed feed position, smaller biomass particles should lead to more complete conversion of the char and possibly a reduction in the tar content of the producer gas from a fluidized bed gasifier. From an over-bed feed position, the situation is more complex. Biomass particles which are small enough to become entrained in the gas flow before entering the bed region should result in increased tar content and reduced char conversion. This is especially important for particles small enough to become entrained but large enough so that devolatilization rates are still limited by heat transfer considerations. Larger particle sizes

fed into fluid bed gasification systems should increase the amount of char held up in the bed. The reduced reactivity of the char formed from large particles may lead to decreased carbon conversion in the gasifier as the elutriated char is less likely to fully gasify, but the catalytic enhancement of tar reforming via char may lead to modest reductions in tar content of the producer gas.

Table 2.4 shows some of the previous experimental works that have been published on the effect of the particle size on the fluidized bed gasification of biomass.

Table 2.4: Previous experimental fluid bed work where particle size was varied

Authors and Year	Experimental Apparatus and Conditions	Range of Results	Effect of Particle Size on the Producer gas	Ref.
K. Pattabhi Raman; Walter P. Walawender; L. T. Fan 1980	• Bubbling Fluidized Bed: 0.229 m ID (bed level) X 1.93 m high • Gasification completed using flue gas from air-propane combustion with injected steam to moderate temperature • Bed material and size: 0.55 mm silica • Feed location: above bed feed • Biomass feedstock : dried manure • Particle sizes tested: -2 +8 mesh (2.36 – 11.2 mm), -8 +14 mesh (1.4 – 2.36 mm), -14 +40 mesh (0.4 mm – 1.4 mm) • Bed temperatures used were between 900 and 994 K (627°C – 721 °C) at feed rates between 10 – 20 kg/h and superficial velocities between 0.28 – 0.33 m/s	• Nitrogen-free gas yield and heating value reported. • Gas yield: 0.3 – 0.6 m^3 / kg_{DAF} • Heating value: 12 – 22 MJ/Nm^3	Particle size effects are not independent from feed rate and superficial velocity. For the finest size fraction (-14 +40 mesh), the nitrogen-free gas yield ranged between 0.38 – 0.47 Nm^3/ kg_{DAF} and for the coarsest size fraction (-2 +8 mesh) ranged between 0.30 – 0.54 Nm^3 / kg_{DAF} where the temperature ranged between 972 – 983 K and 944 – 994 K for the finest and coarsest size fraction, respectively.	(Raman et al., 1980)
S. Rapagnà; A. Latif 1997	• Bubbling Fluidized Bed: 0.06 m ID X 0.54 m tall • Steam gasification • Feed location: biomass feed into the bed • Biomass feedstock and size: Four sizes of ground almond shells used as feed with average diameters of 0.287 mm, 0.533 mm, 0.747 mm, and 1.09 mm • Bed material and size: alumina with a particle diameter of 0.103 mm. • Feed rate of 1 g/min used with S/B ratio of 0.8	• H_2 yield of 0.2 – 0.7 $m^3/kg_{biomass}$ • Gas yield of 0.3 – 1.5 $m^3/kg_{biomass}$ • Char + tar production of 0 – 0.35 $kg/kg_{biomass}$	The amount of char + tar produced increased as particle size increased from <0.1 $kg/kg_{biomass}$ for 0.287 mm at all temperatures to 0.2 – 0.35 $kg/kg_{biomass}$ for particle sizes of 1.09 mm. Gaseous and H_2 yields decreased with increasing particle size The effect of particle size was	(Rapagnà and Latif, 1997)

	• Temperatures tested ranged from 600 – 800°C		less pronounced at higher temperatures	
J. Schoeters; K. Maniatis; A. Buekens 1989	• Bubbling Fluidized Bed: 0.15m ID (bed level) X 1 m tall • Air blown gasification • Feed location: Feed from the top • Biomass feedstock: Wood shavings used to evaluate the effect of particle size, material was sieved to create three size profiles (fines, coarse, unsieved). • Particle size: Sieve size not specified • Bed material and size: Silica sand, average diameter of 0.58 mm • Feed rate: 1.3 to 3.1 kg/h of wood shavings fed to reactor	• HHV of fuel gas: up to 5.72 MJ/m^3 • H_2 content of gas: up to 6.8 %	The particle size was not found to have an effect on the higher heating value or gas yield from the experiments.	(Schoeters et al., 1989)
A. van der Drift; J. van Doorn 2000	• Circulating Fluidized Bed: 0.2 m ID x 6 m tall • Air blown gasification • Temperature varied axially based on the fuel size used, between 790 and 950°C • Biomass feedstock: Willow feed used • Particle size: 2 x 2 mm, 10 x 10 mm, and 10 x 40 mm particles • Bed material and size: Silica sand ~ 0.5 mm		Heavy tar production was at maximum with 2x2 mm particles and at minimum with 10 x 10 mm particles. The effect of the particle size on other parameters such as carbon conversion, and HHV of the fuel gas was less pronounced than the effect on tar production. Authors attribute the high tar production with fine particles due to entrainment of fines in the flow, which is supported by the axial temperature profiles in the reactor.	(van der Drift and van Doorn, 2000)
X.T. Li; J.R.	• Circulating Fluidized Bed: 0.1 m ID X 6.5 m tall	• H_2 content of gas: 3.0	Over the range of particle sizes	(Li et al.,

Grace; C.J. Lim; A.P. Watkinson; H.P. Chen; J.R. Kim 2004	• Air blown gasification • Temperature range 700-850°C • Biomass feedstock: Sawdust feed, variety of woody biomasses tested including Cypress, Hemlock, Cedar, Spruce, Pine, and Fir. • Particle size: between 0.38 and 1.49 mm with a moisture range of 4-22.0 wt%. • Sawdust feed rate between 16 – 45 kg/h with superficial velocities between 4 and 10 m/s • Steam injection also used	– 7.3 %, dry basis • ER: 0.218 – 0.536 • Gas heating value: 2.43 – 6.13 MJ/m^3 • Tar yield: 0.04 – 15.13 g/m^3 (catalyst used for some tests)	used (0.38 – 1.49 mm) no clear effect of particle size was detected in the results	2004)
P.M. Lv; C.Z. Wu; Z.H. Xiong; Y. Chen; J. Chang; J.X. Zhu 2004	• Bubbling Fluidized Bed: 0.04 m ID X 1.4m tall • Air blown gasification with steam injection Electrically heated to compensate for heat loss / provide additional heat to the system • Bed material and size: Silica sand, 0.2 – 0.3 mm • Biomass feedstock: Four sizes of pine sawdust used: • Particle size: 0.6-0.9 mm, 0.45-0.6 mm, 0.3-0.45 mm, and 0.2-0.3 mm • Feed location: not explicitly described but based on the author's diagram appears to feed into the bed • For the effect of particle size tests: Temperature = 800°C, Feed rate = 0.512 kg/h, ER = 0.23, S/B = 1.56	(For particle size experiments only) • Gas yield ranged between 1.53 – 2.57 $m^3/kg_{biomass}$ • Gas LHV ranged between 6.98 – 8.74 MJ/m^3 • Carbon conversion between 77.6 – 95.1 %	The gas yield, gas LHV, and carbon conversion all increased when the particle size decreased.	(Lv et al., 2004)

Table 2.4 shows that much of the previous works have been performed using very small particle sizes. Only two of the studies listed above used particle sizes greater than 2 mm. This can often be related to the scale of the gasifier and feeding point location, as well as the tendency of research to be completed with easy to feed materials. At the small particle size (<2 mm), the research often reports that the particle size has no effect or that a smaller particle size increases conversion of solid fuel to gas and reduces the tar yield. At such small sizes, it is likely that the particles fall within the kinetic regime or the thermally thin regime where the drying, devolatilization, and char gasification take place uniformly within the particle. At larger particle sizes (>2 mm), in the thermally thick regime, the drying, devolatilization, and char gasification can all be occurring simultaneously depending on the location within the particle. Larger particles will also have a tendency to mix better in the fluidized bed since the particle density of biomass is typically low compared to the bulk density of the bed material.

Since it can be very costly and energy intensive to comminute biomass to particle sizes less than 2 mm, there is a great need for further research evaluating whether adequate gasification performance can be obtained using larger particles in a fluidized bed gasifier and whether optimal size ranges can be determined.

2.3.3 Physical Densification

One of the most important physical properties of biomass for use in energy processes is the bulk density. The bulk density affects the transport costs, storage volumes, and handling system sizes required in order to process biomass. In an effort to increase the bulk density of biomass, physical processes such as pelletization or briquetting are used to compact biomass into a denser product. These densification processes have the added benefit of producing feedstock with a standardized size and shape distribution which can facilitate the formulation of uniform feed standards for gasifiers. For dry wood and bark, species commercially important to the United States, the dry particle density of chips is generally between 300 and 550 kg/m^3 (Ragland et al., 1991). The particle density of woody pellets is increased to between 1000 and 1500 kg/m^3 (Dai and Grace, 2011; Wu et al., 2011).

Densifying biomass, affects the physical properties of the biomass particles. The mechanical strength of the biomass particle becomes altered, as does the macroscopic pore size. For

woody biomass the directional pore structure of the biomass is partially destroyed in the size reduction and densification process leading to differences in the mass transfer characteristics in and out of the particle. The pelletization process also imparts changes to the permeability, effective thermal conductivity, and mechanical strength of the particles. The increased particle density of the fuel pellets should allow for more favorable mixing in fluid bed. Segregation of the relatively light biomass to the top of a fluid bed will result in devolatilization occurring in the top of the bed and in the splash zone which will eject pyrolysis vapours directly into the freeboard. These pyrolysis products will not spend any significant residence in contact with the marginally catalytic bed material. It is hypothesized that the improved mixing of particles with density closer to that of the bed material will result in more mature gas and tar products from a fluidized bed gasifier.

Changes to the permeability and thermal conductivity of the particle from the pelletization process will also lead to different heat conduction rates through the particle, different devolatilization rates, and different vapour residence times in the particle. This will affect the degree of secondary reactions occurring within the particle.

Investigation of the fragmentation and attrition behaviour of wood and wood-coal pellets has shown that pellets are relatively resistant to primary fragmentation, indicating the pelletization process imparts significant strength to the pellet. However, secondary fragmentation and attrition processes led to significant elutriation of char from the system, indicating that as gasification takes place, the erosion of char structure reduces the mechanical stability of the particle (Ammendola et al., 2011).

Pelletized biomass forms used in fluidized bed gasification are frequently presented in published literature for their positive handling and feeding characteristics. Thus, plenty of work can be found where a fluidized bed gasifier was used and at least one of the gasification feedstocks tested in the study was biomass in pelletized form (Campoy et al., 2009; Gómez et al., 1999; Gustafsson et al., 2001; Meng et al., 2011; Michel et al., 2011; Pfeifer et al., 2009; Schoeters et al., 1989; van der Drift et al., 2001; Weerachanchai et al., 2009). However in the aforementioned studies no direct comparison between the parent material and pellets were made for their effects on the fluidized bed gasifier. In another work, the pyrolysis and gasification behaviour of pellets in a TGA has been reported (Erlich

et al., 2007). The data from this study indicates that the shrinkage behaviour of the pellets during gasification is significantly different from the parent material. While the parent wood material shows increased variance in shrinkage perpendicular to the wood fibres, the wood pellets experience uniform shrinkage in all directions. In addition, pellets tended to yield higher density char which took longer to gasify with steam at 800°C.

Siedlecki and de Jong (2011) compared the performance of pellets and crushed pellets in a steam-oxygen circulating fluidized bed fed at approximately 20 kg/h. This was a somewhat accidental comparison since the use of crushed pellets was originally dictated by feeding issues. Since the comparison was accidental, the gasifier conditions are not identical between crushed and non-crushed pellets, but over the range of conditions, the data appears to suggest that the use of pellets led to an increase in the hydrogen content of the gas with a decrease in the methane content. They found that for the whole pellets, there were lower concentrations of phenols and PAHs in the producer gas. They noted that the crushed pellets led to an increase in the carbon conversion of the process.

The only comparison found in literature between the fluidized bed performance of pellets and the parent material used to make the pellet is by Wilk and Hofbauer (2013). Their comparison was deliberate and they took efforts to make sure that a strong comparison could be drawn between the parent and the pelletized material. However, they could not feed 100% sawdust to their system. Thus, their comparison was limited to a comparison between a pellet / sawdust mixture (31/69 weight ratio) and pure pellets. Wilk and Hofbauer also included some woody waste materials with varying particle size distributions in their experimental campaign. They compared many of their results on a basis of the content of the feedstock having an equivalent diameter of less than 1 mm. For the sawdust / pellet mixture they found a decreased hydrogen content in the gas while there was an increase in the carbon monoxide and methane content compared to the pure pellets. The tar content of the gas was increased (both gravimetric and GC/MS tar) for the pellet / sawdust mixture compared to the pellets.

Table 2.5 shows the results of previous experimental work that is published which compares pelletized to either the parent sawdust or to crushed pellets in fluidized bed gasifiers.

Table 2.5: Previous experimental fluid bed work where pelletized biomass was compared to other biomass

Authors and Year	Experimental Apparatus and Conditions	Range of Results	Effect of pelletization on the Producer gas	Ref.
M. Siedlecki and W. de Jong 2011	• Circulating fluidized bed, • Steam-oxygen blown, 0.083 m inner diameter riser. • Clean and demolition wood pellets tested ER 0.20- 0.40, S/B 0.5 – 1.5 • Temperature 800 – 850°C and superficial fluidization velocity used 3 – 4.5 m/s • Pelletized and milled pellets were compared (somewhat accidentally) using a sand material • Maximum feed rate of the system ~20 kg/h • Feed point 0.90 m from distributor	Milled A-wood: • H2: 21-26 vol% • CH4: 9.4-10.6 vol% • CO: 36-41 vol% Pelletized A-wood: • H2: 28-35 vol% • CH4: 7.9-8.9 vol% • CO: 30-35 vol%	The gas composition results appear to indicate a slightly different gas composition for the pellets relative to the milled pellets, an increase in the H_2/CO ratio and a decrease in methane. This is hard to conclusively say since the milled and pelletized material was not run at exactly the same conditions. The authors also noted a substantial increase in the PAH and phenolic concentration for milled pellets vs. the original pellets	(Siedlecki and Jong, 2011)
V. Wilk; H. Hofbauer 2013	• Dual fluidized bed • Steam gasification. • Gasification bed is 0.302 m ID x 2.3 m high • 400-660 µm olivine at 0.62 m/s • Sawdust, pellets made from the sawdust and varying woody waste material used • Fuel input ~100 kW. • Gasification temperature 850°C.	• H2: 34-40 vol% • CH4: 10-12 vol% • CO: 27-34 vol% • Grav. tar 6-13 g/Nm^3 • GC/MS tar 10-29 g/Nm^3	Pellets (compared to pellet-sawdust mixture): Favoured H_2 with lower CO and CH_4 content. Lower tar content gas (about ½). Increased gas yield.	(Wilk and Hofbauer, 2013)

Based on the two research findings summarized in Table 2.5, it appears that the use of pellets may lead to a favorable increase in the hydrogen content of the producer gas at the expense of carbon monoxide and methane. Tar content in the gas may also be reduced through pelletization. It should be noted that both of the studies compare the pellets to material that has a smaller particle size. Thus, the effect of pelletization and the effect of particle size are confounded in both of these cases.

2.3.4 Torrefaction

Torrefaction is a mild thermal treatment of biomass to produce a solid fuel which compared to the original fuel is hydrophobic, has an increased specific calorific value (i.e. MJ/kg), has increased friability and is essentially moisture-free (Girard and Shah, 1991). The altered properties of the biomass by torrefaction have several advantages related to transport, storage, and handling. They are:

- The hydrophobicity protects against biodegradation and limits moisture uptake during storage to between 1-6 wt% (Bergman, 2005).
- The increased friability reduces the cost of grinding or milling. The energy requirement for milling or grinding torrefied biomass in reported to be between 3 and 7 times lower than raw biomass (Deng et al., 2009).

The torrefaction process is endothermic reaction carried out at between 230 and 300 °C where various volatile components are released such as water vapour, acetic acid, carbon dioxide (Prins et al., 2006). Depending on the severity of the torrefaction (temperature and residence time), varying amounts of calorific value is retained in the torrefied biomass. In comparison to the original biomass, torrefied biomass has a decreased fraction of volatile carbon, and lower oxygen to carbon ratio (O/C ratio). The off gases and vapours from the torrefaction process are often used to supply some or all of the energy required for the torrefaction and drying of the parent material. Figure 2.7, which is adapted from Bergman et al. (2005), shows a typical mass and energy balance reported for torrefaction processes, where M is a unit of mass and E is a unit of energy.

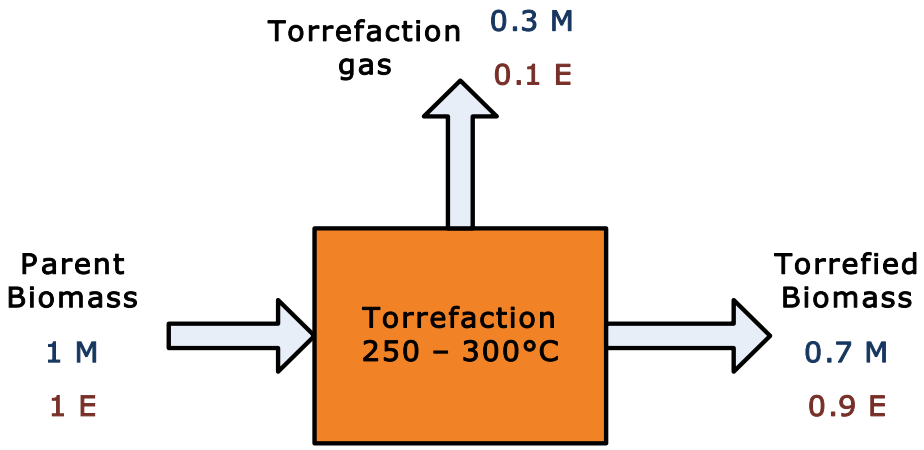

Figure 2.7: Typical mass and energy balance for torrefaction (Reproduced from Bergman, 2005)

The mass loss as gas during the torrefaction causes the biomass to become more porous resulting in a decreased bulk density (Bergman and Kiel, 2005).

Much of the interest surrounding the use of torrefied biomass as a feed for gasifiers is directed at the entrained flow gasifiers. This is because entrained flow gasifiers require very finely ground biomass on the order of hundreds of micrometers (Couhert et al., 2009). The fibrous structure of raw biomass makes this size reduction very difficult and energy intensive. Torrefied biomass has greatly reduced energy demands for size reduction.

Considerable attention has also been given to combining pelletization and torrefaction processes. Since the energy requirement for size reduction and densification is decreased for torrefied biomass relative to the parent material, some studies suggest that it may be cheaper and more energy efficient to produce torrefied pellets as compared to traditional pellets (Bergman, 2005). Torrefied pellets also have greatly increased energy density as compared to traditional pellets. Torrefied pellets have an energy density in the range of 15 to 18.5 GJ/m^3 compared to 8 – 11 GJ/m^3 for traditional pellets (Bergman and Kiel, 2005). This large increase in energy density means that torrefied pellets could serve as platform which would make biomass suitable for large-scale import / export due to the reduction in transport costs.

The torrefaction process destroys a large portion of the hemicellulose and depending on the severity of the conditions some of the cellulose (Lee et al., 2012). The loss of hemicellulose and potentially cellulose results in producing a product that is richer in lignin compared to the parent material. The loss in mass from parent material to torrefied material also has the impact of slightly concentrating the ash. The chars produced at high heating rates (>100°C/s) from torrefied willow showed depressed reactivity compared to the char produced under the same conditions from the parent material (Fisher et al., 2012). Under a steam environment the char reactivity reduced by a factor of three. Similar reductions in char reactivity were observed in an oxygen-containing environment. It can be speculated that the reduction in char reactivity is caused by the partial thermal stabilization of the material during torrefaction, annealing of the surfaces, or a reduction in stresses and material loss due to the lower volatile content leading to reduced pore volume and surface area for reaction. Under the high heating rate conditions of fluidized bed gasification, it can be imagined that the depressed char reactivity from torrefied materials will lead to an increase of char retained in the bed. This may help to reform tar and primary vapours as well as increasing the amount of char available for water-gas reactions.

Very limited information is available in open literature regarding fluidized bed gasification studies on torrefied biomass. Some studies have been performed with torrefied biomass using entrained flow gasifiers. In an entrained flow gasifier, using steam (diluted in nitrogen) as a gasifying agent, feeding in beechwood and torrefied beechwood at 30 g/h, it was determined that (Couhert et al., 2009) torrefied wood yielded more hydrogen and carbon monoxide as compared to the parent wood and that the torrefied wood produced less reactive char, resulting is larger amounts of collected residual char.

A few studies have also looked at the gasification of torrefied biomass from a theoretical perspective. In an analysis of the exergy efficiency of gasification via torrefaction versus untorrefied wood (Prins et al., 2006) it was determined that due to the lower O/C ratio of torrefied wood it is possible to achieve more efficient gasification with torrefied wood if the gasification and torrefaction processes are integrated. However for the scenarios considered, it was shown that without integration of the torrefaction process with the

gasification process, circulating fluidized bed gasification of torrefied biomass is expected to result in lower efficiencies than untorrefied wood.

Torrefaction has been shown to produce different results in a fluidized bed fast pyrolysis. The torrefied wood produced lower oil yields, more char, and similar amounts of gas compared to the parent material (Meng et al., 2012). The composition of the oil was also substantially affected, there was a much lower O/C ratio in the product oil from torrefied materials and consisted of a greater proportion of phenolic compounds. Although gasification is not the same as fast pyrolysis due to different temperature regime and presence of a gasification medium such as air or steam, the indication from pyrolysis is that torrefied materials could produce a higher amount of char with primary tars containing more phenolic character. It is speculated that these phenolic tars may be more difficult to reform than the saccharides, aldehydes, and other heavily oxygenated primary tars.

Due to the altered chemical nature of the torrefied material, the change in char reactivity, the change in pore structure, and the reduction of volatiles in torrefied materials versus its parent material it is expected that torrefied biomass will lead to substantially different producer gas from fluidized bed gasifiers.

2.4 **Research Needs**

This chapter has shown that plenty of fundamental work has been performed on understanding as how the different components of biomass (cellulose, hemicellulose, and lignin) devolatilize. There has also been plenty of effort directed at understanding how particle heating rates influence pyrolysis products and the properties of the resultant char. However, the gasification of biomass in a fluidized bed is a complex interaction of many phenomena under conditions that can sometimes be hard to replicate (such as studying the interaction of immature devolatilization products and char at gasification temperatures) and there are some aspects of the fluidized bed hydrodynamics that are hard to predict (such as the segregation of devolatilizing particles of a polydisperse feed material in a fluidized bed composed of both char, the original bed material and the generated bottom ash). In order to truly appreciate the effect of the pre-treatments on the performance of

fluidized bed gasification of biomass, experimental work in continuously-fed, fluidized bed gasifiers is required.

The effect of comminution and drying had been tested in experimental systems more often than the impact of pelletization and torrefaction. There remains a large gap in the knowledge of the effect of comminution: Small particle sizes (<2 mm) have been the predominant size range tested in experimental, continuously-fed, fluidized bed gasifiers. This is often a result of the small scale of the systems used to report data in literature and the fact that finely ground biomass is easier to handle and feed into an experimental system than large particles. For large scale applications where low cost feed materials are essential to the profitability of a gasifier, such as a gasifier using residual materials at a pulp mill in order to displace existing fossil fuels, it would be desirable to use as little comminution as possible. This requires an understanding of how large particles (much greater than 2 mm) behave in gasification systems in order to assess the cost and benefit of comminution. At larger particle sizes, where the devolatilization rate is limited by internal heat transfer, many different phenomena come into play such as the potential for extensive conversion of pyrolysis products occurring within the particle. Even in the data that does exist on the effect of comminution in open literature, the results are occasionally contradictory – ranging from the suggestion that smaller particles lead to superior gasification performance, to the suggestion that particle size has no effect, to the suggestion that there is an optimal particle size in the 10x10 mm range. Research on the effect of particle must be comprehensive in its evaluation of the gasifier performance, both the amount and composition of producer gas needs to be evaluated in addition to the presence of contaminants and the conversion limitations.

Given the importance of pelletization as a pre-treatment process for biomass materials and the number of articles already in literature that have used pelletized biomass as a feedstock for gasification, an unexpectedly small amount of research has ever directly compared the performance of the same material in a pellet and non-pellet form. Even to interpret results from existing studies on gasification of biomass pellets, a basic understanding is required of how the pelletization pre-treatment can impact the results from a fluidized bed gasifier. It is well appreciated that pelletization can help in reducing the transport costs and increase the

ease of handling. A similar appreciation of whether it is possible that pelletization could be used as a tool to optimize the performance of a fluidized bed gasifier has not been achieved. The few results that could be found in the open literature seem to suggest that it is possible, as they show that pellets compared to sawdust favours hydrogen production and decreases tar production.

Torrefaction has received great interest in recent years as a biomass pre-treatment for many good reasons. Largely, the interest has been concentrated in an interest for a biomass product that is easier to transport, store, comminute, and feed into existing coal or new bioenergy processes. It is necessary to understand what will be the impact of torrefaction on the performance of fluidized bed gasifiers if torrefaction is to be widely adopted as a pre-treatment method. For example, because of the reduced oxygen content of the torrefied materials, it may be possible from a theoretical perspective to achieve more efficient gasification through torrefaction. This does not consider some of the limitations that are expected to exist such as the fact that the same level of conversion may not be achieved at the same temperature for torrefied materials compared to the parent materials due to the depressed char reactivity as discussed in section 2.3.4. Torrefaction as a fuel beneficiation strategy for biomass is still a nascent process - there exists debate on what the definition of a torrefied material is and there may be a lot of variation between materials both called "torrefied" based on the severity of the process. In order for the results to be as widely applicable as possible, an understanding of how a broad range of thermal pre-treatments affect gasification is required.

These research gaps are what this thesis hopes to attempt to experimentally address. Ideally, the work should produce datasets and knowledge suitable to:

- Select optimal pre-treatment strategies for gasification based on application of the producer gas.
- Gain some insight to what appropriate feedstock criteria to specify for formulating supply contracts for operating fluidized bed gasifiers.
- Develop design and feedstock strategies in order to deal with performance shortfalls in fluidized bed gasifiers.

This chapter produced a paper published in *Environmental Progress & Sustainable Energy* section of *AIChE* in 2012 *("Bronson B, Preto F, Mehrani P. Effect of pretreatment on the physical properties of biomass and its relation to fluidized bed gasification. Environmental Progress & Sustainable Energy 2012; 31: 335-339"*). The paper summarized the key results found from reviewing the literature with regards to various pre-treatment methods (drying, comminution, and pelletization) affecting the physical properties of biomass and its gasification.

References

Abu El-Rub, Z., E.A. Bramer and G. Brem, "Experimental comparison of biomass chars with other catalysts for tar reduction," Fuel. **87**, 2243-2252 (2008).

Alauddin, Z.A.B.Z., P. Lahijani, M. Mohammadi and A.R. Mohamed, "Gasification of lignocellulosic biomass in fluidized beds for renewable energy development: A review," Renewable and Sustainable Energy Reviews. **14**, 2852 (2010).

Alén, R., E. Kuoppala and P. Oesch, "Formation of the main degradation compound groups from wood and its components during pyrolysis," J. Anal. Appl. Pyrolysis. **36**, 137-148 (1996).

Ammendola, P., R. Chirone, F. Miccio, G. Ruoppolo and F. Scala, "Devolatilization and Attrition Behavior of Fuel Pellets during Fluidized-Bed Gasification," Energy Fuels. **25**, 1260-1266 (2011).

Asadullah, M., S. Zhang, Z. Min, P. Yimsiri and C. Li, "Effects of biomass char structure on its gasification reactivity," Bioresour. Technol. **101**, 7935-7943 (2010).

Bacon, D.W., J. Downie, J.C. Hso and J. Peters, "Modelling of Fluidized Bed Wood Gasifiers," in "Fundamentals of Thermochemical Biomass Conversion," R. P. Overend, T. A. Milne and L. Mudge, Eds. (1985), pp. 717-732.

Basu, P., "Biomass Gasification Design Handbook," Academic Press, Boston (2010).

Bauen, A., G. Berndes, M. Junginger, M. Londo and F. Vuille, "Bioenergy - A sustainable and reliable energy source, a review of status and prospects," (2009).

Bergman, P.C.A., "Combined torrefaction and pelletisation," **ECN-C--05-073** (2005).

Bergman, P.C.A. and J.H.A. Kiel, "Torrefaction for biomass upgrading," **ECN-RX--05-180** (2005).

Berndes, G., M. Hoogwijk and R. van den Broek, "The contribution of biomass in the future global energy supply: a review of 17 studies," Biomass Bioenergy. **25**, 1-28 (2003).

Bharadwaj, A., L.L. Baxter and A.L. Robinson, "Effects of Intraparticle Heat and Mass Transfer on Biomass Devolatilization: Experimental Results and Model Predictions," Energy Fuels. **18**, 1021-1031 (2004).

Bridgwater, A.V., "The technical and economic feasibility of biomass gasification for power generation," Fuel. **74**, 631-653 (1995).

Bridgwater, A.V., A.J. Toft and J.G. Brammer, "A techno-economic comparison of power production by biomass fast pyrolysis with gasification and combustion," Renewable and Sustainable Energy Reviews. **6**, 181-246 (2002).

Campoy, M., A. Gómez-Barea, F.B. Vidal and P. Ollero, "Air-steam gasification of biomass in a fluidised bed: Process optimisation by enriched air," Fuel Process Technol. **90**, 677-685 (2009).

Caputo, A.C., M. Palumbo, P.M. Pelagagge and F. Scacchia, "Economics of biomass energy utilization in combustion and gasification plants: effects of logistic variables," Biomass Bioenergy. **28**, 35-51 (2005).

Carpenter, D.L., R.L. Bain, R.E. Davis, A. Dutta, C.J. Feik, K.R. Gaston, W. Jablonski, S.D. Phillips and M.R. Nimlos, "Pilot-Scale Gasification of Corn Stover, Switchgrass, Wheat Straw, and Wood: 1. Parametric Study and Comparison with Literature," Ind Eng Chem Res. **49**, 1859-1871 (2010).

Cetin, E., B. Moghtaderi, R. Gupta and T.F. Wall, "Influence of pyrolysis conditions on the structure and gasification reactivity of biomass chars," Fuel. **83**, 2139-2150 (2004).

Chan, W.R., M. Kelbon and B.B. Krieger, "Modelling and experimental verification of physical and chemical processes during pyrolysis of a large biomass particle," Fuel. **64**, 1505-1513 (1985).

Corella, J., J. Herguido and F.J. Alday, "Pyrolysis and steam gasification of biomass in fluidized beds: Influence of the type and location of the biomass feed point on the product distribution," in "Research in Thermochemical Biomass Conversion," A. V. Bridgewater and J. L. Kuester, Eds. Elsevier Applied Science, London, UK (1988), pp. 384-398.

Couhert, C., S. Salvador and J. Commandré, "Impact of torrefaction on syngas production from wood," Fuel. **88**, 2286-2290 (2009).

Cui, H. and J.R. Grace, "Fluidization of biomass particles: A review of experimental multiphase flow aspects," Chemical Engineering Science. **62**, 45-55 (2007).

Cummer, K.R. and R.C. Brown, "Ancillary equipment for biomass gasification," Biomass Bioenergy. **23**, 113-128 (2002).

Dai, J. and J.R. Grace, "Biomass granular screw feeding: An experimental investigation," Biomass Bioenergy. **35**, 942-955 (2011).

Demirbas, A., "Combustion characteristics of different biomass fuels," Progress in Energy and Combustion Science. **30**, 219-230 (2004a).

Demirbas, A., "Effect of initial moisture content on the yields of oily products from pyrolysis of biomass," J. Anal. Appl. Pyrolysis. **71**, 803-815 (2004b).

Deng, J., G. Wang, J. Kuang, Y. Zhang and Y. Luo, "Pretreatment of agricultural residues for co-gasification via torrefaction," J. Anal. Appl. Pyrolysis. **86**, 331-337 (2009).

Di Blasi, C., "Influences of physical properties on biomass devolatilization characteristics," Fuel. **76**, 957-964 (1997).

Di Blasi, C., "Kinetic and Heat Transfer Control in the Slow and Flash Pyrolysis of Solids," Ind Eng Chem Res. **35**, 37-46 (1996).

Di Felice, R., G. Coppola, S. Rapagnà and N. Jand, "Modeling of Biomass Devolatization in a Fluidized Bed Reactor," Can. J. Chem. Eng. **77**, 325-332 (1999).

El-Rub, Z.A., E.A. Bramer and G. Brem, "Review of Catalysts for Tar Elimination in Biomass Gasification Processes," Ind Eng Chem Res. **43**, 6911-6919 (2004).

Erlich, C., E. Bjirnbom, D. Bolado, M. Giner and T.H. Fransson, "Pyrolysis and gasification of pellets from sugar cane bagasse and wood," Fuel. **85**, 1535-1540 (2007).

Evans, R.J. and T.A. Milne, "An Atlas of Pyrolysis Mass Spectograms for Selected Pyrolysis Oils," (1987).

Fagernäs, L., J. Brammer, C. Wilén, M. Lauer and F. Verhoeff, "Drying of biomass for second generation synfuel production," Biomass Bioenergy. **34**, 1267-1277 (2010).

Fisher, E.M., C. Dupont, L.I. Darvell, J.-. Commandré, A. Saddawi, J.M. Jones, M. Grateau, T. Nocquet and S. Salvador, "Combustion and gasification characteristics of chars from raw and torrefied biomass," Bioresour. Technol. **119**, 157 (2012).

Fiorentino, M., A. Marzocchella, and P. Saltino, “Segregation of fuel particles and volatile matter during devolatilization in a fluidized bed – II. Experimental”, Chem Eng Sci. **52,** 1909-1922 (1997).

Fushimi, C., K. Araki, Y. Yamaguchi and A. Tsutsumi, "Effect of Heating Rate on Steam Gasification of Biomass. 1. Reactivity of Char," Ind Eng Chem Res. **42**, 3922-3928 (2003).

Gil, J., J. Corella, M.P. Aznar and M.A. Caballero, "Biomass gasification in atmospheric and bubbling fluidized bed: Effect of the type of gasifying agent on the product distribution," Biomass Bioenergy. **17**, 389-403 (1999).

Girard, P. and N. Shah, "Recent developments on torrefied wood, an alternative to charcoal for reducing deforestation," REUR Technical Series. **20**, 101-114 (1991).

Gómez, E.O., L. Augusto Barbosa Cortez, E.S. Lora, C.G. Sanchez and A. Bauen, "Preliminary tests with a sugarcane bagasse fueled fluidized-bed air gasifier," Energy Conversion and Management. **40**, 205-214 (1999).

Gómez-Barea, A. and B. Leckner, "Modeling of biomass gasification in fluidized bed," Prog. Energy Comb. Sci. **36**, 444-509 (2010).

Gustafsson, E., L. Lin and M. Strand, "Characterization of particulate matter in the hot product gas from atmospheric fluidized bed biomass gasifiers," Biomass Bioenergy. **35**, S71-S78 (2011).

Hanaoka, T., S. Inoue, S. Uno, T. Ogi and T. Minowa, "Effect of woody biomass components on air-steam gasification," Biomass Bioenergy. **28**, 69 (2005).

Herguido, J., J. Corella and J. Gonzalez-Saiz, "Steam gasification of lignocellulosic residues in a fluidized bed at a small pilot scale. Effect of the type of feedstock," Ind Eng Chem Res. **31**, 1274-1282 (1992).

Higman, C. and M. van der Burgt, "Gasification," Gulf Professional Publishing, Burlington (2008).

Hosoya, T., H. Kawamoto and S. Saka, "Pyrolysis behaviors of wood and its constituent polymers at gasification temperature," J. Anal. Appl. Pyrolysis. **78**, 328 (2007).

Igathinathane, C., A.R. Womac, S. Sokhansanj and S. Narayan, "Size reduction of high- and low-moisture corn stalks by linear knife grid system," Biomass Bioenergy. **33**, 547-557 (2009).

Igathinathane, C., A.R. Womac, S. Sokhansanj and S. Narayan, "Knife grid size reduction to pre-process packed beds of high- and low-moisture switchgrass," Bioresour. Technol. **99**, 2254-2264 (2008).

International Energy Agency, "World Energy Outlook," (2008).

Jand, N. and P.U. Foscolo, "Decomposition of Wood Particles in Fluidized Beds," Ind Eng Chem Res. **44**, 5079-5089 (2005).

Kaewluan, S. and S. Pipatmanomai, "Gasification of high moisture rubber woodchip with rubber waste in a bubbling fluidized bed," Fuel Process Technol. **92**, 671 (2011).

Koufopanos, C.A., N. Papayannakos, G. Maschio and A. Lucchesi, "Modelling of the pyrolysis of biomass particles. Studies on kinetics, thermal and heat transfer effects," The Canadian Journal of Chemical Engineering. **69**, 907-915 (1991).

Kurkela, E. and P. Ståhlberg, "Air gasification of peat, wood and brown coal in a pressurized fluidized-bed reactor. I. Carbon conversion, gas yields and tar formation," Fuel Process Technol. **31**, 1 (1992).

Lee, J., Y. Kim, S. Lee and H. Lee, "Optimizing the torrefaction of mixed softwood by response surface methodology for biomass upgrading to high energy density," Bioresour. Technol. **116**, 471 (2012).

Li, X.T., J.R. Grace, C.J. Lim, A.P. Watkinson, H.P. Chen and J.R. Kim, "Biomass gasification in a circulating fluidized bed," Biomass Bioenergy. **26**, 171-193 (2004).

Lv, P.M., Z.H. Xiong, J. Chang, C.Z. Wu, Y. Chen and J.X. Zhu, "An experimental study on biomass air–steam gasification in a fluidized bed," Bioresour. Technol. **95**, 95-101 (2004).

Maniatis, K., "Progress in Biomass Gasification: An Overview," in "Progress in Thermochemical Biomass Conversion," A. V. Bridgewater, Ed. Oxford: Blackwell Science (2001).

McKendry, P., "Energy production from biomass (part 1): overview of biomass," Bioresour. Technol. **83**, 37-46 (2002).

Meng, J., J. Park, D. Tilotta and S. Park, "The effect of torrefaction on the chemistry of fast-pyrolysis bio-oil," Bioresour. Technol. **111**, 439 (2012).

Meng, X., W. de Jong, N. Fu and A.H.M. Verkooijen, "Biomass gasification in a 100 kWth steam-oxygen blown circulating fluidized bed gasifier: Effects of operational conditions on product gas distribution and tar formation," Biomass Bioenergy. **35,** 2910-2924 (2011).

Miao, Z., T.E. Grift, A.C. Hansen and K.C. Ting, "Energy requirement for comminution of biomass in relation to particle physical properties," Industrial Crops and Products. **33**, 504-513 (2011).

Michel, R., S. Rapagnà, M. Di Marcello, P. Burg, M. Matt, C. Courson and R. Gruber, "Catalytic steam gasification of Miscanthus X giganteus in fluidised bed reactor on olivine based catalysts," Fuel Process Technol. **92**, 1169-1177 (2011).

Milne, T.A., R.J. Evans and N. Abatzoglou, "Biomass Gasifier "Tars": Their Nature, Formation, and Conversion," **NREL/TP-570-25357** (1998).

Mozaffarian, M., R.W.R. Zwart, H. Boerrigter and E.P. Deurwaader, "Biomass and Waste-Related SNG Production Technologies," (2004).

Pan, Y.G., X. Roca, E. Velo and L. Puigjaner, "Removal of tar by secondary air in fluidised bed gasification of residual biomass and coal," Fuel. **78**, 1703 (1999).

Pfeifer, C., B. Puchner and H. Hofbauer, "Comparison of dual fluidized bed steam gasification of biomass with and without selective transport of CO2," Chemical Engineering Science. **64**, 5073-5083 (2009).

Prins, M.J., K.J. Ptasinski and F.J.J.G. Janssen, "More efficient biomass gasification via torrefaction," Energy. **31**, 3458-3470 (2006).

Qin, Y., J. Feng and W. Li, "Formation of tar and its characterization during air–steam gasification of sawdust in a fluidized bed reactor," Fuel. **89**, 1344-1347 (2010).

Ragland, K.W., D.J. Aerts and A.J. Baker, "Properties of wood for combustion analysis," Bioresour. Technol. **37**, 161-168 (1991).

Raman, K.P., P.W. Walter and L.T. Fan, "Gasification of Feedlot Manure in a Fluidized Bed Reactor," Ind. Eng. Chem. Process Des. Dev. **19**, 623-629 (1980).

Rapagnà, S. and A. Latif, "Steam Gasification of Almond Shells in a Fluidised Bed Reactor: The Influence of Temperature and Particle Size on Product Yield and Distribution," Biomass Bioenergy. **12**, 281-288 (1997).

Rauch, R., "Technology Brief: Biomass Gasification to Produce Synthesis Gas for Fuel Cells, Liquid Fuels, and Chemicals," (2002).

Raveendran, K., A. Ganesh and K.C. Khilar, "Pyrolysis characteristics of biomass and biomass components," Fuel. **75**, 987-998 (1996).

Richard, T.L., "Challenges in Scaling Up Biofuels Infrastructure," Sci. **329**, 793-796 (2010).

Schoeters, J., K. Maniatis and A. Buekens, "The fluidized-bed gasification of biomass: Experimental studies on a bench scale reactor," Biomass. **19**, 129-143 (1989).

Schuster, G., G. Löffler, K. Weigl and H. Hofbauer, "Biomass steam gasification – an extensive parametric modeling study," Bioresour. Technol. **77**, 71-79 (2001).

Scott, D.S., J. Piskorz, M.A. Bergougnou, R. Graham and R.P. Overend, "The role of temperature in the fast pyrolysis of cellulose and wood," Ind Eng Chem Res. **27**, 8-15 (1988).

Shafizadeh, F., "Introduction to pyrolysis of biomass," J. Anal. Appl. Pyrolysis. **3**, 283-305 (1982).

Shen, L., J. Xiao, F. Niklasson and F. Johnsson, "Biomass mixing in a fluidized bed biomass gasifier for hydrogen production," Chemical Engineering Science. **62**, 636-643 (2007).

Siedlecki, M. and W.d. Jong, "Biomass gasification as the first hot step in clean syngas production process gas quality optimization and primary tar reduction measures in a 100 kW thermal input steam-oxygen blown CFB gasifier," Biomass Bioenergy. **35, Supplement 1**, S40 (2011).

Simmons, G.M. and M. Gentry, "Particle size limitations due to heat transfer in determining pyrolysis kinetics of biomass," Journal of Analytical and Applied Pyrolysis. **10**, 117-127 (1986).

Smeets, E.M.W., A.P.C. Faaij, I.M. Lewandowski and W.C. Turkenburg, "A bottom-up assessment and review of global bio-energy potentials to 2050," Progress in Energy and Combustion Science. **33**, 56-106 (2007).

Stevens, D.J., "Hot Gas Conditioning: Recent Progess With Larger-Scale Biomass Gasification Systems," **NREL/SR-510-29952** (2001).

Sudhakar, D.R., K.S. Reddy, A.K. Kolar and B. Leckner, "Fragmentation of wood char in a laboratory scale fluidized bed combustor," Fuel Process Technol. **89**, 1121-1134 (2008).

Sun, Q., S. Yu, F. Wang and J. Wang, "Decomposition and gasification of pyrolysis volatiles from pine wood through a bed of hot char," Fuel. **90**, 1041-1048 (2011).

Tremel, A., D. Becherer, S. Fendt, M. Gaderer and H. Spliethoff, "Performance of entrained flow and fluidised bed biomass gasifiers on different scales," Energy Conversion and Management. **69**, 95 (2013).

US Department of Energy - Energy Efficiency and Renewable Energy, "Biopower Technical Strategy Workshop - Summary Report," (2010).

van der Drift, A. and H. Boerrigter, "Synthesis Gas from Biomass for Fuels and Chemicals," **ECN-C--06-001** (2006).

van der Drift, A. and J. van Doorn, "Effect of fuel size an process temperature on fuel gas quality from CFB gasification of biomass," **ECN-RX--00-026** (2000).

van der Drift, A., J. van Doorn and J.W. Vermeulen, "Ten residual biomass fuels for circulating fluidized-bed gasification," Biomass Bioenergy. **20**, 45-56 (2001).

van der Meijden, C.M., H.J. Veringa and L.P.L.M. Rabou, "The production of synthetic natural gas (SNG): A comparison of three wood gasification systems for energy balance and overall efficiency," Biomass Bioenergy. **34**, 302-311 (2010).

van Paasen, S.V.B. and J.H.A. Kiel, "Tar formation in a fluidised-bed gasifier," **ECN-C--04-013** (2004).

Vriesman, P., E. Heginuz and K. Sjöström, "Biomass gasification in a laboratory-scale AFBG: influence of the location of the feeding point on the fuel-N conversion," Fuel. **79**, 1371-1378 (2000).

Weerachanchai, P., M. Horio and C. Tangsathitkulchai, "Effects of gasifying conditions and bed materials on fluidized bed steam gasification of wood biomass," Bioresour. Technol. **100**, 1419-1427 (2009).

Wilk, V. and H. Hofbauer, "Influence of fuel particle size on gasification in a dual fluidized bed steam gasifier," Fuel Process Technol. **115**, 139 (2013).

Wu, M.R., D.L. Schott and G. Lodewijks, "Physical properties of solid biomass," Biomass Bioenergy. **35**, 2093-2105 (2011).

Yang, H., R. Yan, H. Chen, D.H. Lee and C. Zheng, "Characteristics of hemicellulose, cellulose and lignin pyrolysis," Fuel. **86**, 1781 (2007).

Zhang, L., C.(. Xu and P. Champagne, "Overview of recent advances in thermo-chemical conversion of biomass," Energy Conversion and Management. **51**, 969-982 (2010).

Zhang, W., "Automotive fuels from biomass via gasification," Fuel Process Technol. **91**, 866-876 (2010).

Zhang, Y., B. Jin and W. Zhong, "Experimental investigation on mixing and segregation behavior of biomass particle in fluidized bed," Chemical Engineering and Processing: Process Intensification. **48**, 745-754 (2009).

Chapter 3. Effect of Biomass Particle Size, Moisture Level and Pelletization

The focus of this thesis was to understand how biomass feedstock pre-treatment affects the performance of a fluidized bed gasifier; this chapter describes the equipment, methods and results from the experimental campaign carried out to determine the effect of conventional pre-treatments: comminution, drying, and pelletization on the performance of a small pilot scale, air blown, bubbling fluidized bed gasifier.

3.1 Materials

3.1.1 Feedstock

The feedstock used was a hog fuel[3] originating from a pulp mill located in the interior of British Columbia, Canada. The fuel, as delivered, had been comminuted to approximately 50 mm or smaller and was dried to between 10 and 25 wt% moisture. A sample of the fuel was characterized upon delivery. The composition of the fuel as received is given in Table 3.1 and an analysis of the mineral composition of its ash is presented in Table 3.2.

Table 3.1: Feedstock analysis of the as received interior BC hog fuel

Parameter	Method	Value
Moisture TGA (wb wt%)	ASTM D7582	**13.89**
Ash TGA (db wt%)	ASTM D7582	**3.67**
Volatile (db wt%)	ISO 562	**76.91**
Fixed Carbon (db wt%)	ASTM D7582	**19.42**
Carbon (db wt%)	ASTM D5373	**51**
Hydrogen (db wt%)	ASTM D5373	**5.61**
Nitrogen (db wt%)	ASTM D5373	**0.24**
Total Sulfur (db wt%)	ASTM D4239	**<0.05**
Oxygen by Difference (db wt%)	in-house	**39.48**
Gross Calorific Value (cal/g)	ISO 1928	**4900**
Total Chlorine by Pyrohydrolysis (ug/g db)	in-house	**550**
Total Fluorine by Pyrohydrolysis (ug/g db)	in-house	**<10**
Total Bromine by Pyrohydrolysis (ug/g db)	in-house	**<10**

[3] A hog fuel is a residual product often available at pulp mill which is a mixture of bark and wood chips.

Table 3.2: X-Ray Fluorescence (XRF) analysis of the ash of the as received interior BC softwood hog fuel

Parameter	Method	Value
SiO2 (wt%)	ASTM D4326	**13.85**
Al2O3 (wt%)	ASTM D4326	**3.35**
Fe2O3 (wt%)	ASTM D4326	**2.27**
TiO2 (wt%)	ASTM D4326	**0.11**
P2O5 (wt%)	ASTM D4326	**9.78**
CaO (wt%)	ASTM D4326	**29.7**
MgO (wt%)	ASTM D4326	**11.11**
SO3 (wt%)	ASTM D4326	**3.81**
Na2O (wt%)	ASTM D4326	**1.31**
K2O (wt%)	ASTM D4326	**9.52**
Barium (ppm)	ASTM D4326	**1519**
Strontium (ppm)	ASTM D4326	**754**
Vanadium (ppm)	ASTM D4326	**<50**
Nickel (ppm)	ASTM D4326	**102**
Manganese (ppm)	ASTM D4326	**6993**
Chromium (ppm)	ASTM D4326	**175**
Copper (ppm)	ASTM D4326	**94**
Zinc (ppm)	ASTM D4326	**1299**
Loss on Fusion (wt%)	ASTM D4326	**14.11**
Sum (wt%)	ASTM D4326	**100**

In order to create different size fractions (as a surrogate for comminution), the hog fuel was sieved into three different size fractions. The size fractions were determined based on size analysis of the fuel and screen sizes that are standardly available. The finest size fraction created was the material that passed through a 3.175 mm (1/8") screen. The mid-sized fraction was the fuel that was retained between 3.175 mm and 6.35 mm (1/8" and 1/4") screens. The coarse fraction was the material that was retained between a 6.35 mm and 19.05 mm (1/4" and 3/4") screens. The material that was retained above the 3/4" screen was not used. Caution should be made when interpreting results since the average size of the fuel does not necessarily fall between the screen sizes that were used to generate it. For example, within the material that was retained between a 1/4" and 3/4" screens there were pieces that were measured to be in excess of 127 mm (5") in their longest dimension. This was due to the typical particle shape. Pieces were typically shaped like "needles" in the sense that they had a longest dimension that was much greater than its two smaller

dimensions. It also should be noted that the use of the screens does not guarantee that a particle smaller than 3.175 mm ends up in the fines fraction. The particles may have exited the sieve shaker before having a chance to pass through the appropriate screen due to interactions with other particles. Also, particles will often only have one orientation through which they will fall through the appropriate screen - there is the possibility that they get retained in a larger fraction since they did not have adequate residence time on the screen in order to hit the screen with the appropriate orientation. Pellets were also made from the hog fuel. In order to make the pellets, the finest fraction (the fraction of fuel passing through a 1/8" screen) was processed in a 50 kg/h California Pellet Mill using a 6.35 mm (1/4") die to produce pellets that were approximately 25.4 mm (1") x 6.35 mm (1/4"). A collage of the created fuel sizes / forms used in this research are shown in Figure 3.1. Throughout this thesis, the fuel fractions created are referred to as ***fines, mids, coarse***, and ***pellets***.

(A) **Fines**: Material passing through a 3.18 mm (1/8") sieve screen

(B) **Mids:** Material retained between 3.18 and 6.35 mm (1/8" and 1/4") sieve screens

(C) **Coarse:** Material retained between 6.35 and 19.05 mm (1/4" and 3/4") sieve screens

(D) **Pellets:** Produced using fines using a 6.35 mm (1/4") die

Figure 3.1: Images of various hog fuel particles sizes and shapes used. (A) fines, (B) mids, (C) coarse, and (D) Pellets.

It is possible that the sieving process introduced differences in the composition of the fuel fractions. Bark and soil contamination may have a tendency to form smaller particles which would mean that the fines and pellets may bias bark and ash compared to the mid and coarse fraction. In order to determine how similar the different fuel fractions were, some of the key fuel characterization analyses were repeated on the individual size fractions. The results of the analyses are presented in Table 3.3 and the results normalized to an ash free basis are shown in Table 3.4.

Table 3.3: Fuel analyses of each particle size / form

Parameter	Method	Fines	Mid	Coarse	Pellets
Ash (db wt%)	ASTM D7582	12.5	4.3	4.2	9.4
Volatile (db wt%)	ISO 562	69.9	75.8	76.0	72.0
Fixed Carbon (db wt%)	ASTM D7582	17.6	19.9	19.8	18.6
Carbon (db wt%)	ASTM D5373	46.5	49.5	49.8	47.2
Hydrogen (db wt%)	ASTM D5373	5.5	5.8	5.9	5.5
Nitrogen (db wt%)	ASTM D5373	0.3	0.2	0.2	0.4
Total Sulfur (db wt%)	ASTM D4239	0.2	0.1	0.1	0.2
Oxygen by Difference (db wt%)	in-house	35.0	40.1	39.8	37.3
Gross Calorific Value (MJ/kg)	ISO 1928	18.8	20.0	20.0	19.2

Table 3.4: Fuel analyses of each particle size / form normalized to an "ash-free" basis

Ash-free basis				
	Fines	Mid	Coarse	Pellets
Volatile (wt%)	79.9	79.2	79.3	79.5
Fixed Carbon (wt%)	20.1	20.8	20.7	20.5
Carbon (wt%)	53.2	51.7	52.0	52.1
Hydrogen (wt%)	6.2	6.1	6.2	6.1
Nitrogen (wt%)	0.4	0.2	0.2	0.4
Sulfur (wt%)	0.2	0.1	0.1	0.2
Oxygen (wt%)	40.0	41.9	41.5	41.2
Gross Calorific Value (MJ/kg)	21.5	20.9	20.9	21.2

The results from Table 3.3 and Table 3.4 suggest that the main component of the fuel that was biased between size fractions was the ash. The fines and the pellets (which were made from the fines) had a higher level of ash than the original fuel (Table 3.1) or the coarse and mid fraction. It is not obvious that any other part of the fuel composition was preferentially segregated during the sieving, since the composition of the fines, mid, coarse, and pelletized material have very similar composition on an ash-free basis. If the bark, for example, had been biased in sieve fraction, one would have expected to see a different C/H/O distribution in the fuel on an ash-free basis since bark would have a tendency to be higher in lignin than the core wood (A bias towards bark should push the C/H/O ratio towards carbon). Although, the fines appeared to show a slightly greater amount of carbon than the other

fuels on a dry, ash-free basis, this was more likely an indication of analytical uncertainty because this result was not replicated in the analysis of the pellets. Since the pellets were made from the fines, it would be expected that the pellets and the fines would be identical. However, it can be seen from Table 3.3 that the pellets had essentially the same level of carbon as the mid or coarse material. Another difference was that the measured sample of the pellets and of the fines contained 9.4 and 12.5wt% (dry basis) of ash, respectively.

In order to simulate the effect of different drying levels, moisture was added to the fines, mid, and coarse fuel fractions. Moisture could not be added to the pellets since wood pellets swell and crumble following the addition of water. In order to add moisture to the fuel fractions the following procedure was used:

- Approximately 100 kg of each size fraction was loaded into three or four 45 gal drums (200 L drums).
- The actual weight of the fuel in each drum was measured.
- Enough water was measured in order to bring the moisture content of the fuel up to 30 wt% on a wet basis.
- The 100 kg batch of fuel was loaded into a large feed bin.
- The water was added to the fuel in the feed bin.
- The fuel and the water was hand-mixed using a pitchfork and a shovel.
- The fuel was emptied out of the feed bin by an auger into the drums.
- The drums were emptied back into the feed bin and mixed a second time.
- The fuel was emptied out of the feed bin by an auger into the drums.
- The drums were sealed with a lid until testing.

The moisture content of the fuel was measured in a nitrogen-purged, vacuum oven. A sample of approximately 100 g was placed on a tin tray, the oven was purged with 1 sLpm (1.67×10^{-5} m^3/s) of nitrogen gas, a vacuum pump connected to the oven was then turned on, and the pressure in the oven was adjusted to between 91 - 98 kPa_{abs} (-1 to -3 inHg). The oven was set to a temperature between 100 and 105°C. The weight of the sample was taken before the sample was placed in the oven and immediately after it was removed from the oven. The samples were allowed to dry for at least 15 hours. Multiple measurements were

carried out of the moisture content of each fuel fraction tested. The results from the moisture measurements on the fuels tested are provided in Table 3.5.

Table 3.5: Moisture results of the fuels tested.

Fuel Type	number of samples	Average	*Min*	*Max*	*Std Dev.*
fines	6	11.4%	*9.8%*	*15.2%*	*1.97%*
mid	3	10.1%	*9.5%*	*11.1%*	
coarse	3	10.8%	*10.1%*	*11.3%*	
unsieved	1	12.6%			
Total (unaltered)	**13**	**11.2%**	***9.5%***	***15.2%***	***1.53%***
Pellets	5	7.2%	*6.0%*	*9.0%*	*1.16%*
wet-fines	7	24.9%	*17.1%*	*32.9%*	*4.80%*
wet-mid	6	23.9%	*18.8%*	*29.1%*	*3.91%*
wet-coarse	5	31.0%	*27.9%*	*34.2%*	*2.68%*

Table 3.5 shows that the measured moisture results from the "unaltered" samples had a standard deviation of 1.5% for 13 samples. On the other hand, the moisture content of the "wetted" fuels varied considerably between samples (up to a standard deviation of 4.8% with the finest fraction for 7 samples). Since the moisture content is a key part of the mass balance input this introduces uncertainty to the mass balances which are a vital component of the data analysis.

3.1.2 Bed Material

The bed media used in the system was olivine sand, with an approximate Sauter mean diameter of approximately 350 microns. Size distribution data is presented in the appendix (section A.1). The bulk density of the olivine sand was measured to be between 1500 – 1550 kg/m^3 and the particle density was advertised by the supplier to be between 2700 – 2900 kg/m^3.

Many authors have studied the impact of different bed materials on the products yielded from the fluidized bed gasification of biomass (Corella et al., 2008; Hurley et al., 2012; Miccio et al., 2009). Olivine sand was chosen since some studies have shown that this type of sand to be slightly catalytic towards the reformation of tars while still having acceptable

mechanical stability and is a relatively inexpensive bed material (Koppatz et al., 2011). There is evidence that the origin and structure of the olivine can have an impact on the efficacy of it as a catalyst (Corella et al., 2004). This may explain why some studies have found the tar reforming capability of olivine to be limited.

The olivine material used was not "fresh", rather the material was obtained from previous gasification testing of forestry residues in a larger steam-oxygen gasifier installed at CanmetENERGY (Ottawa, ON, Canada). The purpose of using a bed media that had been previously "aged" in a gasifier was so that the results were more reflective of the behavior of a gasifier operated on a continuous basis as opposed to the behavior of a gasifier during start-up when the bed media is still fresh. There is evidence that the compositional changes of olivine during prolonged exposure to biomass ash components can have an impact on its activity, typically resulting in an increase in tar reforming activity with time (Kirnbauer et al., 2012). The bed media was re-used for the duration of the experimental campaign and the mineral composition of the sand was measured before the testing campaign began and after the testing campaign was completed. The results of the compositional analysis are shown in Table 3.6.

Table 3.6: XRF analysis of olivine bed media used for testing campaign

Parameter	Method	Bed media - start	Bed media - finish
SiO2 (wt%)	ASTM D4326	43.77	47.02
Al2O3 (wt%)	ASTM D4326	3.83	4.20
Fe2O3 (wt%)	ASTM D4326	8.00	5.95
TiO2 (wt%)	ASTM D4326	0.05	0.08
P2O5 (wt%)	ASTM D4326	0.59	0.90
CaO (wt%)	ASTM D4326	4.50	5.63
MgO (wt%)	ASTM D4326	35.60	32.15
SO3 (wt%)	ASTM D4326	<0.10	<0.10
Na2O (wt%)	ASTM D4326	0.97	0.70
K2O (wt%)	ASTM D4326	1.49	2.26
Barium (ppm)	ASTM D4326	254	364
Strontium (ppm)	ASTM D4326	164	196
Vanadium (ppm)	ASTM D4326	114	53
Nickel (ppm)	ASTM D4326	2483	1887
Manganese (ppm)	ASTM D4326	1201	1778
Chromium (ppm)	ASTM D4326	7100	4088
Copper (ppm)	ASTM D4326	133	45
Zinc (ppm)	ASTM D4326	564	585
Loss on Fusion (wt%)	ASTM D4326	0.00	0.21
Sum (wt%)	ASTM D4326	100	100

The compositional analysis shows that the silicon, aluminum, calcium, and potassium content of the bed media rose over the testing campaign while the iron and magnesium content declined. This is in agreement with the other results from the pilot-scale steam-oxygen gasification trials where the bed material showed the same trends as it aged (bed media composition change with progression in experimental run number shown in the appendices, section A.2).

3.1.3 Fluidizing Medium (Gas)

Air was used for the fluidizing the gasifier, supplied from building-wide compressed air system (provided by compressors operating on ambient air at outlet pressures of 100 – 120 psig). Air was assumed for the purposes of mass balances to be dry. The contribution of water from the air is small. The following approximation shows that the mole fraction of water vapour in the air should have been less than 1% even if the compressed air was

saturated at 25°C (the system is equipped with an air dryer, so this approximation is an overestimation):

$$y_{sat,H_2O} = \frac{P_{sat,H_2O,298K}}{P_T} = \frac{3200\text{Pa}}{100\text{psig}\left(\frac{6895\text{Pa}}{1\text{psi}}\right) + 101325\text{Pa}} = 0.0040 \qquad \text{Eq. 3.1}$$

3.2 **Experimental Apparatus**

Gasification of the interior hog fuel was completed in a small pilot-scale, 0.1524 m inner diameter (ID), bubbling fluidized bed reactor located at CanmetENERGY, Natural Resources Canada (Ottawa, ON, Canada). The height of the system from the distributor to the top of the freeboard was 4.5 m. A simplified diagram of the system is provided in Figure 3.2. Instrumentation locations in the bed region of the apparatus are given in Figure 3.3. A photograph of the upper and lower floor of the facility is provided in Figure 3.4.

The feeding system consisted of a feed hopper which was normally kept filled with between 10 – 30 dm^3 of feed material. The feed hopper was shook by an electric vibrator which facilitated the flow of solid feed material through an adjustable opening from the hopper onto the feed belt. The feed belt was driven by an adjustable electric motor and was placed on a weight scale. The power provided to the motor and the weight of the feed belt were recorded and converted into a feed rate through the control software. The feed material fell off of the end of the feed belt where it passed through a rotary airlock before falling onto the top of the fluidized bed. Fluidization air was provided by eight nozzles located at the bottom of the bed. A standpipe was located in the center of the distributor (the eight nozzles that distributed the fluidization air). The standpipe had a ball valve at the bottom which allowed for the bed material to be drained. The gases that were produced in the fluidized bed traveled up through a tall freeboard and subsequently entered a cyclone in order to remove entrained solids (mostly char). The char fell by gravity down through a long pipe (3" NPS, outer diameter = 0.0779 m) and was removed from the char removal port which consisted of a section of pipe and a ball valve. In order to remove the char, the ball valve was shut and

the section of pipe containing the char was emptied. The gases at the top of the cyclone continued onwards towards the gas cooler. However, between the top of the cyclone and the sampling location, electric band heaters were used to ensure that the gas temperature stays above 400°C in order to ensure that tars do not deposit on surfaces (which would lead to plugging as well as erroneous tar measurements). The gas after the gas cooler went to an afterburner which consisted of a propane burner and 2 ports for air injection that was used to combust the producer gas. The gases passed through another heat exchanger and pulled through a blower (draft fan). The draft fan was operated on a variable frequency drive and was adjusted in order to keep the pressure in the feed arm (PT-05 in Figure 3.3) at atmospheric pressure. This minimized the amount of air that could leak into the process through the rotary airlock or the amount of producer gas that could leak back through the feed arm. Up to the gas cooler, the system was insulated externally by ceramic fiber insulation and then clad with tin in order to reduce heat loss.

As might be recognized by examination of Figure 3.2, the system was designed so that it could also be run as a circulating fluidized bed by increasing the fluidizing gas velocity or by using finer bed material. Due to this design feature, this system did not have an expanded diameter freeboard section like many bubbling fluidized beds. The connection between the "L"-valve and the bed was blinded off with a plate of stainless steel so that the circulation of material was not possible.

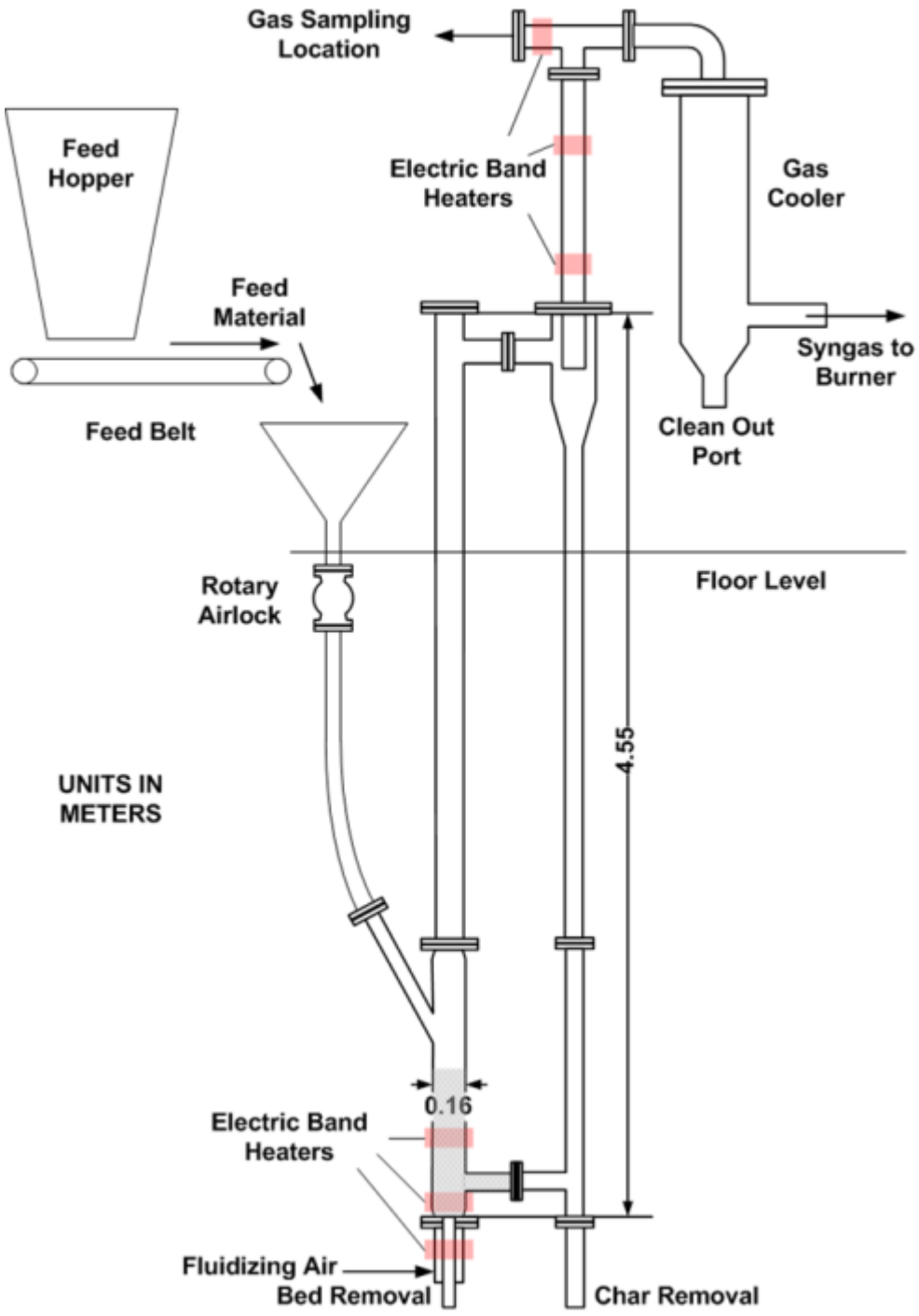

Figure 3.2: Simplified diagram of the small pilot-scale fluidized bed gasifier.

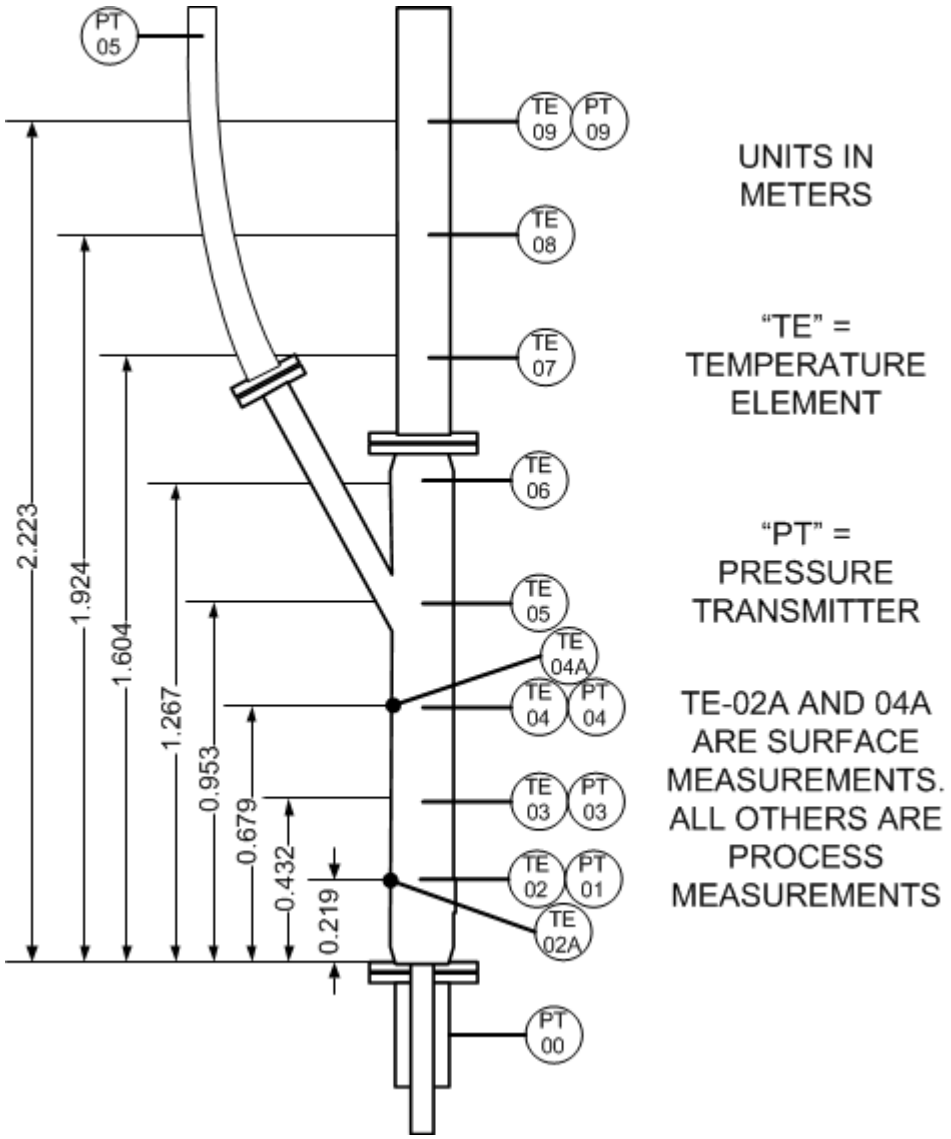

Figure 3.3: Instrumentation locations in the bed region of the small pilot-scale bubbling fluidized bed gasifier

Figure 3.4: Photograph of the upper (left picture) and lower floor (right picture) of the bubbling fluidized bed gasification laboratory.

In this work, an over-bed feed position was used to complete the fluidized bed gasification of biomass. Some sources claim that an in-bed feed position is superior to over-bed feed in fluidized bed biomass gasification. These claims often refer to an article by Corella et al., (1988). The article compares performance of sawdust (small particle sizes) between two different fluidized bed systems, one with an in-bed feed location and one with an over-bed feed location. Although the authors recognized the limitations of the study, the conclusions of the study have often been applied out of context and interpreted that in-bed feeding of biomass is always superior to over-bed feeding. For example, another study on the influence of feeding point on the fluidized bed gasification biomass did not see clear difference with respect to the carbon conversion to tar or char using crushed Miscanthus pellets, although they did find differences in the nitrogenous products of the gas (Vriesman et al., 2000). With small particles, in-bed feeding may be necessary: very small particles will never be well mixed with bed media due to entrainment and particle segregation. For large particles (in this context, large particles mean particles with aerodynamic diameters large enough that they are not entrained in the upward flow of the gas), such as the large majority of hog fuel, wood chips and wood pellets, the differences between over-bed and in-bed feeding are less obvious. For large particles the heating rate of the particle, and thus the time required for devolatilization, is regulated by internal heat transfer. For these particles, a devolatilizing particle will rise through the bed in a much shorter time than the time for devolatilization. Larger particles can also mix with the more dense bed media at appropriate fluidizing conditions. The big advantage of an over-bed feed system is that it is much simpler to construct and operate and thus, less expensive. For an atmospheric pressure fluidized bed gasifier, the pressure differential that an air locking mechanism needs to overcome for over-bed feeding is very small, especially if the gasifier includes a draft fan in order to balance the pressure of the gasifier at the feed point to equal atmospheric pressure. An in-bed feed system on the other hand must always work against the hydrostatic pressure of the bed (depends on bed height but is often greater than 1 psig) which leads to the potential backflow of tars which condense on feed system components and the potential backflow of flammable, carbon monoxide-laden gas through the feed system. Feeding in-bed also relies on some mechanism of injecting the material into the bed such as a quickly rotating auger.

An in-bed auger screw can be expected to experience high wear rates from the high temperature bed material acting on the tip of the screw.

3.3 **Experimental Procedure**

3.3.1 Operational Procedures

In order to warm up the system, electric band heaters were used to heat up the bed to approximately 600°C. The band heaters were normally started at low output the day before the run in order to achieve a bed temperature of approximately 400°C on the morning of an experimental run. Once a bed temperature >450°C was achieved, the system was operated as a combustor by introducing biomass to the bed (at a much reduced rate compared to gasification, normally 2-5 kg/h) in order to heat up the system to approximately 800°C. At around 600°C, the electric band heaters at bed level were switched off. The band heaters were switched off at this temperature based on their temperature limits: they use NiCr wires which melt around 1400°C. At a surface temperature on the heater of about 750°C, the wire temperature can reach the melting temperature if they are powered. Once a suitable bed temperature was reached, the feed rate of biomass was rapidly increased and the air flow was decreased in order to "switch over" from combustion into gasification. The bed level electric band heaters were turned off during gasification for all experiments outlined in this thesis, thus the gasifier was operated with no external heat source in the bed region. In other words, the exothermic reactions of the partial combustion of the materials (such as reaction between oxygen and char to produce to carbon monoxide or carbon dioxide) were balanced by the heat required to raise the temperature of the air and biomass to gasification temperature as well as the endothermic gasification reactions (such as the reaction of char with steam to produce hydrogen gas and carbon monoxide). The system was allowed to stabilize at the gasification conditions. The temperatures and the gas composition were monitored by the operators and once they were not obviously increasing or decreasing, it would be declared that the system was at steady-state[4]. Once steady-state

[4] Steady-state is used loosely in this thesis. It is meant to represent the period of time where the temperatures and gas composition were not obviously increasing or decreasing with time. Sometimes, as an operator it was hard to detect that there is still trending in these data points depending on the variability and the rate of change. This was not a true steady-state in the sense that nothing is changing with respect to time. For example, the bed material is always slowly changing due to attrition, impregnation of ash, sintering, or other

was declared condensate and tar sampling was initiated. The declaration of steady-state was a subjective decision made by the operators. Run charts were examined after the run to assess the validity of such a declaration. The duration over which the system was held at steady state (reactor temperature was reasonably constant, no obvious change in gas composition, and the airflow was constant) lasted between 1 – 2.5 hours is referred to as a *condition*. Most experimental runs consisted of two conditions. After the first condition was completed, changes were made to operating conditions (the amount of air provided to the gasifier was changed and the feed rate was altered) to achieve a second condition. The total operation over the course of a day is referred to as an *experimental run*.

3.3.2 Char Sampling

During each run, char was periodically removed from the "char removal" port (as labeled in Figure 3.2) and a sample from each condition was sent for ultimate and proximate analysis. In order to remove the char, a ball valve (char drain valve) and a section of pipe installed at the char removal port was used. During operation, the char drain valve was left open and the length of pipe was capped. The char would settle into the length of pipe beneath drain valve. Periodically, the char drain valve would be closed (in order to ensure the gasifier remained isolated from the atmosphere) and a bucket would be placed under the pipe. The cap would be removed from the pipe and the char would fall into the bucket. When the section of pipe was empty, the cap would be retightened onto the pipe and the char drain valve re-opened. The bucket into which the char fell was weighed and the time recorded. The removal of char was completed on an "as-necessary" basis which resulted in much more frequent removal for conditions that produced high amounts of char. Normally, the removal frequency varied between 15 – 45 minutes.

3.3.3 Gas Composition Measurements

Figure 3.5 shows the gas sampling arrangement used. In order to measure the gas composition, a slipstream of gas was drawn through a 1 micron stainless steel filter from just after the cyclone. The temperature of the gas prior to and at the filter was always maintained at >400°C to ensure that no tar had yet condensed. The hot-filtered gas

---

factors. It was also very difficult to confirm whether certain parameters are indeed constant with respect to time, such as the level of tar production, based on the measurement methods employed.

(>400°C) was first drawn through a "heavy-tar trap" maintained at 120°C and fiberglass filters at 120°C (in the "heated filter cabinet") in order to remove heavy tar species (which was necessary to protect analytical equipment). In order to measure the amount of water vapor in the product gas, some of the gas was then passed through two impingers in an ice bath and the amount of gas measured by a wet test meter. The impingers were then emptied to collect the amount of water that was condensed from the gas stream (this is what is meant by "condensate sampling"). In order to measure the composition of non-condensable gases, the sample gas (after the heated filter cabinet) was bubbled through water which was cooled to 0°C in order to condense water and remove the light tar components. The sample gas was then filtered (through a coalescing filter to remove aerosols), desiccated, and then filtered once more at ambient conditions. This brought the dew point of the gas down to an acceptable level for the gas analysis (non-condensing at the conditions of the analyzers). This gas sample was then routed to non-dispersive infrared (NDIR) analyzers for CO and CO_2, as well as a magnetopneumatic oxygen analyzer. The oxygen analyzer was necessary for the operators, under gasification conditions the oxygen concentration should be zero, sometimes a small amount (<0.2 vol%) could be detected due to a small leakage in the gas sampling system. If the oxygen was different than zero it indicated a problem (either with the sampling system or with the gasifier). The NDIR analyzers for CO and CO_2 where mostly used for confirmation of the micro-GC results and to assist the operators during the combustion warm up (gauging whether "good" combustion was occurring). A portion of the gas sample was also routed to micro-GC for measurement of H_2, O_2, N_2, CH_4, CO, CO_2, C_2H_6, C_2H_4, C_2H_2, and C_3H_6. The CO, CO_2, and O_2 analyzers were calibrated daily with a "zero" gas and a "span" gas. The micro-GC was calibrated prior to the project using multiple gas standards to generate calibration curves with between 3 and 7 points. The calibration was verified daily to ensure that the calibrations were valid to a tolerance of ±5% relative error on each gas species using gas standards which are reflective of the expected observed gas concentrations during gasification. Gas bags were also periodically taken in order to confirm the results of the micro-GC.

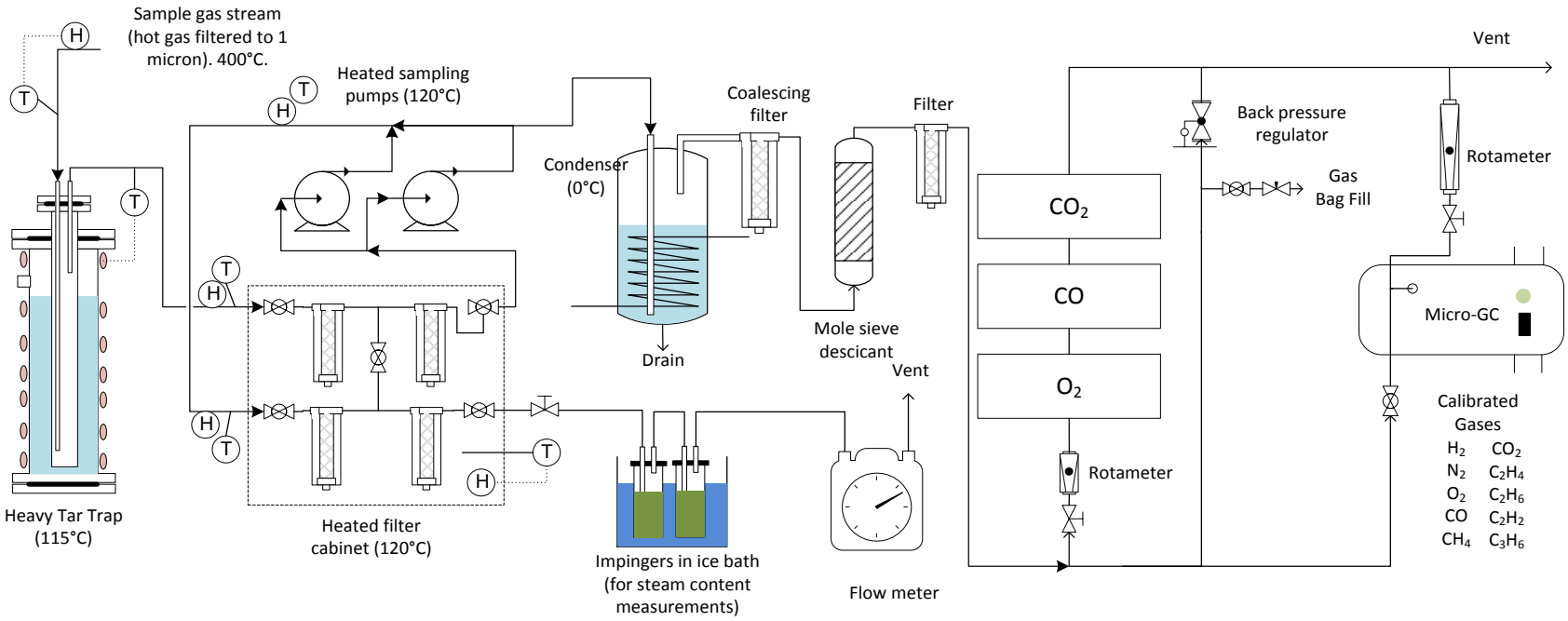

Figure 3.5: Sample gas conditioning and analysis system

3.3.4 Tar Sampling

The measurement of tar was completed by drawing a sample of hot-filtered gas (>400°C) from the top of the gasifier (labeled "gas sampling location" in Figure 3.2) through heated lines (at 400°C) followed by a set of 7 impingers. Each impinger was filled with approximately 200 mL of isopropanol. The first three impingers were placed in a water bath that was neither heated nor cooled and thus reached the ambient temperature of the laboratory which was typically between 20°C and 30°C. The last four impingers were kept in a bath of propylene glycol bath that was cooled to between -5°C and -20°C. Before sampling the impingers were cleaned, assembled and tested to ensure that there were no leaks among the joints of the arrangement. The heating tapes prior to the impingers were also turned on well before the tar sampling began in order to allow the sampling line temperature to reach 400°C. Sampling the gas at 400°C ensures that the gas temperature stays above the tar dewpoint so that the tar does not condense out of the gas phase until the gas reaches the isopropanol. Sampling was begun by zeroing the dials on the wet test meter (the flowmeter used to measure the amount of gas drawn through the sampling arrangement), starting a vacuum pump after the impingers and then opening up sampling valves. The gas flow rate was set to between 3 – 7 L/min by adjusting a bypass-recycle on the sampling vacuum pump. As the gas was drawn through the isopropanol the tar from the gas was dissolved into the isopropanol. After about an hour of sampling, the total volume of gas drawn through the impingers was recorded and the gas sampling was stopped. The impingers were emptied of the isopropanol and the impingers were rinsed with isopropanol to remove any condensed tar from surfaces that were not in contact with the isopropanol. The tar sampling arrangement is shown in Figure 3.5.

In order to determine the amount of tar that was contained in the isopropanol-tar solution (and thus the amount of tar that was in the gas), the isopropanol-tar solution was analyzed by two methods: by evaporation and by gas chromatography / mass spectroscopy (GC/MS). The evaporation method was carried out in a rotary evaporator in two stages using 50 mL of the solution. The first stage was at 60°C and -85 kPa_{gauge} (-25 inHg) for 20 minutes followed by a dissolution of the tar residue into acetone and the second stage of the evaporation was carried out at 60°C and -91 kPa_{gauge} (-27 inHg) for 20 minutes. After the evaporation a viscous or semi-solid black residue was left at the bottom of the evaporation

flask. The difference between the original weight the flask and the weight of the flask at the end of the evaporation was carefully measured. The difference in weight can be attributed to the amount tar that was not evaporated at the conditions stated. The mass of tar determined in this way is referred to as "gravimetric tar". Evaporations were repeated and the average of the measurements has been reported.

Some isopropanol-tar samples were analyzed by GC/MS to determine the composition of the tar. Table 3.7 shows the components that the GC/MS apparatus was calibrated for using standards containing known amounts of the chemical species. The sum of the concentration of the components listed in Table 3.7 is referred to as "GC tar".

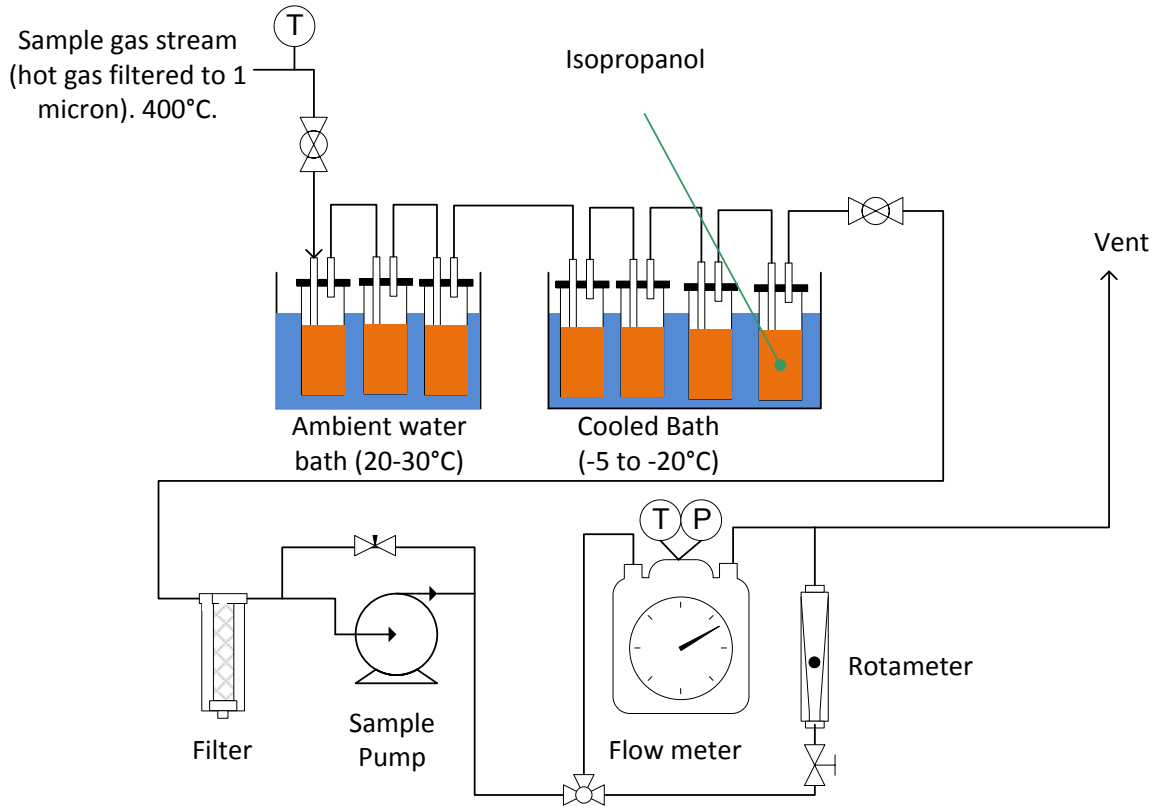

Figure 3.6: Schematic diagram of the tar sampling arrangement used

Table 3.7: Tars quantified by GC/MS arranged according to classification

Class 2	Class 3	Class 4	Class 5
phenol	toluene	indene	fluoranthene
o,m,p-cresol	ethylbenzene	naphthalene	pyrene
	o,m,p-xylene	2-methylnaphthelene	benz(a)anthracene
	styrene	1-methylnaphthalene	chrysene
		biphenyl	benzo(b)fluoranthene
		acenaphthylene	benzo(k)fluoranthene
		acenaphthene	benzo(e)pyrene
		fluorene	benzo(a)pyrene
		phenanthrene	perylene
		anthracene	Indeno(123-cd)pyrene
			Dibenz(a,h)anthracene
			Benzo(ghi)perylene
			coronene

Photographs of some of the key items of the gas sampling and tar sampling system are provided in Appendix E.

3.4 Experimental Design

In order to determine the effects of particle size, moisture level and pelletization of a forestry residue on its fluidized bed gasification, a pseudo-factorial[5] experimental design was followed, with run replication and a randomized run order. The selected levels of the three factors are shown in Table 3.8.

[5] The experimental design is referred to as pseudo-factorial in the sense that a factorial design was used as much as possible, but some factors are not independent. For example, the pelletization and particle size are not independent factors. Also certain combinations of factors are not possible, for example, a fuel cannot be both high moisture and pelletized since wood pellets will not hold together at high moisture levels (they crumble)

Table 3.8: Selected moisture, size, and pelletization levels

Moisture Level	Moisture (w.b.)
1	~30%
-1	As is

Size level	Sieve range (mm)	
1	6.35	19.05
0	3.175	6.35
-1	0	3.175

Pelletization Level	Form
0	Raw
1	Pellets

The factors were investigated over a variety of temperature levels in order to study the effects over a wide range of operating conditions. Temperature is one of the most important operational parameters, and by fixing the fluidizing velocity, it allows a wide range conditions to be studied. Three temperature levels were chosen: 725, 800, and 875°C. 875°C represents a fairly high operating temperature for a fluidized bed gasifier, but still below ash softening points with residual feedstocks in order to avoid bed agglomerations. 725°C represents a relatively low temperature for fluidized bed gasifier operation, but still high enough that a reasonable level of carbon conversion might be possible.

Another operating parameter which is important for the operation of a fluidized bed gasifier is the fluidizing gas velocity. With all the different factors that needed to be varied, it was decided to carry out the experiments at one constant fluidizing velocity, thus no indication as whether the factors tested interact with the fluidizing gas velocity were discussed in this thesis. The constant velocity that is referred to is the fluidizing velocity at the base of the bed considering only the fluidizing air. Since the number of moles of gas produced will depend on feed rate, char conversion and gas composition, the fluidizing velocity at the top of the bed will be unique for each run. The fluidizing velocity chosen was 0.91 m/s which corresponds to a fluidization number of roughly 10 (ten times the minimum fluidization velocity of the bed media used).

With a fixed bed temperature, a constant fluidizing velocity and no heat input from external sources, the only way to adjust the bed temperature was to adjust the biomass feed rate. Thus, as a result of the experimental design, the equivalence ratio[6] (ER) varied based on the characteristics of the gasification of each fuel. The observed ER for each fuel is reported in section 3.8.1.

Table 3.9 shows a layout of the factor levels evaluated and Table 3.10 shows the full list of experiments with bed temperature and air flow rate requirements. Repeats were carried out at the central temperature level (800°C) with the dry fuels and both gravimetric and GC tar measurements were completed. These condition replicates were used to qualitatively evaluate the level repeatability between trials.

Table 3.9: Experimental levels tested and number of replicates

Three level in size, two level in moisture				
Exp No	Moisture	Size	Pelletized	Number of Tests
A	1	1	0	1
B	1	0	0	1
C	1	-1	0	1
D	-1	1	0	2
E	-1	0	0	2
F	-1	-1	0	2
G	-1	"1"	1	2
Total				**11**

As the testing campaign progressed some adjustments were necessary to the original experimental design. The actual (i.e., final) testing order and number of runs are presented in Table 3.10. Firstly, due to feeding problems with the coarse material run D1 could not be accomplished and the runs A and D2 were moved out of the run order until the end of the testing campaign. Secondly, in order to confirm some results that appeared to be suspicious, repeats of a few additional conditions were carried out. Thus, run codes G3, F3, and E3 can be found in the summary of experimental runs. These runs replicated with specific

[6] The equivalence ratio (ER) is the amount of oxygen provided to the system divided by the stoichiometric amount of oxygen required to completely combust the fuel.

conditions which were deemed to be unexpected in order to confirm whether or not the observed results were repeatable or not.

Table 3.10: Actual experimental campaign

Run Code	Moisture	Size / form	Air flow Condition 1 sLpm	Air flow Condition 2 sLpm	Bed Temperature Condition 1 °C	Bed Temperature Condition 2 °C	Run Order
A	Added	Coarse	275	296	800	725	13
B	Added	Mid	275	296	800	725	3
C	Added	Fine	275	296	800	725	8
D1	As is	Coarse	275	296	800	725	abandoned
D2	As is	Coarse	275	257	800	875	12
E1	As is	Mid	275	296	800	725	7
E2	As is	Mid	275	257	800	875	4
E3	As is	Mid	296	-	725	-	11
F1	As is	Fine	275	296	800	725	2
F2	As is	Fine	275	257	800	875	5
F3	As is	Fine	257	296	875	725	10
G1	As is	Pellets	275	296	800	725	1
G2	As is	Pellets	275	257	800	875	6
G3	As is	Pellets	275	296	800	725	9

3.5 **Experimental Conditions**

A summary of the experiments performed and the operational measurements taken from each experiment are outlined in Table 3.11. The bed mass represents the total initial mass of bed media (olivine sand) loaded into the reactor. The two first runs (4 conditions) were completed with a greater initial charge of sand than the following eleven runs (21 conditions). The higher bed level led to operational problems (back pressure in the feed arm). Thus, interpretation of the results needs to respect the fact that the initial two runs were completed at different bed levels (Run code F1 and G1).

The airflow is the amount of air fed to the reactor measured in standard liters per minute (sLpm). For these experiments, the only location that air entered the reactor was through the distributor (in other words, staged injection of the air was not used). The feed rate was measured by two independent methods. This provided back-up verification of the feed rate. The “LabView feed rate” was computed by the data acquisition software from the measured weight of feed on the feed belt, the distance of the belt that feed was distributed, and the

power provided to the feed belt (which was correlated with the speed of the feed belt). The LabView feed rate was useful for displaying an instantaneous measurement of feed rate and to show how the feed rate varied over the course of a condition. In Table 3.11, the presented LabView feed rate is the average measurement over the duration of the condition. The "bucket feed rate" was the feed rate measured by weighing and recording each bucket of material loaded into the feed hopper. The data in Table 3.11 shows that there are differences in the feed rate as reported by the LabView method or by the bucket method. The LabView method relies on correlations between the power provided to the DC motor and the speed of the belt in addition to interferences like the effect of the vibrator on the weight measurement. The bucket feed rate should be very reliable over the course of a condition as long as the feed hopper was always filled at the same level (which was done as best as possible).

The "Avg. Bed T." is the average bed temperature which was the average of the readings from the three bed level thermocouples (those located at 0.219, 0.432, and 0.679 m from the distributor plate) over the duration of the condition. The "Bed P." is the bed pressure which was recorded by the pressure transmitter located at 0.219 m from the distributor plate. The char recovery is the amount of char recovered from the cyclone converted to an average rate over the duration of a condition.

Table 3.11: Operation parameters and measured parameters for the experimental campaign

Run Code	Fuel	Bed Mass kg	Air flow sLpm	LabView feed rate kg/h	Bucket feed rate kg/h	Avg. Bed T. °C	Bed P (at 0.219 m) kPa	Char recovery kg/h	
F3	Fines	11	257	9.8	9.4	871	2.8	0.9	
F2	Fines	11	257	10.8	10.1	862	2.9	1.2	
F2	Fines	11	275	17.2	16.9	801	2.5	0.9	
F1	Fines	15	275	13.6	15.4	799	4.5	1.6	
F3	Fines	11	296	22.4	24.1	726	3.2	3.7	
F1	Fines	15	296	17.5	20.1	725	4.4	1.6	
C	Fines-wet	11	275	13.9	14.7	800	2.8	1.2	
C	Fines-wet	11	296	18.1	20.4	725	3.0	2.3	
E2	Mid	11	257	11.7	10.6	875	2.3	[2]	
E2	Mid	11	275	15.0	14.6	801	2.3	[2]	
E1	Mid	11	275	14.0	15.7	801	2.5	0.7	
E1	Mid	11	296	18.0	22.7	725	2.7	1.3	
E3	Mid	11	296	18.5	21.1	725	2.8	1.8	
B	Mid-wet	11	275	13.9	13.8	802	2.2	1.5	
B	Mid-wet	11	296	18.1	17.9	725	2.5	0.8	
D2	Coarse	11	257	10.9	10.8	875	2.9	0.5	
D2	Coarse	11	275	14.6	14.6	800	2.9	1.0	
A	Coarse-wet	11	275	13.0	12.6	800	2.9	0.5	
A	Coarse-wet	11	296	17.0	16.8	725	3.2	1.1	
G2	Pellets	11	257	10.5	10.1	875	3.1	[2]	
G2	Pellets	11	275	14.8	14.8	801	3.4	[2]	
G3	Pellets	11	275	15.2	14.6	801	3.3	1.7	
G1	Pellets	15	275	13.5	13.7	800	4.6	1.8	
G1	Pellets	15	296	21.2	22.5	725	3.1	4.9	[1]
G3	Pellets	11	296	20.3	22.0	725	4.2	3.1	

[1] **Pressure trends indicate loss of bed material, char is likely heavily contaminated with bed material**
[2] **Invalid char data, substantial levels of plugging found in cyclone after the run**

3.6 **Data Analysis Methodology (Mass Balancing Procedure)**

Mass balances must be carried out in order to determine the yields of gases, tar, water, and char, as well as the carbon conversion, and the efficiency of the gasification experiments. The mass balances are sensitive to the uncertainties in the measurement of the inputs and outputs of the process. An example of such uncertainty would be how representative the fuel sample that was analyzed is compared to the entire amount of fuel fed to the gasifier. Different approaches can be used to complete the mass balance by using a different set of assumptions. Two approaches for performing the mass balance are presented in this thesis. In theory, both strategies should produce the same results. However, in practice there are differences. Since the two approaches are fundamentally different, if the two different

approaches give the same trends and conclusions it is reassuring[7] that the conclusion is real and not an artifact of experimental error. The detailed calculations and assumptions of the two methods are outlined in Appendix B.

The first strategy has been named the ***traditional*** method and the second method has been called the ***CHO*** method. For the mass balances:

- the mass input of air and feed material is measured
- the composition of the dry feed material has been measured
- the amount of moisture (water) in the feed has been measured
- the composition of water is known
- the composition of air is known
- the mass output of producer gas is not known

Practically, it is very difficult[8] to get a direct measurement of the product gas flow rate (changing gas composition, presence of contaminants that interfere with traditional measurement techniques, pressure fluctuations that interfere with differential pressure techniques, etc…). The product gas composition was however measured. The salient feature of the traditional method is that the nitrogen composition is used to determine the flow rate of product gas. The amount of nitrogen into the system is known and molecular nitrogen is assumed to be inert, thus the concentration of nitrogen in the gas can be related to the total gas flow rate. The assumption here is that all the input nitrogen in the system reports to N_2. Although gasification does produce NH_3, HCN and other nitrogen species, their amounts are small compared to the total amount of nitrogen in an air-blown gasifier. Since the concentration of water in the gas, the tar, and the amount of char recovered is measured, then the performance of this method can be assessed by knowing whether or not the mass

[7] What is be claimed here is not that if the two methods give the same trend that it is proof that the trend is real as opposed to an artifact of experiment error. What is being proposed is that if both methods give the same trend, there is an increased chance that the result is not an artifact of experimental error.

[8] This is not to say it can't be done. People do measure the mass output of gas. However, this often involves the use of expensive measurement devices or repeatedly ruining measuring devices. Measuring the gas can also come with its own set of assumptions.

of carbon, hydrogen, and oxygen fed into the system equals the mass of the output carbon, hydrogen, and oxygen.

The first approach relies on accurate knowledge of the amount of nitrogen input to the process and the concentration of nitrogen in the dry product gas. Any leakage of air into the system (such as the small amount that comes in with the feed material through the rotary airlock) can contribute to error with this method. A relatively small inaccuracy in the nitrogen measurement can lead to a big change in the calculated gas flow rate (especially as the ER rises and concentration of nitrogen in the producer gas tends towards that in air). This method also relies on accurate knowledge of the amount of ash in the char and that all the char is recovered. The char is hard to fully recover (cyclones are only effective for large particles) and it was observed that the char samples can be heterogeneous in ash. There is also difficulty in ascertaining whether the ash in the char originates from the feed material or the bed media.

In order to address some of the issues with the traditional method, a second mass balancing method was developed for this thesis. In the second method, the carbon, hydrogen, and oxygen balances were fixed instead of nitrogen balance. This method is referred to in this thesis as ***CHO*** method. The method attempts to take advantage of the measurements that have been completed the most frequently and have the highest level of accuracy. The procedure was chosen since it was assumed that through the number of measurements completed, the knowledge of the carbon-hydrogen-oxygen (C-H-O) composition of the feed, air, product gas, tar, and char have a high level of certainty (i.e. the level of certainty on the C-H-O composition of char is much greater than the level of certainty on the amount of char produced). This method takes the C-H-O mass input and the C-H-O composition of the output products in order to predict the mass output of three products. For ease of the calculation, these three mass outputs have been defined as: gas + tar, water, and char. Tar in this mass balance strategy is accounted for as a component of the gas just like CH_4 or H_2. It is treated in this way because this reflects how it is measured (it is measured as the amount found in the dry gas). The performance of this method can be evaluated by comparing the predicted and measured nitrogen, water concentration in the gas and the amount of char produced. Since the composition of water does not change and the ash-free composition of

char does not vary much (close to pure carbon), the only real sensitivities of the method are the knowledge of the composition the feed material, the mass input of the feed and air, and the C-H-O composition of the dry gas+tar.

3.7 **Experimental Results**

The gas composition, the amount of tar, and the amount of water are among the most important measurements taken during the gasification trials. Table 3.12 shows the average recorded gas composition over the steady state duration of each condition along with results from the tar and condensate sampling activities. Although certain trends are visible, the remainder of this chapter deals with the thorough analysis of this data from mass and energy perspectives. The time resolved data is provided in the appendix of this section in detailed run charts (Figure C.1 through Figure C.26).

Table 3.12: Measured gas composition for the experimental campaign

Run Code	Fuel	Avg. Bed T. °C	CO %vol	CO_2 %vol	H_2 %vol	CH_4 %vol	N_2 %vol	C2 gases [4] %vol	Grav. Tar g/m^3 [3]	Water g/m^3 [3]
F3	Fines	871	9.5	17.8	3.8	2.5	65.0	1.17	8.9	124.9
F2	Fines	862	10.3	17.2	3.8	2.8	64.2	1.26	7.4	156.3
F2	Fines	801	14.8	17.4	6.9	4.0	54.8	1.68	27.9	182.3
F1	Fines	799	13.0	17.7	5.8	3.7	57.9	1.56	17.9	150.8
F3	Fines	726	15.1	17.8	6.6	4.0	54.2	1.45	45.3	232.5
F1	Fines	725	15.9	17.7	6.2	4.2	53.9	1.52	59.0	200.2
C	Fines-wet	800	12.3	18.0	5.7	3.5	58.5	1.51	23.4	219.3
C	Fines-wet	725	12.2	18.9	6.4	3.3	57.5	1.19	38.4	301.1
E2	Mid	875	13.0	17.4	9.8	3.8	54.4	1.45	6.9	111.5
E2	Mid	801	14.4	17.6	10.8	4.2	51.1	1.65	11.9	134.3
E1	Mid	801	14.2	17.7	10.6	4.2	51.3	1.68	11.9	140.2
E1	Mid	725	13.7	19.1	11.2	4.5	49.4	1.50	10.1	202.0
E3	Mid	725	14.2	18.4	10.5	4.5	50.2	1.51	24.1	188.5
B	Mid-wet	802	9.8	19.2	10.2	3.0	56.4	1.21	9.2	191.8
B	Mid-wet	725	10.4	19.9	10.6	3.3	54.3	1.13	16.6	260.0
D2	Coarse	875	11.6	17.7	9.8	3.2	56.2	1.25	2.0	111.9
D2	Coarse	800	12.7	18.3	11.7	3.8	51.6	1.46	7.3	125.1
A	Coarse-wet	800	7.7	20.0	8.5	2.5	60.2	1.04	5.8	241.9
A	Coarse-wet	725	8.6	20.3	8.5	2.6	58.8	0.98	16.6	308.5
G2	Pellets	875	12.9	16.7	11.6	3.1	54.7	0.88	3.2	87.7
G2	Pellets	801	12.3	18.4	12.1	4.0	51.6	1.35	13.3	126.3
G3	Pellets	801	12.7	18.1	13.0	3.9	50.5	1.31	9.1	119.0
G1	Pellets	800	12.9	17.7	12.6	3.6	52.0	1.12	8.1	93.2
G1	Pellets	725	12.8	19.7	13.0	4.7	48.1	1.34	36.7	158.5
G3	Pellets	725	11.4	19.7	12.9	4.3	49.8	1.22	16.0	[5]

[3] **One m^3 is standardized to 0°C, 1 atm on a dry basis.**
[4] **"C2 gases" is the sum of ethylene, ethane, and acetylene**
[5] **Sampling error during the condensate sample, invalid result**

3.7.1 Results of Mass Balancing

Many of the most important parameters such as the yield of the gas, tar, and char can only be determined after conducting a mass balance over the process. From the mass balance results, calculations such as the carbon conversion and the cold gas efficiency can be determined. Table 3.13 shows the results obtained from the traditional mass balance approach and Table 3.14 shows the results obtained from the CHO mass balance strategy[9]. It should be cautioned when interpreting the results from this table that a result of 0.00 can often indicate that a measurement was not carried out or that there was an error with the measurement.

[9] The yield of "light HC gases" presented in the following tables is the sum of the yield of methane, ethane, ethylene, acetylene, and propylene.

Table 3.13: Tabulated results from the traditional mass balance method

Run Code	Fuel	Airflow	Feed rate	Average Bed T.	dry gas yield	Hydrogen	Carbon Monoxide	Methane	Ethylene	Carbon Dioxide	Ethane	Acetylene	Propylene	Light HC gases
		sLpm	kg/h	°C	kg/kg-biomass DAF	kg/kg-biomass DAF	kg/kg-biomass DAF	kg/kg-biomass DAF	kg/kg-biomass DAF	kg/kg-biomass DAF	kg/kg-biomass DAF	kg/kg-biomass DAF	kg/kg-biomass DAF	kg/kg-biomass DAF
F3	Fines	257	10.1	862	3.131	0.008	0.307	0.048	0.028	0.807	0.005	0.004	0.001	0.087
F2	Fines	257	9.4	871	3.346	0.009	0.302	0.046	0.027	0.887	0.005	0.005	0.000	0.084
F2	Fines	275	15.4	799	2.405	0.010	0.304	0.050	0.028	0.647	0.007	0.002	0.008	0.094
F1	Fines	275	16.9	801	2.285	0.011	0.332	0.052	0.029	0.612	0.007	0.002	0.009	0.099
F3	Fines	296	20.1	725	2.124	0.009	0.328	0.050	0.023	0.576	0.009	0.001	0.014	0.096
F1	Fines	296	24.1	726	1.752	0.008	0.260	0.040	0.018	0.479	0.007	0.001	0.011	0.076
C	Fines-wet	275	14.7	800	2.952	0.012	0.352	0.057	0.033	0.808	0.008	0.002	0.009	0.109
C	Fines-wet	296	20.4	725	2.331	0.010	0.275	0.042	0.019	0.668	0.008	0.001	0.012	0.081
E2	Mid	257	10.6	875	3.052	0.022	0.401	0.068	0.037	0.842	0.007	0.001	0.002	0.115
E2	Mid	275	14.6	801	2.501	0.020	0.366	0.061	0.033	0.704	0.008	0.001	0.007	0.111
E1	Mid	275	15.7	801	2.322	0.018	0.335	0.057	0.031	0.657	0.007	0.002	0.007	0.103
E1	Mid	296	22.7	725	1.796	0.015	0.249	0.046	0.020	0.546	0.008	0.001	0.011	0.085
E3	Mid	296	21.1	725	1.906	0.015	0.274	0.049	0.021	0.559	0.008	0.001	0.012	0.091
B	Mid-wet	275	13.8	802	2.852	0.021	0.280	0.048	0.026	0.859	0.007	0.001	0.005	0.088
B	Mid-wet	296	17.9	725	2.458	0.019	0.254	0.046	0.020	0.769	0.008	0.000	0.011	0.085
D2	Coarse	257	10.8	875	2.901	0.021	0.338	0.054	0.030	0.812	0.005	0.001	0.001	0.091
D2	Coarse	275	14.6	800	2.461	0.021	0.319	0.054	0.029	0.724	0.007	0.001	0.007	0.098
A	Coarse-wet	275	12.6	800	3.300	0.020	0.249	0.046	0.026	1.012	0.007	0.001	0.004	0.084
A	Coarse-wet	296	16.8	725	2.729	0.016	0.228	0.040	0.019	0.846	0.007	0.001	0.010	0.076
G2	Pellets	257	10.1	875	3.160	0.027	0.419	0.058	0.023	0.850	0.006	0.001	0.000	0.087
G2	Pellets	275	13.7	800	2.614	0.024	0.348	0.056	0.023	0.748	0.007	0.001	0.004	0.091
G3	Pellets	275	14.8	801	2.456	0.022	0.311	0.058	0.026	0.727	0.007	0.001	0.005	0.098
G1	Pellets	275	14.6	801	2.511	0.024	0.332	0.058	0.026	0.742	0.007	0.001	0.005	0.097
G1	Pellets	296	22.5	725	1.859	0.018	0.244	0.052	0.018	0.590	0.008	0.001	0.010	0.088
G3	Pellets	296	22	725	1.837	0.017	0.216	0.047	0.016	0.583	0.007	0.000	0.009	0.080

Table 3.13: Tabulated results from the traditional mass balance method (Continued)

Fuel	Airflow	Feed rate	Average Bed T.	Water (Gross)	Water (Net)	GC Tar + Benzene	Grav. Tar	Char	ER	HHV(gas)	MW(gas)	Gas density [6]	Carbon conversion [7]	Carbon conversion [8]	Cold Gas Efficiency
	sLpm	kg/h	°C	kg/kg-biomass DAF	kg/kg-biomass DAF	kg/kg-biomass DAF	kg/kg-biomass DAF	kg/kg-biomass DAF	mol/mol	MJ/kg	g/mol	kg/m^3	kg/kg	kg/kg	MJ/MJ
Fines	257	10.1	862	0.374	0.230	0.000	0.018	0.153	0.39	2.84	29.30	1.31	79.2%	82.3%	41.4%
Fines	257	9.4	871	0.317	0.173	0.040	0.023	0.126	0.42	2.61	29.51	1.32	82.5%	89.5%	40.7%
Fines	275	15.4	799	0.281	0.137	0.045	0.033	0.134	0.27	3.93	28.91	1.29	71.9%	79.5%	44.0%
Fines	275	16.9	801	0.328	0.183	0.039	0.050	0.069	0.25	4.45	28.51	1.27	73.1%	81.5%	47.4%
Fines	296	20.1	725	0.331	0.187	0.037	0.098	0.103	0.23	4.57	28.79	1.28	70.4%	86.3%	45.2%
Fines	296	24.1	726	0.319	0.175	0.020	0.062	0.198	0.19	4.46	28.63	1.28	56.9%	67.0%	36.4%
Fines-wet	275	14.7	800	0.501	0.122	0.040	0.053	0.124	0.34	3.73	28.96	1.29	86.3%	95.3%	51.3%
Fines-wet	296	20.4	725	0.543	0.164	0.022	0.069	0.172	0.26	3.67	28.97	1.29	68.6%	79.8%	39.8%
Mid	257	10.6	875	0.274	0.142	0.000	0.017	*0.000*	0.36	4.34	27.80	1.24	95.2%	98.2%	63.3%
Mid	275	14.6	801	0.273	0.141	0.045	0.024	*0.000*	0.28	4.96	27.54	1.23	84.5%	92.4%	59.3%
Mid	275	15.7	801	0.264	0.133	0.032	0.022	0.052	0.26	4.92	27.61	1.23	78.3%	84.0%	54.5%
Mid	296	22.7	725	0.295	0.163	0.000	0.015	0.067	0.19	5.08	27.60	1.23	62.5%	65.0%	43.5%
Mid	296	21.1	725	0.291	0.159	0.019	0.037	0.100	0.21	5.07	27.69	1.24	66.1%	72.4%	46.1%
Mid-wet	275	13.8	802	0.436	0.108	0.029	0.021	0.149	0.34	3.68	28.09	1.25	82.1%	87.1%	50.1%
Mid-wet	296	17.9	725	0.510	0.182	0.000	0.033	0.061	0.28	3.97	28.08	1.25	74.7%	80.1%	46.6%
Coarse	257	10.8	875	0.261	0.130	0.018	0.005	0.056	0.34	3.86	27.85	1.24	84.3%	87.5%	53.5%
Coarse	275	14.6	800	0.252	0.120	0.025	0.015	0.081	0.27	4.65	27.40	1.22	79.3%	83.6%	54.8%
Coarse-wet	275	12.6	800	0.622	0.153	0.025	0.015	0.060	0.41	2.96	28.75	1.28	86.5%	90.8%	46.7%
Coarse-wet	296	16.8	725	0.656	0.187	0.021	0.035	0.099	0.33	3.17	28.77	1.28	74.9%	80.8%	41.4%
Pellets	257	10.1	875	0.228	0.142	0.000	0.008	*0.000*	0.37	4.05	27.25	1.22	92.1%	93.6%	60.5%
Pellets	275	13.7	800	0.201	0.115	0.026	0.017	0.157	0.29	4.53	27.16	1.21	81.6%	86.0%	56.0%
Pellets	275	14.8	801	0.254	0.169	0.038	0.027	*0.000*	0.27	4.67	27.34	1.22	78.4%	85.1%	54.2%
Pellets	275	14.6	801	0.248	0.162	0.031	0.019	0.138	0.28	4.78	27.01	1.20	80.9%	86.3%	56.8%
Pellets	296	22.5	725	0.242	0.157	0.028	0.056	0.259	0.19	5.21	27.25	1.22	64.3%	73.6%	45.7%
Pellets	296	22	725	*0.000*	*-0.086*	0.000	0.024	0.168	0.20	4.85	27.26	1.22	60.4%	64.4%	42.1%

[6] at 0°C, 1 atm

[7] Carbon conversion to gas only

[8] Carbon conversion to gas and any condensable organics (tar)

Table 3.14: Tabulated results from the CHO mass balance method

Run Code	Fuel	Airflow	Feed rate	Average Bed T.	dry gas yield	Hydrogen	Carbon Monoxide	Methane	Ethylene	Carbon Dioxide	Ethane	Acetylene	Propylene	Light HC gases
		sLpm	kg/h	°C	kg/kg-biomass DAF	kg/kg-biomass DAF	kg/kg-biomass DAF	kg/kg-biomass DAF	kg/kg-biomass DAF	kg/kg-biomass DAF	kg/kg-biomass DAF	kg/kg-biomass DAF	kg/kg-biomass DAF	kg/kg-biomass DAF
F3	Fines	257	9.4	871	3.116	0.008	0.281	0.043	0.025	0.826	0.004	0.005	0.000	0.078
F2	Fines	257	10.1	862	2.959	0.008	0.291	0.045	0.027	0.762	0.005	0.004	0.001	0.082
F2	Fines	275	16.9	801	1.965	0.010	0.286	0.044	0.025	0.527	0.006	0.002	0.008	0.085
F1	Fines	275	15.4	799	2.140	0.009	0.271	0.044	0.025	0.576	0.006	0.002	0.007	0.084
F3	Fines	296	24.1	726	1.450	0.007	0.215	0.033	0.015	0.396	0.006	0.001	0.009	0.063
F1	Fines	296	20.1	725	1.747	0.008	0.270	0.041	0.019	0.474	0.007	0.001	0.012	0.079
C	Fines-wet	275	14.7	800	2.581	0.010	0.308	0.050	0.029	0.707	0.007	0.002	0.008	0.096
C	Fines-wet	296	20.4	725	1.928	0.009	0.228	0.035	0.015	0.552	0.006	0.001	0.010	0.067
E2	Mid	257	10.6	875	2.940	0.021	0.387	0.065	0.036	0.811	0.006	0.001	0.002	0.110
E2	Mid	275	14.6	801	2.385	0.019	0.349	0.059	0.032	0.671	0.007	0.001	0.007	0.106
E1	Mid	275	15.7	801	2.169	0.017	0.313	0.053	0.029	0.613	0.007	0.001	0.006	0.096
E1	Mid	296	22.7	725	1.564	0.013	0.217	0.040	0.017	0.476	0.007	0.000	0.009	0.074
E3	Mid	296	21.1	725	1.736	0.013	0.249	0.045	0.019	0.509	0.007	0.001	0.011	0.083
B	Mid-wet	275	13.8	802	2.754	0.020	0.270	0.047	0.026	0.830	0.007	0.001	0.005	0.085
B	Mid-wet	296	17.9	725	2.228	0.017	0.230	0.042	0.018	0.697	0.007	0.000	0.010	0.077
D2	Coarse	257	10.8	875	2.778	0.020	0.323	0.052	0.029	0.778	0.005	0.001	0.001	0.087
D2	Coarse	275	14.6	800	2.279	0.020	0.295	0.050	0.027	0.671	0.007	0.001	0.006	0.091
A	Coarse-wet	275	12.6	800	3.066	0.018	0.231	0.043	0.024	0.940	0.006	0.001	0.004	0.078
A	Coarse-wet	296	16.8	725	2.456	0.015	0.205	0.036	0.017	0.761	0.006	0.001	0.009	0.069
G2	Pellets	257	10.1	875	3.088	0.027	0.410	0.057	0.022	0.830	0.005	0.001	0.000	0.085
G2	Pellets	275	14.8	801	2.379	0.021	0.301	0.056	0.025	0.705	0.007	0.001	0.005	0.095
G3	Pellets	275	14.6	801	2.389	0.023	0.316	0.055	0.025	0.706	0.007	0.001	0.005	0.093
G1	Pellets	275	13.7	800	2.508	0.023	0.334	0.054	0.022	0.718	0.006	0.001	0.004	0.087
G1	Pellets	296	22.5	725	1.690	0.016	0.222	0.047	0.016	0.536	0.007	0.000	0.009	0.080
G3	Pellets	296	22	725	1.659	0.016	0.195	0.042	0.015	0.527	0.006	0.000	0.008	0.072

Table 3.14: Tabulated results from the CHO mass balance method (Continued)

Fuel	Airflow	Feed rate	Average Bed T.	Bed P at 21.9 cm	Water (Gross)	Water (Net)	GC Tar + Benzene	Grav. Tar	Char	ER	HHV(gas)	MW(gas)	Gas density [6]	Carbon conversion [7]	Carbon conversion [8]	Cold Gas Efficiency
	sLpm	kg/h	°C	"WC	kg/kg-biomass DAF	kg/kg-biomass DAF	kg/kg-biomass DAF	kg/kg-biomass DAF	kg/kg-biomass DAF	mol/mol	MJ/kg	g/mol	kg/m^3	kg/kg	kg/kg	MJ/MJ
Fines	257	9.4	871	11.2	0.449	0.304	0.038	0.021	0.342	0.42	2.61	29.51	1.32	76.8%	83.3%	37.9%
Fines	257	10.1	862	11.5	0.445	0.301	0.000	0.017	0.478	0.39	2.84	29.30	1.31	74.9%	77.8%	39.1%
Fines	275	16.9	801	10.1	0.398	0.254	0.034	0.043	0.462	0.25	4.45	28.51	1.27	62.9%	70.1%	40.8%
Fines	275	15.4	799	17.9	0.412	0.268	0.040	0.030	0.539	0.27	3.93	28.91	1.29	64.0%	70.7%	39.1%
Fines	296	24.1	726	12.7	0.438	0.293	0.017	0.051	0.695	0.19	4.46	28.63	1.28	47.1%	55.5%	30.1%
Fines	296	20.1	725	17.8	0.404	0.259	0.031	0.080	0.343	0.23	4.57	28.79	1.28	58.0%	71.0%	37.2%
Fines-wet	275	14.7	800	11.1	0.621	0.242	0.035	0.047	0.201	0.34	3.73	28.96	1.29	75.4%	83.3%	44.9%
Fines-wet	296	20.4	725	11.9	0.656	0.277	0.018	0.057	0.365	0.26	3.67	28.97	1.29	56.8%	66.0%	33.0%
Mid	257	10.6	875	9.1	0.267	0.135	0.000	0.016	0.046	0.36	4.34	27.80	1.24	91.7%	94.6%	61.0%
Mid	275	14.6	801	9.2	0.275	0.143	0.043	0.023	0.100	0.28	4.96	27.54	1.23	80.6%	88.1%	56.5%
Mid	275	15.7	801	10.2	0.314	0.182	0.030	0.021	0.163	0.26	4.92	27.61	1.23	73.1%	78.4%	50.9%
Mid	296	22.7	725	10.7	0.377	0.245	0.000	0.013	0.295	0.19	5.08	27.60	1.23	54.5%	56.6%	37.9%
Mid	296	21.1	725	11.3	0.352	0.220	0.017	0.034	0.234	0.21	5.07	27.69	1.24	60.2%	65.9%	42.0%
Mid-wet	275	13.8	802	9	0.489	0.161	0.028	0.020	0.455	0.34	3.68	28.09	1.25	79.2%	84.1%	48.4%
Mid-wet	296	17.9	725	10	0.537	0.209	0.000	0.030	0.283	0.28	3.97	28.08	1.25	67.7%	72.6%	42.2%
Coarse	257	10.8	875	11.5	0.320	0.188	0.017	0.004	0.186	0.34	3.86	27.85	1.24	80.7%	83.8%	51.3%
Coarse	275	14.6	800	11.6	0.307	0.175	0.023	0.014	0.201	0.27	4.65	27.40	1.22	73.4%	77.4%	50.7%
Coarse-wet	275	12.6	800	11.6	0.685	0.216	0.023	0.014	0.212	0.41	2.96	28.75	1.28	80.3%	84.3%	43.4%
Coarse-wet	296	16.8	725	12.8	0.715	0.246	0.019	0.032	0.248	0.33	3.17	28.77	1.28	67.4%	72.7%	37.2%
Pellets	257	10.1	875	12.6	0.218	0.132	0.000	0.008	0.100	0.37	4.05	27.25	1.22	90.0%	91.4%	59.1%
Pellets	275	14.8	801	13.7	0.225	0.139	0.037	0.026	0.268	0.27	4.67	27.34	1.22	76.0%	82.4%	52.5%
Pellets	275	14.6	801	13.4	0.219	0.133	0.030	0.018	0.145	0.28	4.78	27.01	1.20	77.0%	82.1%	54.0%
Pellets	275	13.7	800	18.3	0.228	0.143	0.025	0.017	0.185	0.29	4.53	27.16	1.21	78.3%	82.5%	53.7%
Pellets	296	22.5	725	12.6	0.275	0.189	0.025	0.051	0.265	0.19	5.21	27.25	1.22	58.4%	66.9%	41.6%
Pellets	296	22	725	16.9	0.306	0.221	0.000	0.022	0.344	0.20	4.85	27.26	1.22	54.5%	58.2%	38.1%

[6] at 0°C, 1 atm

[7] Carbon conversion to gas only

[8] Carbon conversion to gas and any condensable organics (tar)

3.7.2 Comparison of Mass Balance Strategies

In order to determine how the choice of a mass balance strategy could influence the results, the two mass balancing strategies described were compared to each other using the data presented in this chapter. Case studies were undertaken in order to gather understanding on the sensitivity of each strategy to uncertainties in key measurements. The details of the comparison and the sensitivity case studies are given in the appendices, section B.3.

The studies show that the CHO method is effective in its main goal, which was to minimize the sensitivity of the mass balance to perfect knowledge of the nitrogen concentration in the producer gas. Under the case studied, if the measured nitrogen concentration was actually different from the true nitrogen concentration by +/- 5%, then the traditional method would predict a gas yield that could be as much as 7% different. With the CHO mass balancing method, the gas yield was affected by less than 0.5% for a nitrogen concentration measurement error of 5%.

The mass balance results from the CHO method (such as the gas yield) showed similar levels of sensitivity to the traditional method for the two other cases simulated: an error in the measurement of carbon monoxide and an error in the amount of ash in the feed material.

The traditional mass balance gave persistently low carbon closures with an average carbon mass balance closure of 92% (in other words the amount of carbon recovered was persistently lower than the amount of carbon that was calculated to have been fed to the gasifier during the conditions). On the other hand the CHO method persistently gave a low nitrogen balance closure, which coincidentally also averaged 92% (in other words the amount of nitrogen in the producer gas was 92% of the amount of nitrogen fed to the gasifier). Some of the potential causes of these errors are discussed in the appendix section dealing with this study, section B.3.

3.7.3 *Effect on Gas Composition and Yield*

One of the biggest parameters that appeared to be influenced by the particle size was the hydrogen to carbon monoxide ratio (H_2/CO) of the product gas. A general trend can be established which appears to be true for all three temperature levels:

$$H_2/CO_{fines} < H_2/CO_{mid} < H_2/CO_{coarse} < H_2/CO_{pellets}$$

This trend, although clearly evident in the data, is hard to explain. All of the particle sizes, with the possible exception of the fines, will be in the thermally thick regime. In this region of particle sizes, the rate of devolatilization will vary with particle size. From the literature reviewed in the previous chapters, larger particles should be associated with lower gas yields from the initial fuel particle and higher char yields. The results of this study could suggest that the conversion of char to hydrogen and carbon monoxide by water vapour is more significant than the steam reformation of volatiles to hydrogen and carbon monoxide. This is quite easy to understand if we assume that the char from large particles spends a large residence time in the fluidized bed (on the order of minutes) compared to the residence time of vapours and gases which are on the order of seconds. Additionally, it may be possible that the additional char in the bed acted catalytically in order to promote the approach of the gas phase towards equilibrium. If this was the case, the gas compositions from the large particle sizes should deviate less from thermodynamic equilibrium than small particles. A thermodynamic approach to this data was evaluated and the deviation from thermodynamic equilibrium of these results is evaluated in section 3.8.

Another trend evident in the data is that the H_2/CO ratio also increased with increasing fuel moisture. This has a relatively obvious explanation since the increase in moisture content in the gasifier promotes the water gas shift reaction in addition to promoting steam reforming reactions of char, tar, and light hydrocarbons. Figure 3.7 shows the measured H_2/CO for each of the tests completed. The H_2/CO given represents the average measurement for the duration of the condition or conditions. Since some conditions were repeated, the number of trials completed is signified by a bracketed number along with the data label on the x-axis. In the case where more than one trial at a given condition was completed, the

presented results are the average of all the data from that condition. In these cases, error bars are provided which signify the range of observed conditions.

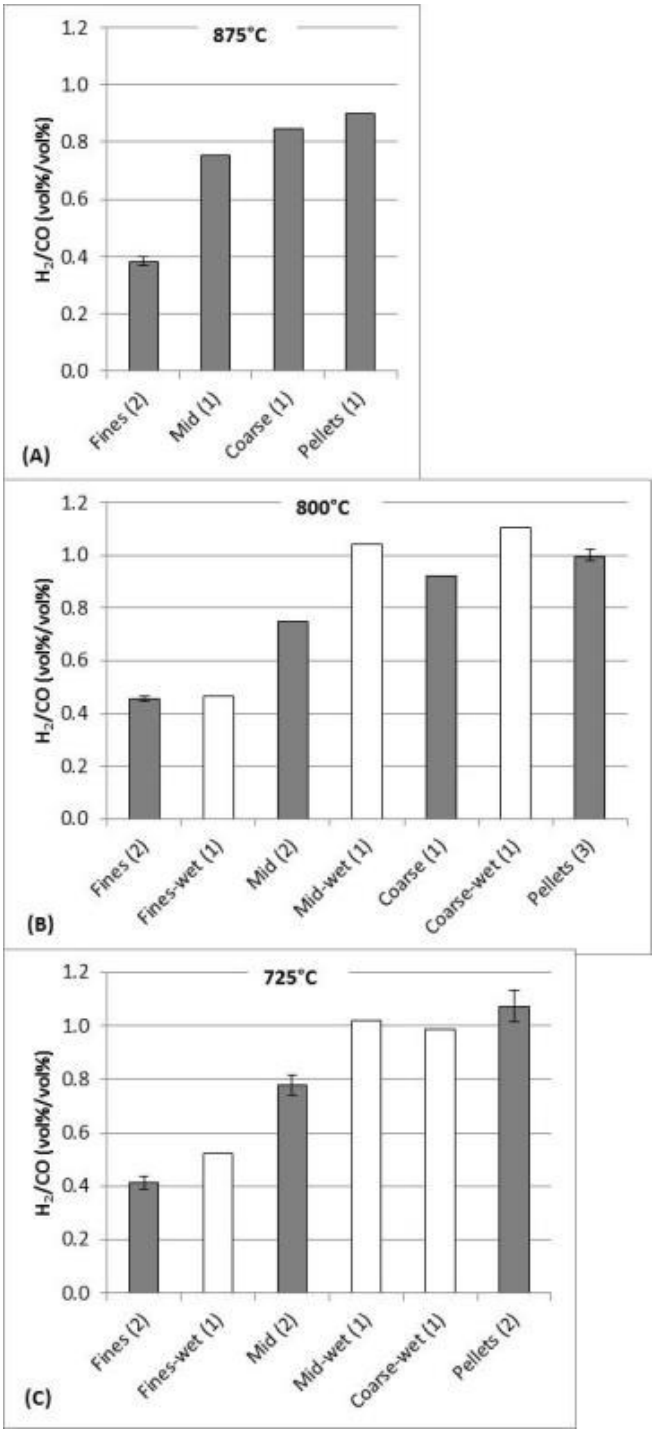

Figure 3.7: Observed hydrogen to carbon monoxide ratio for the different particle sizes, forms, and moisture levels. (A) Gasification at 875°C, (B) gasification at 800°C and (C) gasification at 725°C.

A noteworthy observed effect of the higher moisture fuels compared to the dry fuels was the depressed heating value of the producer gas for the moist fuels. Figure 3.8 highlights this trend. As discussed in earlier, one of the key operational differences between the moist and dry fuels was that less fuel input was required at the same air flow rate (and thus higher equivalence ratio) in order to achieve the same bed temperature. Because of this, the depressed heating value of the producer gas from the wet fuels was impacted by the fact that the producer gas from the moist fuels was more diluted with nitrogen from air.

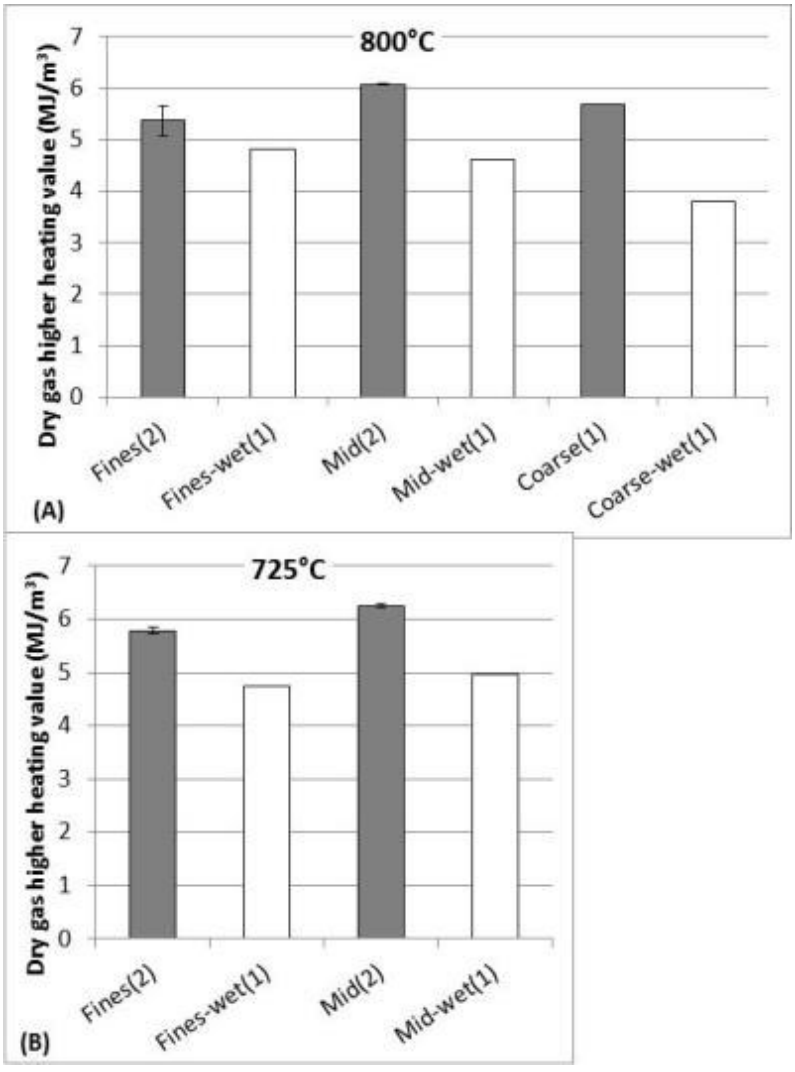

Figure 3.8: Comparison of higher heating value of the dry gas for dry and moist biomass feed. (A) Gasification at 725°C, and (B) Gasification at 800°C.

Figure 3.9 shows the hydrogen yield from each of the particle sizes and forms of the dry fuels with respect to the gasification temperature. The trend lines in the figure represent a quadratic best fit of the data series. The trend lines are not meant to represent a modeled prediction or an accurate description of the behavior of the trend of the data. The trend lines are meant to help data points of the same particle size or form and to help recognize the implied direction of the trend.

The hydrogen yield reported in Figure 3.9 is based on the yield determined by the CHO mass balance technique. The hydrogen yield from the traditional mass balance approach is provided in Appendix D. The CHO and the traditional mass balance techniques display the same trends although the absolute values can be different (the relative differences between the values from the traditional and CHO mass balance technique are up to 10% in some cases). The pelletized material showed the highest yield of hydrogen gas (per kg of dry ash-free biomass fed to the gasifier) than any other fuel type despite the fact that the pellets were actually marginally drier than the other fuels (less elemental hydrogen input from moisture). For the mid and pelletized biomass the yield of hydrogen gas also increased with increasing bed temperature.

Figure 3.10 shows the yield of light hydrocarbon gases from each of the dry fuels. In this case, the mid fraction yielded the greatest amount of light hydrocarbons gases[10]. The difference between the yields of light hydrocarbon gases for the mid fraction compared to the yields of light hydrocarbon gases from the fines, coarse, and pelletized material increased with increasing gasification temperature.

[10] In this thesis "light hydrocarbon gases" refers to the sum of methane, acetylene, ethylene, ethane, and propylene.

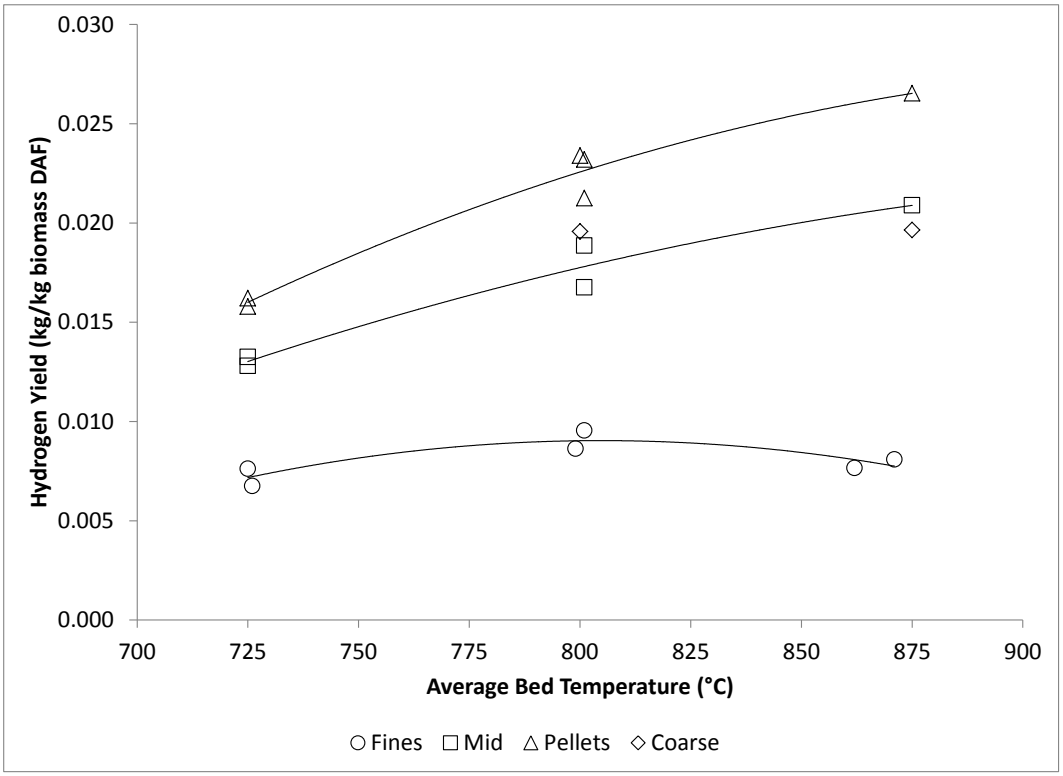

Figure 3.9: Hydrogen gas yield based on the CHO mass balancing approach.

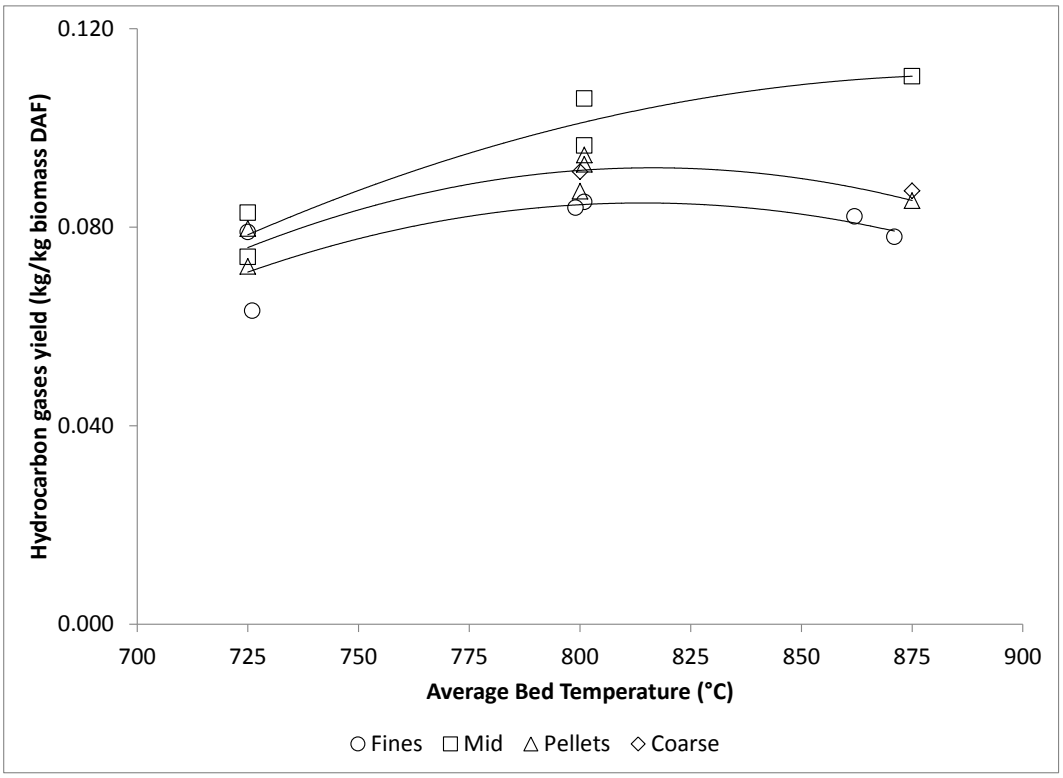

Figure 3.10: Light hydrocarbon gases (C1-C3) yield based on the CHO mass balance approach.

3.7.4 Effect on Tar Composition and Yield

The amount of gravimetric tar measured was also affected by the different particle sizes and bed temperatures. Figure 3.11 shows the gravimetric tar measurements from each test. One of the most apparent effects is that the amount of gravimetric tar greatly decreased with increasing temperature. The tar measurements also displayed a high level of irreproducibility; many of the repeated runs show substantially different tar measurements from the original run. This uncertainty stems for a variety of factors which may include:

- *Temporal effects:* It is recognized that the bed material ages with time. As the bed material is recycled, the concentration of some components, such as potassium and calcium increases while other components like iron and magnesium decrease. The composition of the bed material has been shown in various works to be able to have a strong impact on the amount of tar produced from biomass gasification.
- *Fuel heterogeneity*: The differences between the fuel analysis of the "fines" and of the "pellets" were previously discussed. Although the pellets and fines were the same material (the pellets were made from the fines), their fuel analysis showed differences. This is indicative of fuel heterogeneity and the level of differences possible within a fuel.
- *Methods*: The evaporation method for the determination of gravimetric tar was studied during this research and was covered in another undergraduate student thesis (Robinson, 2012). It was found that it is reasonable to expect a standard error on the evaporation methods of 20%.
- *Sampling error*: The tar sampling methods are cumbersome methods consisting of many steps, thus it is possible that some error may have occurred. Examples of the possible errors could include a transposition error while recording values from the tar sampling activities, electrical failure of heated line, and vibration of impinger assembly opening one of the joints to a small leak of ambient air. Although this is not expected to happen often, even if this were to occur once every 10 measurements, it could introduce some difficulty into interpreting the data. The reason for a repeat of the dry, mid-size fuel fraction at 725°C was because the gravimetric tar results appeared suspiciously low compared to expected results. A repeat was carried out to

see if the suspiciously low result was reproducible. The repeat showed a much greater tar level in the gas than the original run, much closer to the expected trend widely reported in literature (increasing tar content with decreasing gasification temperature).

- *Bed Level*: The first two experimental runs (first four conditions) were completed with a larger amount of bed material (the initial bed charge was 36% greater in these cases). It has been elected to still include those results in all the tables. The bed level varied according to how carbon and bottom ash accumulated in the bed over the duration of the run which led to differences in the bed height between the fuels. This means that keeping a constant bed height between runs was not possible, even if a constant initial charge of bed material was used. For all discussions within this chapter it should be recognized that the results are possibly confounded with the bed height although no clear biases could be detected that are attributable to bed level.

From Figure 3.11, it can be observed that the fines consistently yielded a product gas with the highest gravimetric tar loading at all temperatures. It appears that the following relation between the gravimetric tar content of the gas and the particle size or form existed:

$$C_{tar,fines} > C_{tar,mids} \approx C_{tar,pellets} > C_{tar,coarse}$$

There does not appear to be any difference in the gravimetric tar content of the gases produced with moist materials compared to the dry (at least no different that can be claimed to be outside of the variation in the tar measurements). It must also be considered that the more moist fuels had to be run at a higher ER in order to achieve the same bed temperature. The higher ER also has a tendency to lead to a higher gas yield (due to the increased contribution of air to gas yield).

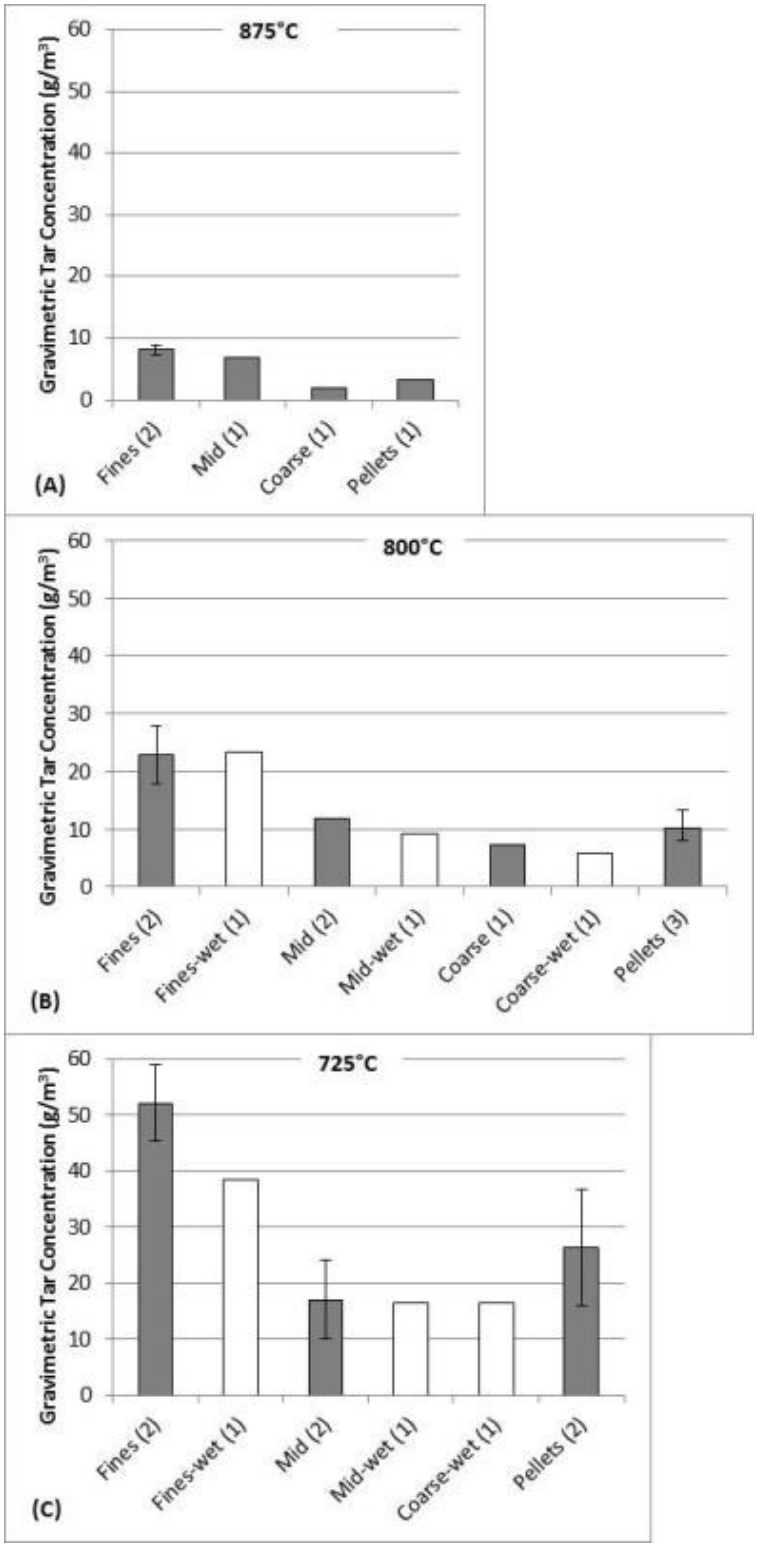

Figure 3.11: Comparison of measured gravimetric tar levels across different particle sizes, forms, moisture level, and bed temperatures. (A) Gasification at 875°C, (B) gasification at 800°C and (C) gasification at 725°C.

Figure 3.12 shows the measured gravimetric tar yield with specific emphasis on the comparison between the dry and wet fuels. On the basis of the amount of tar that was yielded (as opposed to the tar concentration in the gas), the yield of the tar for the moist materials appears to be essentially the same as the dry material. This indicates that extra moisture in the particle had essentially no impact of the reformation of tars.

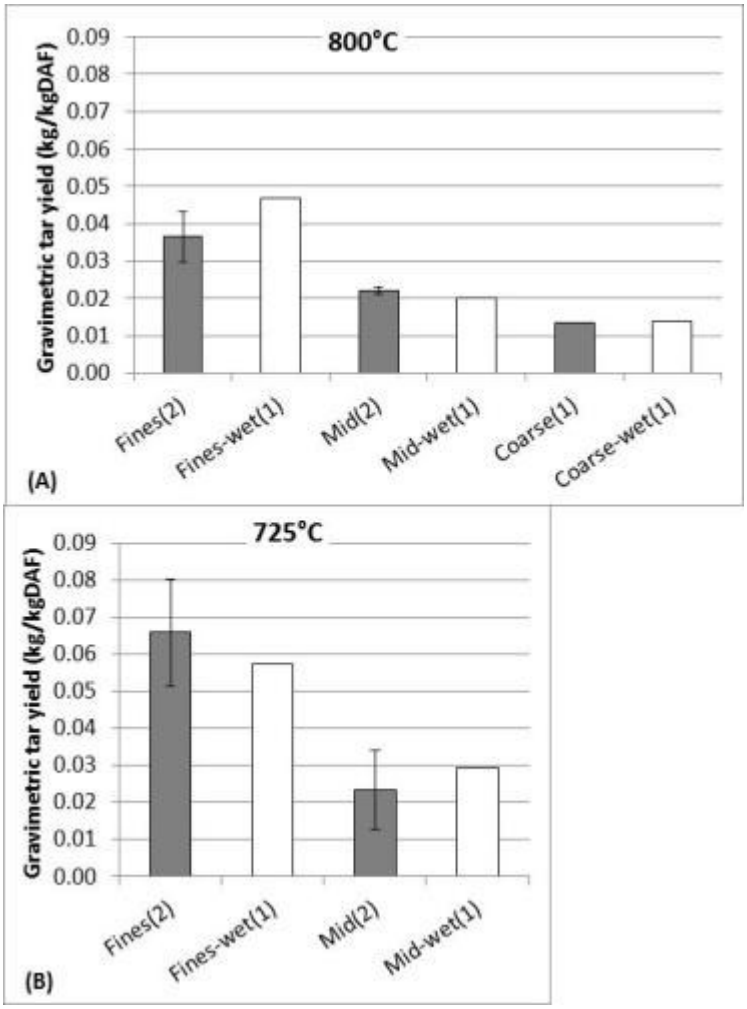

Figure 3.12: Comparison of gravimetric tar yield for dry and moist feed. (A) Gasification at 800°C, and (B) gasification at 725°C.

Measurements of the tar composition were also carried out by GC/MS on select conditions. The objective was to carry out GC/MS analysis of the tar on every run completed at the central bed temperature (800°C). Research was also being conducted during the runs on alternative tar sampling methods, which required that additional tar samples be analyzed by GC/MS from the reference tar sampling method. Thus compositional data for the tars is

available for all conditions at the 800°C plus some data at 725°C and 875°C. Table 3.15 shows the GC/MS data obtained during the experimental campaign that has been grouped according to tar classification[11].

Table 3.15: Results of tar analysis by GC/MS for the testing campaign.

Fuel	Avg. Bed T. °C	Benzene g/m^3 [9]	Class 2 tar g/m^3 [9]	Class 3 tar g/m^3 [9]	Class 4 & 5 tar g/m^3 [9]
Fines	871	7	0.7	3.9	4.3
Fines	801	6.8	4.3	7.7	3
Fines	799	8.6	3.9	8.7	2.8
Fines	726	2.8	5.8	5.2	1.2
Fines	725	4.4	8.2	8.4	1.5
Fines-wet	800	5.6	3.3	6.1	2.7
Fines-wet	725	2.4	4.7	4.2	0.9
Mid	801	7.4	3.2	7.8	3.7
Mid	801	5.9	2.3	6.3	2.7
Mid	725	2.3	4.3	4.4	1.4
Mid-wet	802	5	1.3	4.3	2.1
Coarse	875	3.8	0.2	2.1	1.6
Coarse	800	4.4	1.7	4.1	2
Coarse-wet	800	3.7	1	3.1	1.8
Coarse-wet	725	2.5	2.9	3.3	1
Pellets	801	6.5	2.8	6.4	3.5
Pellets	801	6.4	2	4.7	1.9
Pellets	800	4.5	1.6	4.1	1.6
Pellets	725	4.3	6.1	6.1	1.6

[9] **One m^3 is standardized to 0°C, 1 atm on a dry basis.**

Figure 3.13 shows the measured concentration of benzene and GC/MS tar classes in the dry gas from each fuel type. The trends from the GC/MS tar data are not the same, or as prominent, as the trends from the gravimetric tar measurements. The GC/MS tar results appear to indicate that there are only small differences between the amounts of tar produced by different particle sizes and forms. The fact that different conclusions can be drawn based on whether gravimetric tar or GC/MS is considered falls in-line with previous experience at CanmetENERGY. Depending on the gasification conditions, the amount of tar reported from GC/MS and that reported from gravimetric measurements can be

[11] A simplified summary of the tar classification system is that class 2 tars comprise the oxygenated tar species, class 3 tars are benzene derivatives, class 4 tars are 2-3 ring PAHs, and class 5 tars are 4-5 ring PAHs. For the presentation of this thesis, class 4 and 5 tars have been grouped together.

substantially different and do not necessarily follow the same trends. The GC/MS results still suggest that the highest amount of tar is measured in the gas from the gasification of the smallest particle size tested and the lowest amount for the largest particles tested. The difference is not as profound as with the gravimetric tar measurements. For example, at 800°C the fines produced a gas which on average contained 125% more gravimetric tar than the pellets, but only 59% more GC/MS tar. This difference between gravimetric and GC/MS tar is even more profound when comparing the fines to the mid material. At 800°C, the fines on average produced 92% more tar than the mid material but only 17% more GC/MS tar.

The GC/MS results show also that the composition of the tar does not seem to vary much with particle size and form. The reader is reminded that only certain components are measured by GC/MS. The components detected by GC/MS are typically the more stable, most mature tar species. This may be an indication that many of the reactions that transform primary tar to secondary to tertiary tar are occurring under similar conditions and are thus not highly dependent on the conditions within the particle. The mismatch between gravimetric tar and GC/MS tar results suggest that the fines produce the highest amount of tar that is not amenable to quantification by GC/MS. As such a significant portion of the tars from the fines may be immature (or in other words produced at some combination of low temperature or short residence time). This is indication that the gasification of some portion of the fines was taking place outside of the bed (on the surface and in the freeboard).

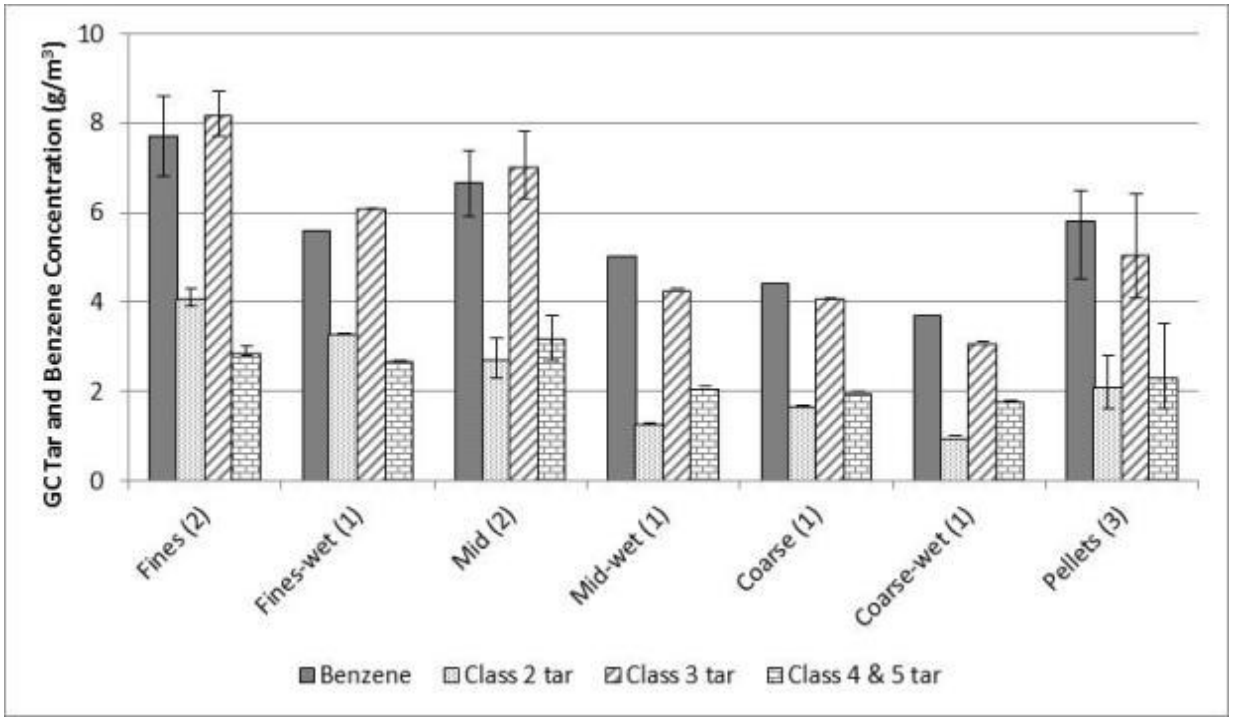

Figure 3.13: Comparison of measured concentration of benzene and GC/MS tar levels across different particle sizes, forms, and moisture level at bed temperature of 800°C.

3.7.5 Effect on Char Conversion and Cold Gas Efficiency

The char was recovered and analyzed in every run. The results however indicate that the recovery of char was incomplete (based on the mass balances) and obtaining a representative char sample was challenging. The appendices (section A.2) present the char results in detail. Because of the unreliability of the char results, the carbon conversion presented in this thesis is based on the carbon content and yield of the producer gas (instead of the opposite approach of subtracting the amount of carbon in the char from the amount of input carbon).

Figure 3.14 shows the comparison of carbon conversion to gas with specific emphasis on the comparison between dry and moist fuels (this is only the conversion to gas and does not include amount of carbon converted to tar).

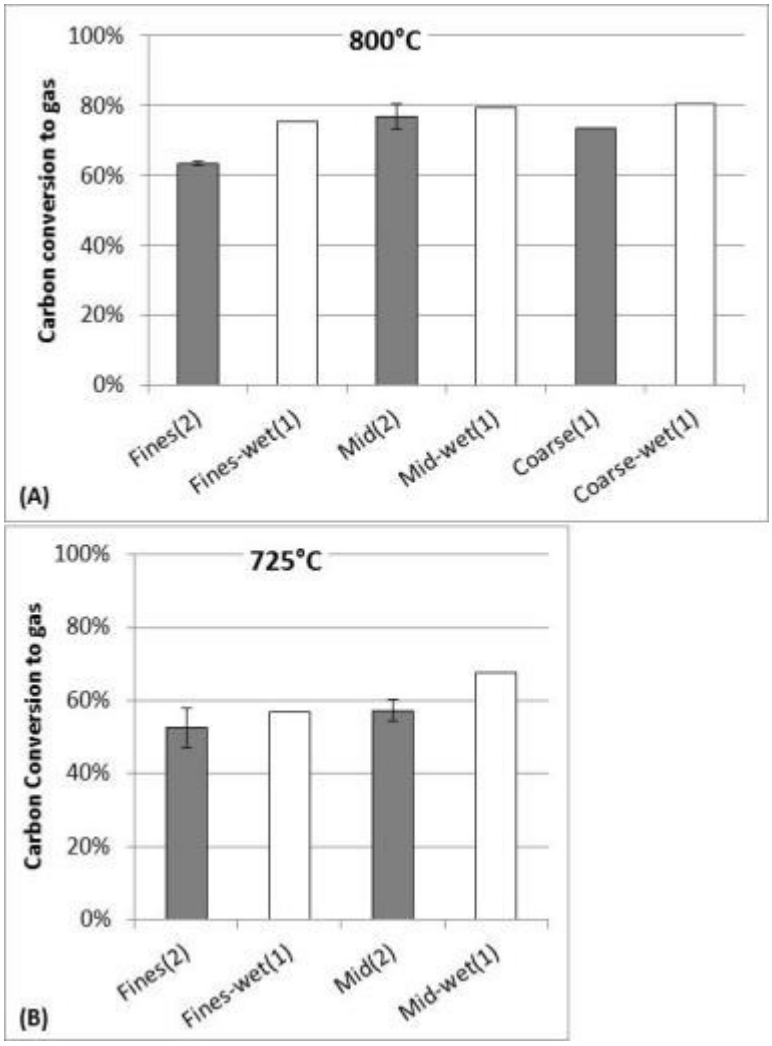

Figure 3.14: Comparison of the carbon conversion to gas for the dry and moist feeds. (A) Gasification at 800°C, and (B) Gasification at 725°C.

Figure 3.14 appears to indicate that there may be a slight enhancement of carbon conversion to gas due to increased particle moisture. At 800°C, the average carbon conversion to gas for dry fuels (excludes pellets since there are no "wet" pellets), is 71% compared to 78% for the moist fuels.

Figure 3.15 shows the carbon conversion comparison between the dry fuels. This is the only result where a different trend might be interpreted depending on whether the data was evaluated from the traditional or the CHO mass balance technique. From the CHO method it appears that at lower temperatures the pellets have the greatest level of carbon conversion.

From the traditional approach (see Figure D.3 in the appendices) it appears that the level of carbon conversion for the mid material and the pelletized fuel is equivalent.

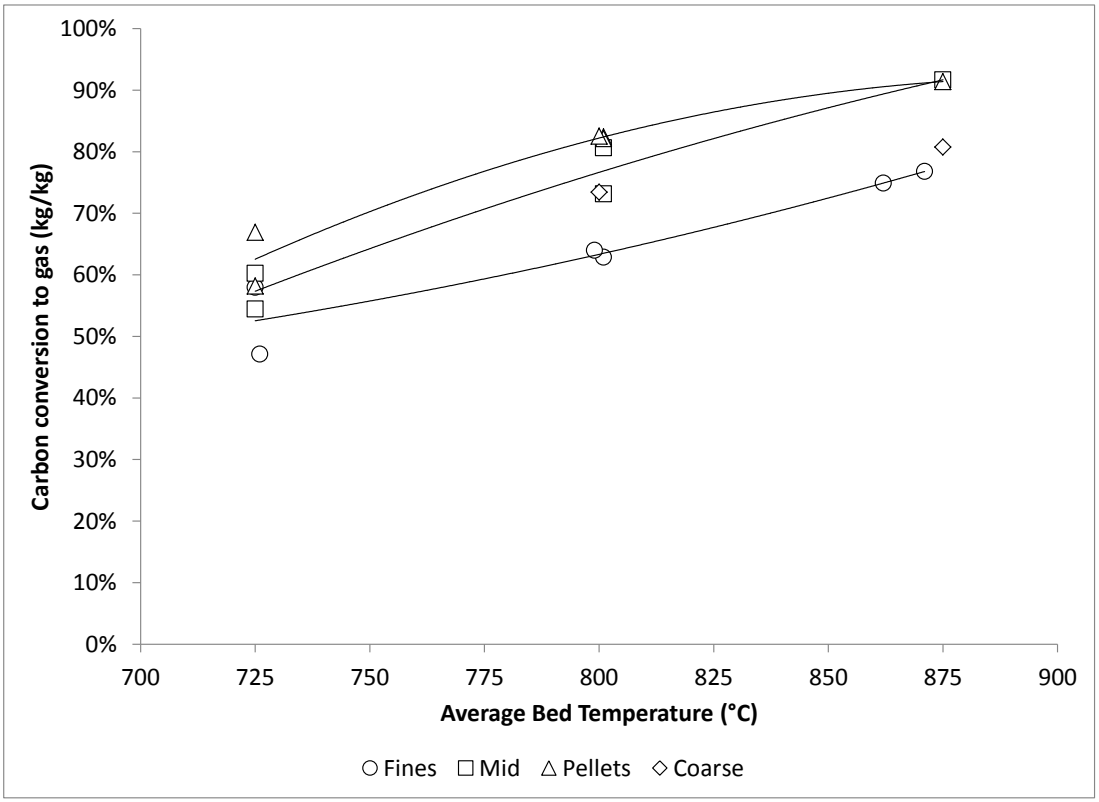

Figure 3.15: Percentage of carbon converted to gases based on the CHO mass balance approach.

Figure 3.15 shows that the carbon conversion to gas increases with increasing temperature for all the fuel sizes and forms. Despite their small particle size, the fines show a depressed carbon conversion to gas compared to the larger particle sizes. This probably is heavily related to the increased entrainment of char from fines and poor mixing of the fines with the bed media. Once again this is evidence that some of the conversion of the fines is taking place outside of the bed.

Figure 3.16 shows a comparison of the determined cold gas efficiency with an emphasis on the comparison between the moist and dry fuels. Across the variability of the data, there is not a major difference between the cold gas efficiency of the wet fuels and the dry fuels. The wet fuels were gasified at an increased equivalence ratio. For the cold gas efficiency, a big factor was that the moist fuels showed an elevated level of carbon conversion relative to the

dry fuels (this could be due to the increased ER or it could be due to the influence of steam). Because of the increase in carbon conversion for the moist fuels, the cold gas efficiency of the dry and the wet fuels was fairly similar.

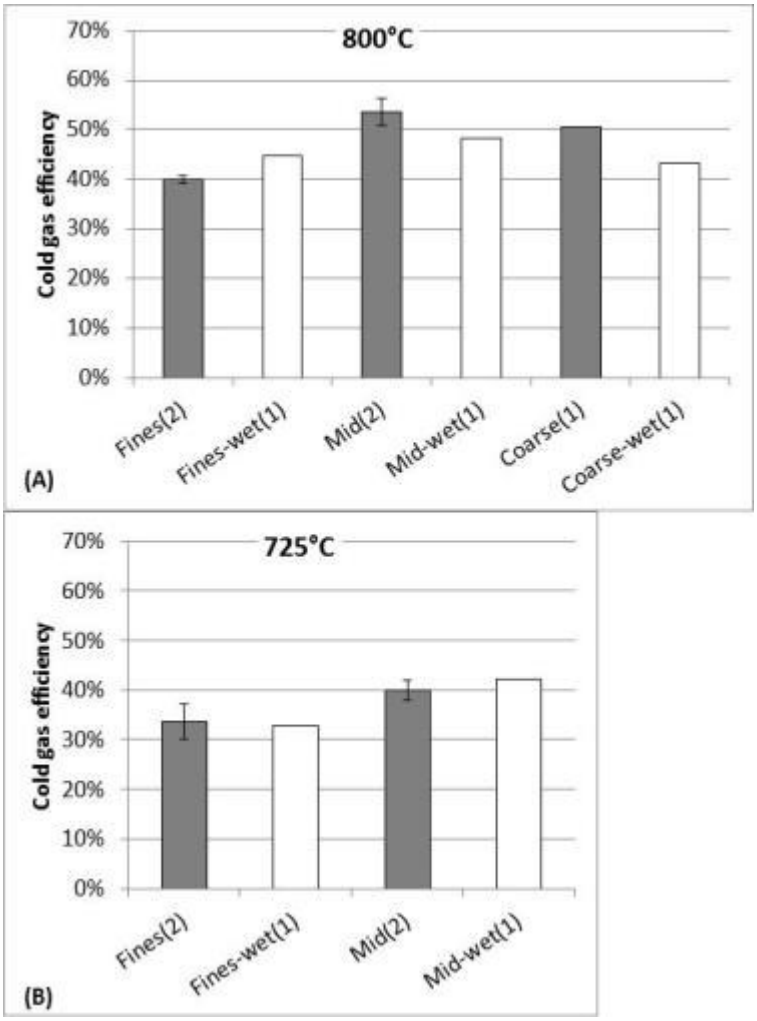

Figure 3.16: Comparison of the cold gas efficiency of the dry and moist fuels. (A) Gasification at 800°C, and (B) Gasification at 725°C.

Figure 3.17 shows the cold gas efficiency of each of the dry fuels with respect to temperature (whereas the last figure focused on the dry vs. moist comparison). The cold gas efficiency of the gasification of dry fines stays in between 30 and 41% across all three bed temperature levels (the highest cold gas efficiency actually being observed at 800°C) whereas for the mid and pellets the cold gas efficiency rises from 37 to 61% as the temperature increases from 725°C to 875°C.

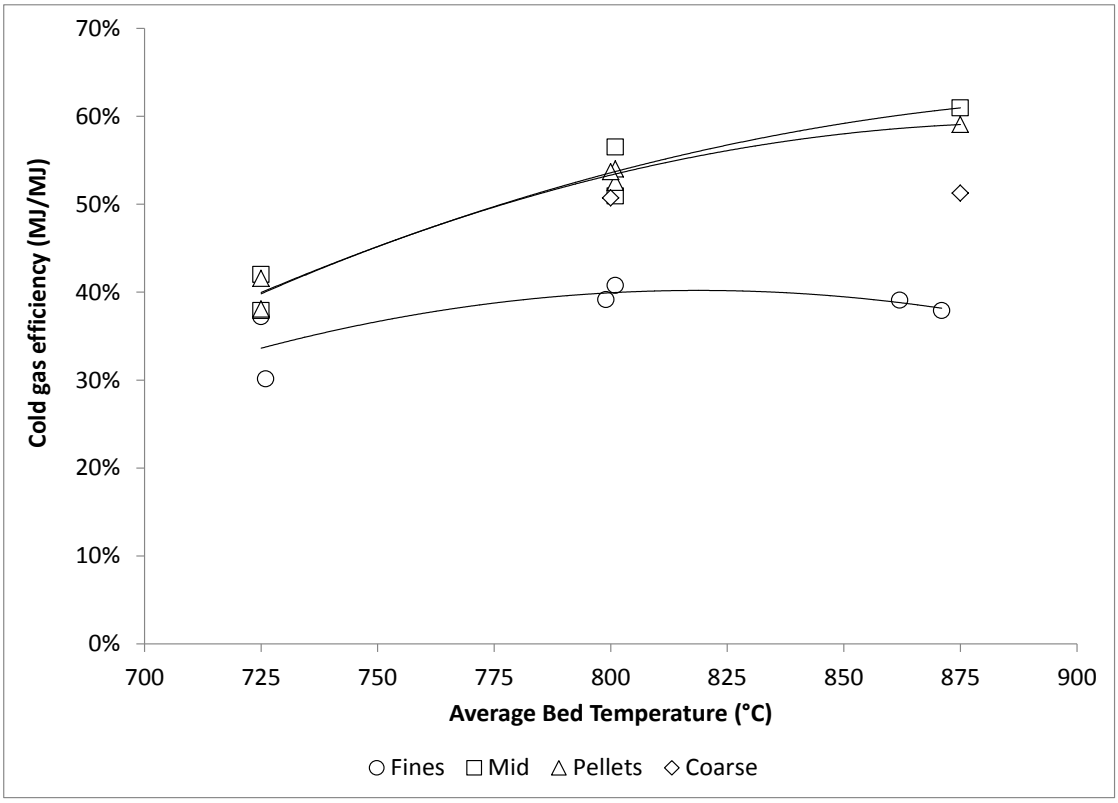

Figure 3.17: Cold gas efficiency as calculated based on the CHO mass balance approach.

3.7.6 Energy Balance Results

So far, the measure of efficiency that has been considered has been the cold gas efficiency. The cold gas efficiency does not account for the useful energy that is still contained in the char and tar or the sensible heat of the gas. The tar and char could be separated in order to be recycled into the gasifier to produce more gas, or the char and tar could be separately used as an energy product. The sensible heat of the producer gas could be used within heat integration strategies (i.e. for example providing heat for the production of steam in a pulp mill) or the heat could be used to preheat the gasification medium which would enhance process efficiency. In order to understand the distribution of the energy in the products from the gasification, an energy balance was performed on the experiments using the mass balance data obtained from the CHO technique. Tabulated energy input and the energy outputs are given in the appendices (section D.2). In order to carry out the energy balances, the heating value of the tar is assumed since it was not measured. The higher heating value of the tar is assumed to be 40 MJ/kg which is a crude approximation. For comparison, the higher heating value of benzene and naphthalene is 41.8 MJ/kg and 40.2 MJ/kg,

respectively. Since the contribution of tar to the energy balances is small, the coarseness of this estimate should not have a substantial impact on the results.

Figure 3.18, Figure 3.19, and Figure 3.20 give the calculated energy distribution for the products of the gasification at bed temperatures of 875°C, 800°C, and 725°C, respectively. The energy value given in the graphs only accounts for the heat of combustion of the component. The *thermal losses* portion includes heat loss from the system, sensible heat contained by the products, and the latent heat of the products. It is important to note that the thermal losses have been determined by difference (instead of being measured or rigorously calculated).

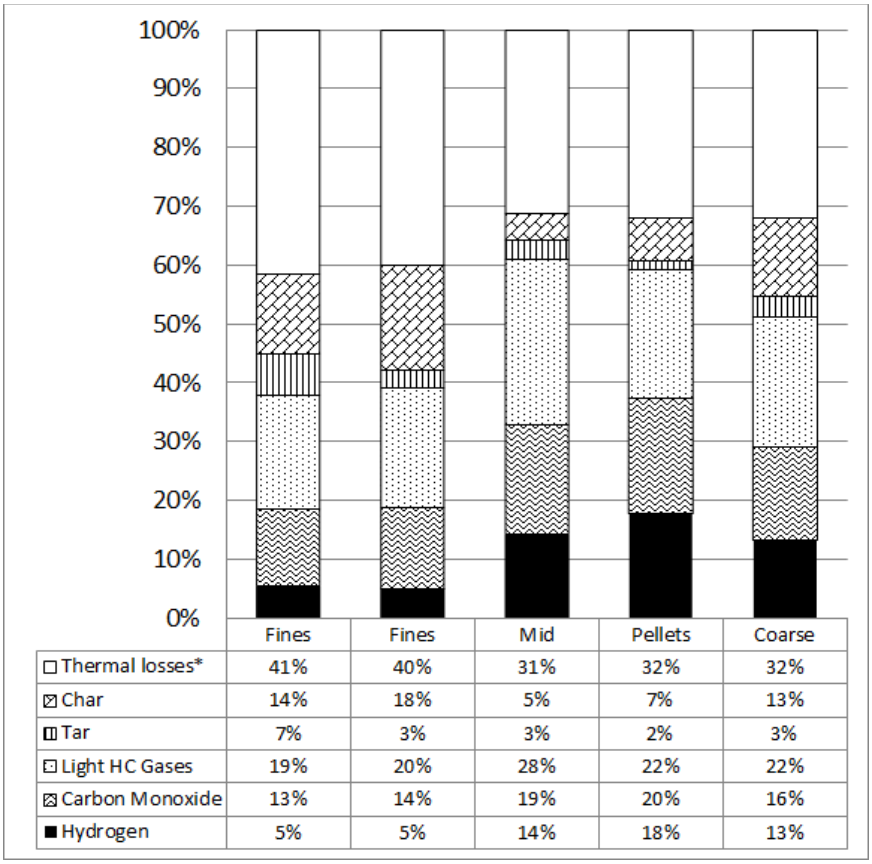

	Fines	Fines	Mid	Pellets	Coarse
Thermal losses*	41%	40%	31%	32%	32%
Char	14%	18%	5%	7%	13%
Tar	7%	3%	3%	2%	3%
Light HC Gases	19%	20%	28%	22%	22%
Carbon Monoxide	13%	14%	19%	20%	16%
Hydrogen	5%	5%	14%	18%	13%

Figure 3.18: Energy distribution of the gasification experiments carried out at bed temperature of 875°C.

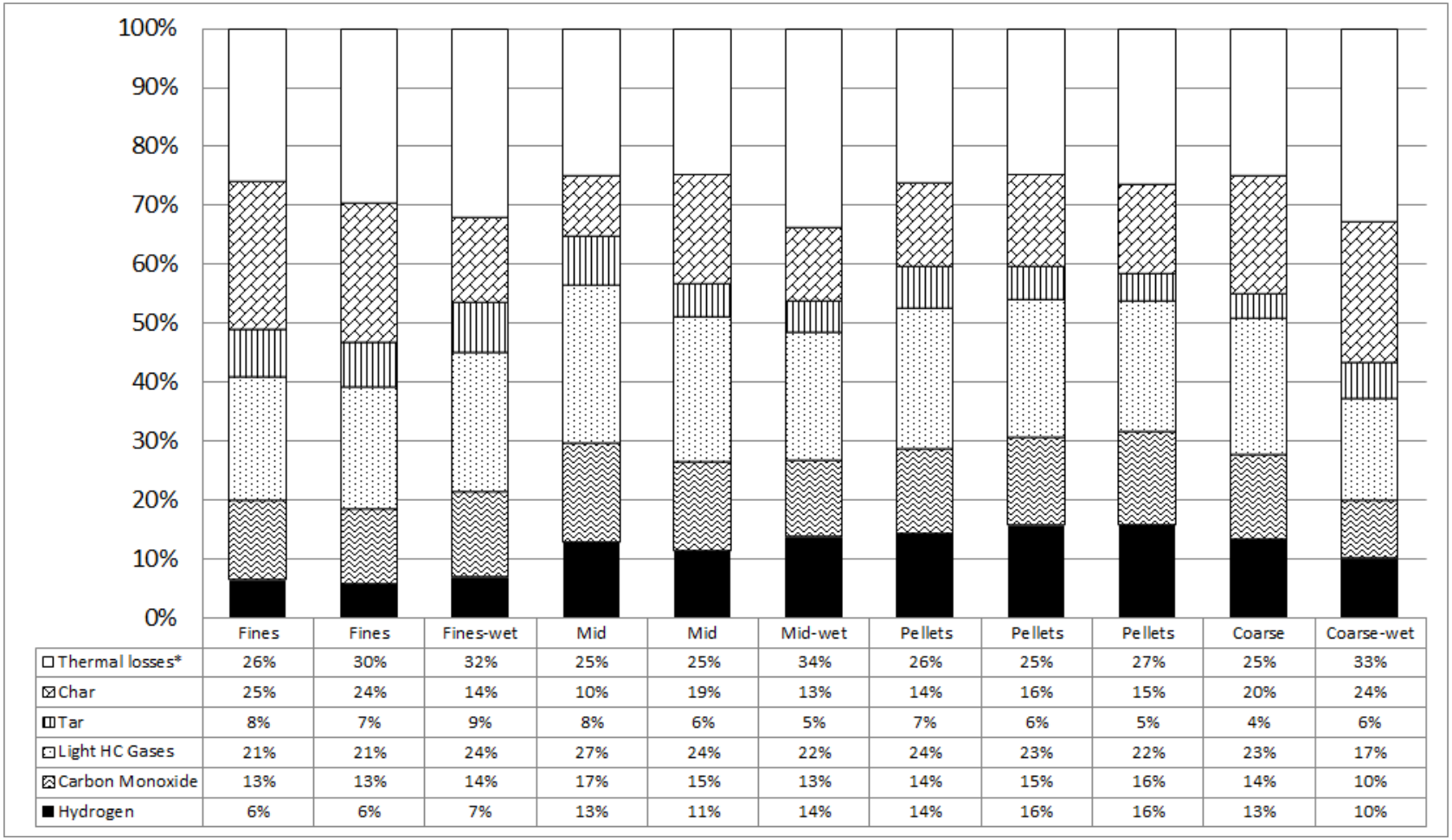

	Fines	Fines	Fines-wet	Mid	Mid	Mid-wet	Pellets	Pellets	Pellets	Coarse	Coarse-wet
Thermal losses*	26%	30%	32%	25%	25%	34%	26%	25%	27%	25%	33%
Char	25%	24%	14%	10%	19%	13%	14%	16%	15%	20%	24%
Tar	8%	7%	9%	8%	6%	5%	7%	6%	5%	4%	6%
Light HC Gases	21%	21%	24%	27%	24%	22%	24%	23%	22%	23%	17%
Carbon Monoxide	13%	13%	14%	17%	15%	13%	14%	15%	16%	14%	10%
Hydrogen	6%	6%	7%	13%	11%	14%	14%	16%	16%	13%	10%

Figure 3.19: Energy distribution of the gasification experiments carried out at bed temperature of 800°C.

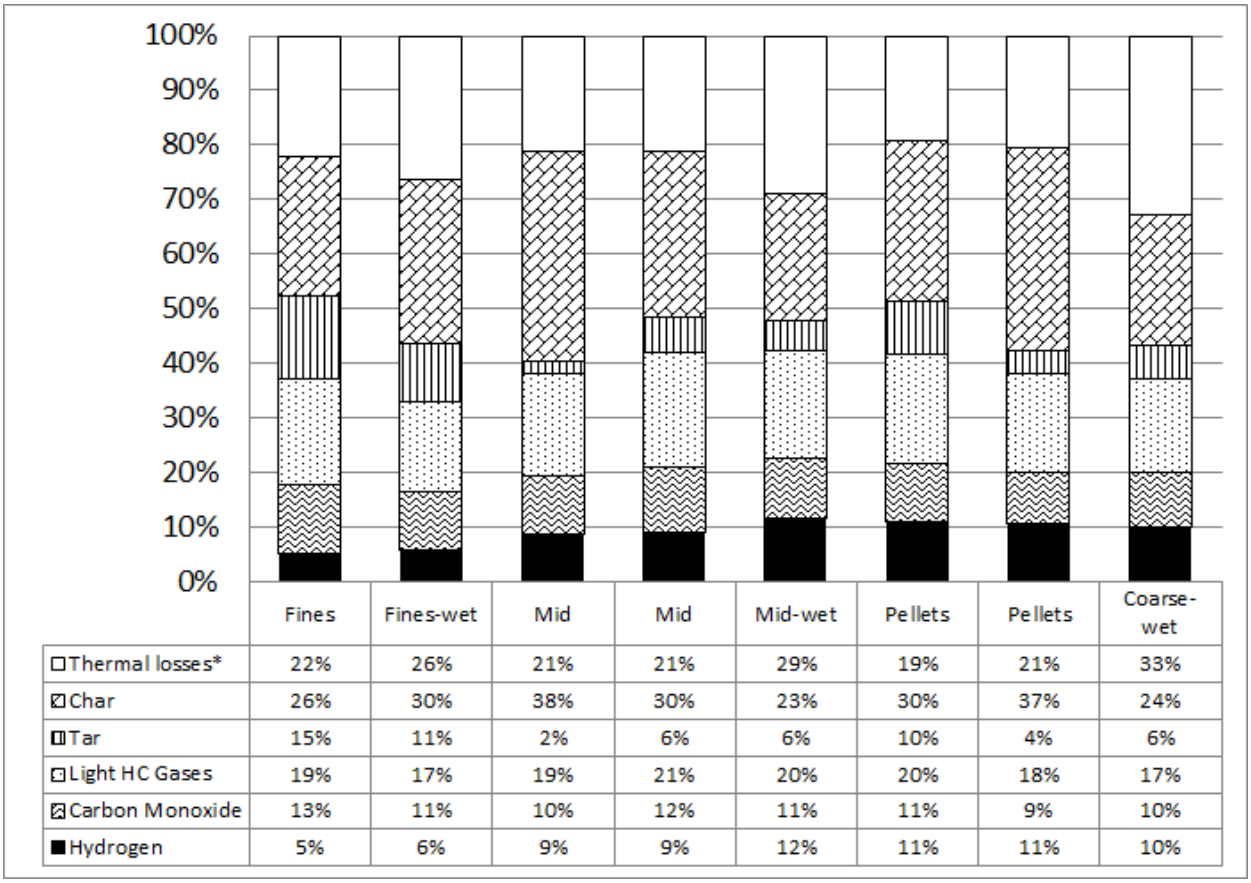

	Fines	Fines-wet	Mid	Mid	Mid-wet	Pellets	Pellets	Coarse-wet
Thermal losses*	22%	26%	21%	21%	29%	19%	21%	33%
Char	26%	30%	38%	30%	23%	30%	37%	24%
Tar	15%	11%	2%	6%	6%	10%	4%	6%
Light HC Gases	19%	17%	19%	21%	20%	20%	18%	17%
Carbon Monoxide	13%	11%	10%	12%	11%	11%	9%	10%
Hydrogen	5%	6%	9%	9%	12%	11%	11%	10%

Figure 3.20: Energy distribution of the gasification experiments carried out at bed temperature of 725°C.

If the entire product distribution is considered (the tar, char, and gas) as opposed to just the gas, the efficiency of the dry fuels of mids, coarse, and pelletized material are roughly equivalent. At 875°C, the total cold efficiency[12] of conversion from biomass to gas, tar, and char for dry-mids, dry-coarse, and pelletized feed is 68 – 69 %. At 800°C, the efficiency of the conversion for dry-mids, coarse and pellets is between 73-75%. At 725°C the efficiency for the dry-mids and pellets is 79-81%. The observed total cold efficiencies are also important because they imply that although the gas composition may be altered with different particle sizes, the total cold efficiency is roughly independent of particle size.

[12] The efficiency of conversion from biomass to gas, tar, and char has been termed *total cold efficiency* which is in contrast to cold gas efficiency which is the conversion efficiency from biomass to gas only. The efficiencies are "cold" because they compare the energy in the products at 25°C and do not consider the energy tied up as sensible or latent heat.

The relationship between bed temperature and total cold efficiency is the opposite of what was observed for the cold gas efficiency. In contrast to the total cold efficiency, the cold gas efficiency for the mid and pelletized material increased as the bed temperature increased between 725 – 875°C, whereas for the fines and coarse material the cold gas efficiency was flat across the same temperature range. The biggest contributor to the difference between cold gas efficiency and the total cold efficiency is the char. At 725°C, the heating value of the char can account for up to 38% of the input energy. This emphasizes on the importance of utilizing the char either by recycling it to the gasifier, using it as a by-product, or making process modifications to achieve better char conversion to gas.

The moisture does have an impact on the total cold efficiency. Although the cold gas efficiency was not greatly affected by moisture level, the total cold efficiency was lower for the moist fuels than the dry fuels at a constant temperature level in every case. This is expected since for the moist fuels, energy from the gasifier must be expended in order to evaporate the moisture in the fuels. The energy tied up in the latent heat of water is included in the "thermal losses".

Traditionally, the aim of gasification has been to convert the feed material into a mix of carbon monoxide and hydrogen. The energy distributions show that with the system, conditions, and feed used for this experimental campaign that a substantial portion of the energy contained in the gas phase is attributed to light hydrocarbon gases (instead of hydrogen and carbon monoxide). With the fines, the amount of heating value contained in the light hydrocarbons is always greater than the heating value of the carbon monoxide and hydrogen combined. In order to get good efficiency for any process that requires syngas[13] (a process that cannot use producer gas), the light hydrocarbons will need to be reformed to produce carbon monoxide and hydrogen. The combined cold efficiency from feed material to carbon monoxide and hydrogen reached a maximum of 38% (pellets at 875°C) and was as low as 17% (fines-wet at 725°C) over the range of conditions tested. In other words, the amount of energy contained in carbon monoxide and hydrogen was always less than half, in many cases less than one quarter, of the energy contained in the feed material over a range

[13] In this document the term *syngas* refers to a mixture where CO and H_2 are the only combustible components.

of conditions. For processes requiring syngas (exclusively H_2 and CO), this emphasizes the importance of research for gas cleaning technologies that are also capable of reforming light hydrocarbons in addition to removing tars and other gaseous contaminants if producer gas from biomass gasification in fluidized beds is to be used for syngas processes based on carbon monoxide and hydrogen chemistry. On the other hand, this data may also point to a promising potential for the single step conversion of biomass to light hydrocarbons if through process optimization the yield of light hydrocarbons could be modestly improved. A product gas rich in light hydrocarbons could potentially be purified and directly injected in natural gas distribution networks depending on gas characteristics (gas dewpoint, Wobbe index, flame speed, etc.). This would greatly simplify current strategies for the manufacture of renewable natural gas (RNG) from biomass if biomass can be thermochemically converted in a single step to a product suitable, after clean-up, for injection into the natural gas grid.

The energy balances also show the variability of the contribution to the energy balance from char. This emphasizes the importance of improving the methods for collecting and measuring the amount of char produced from this system. It is important to understand whether the amount of char produced is indeed that variable or whether the variability observed is an artifact of the collection and data analysis methods.

3.8 **Interpretation of the Results**

3.8.1 Operational Observations

The purpose of the experimental design was to be able to compare different particle sizes, moisture levels, and the impact of pelletization from the same parent material at directly comparable conditions. The conditions tested are not always directly comparable. For example, due to the level of conversion of the solid fuel and due to gas composition differences, the gas velocity in the upper regions of the bed may not be the same between different trials despite the fact that the amount of input fuel is similar and the amount of fluidizing air provided is the same. This section outlines some of operational differences between the different particle sizes, moisture levels, and forms. These operational differences may be useful in explaining why there were some of the observed differences in measured parameters (i.e. gas composition or tar concentration) or they may be useful in

providing insight for what to expect when fuel pre-treatment regiments are adjusted in operating gasifiers.

Since the feed rate of each fuel needed to be varied in order to control a desired bed temperature and a constant airflow rate was used during the gasification, it is possible that each fuel type would result in a different equivalence ratio. Equivalence ratio has been shown by many authors to have an impact on the performance of fluidized bed gasifiers, most notably in the work of Narváez et al. (1996). Figure 3.21 shows a comparison of the ER that each of the tests was carried out at. From the figure it can be seen that for all the dry fuels, a similar ER value was used in order to maintain the same bed temperature. The two tests of the finest fuel at 875°C appear to indicate that those tests required a slightly elevated ER to run these fuels compared to the mid, pellets, and coarse material. Based on the results it is reasonable to directly compare all the dry fuels at the same bed temperature without any concerns about confounding effects from the equivalence ratio. The wet fuels required a higher ER to run at the same bed temperature as the dry fuels. This may have had an effect on one of the observed results - it was observed that slightly better carbon conversion to gas was observed with the moist fuels. Was this effect due to the presence of the additional water vapour or was it because there was more oxygen available in the gas? Although all of the wet fuels were intended to have the same moisture content of roughly 30%, the moisture measurements show that the actual obtained moisture content was 25, 24, and 31 wt% for the fines, mid, and coarse material, respectively. This likely explains the fact that the wetted coarse fuel required the highest equivalence ratio to run at the same bed temperature because it was the wettest of all the fuels by a significant margin.

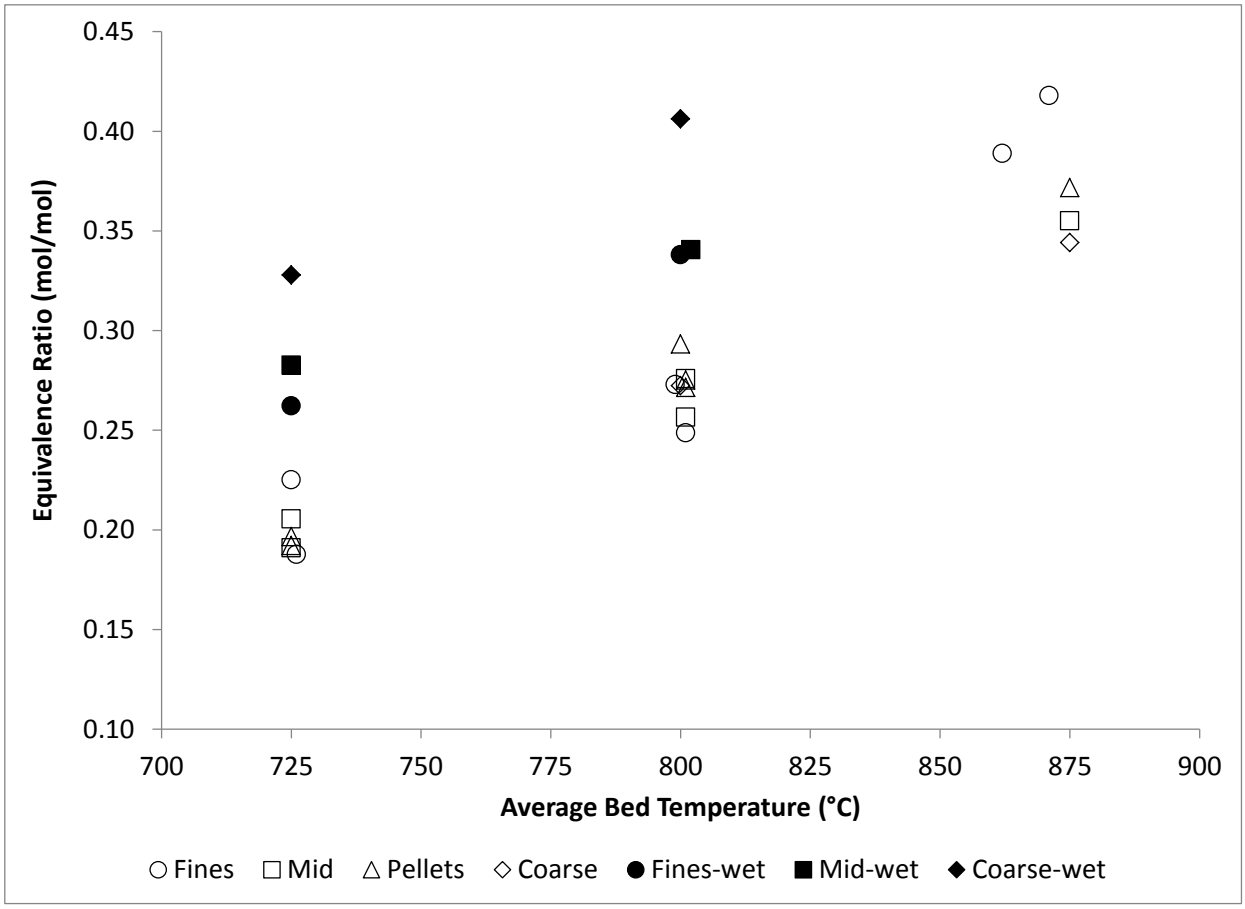

Figure 3.21: Comparison of the operating equivalence ratio between dry and wet fuels.

Another element of the analysis to keep in mind is that although particle sizes were compared at three bed temperatures, the temperature profile in the freeboard cannot be fixed since it will depend on a variety of factors including gas production, heat loss through the freeboard, and reactions occurring in the freeboard. Figure 3.22 shows how the temperature varied with height inside the gasifier for the dry fuels gasified at an average bed temperature of 800°C. Figure D.5 to Figure D.8 in the appendices (section D.2) show the temperature profile for each condition tested.

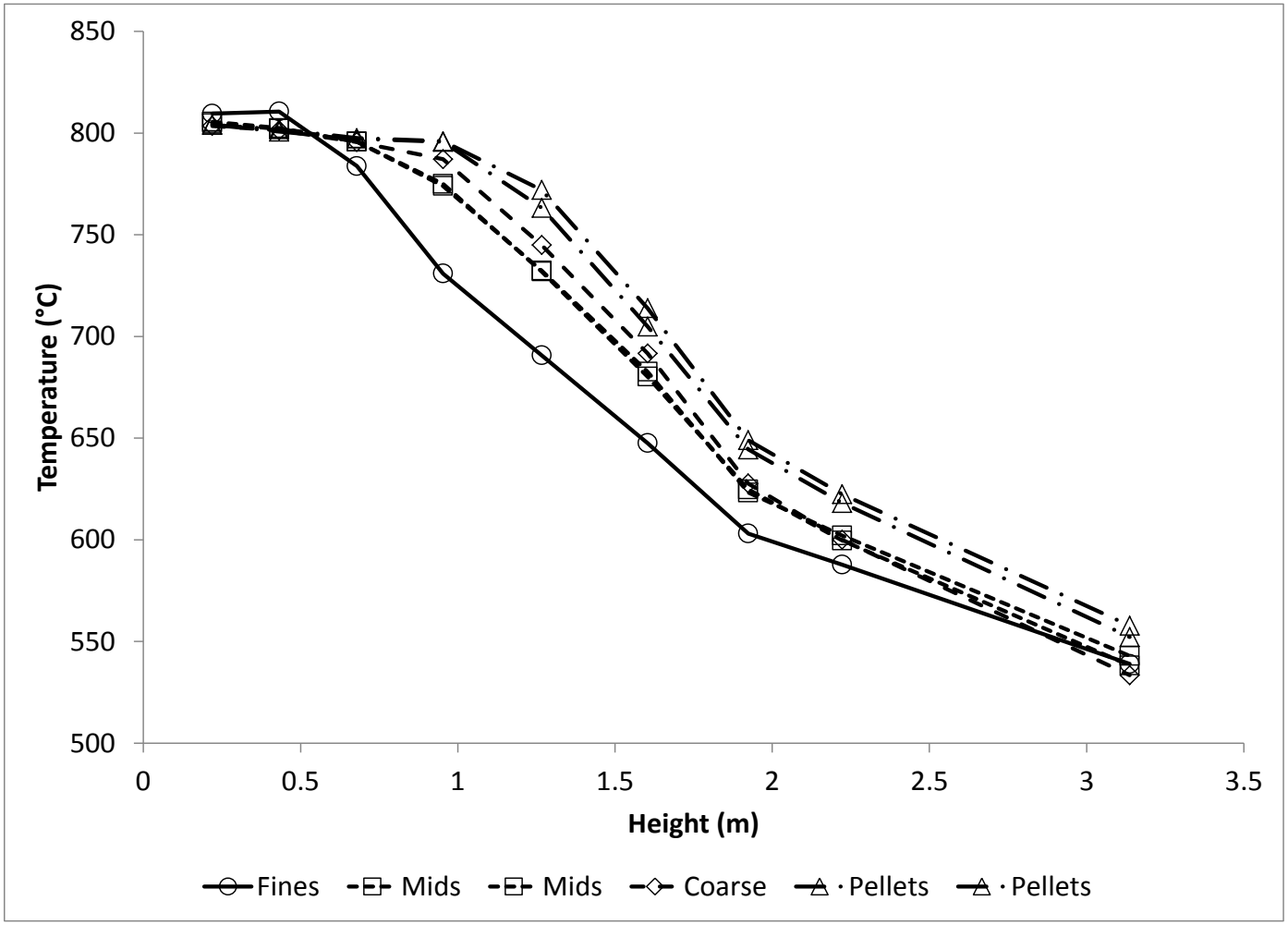

Figure 3.22: Comparison of observed temperature profiles along the height of the gasifier at an average bed temperature of 800°C with an initial 11 kg charge of bed material.

Figure 3.22 shows that the temperature in the reactor drops sharply beyond the bed level. The "freeboard" region of the bed of this system could be considered a "cool freeboard". In an industrial scale gasifier heat loss through the reactor will play a much smaller role (due to the decrease in the ratio of surface area to volume - see chapter 5 for the temperature profiles in a large pilot-scale gasifier). Thus, the freeboard temperature would be expected to be much closer to the bed temperature for an industrial gasifier. This factor could have exacerbated the poor performance (high tar content gas, low carbon conversion to gas) observed with the finest materials. It is expected that a hot freeboard could help to contribute to tar conversion and char conversion, especially with the small particle sizes of the fine material. For example, van Paasen and Kiel (2004) found subtle changes to the gas composition, but fairly significant changes to the amount and character of the tar with increasing reactor height in a fluidized bed gasifier (increasing gas residence time). In their work, the freeboard temperature was maintained very close to the bed temperature. One of these effects was a reduction in the amount of class 2 tar from 2.5 g/m^3 to 0.7 g/m^3 between a height where the gas residence time was 1.3 s compared to 4.0 s. Based on this observation it might be reasonable to use class 2 tar as an indicator of the amount of time gases have spent at elevated temperature. In this work, the fines yielded gases with a class 2 tar concentrations of about 3 – 4 g/m^3 at 800°C bed temperature compared to the other particle sizes which yielded about 1 - 3 g/m^3. This may be an indicator that the product gases and tars from fines gasification are spending less time at elevated temperatures (or were generated outside of the mildly catalytic bed) compared to the other particle sizes. The temperature profile however also shows that the majority of the freeboard with fines gasification was at a lower temperature than with the other particle sizes which may also contribute to the observation of greater class 2 tar levels. These observations also have to be balanced with the fact that overall more tar was observed from the fines.

The repeat runs show that the temperature profiles in the reactor were quite reproducible, despite the variability that were observed elsewhere in the results (especially in the tar results).

The third thermocouple along the height of the reactor was not always buried in the bed, although it was always used in the calculation of the "average bed temperature". More often

than not, the third thermocouple was in the splash zone of the reactor (there was still a positive pressure relative to the freeboard, but the pressure trends indicated that the solids density at that point was significantly reduced). The fines had a clearly depressed temperature in the splash zone of bed at the 800°C condition relative to the other fuels where the splash zone temperature was very close to the bed temperature. It is expected that the finest particles would have had the greatest tendency to segregate to the top of the bed and the fastest reaction rate (devolatilization of biomass is heat transfer limited for most particles >1 mm, thus the smaller particles react quicker because the amount of heat transfer relative to the mass of the particle is greater). This may indicate that segregation was significant enough that at the top of the bed, most of the endothermic char gasification reactions were taking place in the splash zone for the fines. In the other cases, since the temperature difference between the splash zone and the bed was small, it possibly indicates that the endothermic char gasification reactions were occurring throughout the bed. At 875°C for the fines, a temperature depression of the splash zone relative to the bed zone was not observed, rather it was reversed and there was a temperature increase in the splash zone (see Figure D.5 in the appendices). Under the high temperature conditions (higher ER: more O_2 relative to the amount of feed, higher temperature: faster reaction rate of the char) it is possible that such a small amount of char was mixing deep into the bed that O_2 started to penetrate into the upper reaches of the bed. If it were the case that O_2 was making it to the upper reaches of the bed, the splash zone would likely be a region of exothermic char oxidation and volatiles oxidation as opposed to endothermic char gasification reactions.

One of the factors that could be contributing to the observed differences between the fuels is the amount of carbon held in the bed at steady state. Although the amount of carbon held-up in the bed was not directly measured, evidence of the different levels of carbon hold-up certainly existed in the data. Figure 3.23 shows the pressure trends observed with respect to time at the transition from the combustion warm-up into the gasification for four runs with different particle sizes and pellets. For the fines, no immediate increase in bed pressure was observed when the system was transitioned to gasification, but over time, the bed pressure did start to build. This is likely due to the accumulation of bottom ash (the fines and the pellets are biased high in ash compared to the mid and coarse material). On

the other hand the coarse material and the pellets showed an increase in bed pressure after the transition to gasification which leveled off over time. This was due to the accumulation of carbon in the bed which reached a steady sate as the rate of char gasification started to equal the rate of char formation and the rate of char elutriation. Using the change in bed pressure as basis, it can be postulated that the pellets led to a greater amount of carbon held in the bed media at steady state. Figure 3.24 shows an example of the kind of material that accumulated in the bed material over the course of a run.

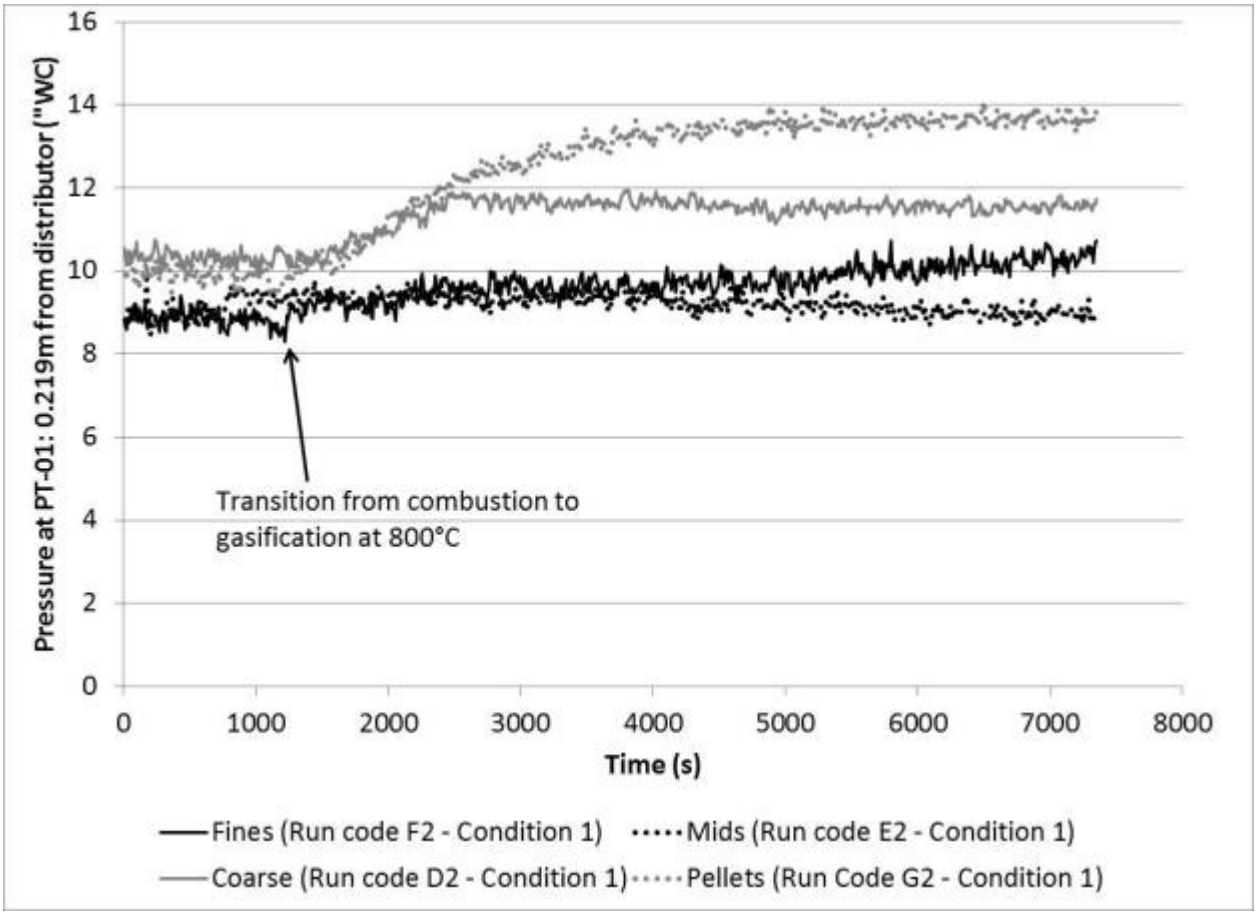

Figure 3.23: Pressure trends in the fluidized bed after transitioning from combustion to gasification.

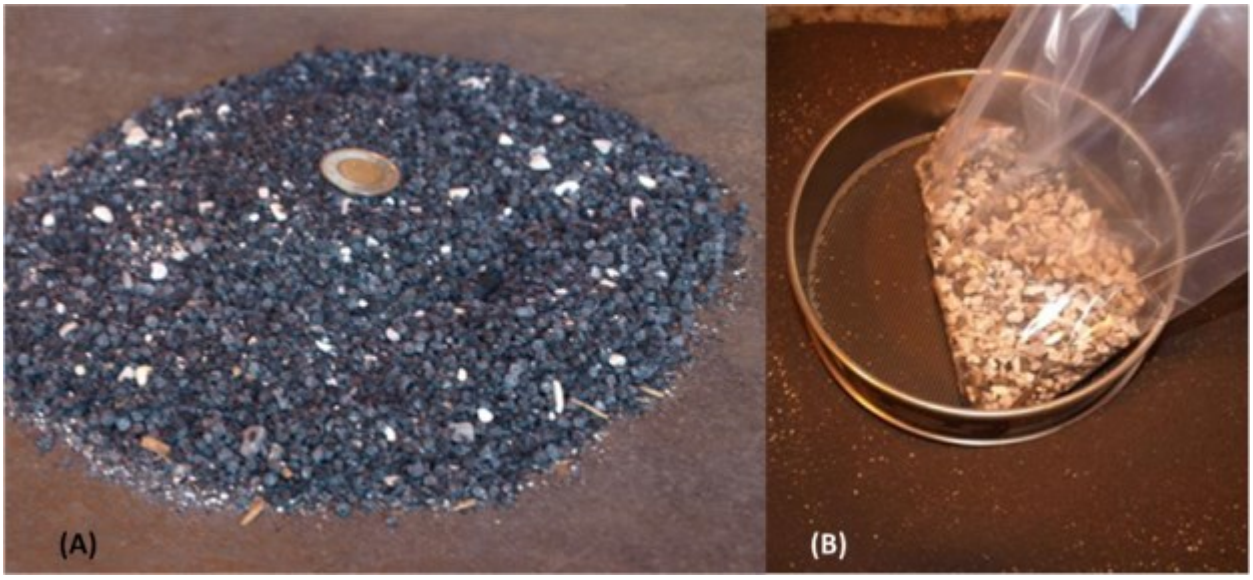

Figure 3.24: Material found in the bed media after the completion of a run. (A) Carbonaceous material sieved from pellet gasification with a toonie for scale. (B) Pebbles and bottom ash from gasification of mid-wet material

The temperature behavior of the system during shut-down provided more evidence that for some fuels there was a large amount of carbon present in the bed at steady-state. Shut-down was completed by stopping the feed-belt. The fluidizing air to the bed was maintained after the feed belt was shut off. The fluidizing air was maintained in order to burn off any residual char from the bed. With the fines, an abrupt, very brief temperature rise was detected during shut-down. With the pellets, a large, steady temperature rise was experienced which lasted for more than 20 minutes after shut-down. The magnitude of temperature rise can be related to the amount of char, and the rate of temperature rise might be related to the reactivity of the char. Figure 3.25 shows the temperature history of the bed after the shut-down of the gasification process for various particle sizes at 725°C.

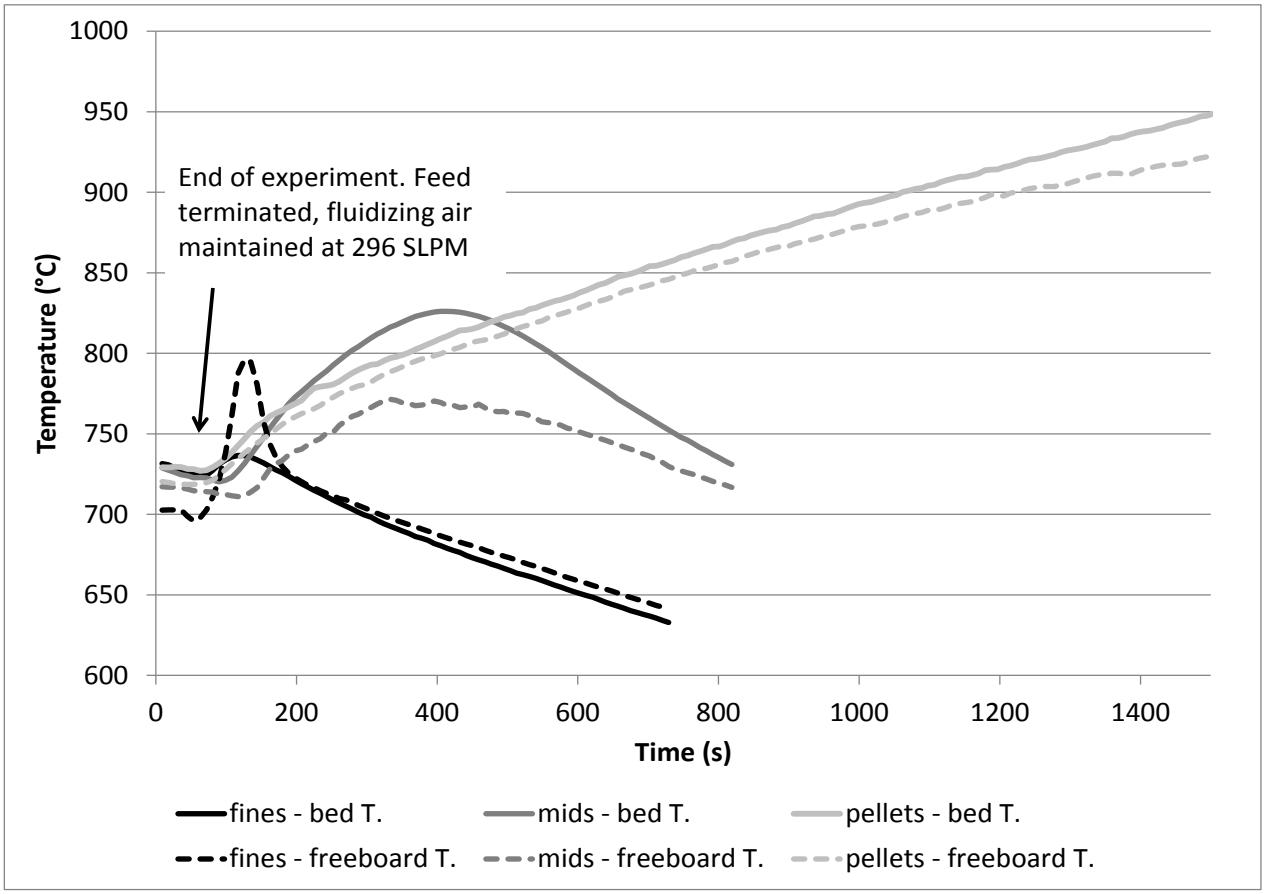

Figure 3.25: Temperature trends after shut-down from gasification at 725°C.

Figure 3.24, which was presented earlier, showed an example of the char that was recovered from the bed material after gasification with pellets. The purpose of the shut-down procedure was to burn out all the char from the bed at the end of a run in order to have relatively clean material that could be recycled for the next run. With the pellets, this could not be achieved as the temperature rise led the reactor to exceed its safe limits. After 950°C, the bed had to be "dumped" regardless of whether char remained in it or not. The dumped bed media showed a considerable amount of char still remaining even 20 minutes after the end of biomass feeding. In order to clean the material for the next run, the char was sieved out from the bed media.

For all experiments, the superficial gas velocity was maintained constant at 0.91 m/s. This gas velocity was calculated at the base of the bed, and thus is reflective of the superficial velocity before the fuel was converted to gas and the oxygen was consumed. The superficial velocity at the top of the bed depends on how much material gets converted to gas and

depends on the composition of the produced gas. The appendices (section D.3) cover the assumptions and methods used to determine the superficial gas velocity. The section also presents the full table of gas velocity results. The superficial velocity, calculated at the top of the bed after feed is gasified, was not constant between experiments. The velocity ranges between 1.34 – 1.82 m/s. The amount of material fed to the gasifier (and thus the bed temperature of the condition) had the greatest effect of the superficial gas velocity at the top of the bed (since less material had to be fed to gasifier in order to reach higher bed temperatures less gas flow was produced). There were also some subtle differences between particle sizes. The gas velocity calculated at the top of the bed, at the 800°C bed temperature condition, varied between 1.52 – 1.57 m/s for the fines, compared to between 1.59 – 1.68 m/s for the other fuels. This implies that the gaseous and vapour products from fines gasification would have spent slightly greater residence compared to the gases and vapours of the other fuel sizes. Greater gas and vapour residence time would suggest improved reduction in tar which is the opposite of what was observed. The differences in gas velocity between the different particle sizes were small.

3.8.2 Thermodynamic Considerations

One possible reason that could be used to explain some of the observed differences in the gas composition between the different particle sizes, forms, and moisture levels is that there are differences in how closely gas phase approaches thermodynamic equilibrium. In this explanation, the differences could plausibly result from:

- Based on the different mixing patterns of large and small particles in denser bed media, larger particles produce the gas in a distributed manner throughout the bed (as opposed to the top of the bed) allowing the gas phase to more closely approach equilibrium.
- Based on the particle size differences, the intraparticle residence time of the gas phase becomes greater for large particles and the char layers of a large particle act as a heterogeneous catalyst to reform devolatilization products that are formed within the interior of the particle.
- Based on char reactivity and char elutriation rates, the steady state hold up of char in the bed is different for the different particle sizes, moisture levels, and forms. The

increased amount of char from some particle sizes and forms acts as a heterogeneous catalyst to push gas phase reactions towards thermodynamic equilibrium.

- The finest materials, owing to their possible entrainment in the gas flow before conversion, would devolatilize outside of the bed and possibly along the height of the reactor. This would produce gases that spend a wide distribution of residence time in the reactor at lower temperatures than that of the bed.

If these explanations were the major contributing factor to the gas composition differences from different particle sizes, then it would be expected to find that the gas phase from one of larger particles, especially the pellets (owing to observed increase of char hold-up in the bed), to yield a gas phase that was closer to the thermodynamic equilibrium composition than the finer materials.

In order to determine whether this hypothesis was indeed valid, it was necessary to perform a simulation on the system to determine the position of chemical equilibrium in the gas phase. In order to accomplish this, UniSim software was used. The simulation developed took as an input a flow of hydrogen, oxygen, nitrogen and solid carbon at atmospheric temperature. The streams of hydrogen, oxygen, nitrogen and carbon were used to specify the appropriate carbon, hydrogen, oxygen, and nitrogen stoichiometry of the system. The input carbon stream was split in order to simulate different levels of carbon conversion to gaseous products by adjustment of the split ratio. These mass inputs were fed into a Gibbs reactor at atmospheric pressure and the reaction temperature. The output gaseous stream from the Gibbs reactor was a representation of the gaseous products from this reaction at thermodynamic equilibrium. Since the gas phase composition in these experiments was measured on a dry basis, the steam was separated from the product gas in the simulation by means of a splitter in order to provide a gas composition that can be directly compared to the measured gas composition. A screenshot from UniSim is provided in the appendices in order to provide a reader familiar with UniSim an overview of the simulation (section D.5, Figure D.9).

Based on the measured feed rate and subtle differences in the compositional analysis of each of the materials, the mass input of carbon, oxygen, hydrogen, and nitrogen was unique

for each run condition. However these differences are in fact subtle and the mass input of carbon, hydrogen, oxygen, and nitrogen is similar for run conditions of the same bed temperature and the same fuel moisture level. Thus, for each temperature and moisture level a representative set of mass inputs can be used with little effect on the results.

Although the bed temperature is maintained at a fixed temperature, the temperature of the freeboard decreases with height. Thus, if the gas is approaching equilibrium in the freeboard it may be approaching a different equilibrium position than that predicted at bed temperature (an equilibrium position at a temperature lower than the bed temperature). From this perspective, it made sense to evaluate the equilibrium position across a variety of temperatures to determine the realm of possible gas compositions. The list of gaseous species considered in the simulation is given in the appendices, section D.5.

For a bed temperature of 800°C, the representative stoichiometry for the "dry" and the "wet" fuels are given in Table 3.16.

Table 3.16: Representative stoichiometry for 800°C bed temperature with dry and wet fuels.

Element	Dry fuels at 800°C kg/h	Wet fuels at 800°C kg/h
Carbon	6.5	5
Hyrdogen	0.95	1
Oxygen	11.5	12
Nitrogen	16.1	16.1

The results of the simulation for the two cases are presented in Table 3.16: Representative stoichiometry for 800°C bed temperature with dry and wet fuels Table 3.16 are given in Figure 3.26 and Figure 3.27 where three lines are given for each gas species. The lighter grey line represents the simulated gas composition at 50% carbon conversion, the darker grey line at 75% carbon conversion, and the black line at 100% carbon conversion.

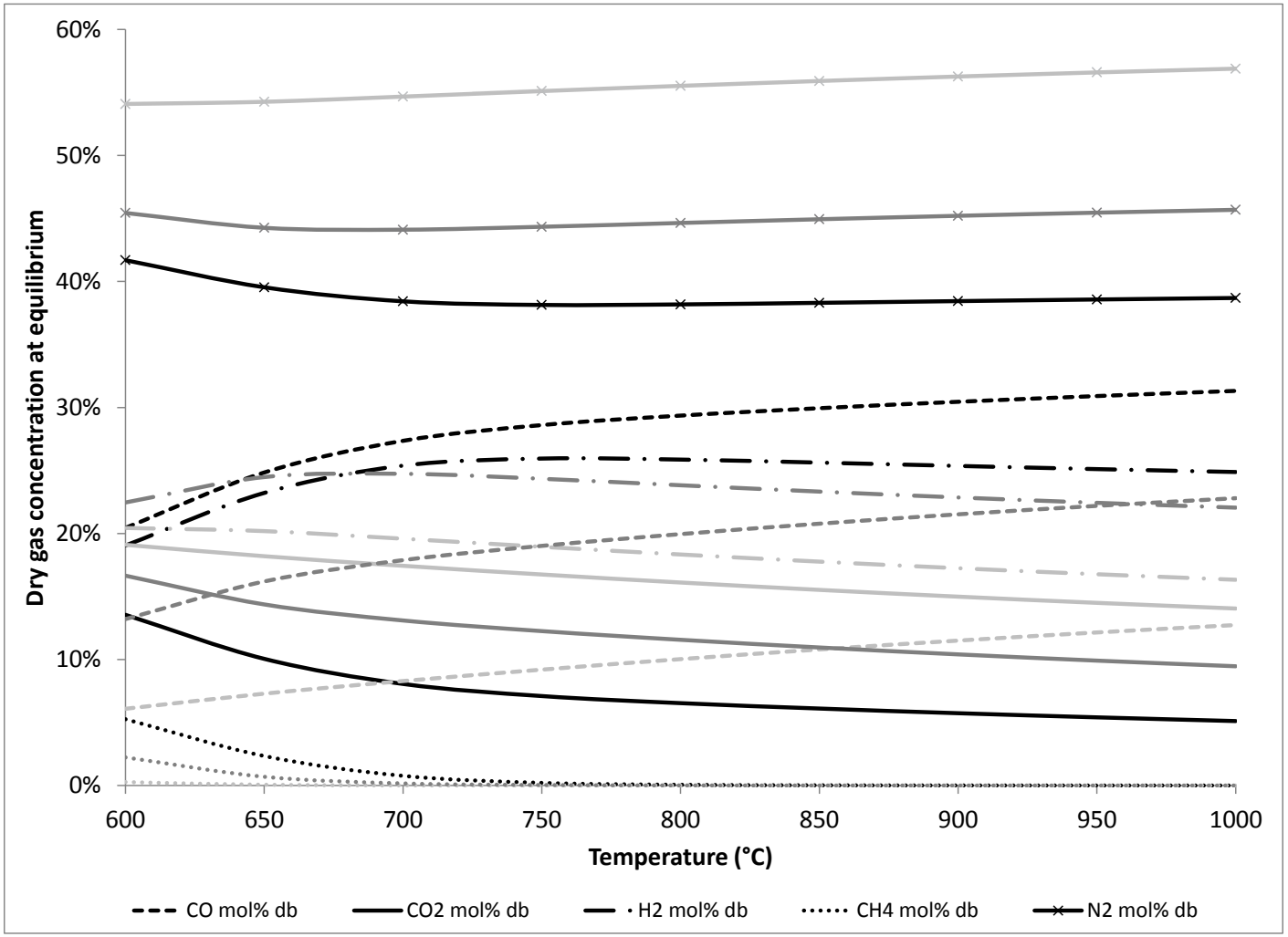

Figure 3.26: Equilibrium gas composition (volume basis) at the representative stoichiometry at 800°C bed temperature for dry fuel. Simulated cases for 50% (light grey), 75% (dark grey) and 100% (black) carbon conversion.

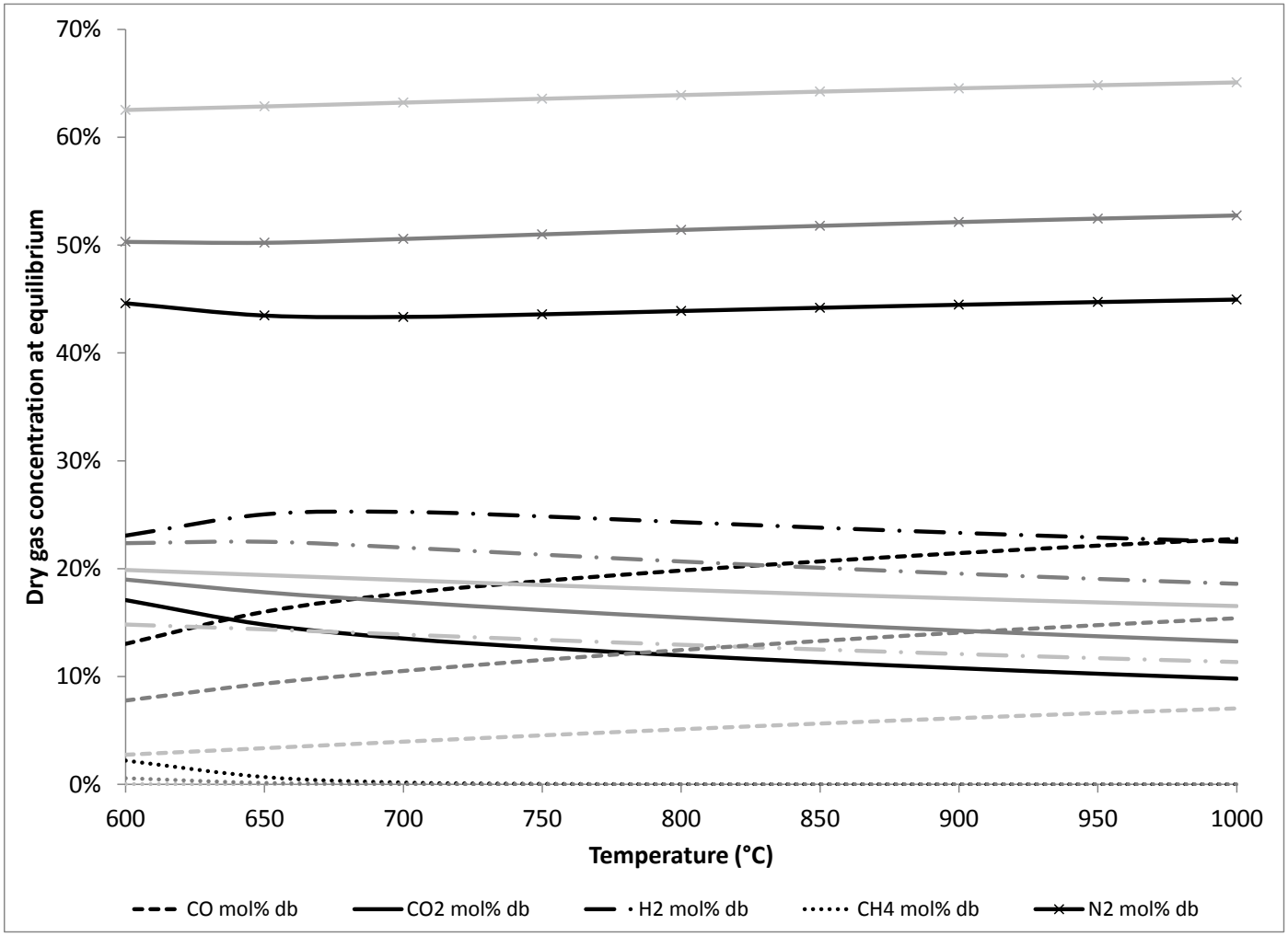

Figure 3.27: Equilibrium gas composition (volume basis) at the representative stoichiometry at 800°C bed temperature for wet fuel. Simulated cases for 50% (light grey), 75% (dark grey) and 100% (black) carbon conversion.

Of the twenty species included in the simulation, the gas composition predicted contains only six species in significant amounts (CO, CO_2, H_2, H_2O, N_2, and CH_4) over a variety of char conversion levels. Other components such as C_2H_4, C_6H_6, or NH_3 are predicted in ppm or sub-ppm levels. Figure 3.26 and Figure 3.27 show that the predicted level of even CH_4 drops to very low levels after 700°C for the typical conditions run in this experimental campaign. This is in contrast to the experimental results where CH_4 and C_2H_4 were measured at percentage levels. Above 700°C, two simplifications for determining the gas composition that minimizes the Gibbs free energy can be reasonably made if gas species at percentage levels are only considered:

- Based on the distribution of nitrogen species (N_2, HCN, and NH_3) at thermodynamic equilibrium, it would be appropriate to assume that all nitrogen converts, or remains as, N_2.
- The balance of the gas composition can be computed by assuming all the converted carbon, hydrogen, and oxygen report to CO, CO_2, H_2, and H_2O according to the water gas shift reaction.

Based on these assumptions, the only equilibrium reaction that needs to be modeled in order to predict thermodynamic equilibrium is the water gas shift reaction. Figure 3.28 shows how the measured gas composition converted to a ***measured K***[14] for the water gas shift reaction compares to the actual equilibrium constant. The data points in Figure 3.28 do not distinguish between wet or dry fuels. The dotted line in Figure 3.28 is the predicted equilibrium gas constant. The solid lines are quadratic best fits of their respective data series. The results of Figure 3.28 show that the mid and coarse material resulted in a similar measured K, but the fines and pellets operated at a very distinct measured K compared to the mid and coarse material.

[14] Measured $K = \frac{[H_2][CO_2]}{[CO][H_2O]}$

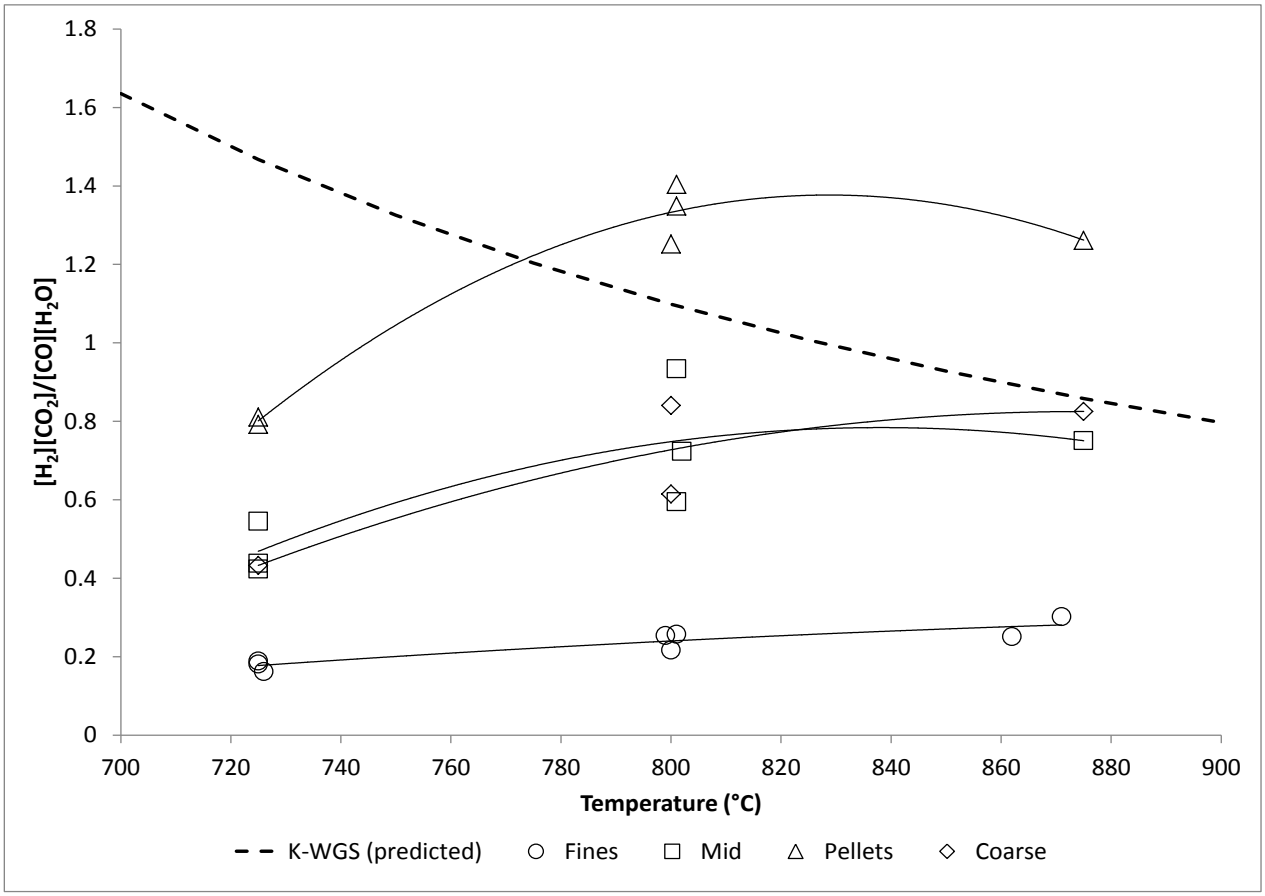

Figure 3.28: Comparison of the equilibrium constant for the water-gas shift compared to the experimental observations.

Other works in literature have pointed out that as the temperature of a gasifier increases the water gas shift starts to be able to predict the relative abundance of CO, CO_2, H_2, and H_2O. An example of this is the work by Schoeters et al. (1989) who postulated that at temperatures above 800°C the water-gas shift equilibrium is virtually attained. The work presented in this thesis does not reach the same conclusion. Rather in this work, it appears that the mid and coarse materials are both still trending towards water-gas shift equilibrium at 875°C. Even this may still only be a coincidence since the pellets and fines are still well off the equilibrium conditions at 875°C. The pellets and fines deviate from the water-gas shift equilibrium in different directions. At 875°C, the amount of hydrogen and carbon dioxide are present in sub-equilibrium amounts for the fines but are present at super-equilibrium amounts for the pellets. This suggests that the CO, CO_2, H_2, and H_2O population of the gas is still dominantly influenced by kinetic limitations even at 875°C. One

important difference between this system and the system described in Scheoters et al. (1989) is that this system does not have a heated freeboard, rather the temperature of the freeboard decreases substantially along its height. Wilk and Hofbauer (2013) concluded in their work with pellets, sawdust, and waste wood gasified in a dual fluid bed gasifier that fine particles (particles <1 mm) led to a greater deviation from the water-gas shift equilibrium. They also found a decreased level of water conversion when the material consisted of a substantial amount of particles less than 1 mm. All of Wilk and Hofbauer's data has H_2 and CO_2 in sub-equilibrium concentrations. The work presented in this thesis is unique in that H_2 and CO_2 were measured at super-equilibrium concentrations which could lead to an entirely new explanation for the deviation from water gas shift.

3.8.3 Comparison with Literature Results

The results from this study at a bed temperature of 800°C compare favorably with those reported in literature. Table 3.17 shows a comparison of results from other air blown fluidized bed gasifiers. In the case where multiple results were given in the literature source, the results produced from conditions that most resembled this study were chosen. The results from this study fell within the range of expected gas composition for air blown gasifiers. The results are arranged in the order of descending H_2/CO ratio in order to emphasize one of the key findings of this work: particle size and pelletization appear to be able strongly influence the relative amount of hydrogen and carbon monoxide produced. From literature, it appears that most of the studies with elevated H_2/CO ratio used large particles or pellets. It must be appreciated that the results presented in Table 3.17 cover a wide variety of conditions, reactor topologies, bed media, ER, and feed positions.

Table 3.17: Comparison of the gasification results from this study with those that could be found in literature.

Reference	Fuel description	Bed T.	ER	Feed position	Fluid bed type	CO	H_2	CO_2	CH_4	H_2/CO ratio
(Corella et al., 2004)	Mix of small pine chips (1-5 mm) olive residue (1 - 4 mm)	847	0.36	In-bed	BFB	12.1	13.2	13.6	4	1.09

(Kim et al., 2013)	wood pellet 8X20mm	775	0.27	Over-bed	BFB	13.8	14.5	16	4	1.05	
This Work	**Softwood forestry residue (pelletized 6.35mm X 10-30mm)**	**800**	**0.28**	**Over-bed**	**BFB**	**12.6**	**12.6**	**18.1**	**3.8**	**1.00**	**{4}**
This Work	**Softwood forestry residue (fraction retained between 6.35mm and 19.05mm screen)**	**800**	**0.27**	**Over-bed**	**BFB**	**12.7**	**11.7**	**18.3**	**3.8**	**0.92**	
(van der Drift et al., 2001)	Verge grass pellets	815	0.36	In dense bed	CFB	10.6	8.45	15.2	2.79	0.79	
(Miccio et al., 1999)	Beech 0 - 5 mm	800	0.15	In-bed	BFB	19.2	15	18.2	6.1	0.78	
This Work	**Softwood forestry residue (fraction retained between 3.175mm and 6.35mm screen)**	**800**	**0.27**	**Over-bed**	**BFB**	**14.3**	**10.7**	**17.7**	**4.2**	**0.75**	**{4}**
(Vriesman et al., 2000)	1 - 1.35 mm crushed miscanthus pellets	800	0.16	Over-bed	BFB	35.2	26.1	22.8	11.8	0.74	{1}
(van der Drift et al., 2001)	Verge grass pellets	803	0.37	In dense bed	CFB	9.89	7.28	15.6	2.58	0.74	
(Ruoppolo et al., 2012)	wood pellets 6x20mm	780	0.3	inbed	BFB	18	12	13	4	0.67	{3}
(van der Drift et al., 2001)	Chip board materials <20 mm	843	0.38	In dense bed	CFB	9.64	6.42	15.6	2.77	0.67	
(Vriesman et al., 2000)	1 - 1.35 mm crushed miscanthus	800	0.16	In-bed	BFB	38.8	25.5	24.4	7.9	0.66	{1}
(Maniatis, 1986)	Wood chips, distributed 0 - 150 mm most 30-50mm	811	0.38	Over-bed	BFB	16.2	10.6	16.7	4.3	0.65	
(van der Drift et al., 2001)	demo wood <35mm	847	0.36	In dense bed	CFB	11.4	7.05	15.8	3.25	0.62	

(van der Drift et al., 2001)	park and public wood waste <25mm	861	0.38	In dense bed	CFB	11.7	6.77	15.5	3.17	0.58	
(van Paasen and Kiel, 2004)	Cellulose 0.7 - 2 mm	827	0.32	In-bed	BFB	15.4	8.9	15.7	3.9	0.58	
(van Paasen and Kiel, 2004)	Beech 0.7 - 2 mm	806	0.25	In-bed	BFB	16.7	8.7	15.7	5	0.52	
(Lahijani and Zainal, 2011)	Sawdust (2 - 6 mm)	850	0.25	Inbed	BFB	14	7	19	3	0.50	{3}
(van Paasen and Kiel, 2004)	Willow 0.7 - 2 mm	801	0.24	In-bed	BFB	16.3	8	16.3	4.8	0.49	
(Kaewluan and Pipatmanomai, 2011)	Rubber wood chips 5x10x10mm	761	0.38	Over-bed?	BFB	31.6	15.5	38.1	8.4	0.49	{1}
This Work	**Softwood forestry residue - fines (passing through 3.175mm screen)**	**800**	**0.26**	**Over-bed**	**BFB**	**13.9**	**6.4**	**17.6**	**3.9**	**0.46**	**{4}**
(Lahijani and Zainal, 2011)	Sawdust (2 - 6 mm)	750	0.25	In-bed	BFB	14	6	17	3	0.43	{3}
(Ergudenler and Ghaly, 1992)	Wheat straw (15x2x0.3mm)	820	0.25	In-bed {2}	BFB {2}	19.7	7.01	14	4.39	0.36	
(Li et al., 2004)	hemlock 0.92 mm mean particle diameter	815	0.52	In dense bed	CFB	9.6	3	17.1	1.9	0.31	
(Li et al., 2004)	hemlock 0.92 mm mean particle diameter	789	0.34	In dense bed	CFB	14.6	4.2	15.7	3	0.29	
(Mansaray et al., 1999)	Rice Husk 0.25 - 0.5 mm	750	0.3	In-bed {2}	BFB {2}	14.4	3.4	16.5	2	0.24	

{1} Nitrogen free

{2} Dual distributor type

{3} Estimated from graph

{4} Average of multiple experiments

BFB – Bubbling Fluidized Bed

CFB – Circulating Fluidized Bed

The data in Table 3.17 provides reassurances that none of the data points observed in this work were outliers. Rather, the gas composition from all the particle sizes tested fall within expectations from a typical air-blown fluidized bed gasifier. Based on the range of observations, it even appears that some of the differences between the results reported in literature are due to particle size differences.

3.9 **Conclusions**

- The gas composition given by each particle size and form is unique. The gas compositions measured in this study compare favorably with those reported in literature. The results of this work, combined with the findings of others, appear to indicate that pelletizing a fine material may be an avenue to increase the hydrogen yield from an air blown fluidized bed gasifier. The increased hydrogen yield effect observed with pellets is partly due to an increase in particle size.
- The observed differences between the gas composition of different particle sizes, moisture levels, and pellets may be due to different amounts of char retained in the bed at steady state and mixing patterns between the fuel and the bed media. Assuming that the gas phase begins to approach thermodynamic equilibrium was not found to be a suitable explanation for describing the differences between different particle sizes, moisture levels, and particle forms.
- Each mass balance strategy produces results that appear have non-random error (for example, the nitrogen closure from the CHO mass balance is not statistically distributed around the expected value, 100%. Rather the nitrogen balance is persistently lower than expected with a sample mean of 92%, a sample standard deviation of 4.6% over 25 samples). Although, neither approach was perfect, most conclusions that can be drawn from the data are independent of the mass balance technique chosen. If the results of the CHO mass balance approach are considered to be accurate, then the moisture measurement methods were not capable of recovering all the moisture from the sample gas and the char measurement methods were severely inadequate (often missing more than 50% of the char produced). It was known before the experiments that the char collection method would likely underestimate the amount of char produced, but the magnitude of the

underestimation suggested by the CHO method was surprising. The idea that a large amount of char was missed (as predicted by the CHO method) is supported by the persistently low carbon closure with the traditional method (average carbon closure of the traditional method: 92%). There also appears to be a systematic error in the CHO method. Since the CHO method relies on perfect knowledge of the gas composition, the sum of all the unaccounted material (C4-C5), low molecular weight oxygenates, tar which is missed, and imperfect knowledge of the tar composition all contribute to the error of the CHO method. The CHO method has the advantage of being less sensitive to the measured dry gas concentration of N_2 and requires fewer measurements (does not require the measurement of char or water in the gas, rather it predicts these values).

- Feed materials with the same moisture cannot be gasified at the same bed temperature with the same ER without external heat input. In these experiments the bed temperature was maintained constant and the ER was increased for higher moisture fuels. At a constant bed temperature, the heating value of the gas decreased with increasing fuel moisture (this comparison is drawn between fuels at 11 % moisture compared to fuels at between 24 – 31 % moisture). The excess moisture led to a slight increase in the H_2/CO ratio of the gas. Increased moisture may have also led to a slight reduction in phenol and cresols in the tar, but overall tar levels were similar between dry and moist fuels. The hypothesized advantages of extra moisture leading to increased char and tar conversion through the promotion of char gasification and steam reforming reactions was partially observed: the addition of fuel moisture did not appear to promote a reduction in the tar yield, but may have slightly promoted char gasification.
- Feeding fines into a fluidized bed gasifier from an over-bed feed position (as was the case in this system) negatively affected the performance of the gasifier by nearly every measure (efficiency, carbon conversion, and tar content) compared to the larger fuel sizes. Pelletizing biomass might be appropriate if there are process advantages of having a gas richer in H_2 at the expense of hydrocarbon gases and carbon monoxide.

- At the highest temperature level (875°C), the best cold gas efficiency was obtained with the pelletized and mid-size material which was approximately 60%. The amount of char produced at the 725°C and the 800°C conditions were a large contributor to the low observed cold gas efficiency at these lower bed temperatures. In order to achieve higher cold gas efficiency in this system, design modifications (such as char recycling) would be required, especially at lower gasification temperatures.
- In agreement with what many other researchers have found, the amount of tar that is produced was greatly reduced at higher temperatures. This was true across all particle forms and moisture level.

References

Corella, J., J. Herguido and F.J. Alday, "Pyrolysis and steam gasification of biomass in fluidized beds: Influence of the type and location of the biomass feed point on the product distribution," in "Research in Thermochemical Biomass Conversion," A. V. Bridgewater and J. L. Kuester, Eds. Elsevier Applied Science, London, UK (1988), pp. 384-398.

Corella, J., J.M. Toledo and R. Padilla, "Olivine or Dolomite as In-Bed Additive in Biomass Gasification with Air in a Fluidized Bed: Which Is Better?" Energy Fuels. **18**, 713-720 (2004).

Corella, J., J.M. Toledo and G. Molina, "Biomass gasification with pure steam in fluidised bed: 12 variables that affect the effectiveness of the biomass gasifier," Int. J. Oil, Gas and Coal Technology. **1**, 194-207 (2008).

Ergudenler, A. and A.E. Ghaly, "Quality of gas produced from wheat straw in a dual-distributor type fluidized bed gasifier," Biomass Bioenergy. **3**, 419 (1992).

Hurley, S., C.. Xu, F. Preto, Y. Shao, H. Li, J. Wang and G. Tourigny, "Catalytic gasification of woody biomass in an air-blown fluidized-bed reactor using Canadian limonite iron ore as the bed material," Fuel. **91**, 170 (2012).

Kaewluan, S. and S. Pipatmanomai, "Gasification of high moisture rubber woodchip with rubber waste in a bubbling fluidized bed," Fuel Process Technol. **92**, 671 (2011).

Kim, Y.D., C.W. Yang, B.J. Kim, K.S. Kim, J.W. Lee, J.H. Moon, W. Yang, T.U. Yu and U.D. Lee, "Air-blown gasification of woody biomass in a bubbling fluidized bed gasifier," Appl. Energy., - (2013).

Kirnbauer, F., V. Wilk, H. Kitzler, S. Kern and H. Hofbauer, "The positive effects of bed material coating on tar reduction in a dual fluidized bed gasifier," Fuel. **95**, 553 (2012).

Koppatz, S., C. Pfeifer and H. Hofbauer, "Comparison of the performance behaviour of silica sand and olivine in a dual fluidised bed reactor system for steam gasification of biomass at pilot plant scale," Chem. Eng. J. **175**, 468 (2011).

Lahijani, P. and Z.A. Zainal, "Gasification of palm empty fruit bunch in a bubbling fluidized bed: A performance and agglomeration study," Bioresour. Technol. **102**, 2068 (2011).

Li, X.T., J.R. Grace, C.J. Lim, A.P. Watkinson, H.P. Chen and J.R. Kim, "Biomass gasification in a circulating fluidized bed," Biomass Bioenergy. **26**, 171-193 (2004).

Maniatis, K., "Fluidized Bed Gasification of Biomass," PhD thesis, Aston University (1986).

Mansaray, K.G., A.E. Ghaly, A.M. Al-Taweel, F. Hamdullahpur and V.I. Ugursal, "Air gasification of rice husk in a dual distributor type fluidized bed gasifier," Biomass Bioenergy. **17**, 315 (1999).

Miccio, F., O. Moersch, H. Spliethoff and K.R.G. Hein, "Generation and conversion of carbonaceous fine particles during bubbling fluidised bed gasification of a biomass fuel," Fuel. **78**, 1473-1481 (1999).

Miccio, F., B. Piriou, G. Ruoppolo and R. Chirone, "Biomass gasification in a catalytic fluidized reactor with beds of different materials," Chem. Eng. J. **154**, 369 (2009).

Narváez, I., A. Orío, M.P. Aznar and J. Corella, "Biomass Gasification with Air in an Atmospheric Bubbling Fluidized Bed. Effect of Six Operational Variables on the Quality of the Produced Raw Gas," Ind Eng Chem Res. **35**, 2110-2120 (1996).

Robinson, T., "Measurement of tar in biomass producer gas and the development of a new sampling device," undergraduate thesis submitted to the University of Ottawa, Dept. of Chemical and Biological Engineering. Ottawa, ON (2012).

Ruoppolo, G., P. Ammendola, R. Chirone and F. Miccio, "H2-rich syngas production by fluidized bed gasification of biomass and plastic fuel," Waste Manage. **32**, 724 (2012).

Schoeters, J., K. Maniatis and A. Buekens, "The fluidized-bed gasification of biomass: Experimental studies on a bench scale reactor," Biomass. **19**, 129-143 (1989).

van der Drift, A., J. van Doorn and J.W. Vermeulen, "Ten residual biomass fuels for circulating fluidized-bed gasification," Biomass Bioenergy. **20**, 45-56 (2001).

van Paasen, S.V.B. and J.H.A. Kiel, "Tar formation in a fluidised-bed gasifier," **ECN-C--04-013** (2004).

Vriesman, P., E. Heginuz and K. Sjöström, "Biomass gasification in a laboratory-scale AFBG: influence of the location of the feeding point on the fuel-N conversion," Fuel. **79**, 1371-1378 (2000).

Wilk, V. and H. Hofbauer, "Influence of fuel particle size on gasification in a dual fluidized bed steam gasifier," Fuel Process Technol. **115**, 139 (2013).

Chapter 4. Effect of Biomass Thermal Pre-treatments (Torrefaction and Carbonization)

This chapter describes the materials, methods and results from the experiments that were designed to understand how a thermal pre-treatment of torrefaction or carbonization can affect the gasification of a forestry residue in a small pilot-scale air-blown fluidized bed gasifier.

4.1 **Materials**

4.1.1 Feedstock

In order to study the effect of thermal pre-treatments, such as torrefaction, on the performance of fluidized bed gasifiers a single feed material was carbonized and torrefied. The feed material was a softwood hog fuel originating from a pulp mill located in the interior of British Columbia, Canada (the same forestry residue that was used and described in chapter 3). In order to minimize the impact of particle size effects, the hog fuel was first sieved to between 3.175 mm (1/8") and 6.35 mm (1/4") screens before thermal pre-treatment. The sieving apparatus and material resulted in a parent material that duplicated the mid-sized fraction from chapter 3. Roughly 950 kg of the mid-sized material that was created by sieving was thermally pre-treated: approximately 360 kg of that material was "torrefied" in a cyclonic bed reactor at a final temperature of 316°C (600°F) and approximately 590 kg of the material was "carbonized" in the same cyclonic bed reactor at a final temperature of 427°C (800°F). The differentiation between torrefied and carbonized is only based on the processing temperature (in other words the torrefied and carbonized material was made from the same feedstock in the same equipment where only the reaction temperature was changed)[15]. Figure 4.1 show how the parent, torrefied, and carbonized material compare visually.

[15] Throughout this chapter a few terms and short forms are used interchangeably, especially in tables and figures. *Parent* or *Mid* may be both used to describe the same material. *Torrefied* may be written in short-form in tables and figures as *Torr*. *Carbonized* material may be written in short-form in tables and figures as *Carb*.

Figure 4.1: Photographic comparison of (A) parent material, (B) torrefied material, and (C) carbonized material.

For creating a torrefied material, 316°C was a slightly elevated temperature compared to that which is normally reported for torrefaction conditions; however a few points should be emphasized:

- The technology chosen has a short residence time at the final temperatures. Much of the literature, which is normally reported from lab and bench-scale studies, relates to torrefaction equipment with longer solids residence times.
- The primary objective was that the thermal pre-treatment conditions were specified in order ensure that a wide range of thermal severity was accomplished in order to be able to clearly see the effects.
- Torrefaction is a process that is still early in its development cycle; there is still debate on the definition of what "torrefaction" is.

A sample from each of the feed materials (the parent (mid), the torrefied, and the carbonized) was submitted for proximate, ultimate, calorific, ash and halogen analyses. The samples that were sent for analysis were created by drawing four small samples of the feedstock at different times during the each experimental run, grinding those samples, combining some of each of the four samples, and then homogenizing the sample bags. A small amount of the material from each of the four samples taken during the experimental run was kept in order to perform thermogravimetric analysis (TGA). The TGA study was undertaken in order to understand the level of fuel heterogeneity present. The results of the proximate, ultimate, calorific, and halogen analyses are presented in Table 4.1. The results

of the TGA analysis (and thus more detailed thermal behaviour of each of the feed materials) are dealt with separately in the appendices (section A.4).

Table 4.1: Proximate, ultimate, calorific and halogen results of the feed parent, torrefied, and carbonized material.

Parameter	Method	Parent (Mid)	Torrefied	Carbonized
Ash (db wt%)	ASTM D7582	4.1	5.6	21.0
Volatile (db wt%)	ISO 562	77.0	59.9	28.7
Fixed Carbon (db wt%)	ASTM D7582	18.9	34.6	50.4
Carbon (db wt%)	ASTM D5373	50.0	58.0	60.8
Hydrogen (db wt%)	ASTM D5373	5.8	5.0	2.8
Nitrogen (db wt%)	ASTM D5373	0.1	0.3	1.1
Sulfur (db wt%)	ATSM D4239	0.1	0.1	0.3
Oxygen by Difference (db wt%)	in-house	39.9	31.1	14.0
Gross Calorifc Value (MJ/kg db)	ISO 1928	19.9	22.2	22.9
Chlorine (µg/g db)	in-house	530	220	4420
Fluorine (µg/g db)	in-house	15	23	30
Bromine (µg/g db)	in-house	<10	<10	<10

The results in Table 4.1 show that the volatile fraction of the feed decreased as the severity of the thermal pre-treatment increased which led to a corresponding increase in the measured amount of fixed carbon. The contribution of devolatilization to the gasification behaviour of the thermally pre-treated materials will be decreased and the importance of gas-solid reactions between the gasification medium and resultant char will be increased for the torrefied and especially the carbonized material. An increase in the ash concentration is evident with thermal pre-treatment, especially in the carbonized material. This is because through the thermal pre-treatment some of the organic material is lost (decomposes into gases and vapours), whereas only a very small amount (if any) of the mineral material is lost. The data also suggests that the sulfur and nitrogen components of the material are largely retained in the solid product, since the nitrogen and sulfur results show similar amplification to the ash concentration. The chlorine content also shows amplification between the parent and carbonized material but not for the torrefied material. It is possible (and in the author's opinion extremely likely) that this is due to sample heterogeneity.

When analyzing single, small samples of a biomass material a risk that always needs to be considered is whether or not a sample that was analyzed was representative of the entire population of material that was used during pilot-scale gasification. Although it would be preferable from a scientific perspective to complete the analysis of multiple samples from the fuel in order to obtain a better estimator of the mean value of the fuel characteristics and additionally to obtain statistical measures regarding the variability within a feedstock, this must be weighed against the cost and effort of such analyses. On the other hand, some of the fuel characteristics can be determined (or at least approximated) with minimal effort. In order to generate some understanding of the mean and variance of the ash content from each of the pre-treatment levels, the four distinct fuel samples that were used to create the final homogenized fuel sample were processed individually in a thermogravimetric analyzer (TGA). The TGA is useful to understand fuel reactivity and also is an easy method to get an estimate of the amount of ash in a fuel sample. The detailed results from the TGA studies are shown in the appendices section A.4, and Figure A.3 to Figure A.5. Some of the key results obtained this non-standard, in-house TGA methodology by include:

- The measured ash content of the parent material varied over 4 samples between 3.6 – 5.2 wt% with an average of 4.3 wt% (compared to 4.1 wt% on a single sample by ASTM D7582).
- The measured ash content of the torrefied material varied over 4 samples between 3.7 – 7.4 wt% with an average of 5.3 wt% (compared to 5.6 wt% on a single sample by ASTM D7582).
- The measured ash content of the carbonized material varied over 4 samples between 12.4 – 26.8 wt% with an average of 17.1 wt% (compared to 21.0 wt% on a single sample by ASTM D7582).
- There were more differences between samples in terms of char reactivity for the carbonized material than for the torrefied or parent material (where the char reactivity is the rate of mass loss in a reactive gas such as CO_2 or O_2).

Since all the measured ash contents (by standard methods) fell within the range of the values from the TGA, it is reassuring that the samples characterized were representative of the entire batch of fuel processed in the gasifier. The fact that there was some fuel

heterogeneity detected in the carbonized material should be factored in when considering the results of the gasification work.

The analysis of the materials was also compared on a dry, ash-free basis which is presented in Table 4.2. The biggest difference that can be observed on a dry, ash-free basis, which is not immediately observable from the dry basis results, is that the calorific value of the dry, ash-free material was substantially enhanced as the thermal pre-treatment severity increased.

Table 4.2: Proximate, ultimate, calorific and halogen results of the feed parent, torrefied, and carbonized material compared on a dry, ash-free basis.

Parameter	Method	Parent (Mid)	Torrefied	Carbonized
Volatile (daf wt%)	ISO 562	80.3	63.4	36.3
Fixed Carbon (daf wt%)	ASTM D7582	19.7	36.6	63.7
Carbon (daf wt%)	ASTM D5373	52.1	61.4	76.9
Hydrogen (daf wt%)	ASTM D5373	6.1	5.3	3.6
Nitrogen (daf wt%)	ASTM D5373	0.1	0.3	1.4
Sulfur (daf wt%)	ATSM D4239	0.1	0.1	0.4
Oxygen by Difference (daf wt%)	in-house	41.6	32.9	17.7
Gross Calorifc Value (MJ/kg daf)	ISO 1928	20.8	23.5	29.0
Chlorine (µg/g daf)	in-house	552	233	5591
Fluorine (µg/g daf)	in-house	16	24	38
Bromine (µg/g daf)	in-house	<10	<10	<10

The presented analyses of the feed materials also displayed another expected effect of thermal pre-treatments: the elemental analysis was much more heavily weighted towards carbon at the expense of hydrogen and oxygen as the thermal pre-treatment severity increases. A Van Krevelen diagram is often used to compare the composition of biomass to other solid fuels such as peat or coal and is used to show how thermal pre-treatment affects the C-H-O distribution of the material. Figure 4.2 shows the position of the feed materials on a Van Krevelen diagram. The reader may want to compare Figure 4.2 and Figure 2.4.

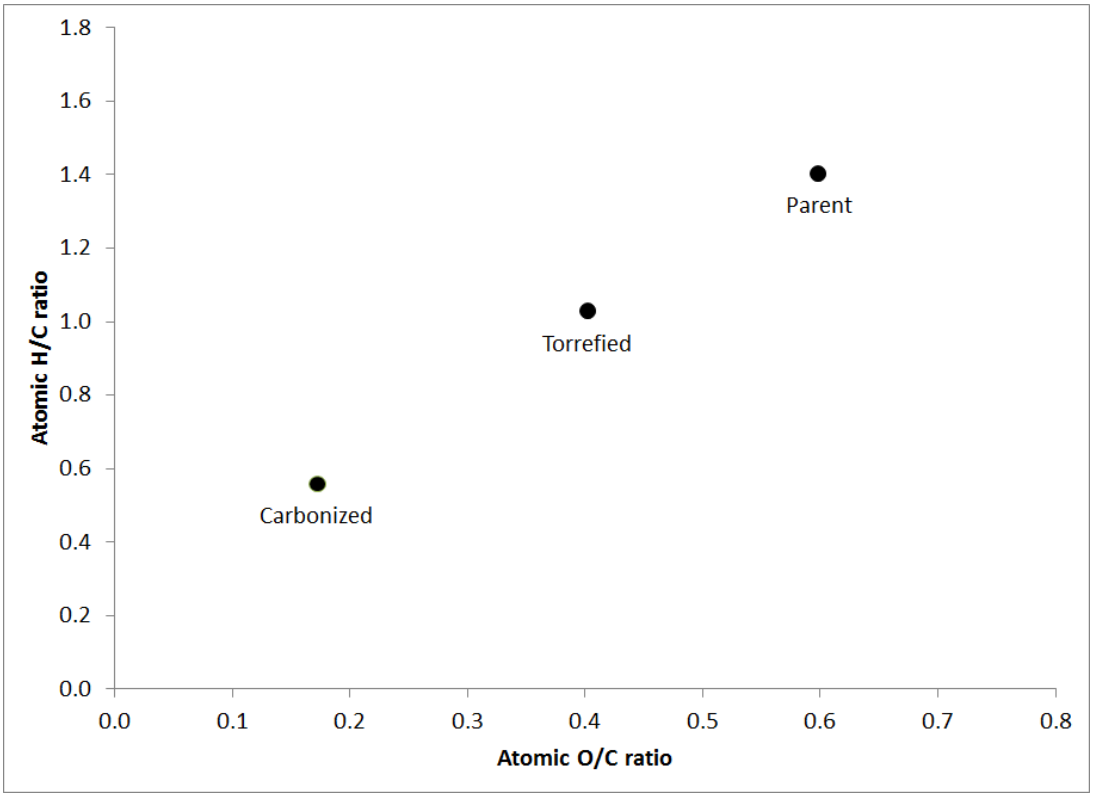

Figure 4.2: Van Krevelen diagram of the parent material and the thermally pre-treated materials (torrefied and carbonized).

The moisture of the feed materials was measured by drying in a purged oven at 100 – 105°C, 91 - 98 kPa_{abs} (-1 to -3 inHg). This is the same technique that was described in section 3.1.1. Table 4.3 shows these results. Interestingly, the torrefied material had less moisture than the carbonized material. The difference in the moisture may be due to differences in the production conditions of the material (relative humidity on the day the material was produced) or it may be that the carbonized material gained some hygroscopic nature based on the composition of the ash coupled with the increased ash concentration and thus had an increased equilibrium moisture content.

Table 4.3: Moisture results from the parent and thermally pre-treated feed materials.

Fuel Type	# points	Average	*min*	*max*	*std dev*
Mids	4	13.7%	*13.0%*	*15.3%*	*1.1%*
Torr	4	3.0%	*2.6%*	*3.6%*	*0.5%*
Carb	4	5.2%	*4.9%*	*5.9%*	*0.5%*

Although a consistent size fraction was used to create the torrefied and carbonized material, the thermal pre-treatment process itself can be expected to reduce the particle size of the material through attrition. The torrefied material and especially the carbonized material were observed to be much more brittle during handling. As was shown in chapter 3, particle size can have a significant impact on the gasification performance, especially if the material contains a substantial portion of fine material. In order to understand how the particle size had been altered by the thermal pre-treatment, the particle size distribution of a sample of each material was determined by sieving. The results are shown in Figure 4.3. From the figure it can be observed that less than 5% of the parent material passed through a 1.18 mm screen. However, around 30% and 73% of the torrefied and carbonized materials passed through a 1.18 mm screen, respectively. This demonstrates that the based on the selected technology of the thermal pre-treatment, the particle size of the material was reduced during the treatment.

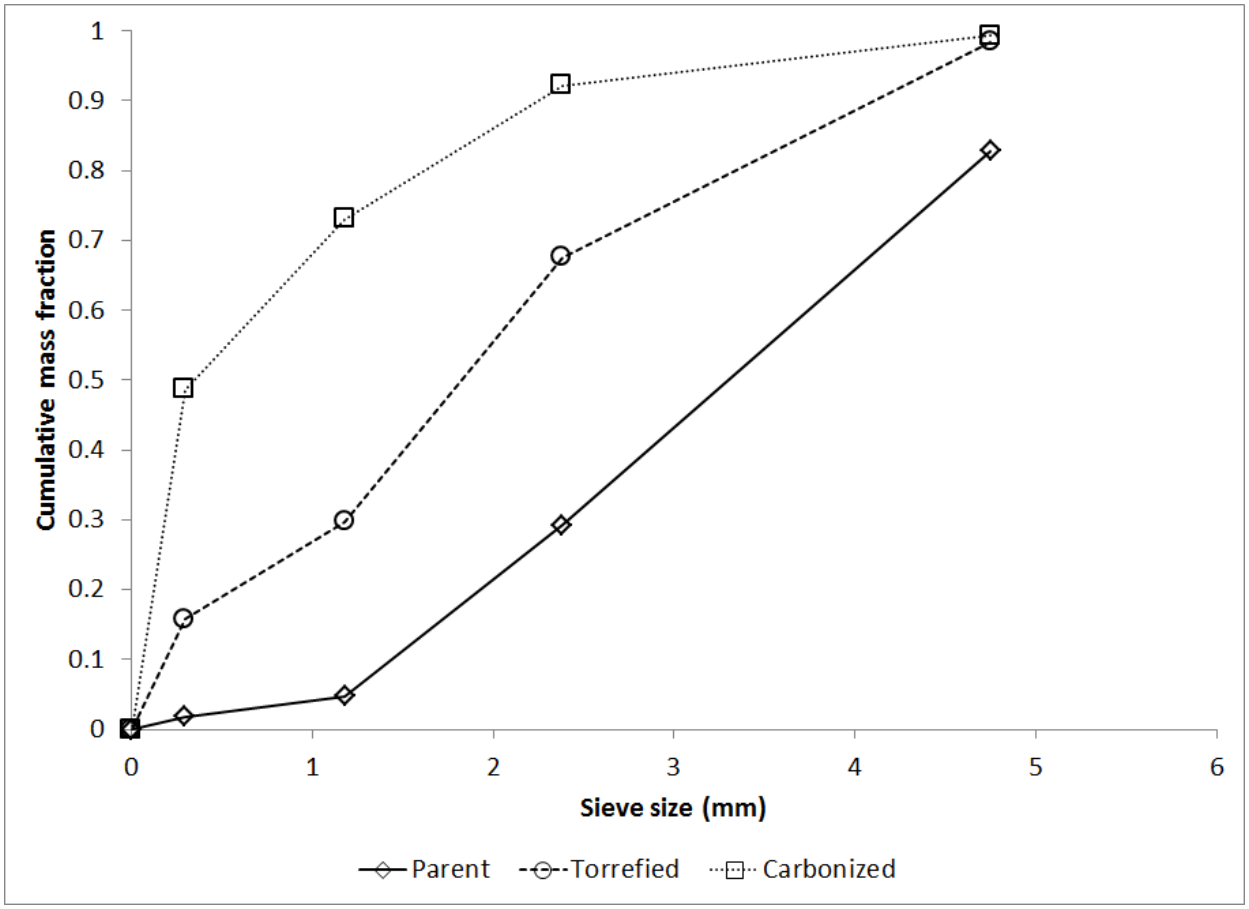

Figure 4.3: Cumulative particle size distribution determined by sieving for the parent, torrefied, and carbonized feed materials.

4.1.2 Bed Material

The same bed material that was used in the work presented in chapter 3 was re-used for the work presented in this chapter. A small amount (~ 3 kg) of fresh new olivine sand had to be added in order to make up for material losses that had occurred from the experimental campaign in chapter 3. Due to the time that had elapsed between the work presented in chapter 3 and the work presented in this chapter 4, there may have been changes to bed media from slow reactions in natural air (such as the hydration or carbonation of CaO to $Ca(OH)_2$ or $CaCO_3$).

4.1.3 Fluidizing Medium (Gas)

The same air supply network was used for the work presented in chapter 3 as was used for the work presented in this chapter.

4.2 **Experimental Apparatus**

The same experimental apparatus (small pilot-scale gasifier) that was described in chapter 3 was used for the work presented in this chapter. There were however a few key changes and improvements to system that are worthwhile noting since they may have an impact on the results:

- A new rotary airlock was installed in the feed system. The original rotary airlock had worn substantially from years of use. The new rotary airlock has a slightly different design in order to reduce the chance of feed jams at the feeder (greater pocket volume and bevelled rotor tips), was constructed of more abrasion resistant grades of metal (to improve longevity), and had a lower temperature rating which required a nitrogen purge in order to dilute or prevent potential backflow of gases. Due to both the better sealing and the presence of the purge, there was less leakage of producer gas back through the feed arm which should have affected the gas movements and temperature in the feed arm. This may have affected how the feed moved through the feed arm and how the feed was distributed onto the top of the bed. The nitrogen purge meant that a small amount of extra nitrogen purge (5 SLPM) was being put into the gasifier which would have a small impact on the gasifier operation (an addition of roughly 2% to the total amount of nitrogen and approximately 1% to the total amount of gas flow).
- The char removal port was modified. Originally, the char removal port consisted of a valve and a section of pipe that was capped off. In order to address problems with the char removal system, its configuration was changed. The old rotary airlock from the feed system was installed directly above the char drain valve. A thick plastic bag with ~ 0.025 m^3 (~ 25 L) of capacity was then sealed to the outlet of the char drain valve.

4.3 **Experimental Procedure**

The experimental procedure was very similar to the experimental procedure described in chapter 3 with a few key changes that will be highlighted in this chapter. Changes to the procedure were made in response to learning experiences from the prior experimental

work carried out on the system. Normally, the objective of a change to the procedures was in order to reduce costs (labour or otherwise) or in order to improve the results that could be obtained from the experimental work.

4.3.1 Operational Procedures

The operational procedures that were described and presented in chapter 3 were also used for the experimental comparison of the thermally pre-treated materials with some small modifications. The key differences in the procedures are highlighted:

- The sand (bed media) was no longer drained after every experimental run. Sand was left in the system, allowing it to cool and then being refilled. This was partly due to the increased difficulty of adding sand through the new rotary airlock.
- A nitrogen purge was used on the rotary airlock.
- As described in section 4.3.2, the char sampling was significantly different.
- As described in section 4.3.4, the tar sampling was significantly different.

4.3.2 Char Sampling

In the procedure described in chapter 3, char was removed from a section of pipe installed at the char removal port. This method had a few challenges and was thereby modified in order to improve operations. A key challenge with the original method was that this procedure took a fair bit of effort and required constant attention. During high levels of char production, one person could spend 5 minutes every 15 minutes emptying the char. When coupled with all the other duties and responsibilities of the operators (condensate sampling, tar sampling, monitoring the gas sampling system, filling the feed hopper, controlling the feed rate to maintain temperature, etc.) this was unreasonable. Secondly, with the original method, the char did not always drain easily. From chapter 3 it can be seen that there were couple experimental runs where char could not be obtained because of plugging during the run in the char drain. For the new char drain set-up employed in the experiments described in this chapter, an empty plastic char bag was sealed to beneath the char drain valve at the start of a run condition. During normal operation the char drain valve was opened and the rotary airlock was powered on. When a run condition ended or

the bag filled with char, the plastic char bag was removed and a clean one placed on the char drain. The amount of char recovered was then weighed.

Based on the results of chapter 3, a sample of the char was not characterized by ultimate and proximate analysis. Instead the char was saved from each condition and multiple TGA runs will be completed in order to get an understanding of the average ash content and to get an estimator for variability within the char samples. The results from the one of each char sample was completed and given in the appendices of this thesis (section A.4, Figure A.6).

4.3.3 Gas Composition Measurement

The system and procedures for measuring the gas composition are the same as those described in chapter 3. The micro-GC was serviced and re-calibrated with 3 – 7 point linear calibrations for each gas during the time between the experiments described in chapter 3 and the experimental work described in this chapter. The CO and CO_2 NDIR analyzers were not relied on during this experimental work.

4.3.4 Tar Sampling

A new tar sampling system developed at CanmetENERGY was used for the experiments described in this chapter instead of the impinger-based sampling method described in chapter 3. This tar sampling system had been compared to the sampling by the impingers and was found to give equivalent results within the error of the data (Robinson, 2012). The new tar sampling apparatus was able to reduce the amount of effort required for the tar sampling activities and hopefully, the simplified procedure reduced the potential for errors or failures.

The tar sampling arrangement is shown in Figure 4.4. The concept of sampling by the tar column is very similar to the impinger sampling method. The tar sampling was completed by drawing a sample of hot-filtered gas (>400°C) from the location labeled “gas sampling location” in Figure 3.2 through heated lines (at 400°C) followed by a vertical arrangement of 3 stages containing isopropanol. The hot gas bubbled through the first stage of isopropanol which is at approximately room temperature. The gas then passed into two further stages of isopropanol, the first stage supported by a coarse glass frit, the second stage supported by a

medium glass frit. The isopropanol in the second and third stage of isopropanol was contained inside condensers which were maintained by a glycol cooling loop at between -5 and -10°C. The amount of gas sampled was measured by a wet test meter.

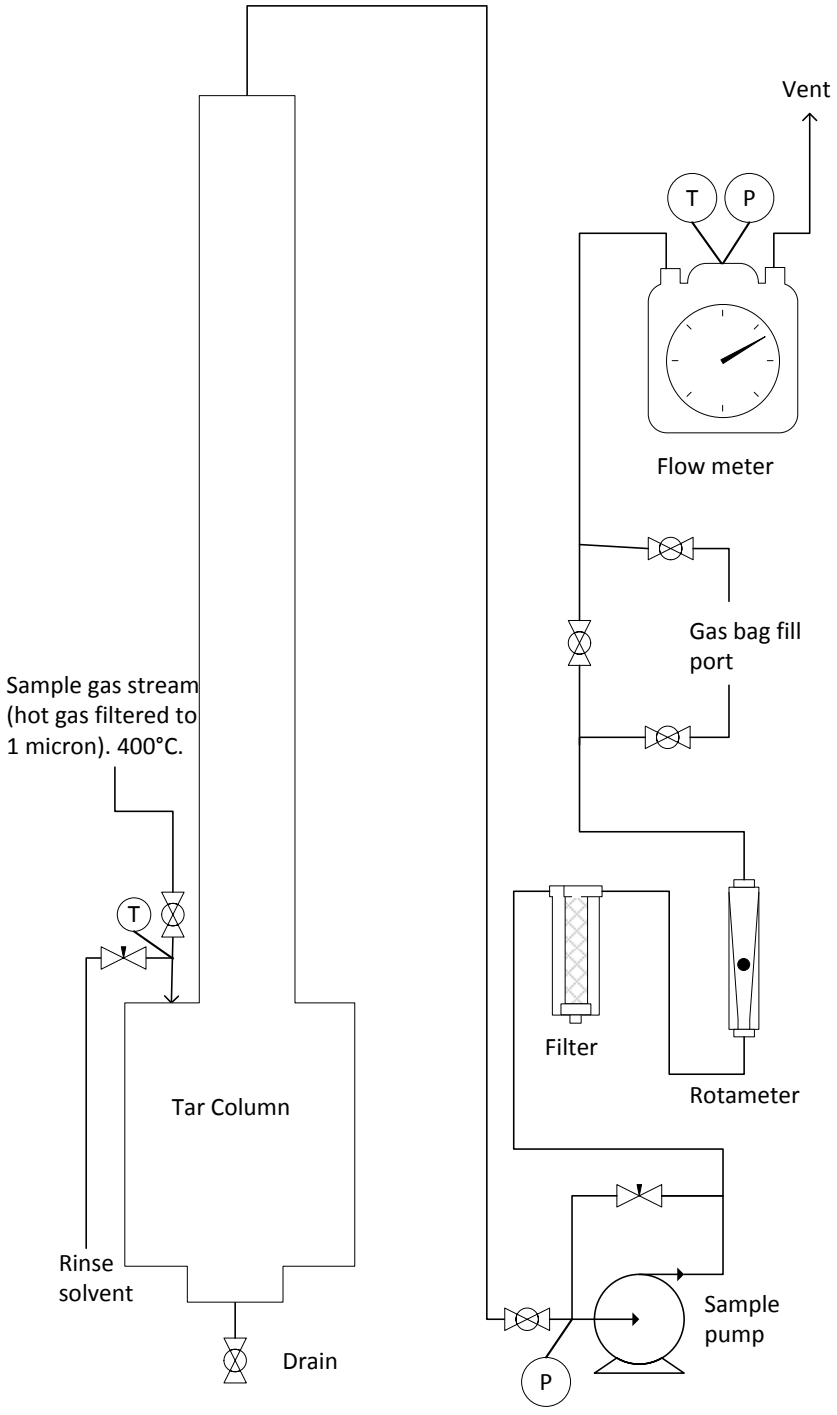

Figure 4.4: Flow diagram of tar sampling by the tar column.

4.4 Experimental Conditions and Operations

One experimental run was completed with each of the materials: the parent, the torrefied, and the carbonized material. Each experimental run had two condition levels. Compared to the experimental work described in chapter 3, the conditions were selected to be identical in order to facilitate comparison of the data sets. For this experimental work only the 875°C and 800°C condition levels were tested (a bed temperature level of 725°C was not tested). The 725°C bed temperature level, based on the results from chapter 3, resulted in the lowest carbon conversion, lowest cold gas efficiency, and highest tar loading meaning that the 725°C condition level produced the least desirable gasification performance. The mass input of fuel for the 725°C condition was also the highest and this required high feed input pushed the limits of the small pilot-scale gasifier's capabilities (the feed system's ability to reliably deliver feed material, ID fan's capacity to handle the volume of gas, and the capacity of the afterburner). It was feared with the torrefied and carbonized material (which have higher specific energy and were drier than the materials tested in chapter 3) that the limits of the system would have been exceeded if a condition at 296 sLpm air and a bed temperature of 725°C had been attempted. Attempting to run this condition level is a part of the future work that is associated with the project. Table 4.4 shows the experimental conditions that were tested.

Table 4.4: Condition levels tested in the experimental campaign to understand the effect of thermal pre-treatments.

Run Code	Pre-treatment Level	Air flow: Condition 1	Air flow: Condition 2	Bed Temperature at Condition 1	Bed Temperature at Condition 2	Run Order
		sLpm	sLpm	°C	°C	
Mid	Parent	275	257	800	875	1
Torr	Torrefied	275	257	800	875	2
Carb	Carbonized	275	257	800	875	3

The experimental conditions given in Table 4.4 represent the objectives that the operators aimed for. Table 4.5 shows some of the key parameters actually achieved during each experimental condition.

Table 4.5: Operational and measured parameters during the comparison of mid, torrefied, and carbonized feed materials.

Run Code	Fuel	Bed Mass	Air flow	LabView feed rate	Bucket feed rate	Avg. Bed T.	Bed P (at 0.219 m)*	Char recovery
		kg	sLpm	kg/h	kg/h	°C	kPa	kg/h
Mid	Parent (mid)	-	257	11.8	11.1	874	1.7	0.6
Mid	Parent (mid)	11	275	14.5	14.7	801	1.9	1.5
Torr	Torrefied	-	257	10.7	9.4	875	2.5	1.7
Torr	Torrefied	-	275	15.1	15.4	801	3.5	3.0
Carb	Carbonized	-	257	8.3	7.3	875	4.2	1.8
Carb	Carbonized	-	275	12.8	12.2	800	4.7	3.6

*After the first experimental run, the pressure trends became erratic, it is possible that plugging in the pressure port or some other measurement error was present

Table 4.5 shows that the objective temperature level was able to be achieved, averaged over the duration of the condition, within 1°C. The feed rate that was required to achieve the desired bed level was unique for each thermal pre-treatment level. The torrefied material required a higher feed rate to maintain an average bed temperature of 800°C. Because the torrefied material is significantly drier, has a similar level of ash, and has greater specific energy, this represents a much larger fuel energy input into gasifier. The feed rate required to achieve an average bed temperature of 875°C with the torrefied and both temperature levels with the carbonized materials was lower than the feed rate required with the parent material. This is in contrast to the work in chapter 3 where roughly equivalent feed rates for the dry materials and the pellets were required to achieve the same average bed temperature. The gasification of the thermally pre-treated materials also resulted in a far greater amount of char being recovered.

Although the average bed temperature is the same for the tests of the differently pre-treated materials, the temperature profile in the gasifier is not. Figure 4.5 and Figure 4.6 show the observed average temperature profiles for the gasifier at the 800°C and 875°C condition. The figures show that at both temperature levels, the thermal pre-treatment appears to lead to elevated temperatures in the region just above the bed (splash zone and beginning of the freeboard). This is despite the fact that the thermally pre-treated materials had smaller particle size distributions (in chapter 3 it was observed that the smaller particles tended to lead to a depression of the temperature in the splash zone and early

freeboard at 800°C). However, it can also be observed from bed pressure measurement at 0.219 m above the distributor was greater for the thermally pre-treated materials. The elevated pressure in the bed, which is evidence that the bed was expanded to a greater height into the freeboard, may be related to the elevated temperature in the freeboard. This was the case that was observed in the temperature profiles presented in the appendices (section D.2) from the chapter 3 data. It does need to be understood that although the objective was to compare all the pre-treatments at equivalent conditions, that is not possible since fixing a parameter such as the fluidizing velocity and the bed temperature means that a different freeboard temperature profile may be observed.

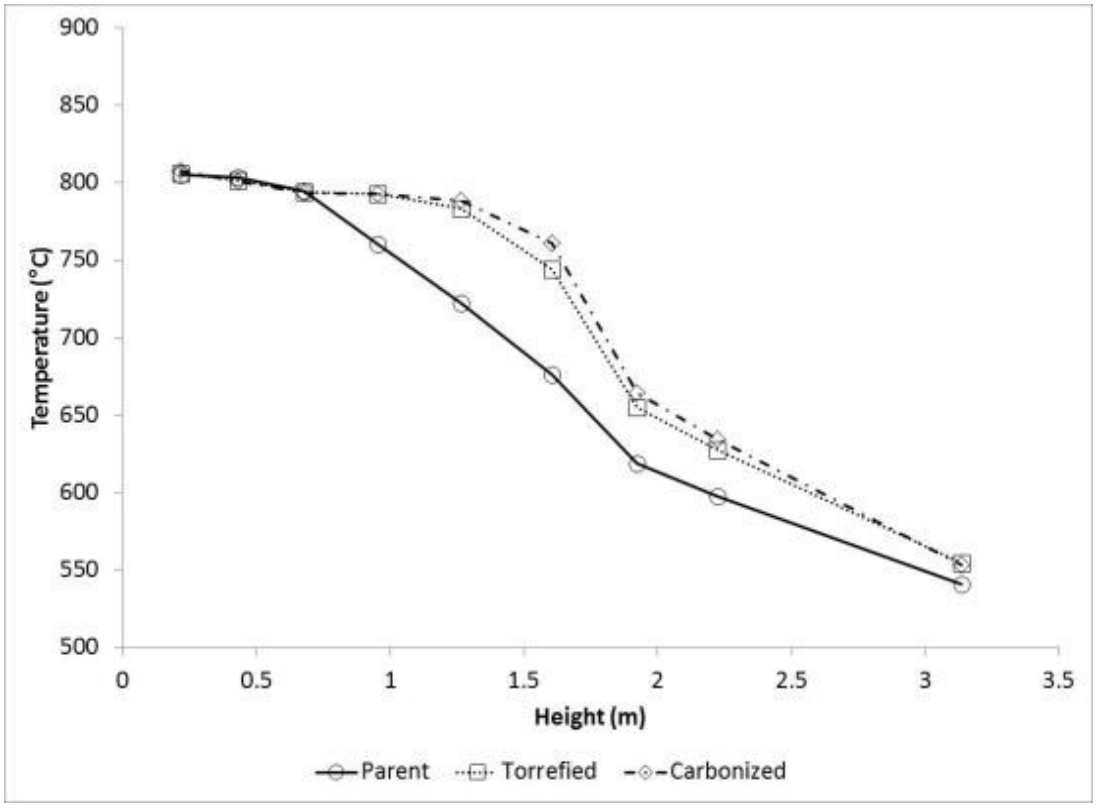

Figure 4.5: Temperature profiles in the gasifier at a bed temperature of 800°C.

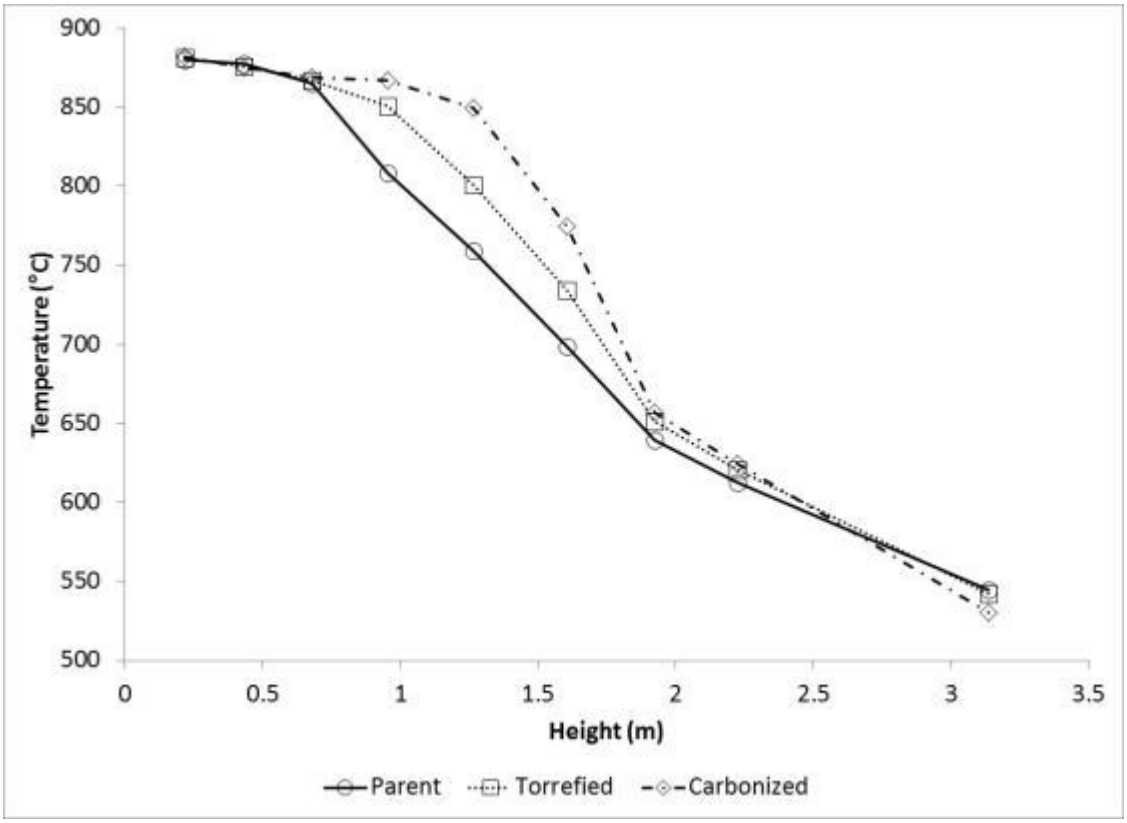

Figure 4.6: Temperature profiles in the gasifier at a bed temperature of 875°C.

4.5 **Results**

The gas composition that was produced from each of the thermal pre-treatment level was distinct. This is similar to the results from chapter 3, where each particle size and particle form led to a distinct producer gas composition. Table 4.6 shows the major gas components measured by the micro-GC (the average results over the "steady-state" duration given in the run charts provided in the appendices, section C.1). The table also provides for reference, the measured amount of condensate (water) and the measured amount gravimetric tar during the condition. As the severity of thermal pre-treatment increases, the hydrocarbon and tar concentration was greatly reduced. Despite the lower input of hydrogen (elemental basis) into the system with thermally pretreated materials, the concentration of hydrogen gas was not severely affected. The methane concentration of the gas was similar for the parent and the torrefied materials (whereas it is greatly depressed for the carbonized materials), but the concentration of C2 gases (ethane, ethylene, and acetylene) was reduced even for the torrefied materials.

Table 4.6: Average measured gas composition of the gasification of parent, torrefied, and carbonized material.

Run Code	Fuel	Avg. Bed T. °C	CO %vol	CO_2 %vol	H_2 %vol	CH_4 %vol	N_2 %vol	C2 gases %vol	Grav. Tar g/m^3 [10]	Water g/m^3 [10]
Mid	Parent (mid)	874	12.6	16.7	8.6	3.6	57.0	1.56	8.9	164
Mid	Parent (mid)	801	12.7	17.5	10.4	3.6	54.1	1.52	22.0	185
Torr	Torrefied	875	15.9	13.6	9.0	3.2	57.2	1.12	7.5	71
Torr	Torrefied	801	14.9	15.1	10.7	3.7	54.5	1.07	12.5	114
Carb	Carbonized	875	16.6	11.0	7.4	0.8	63.9	0.23	1.0 [11]	36
Carb	Carbonized	800	15.1	12.5	9.0	1.1	61.9	0.27	0.4	54

[10] **One m^3 is standardized to 0°C, 1 atm on a dry basis.**

[11] **This gravimetric tar sample was contaminated. Analysis of the tar solution by GC/MS revealed that there was contamination by heptadecane (possibly from improperly cleaned glassware). Actual amount is far less than reported.**

4.5.1 Mass Balance Results

In order to report the amount of carbon converted or the cold gas efficiency or the yield of various components a mass balance must be completed on the system. As described in chapter 3, two mass balancing strategies have been applied to the data generated in the small pilot-scale gasifier. One strategy, the traditional method, uses nitrogen as a tracer gas to determine the amount of gas produced. The measured concentration of tar and water can then be converted into a yield. The char yield is reported as the amount of char that is recovered and it is assumed the recovery is adequate and that there is no interference from elutriated bed media. The other strategy uses the amount of carbon, hydrogen, and oxygen input to the system and the composition of the output products in order to determine the mass outputs. Table 4.7 and Table 4.8 show the results from the CHO and the traditional mass balancing methods, respectively.

Table 4.9 shows the carbon, hydrogen, and oxygen balances that were obtained by the traditional method.

The carbon balance from the traditional method was low on average and showed a high level of variation between runs, whereas the average closure of the hydrogen and oxygen balances were slightly high (averaging 103%). This suggests there may still be an underestimation of the amount of char produced even with the altered char recovery method. The CHO mass balance strategy predicted an amount of nitrogen that was between

91 – 103% percent of the expected value. The char and water measurements predicted by the CHO method were once again in poor agreement with the measured values. A key motivation for performing two different mass balance strategies was to verify the reasonableness of conclusions. If both mass balance techniques draw the same conclusion it provides some level of reassurance that the conclusion is not a product of experimental error on the measurements. Table 4.10 shows the relative difference between the values predicted by the two methods. The relative difference reported was defined as follows:

$$d_r = \frac{a_{CHO} - a_{trad}}{\text{Max}\{a_{trad}, a_{CHO}\}} \qquad \text{Eq. 4.1}$$

Table 4.10 shows that the relative difference between the gas yields (or any value that is calculated from the gas yields, such as tar yields and the cold gas efficiency) is always less than 10%. This is reassuring that conclusions drawn with regards to these numbers are fairly certain. The water yields and the char yields are far less certain and show large relative differences.

In order to better compare the results from this chapter with the results of chapters 3 and 5, the results from the CHO method will be used for further discussions (the mass input of nitrogen is not accurately measured during steam-oxygen gasification in the equipment described in chapter 5, thus the traditional method cannot be applied to the data from chapter 5).

Table 4.7: Tabulated results from the CHO mass balance method.

Run Code	Fuel	Airflow	Feed rate	Average Bed T.	dry gas yield	Hydrogen	Carbon Monoxide	Methane	Ethylene	Carbon Dioxide	Ethane	Acetylene	Propylene	Light HC gases
		sLpm	kg/h	°C	kg/kg-biomass DAF	kg/kg-biomass DAF	kg/kg-biomass DAF	kg/kg-biomass DAF	kg/kg-biomass DAF	kg/kg-biomass DAF	kg/kg-biomass DAF	kg/kg-biomass DAF	kg/kg-biomass DAF	kg/kg-biomass DAF
Mid	Parent	257	11.1	874	3.006	0.019	0.378	0.061	0.038	0.788	0.004	0.003	0.003	0.109
Mid	Parent	275	14.7	801	2.370	0.018	0.305	0.050	0.030	0.658	0.005	0.002	0.007	0.093
Torr	Torrefied	257	9.4	875	3.174	0.021	0.514	0.059	0.029	0.692	0.004	0.002	0.003	0.097
Torr	Torrefied	275	15.4	801	1.926	0.015	0.295	0.042	0.017	0.469	0.004	0.001	0.004	0.068
Carb	Carbonized	257	7.3	875	4.369	0.024	0.734	0.019	0.008	0.763	0.002	0.000	0.000	0.029
Carb	Carbonized	275	12.2	800	2.630	0.017	0.405	0.017	0.006	0.527	0.002	0.000	0.000	0.025

Fuel	Airflow	Feed rate	Average Bed T.	Water (Gross)	Water (Net)	GC Tar + Benzene	Grav. Tar	Char	E/R	HHV (gas)	MW (gas)	Gas density [12]	Carbon conversion [13]	Carbon conversion [14]	Cold Gas Efficiency
	sLpm	kg/h	°C	kg/kg-biomass DAF	kg/kg-biomass DAF	kg/kg-biomass DAF	kg/kg-biomass DAF	kg/kg-biomass DAF	mol/mol	MJ/kg	g/mol	kg/m^3	kg/kg	kg/kg	MJ/MJ
Parent	257	11.1	874	0.310	0.145	0.051	0.021	0.016	0.34	4.09	28.02	1.250	89.1%	98.1%	59.1%
Parent	275	14.7	801	0.355	0.189	0.043	0.042	0.414	0.28	4.45	27.72	1.237	73.8%	81.2%	50.8%
Torrefied	257	9.4	875	0.109	0.077	0.037	0.019	0.119	0.31	4.20	27.46	1.225	79.0%	84.5%	56.7%
Torrefied	275	15.4	801	0.223	0.190	0.022	0.020	0.343	0.20	4.55	27.23	1.215	50.1%	53.3%	37.3%
Carbonized	257	7.3	875	0.120	0.051	0.002	0.004	0.394	0.39	2.82	27.73	1.237	71.0%	71.3%	42.5%
Carbonized	275	12.2	800	0.185	0.115	0.002	0.001	0.752	0.25	2.99	27.53	1.228	43.7%	44.0%	27.1%

[12] at 0°C, 1 atm

[13] Carbon conversion to gas only

[14] Carbon conversion to gas and any measured organic liquids

Table 4.8: Tabulated results from the traditional mass balance method.

Run Code	Fuel	Airflow	Feed rate	Average Bed T.	dry gas yield	Hydrogen	Carbon Monoxide	Methane	Ethylene	Carbon Dioxide	Ethane	Acetylene	Propylene
		sLpm	kg/h	°C	kg/kg-biomass DAF	kg/kg-biomass DAF	kg/kg-biomass DAF	kg/kg-biomass DAF	kg/kg-biomass DAF	kg/kg-biomass DAF	kg/kg-biomass DAF	kg/kg-biomass DAF	kg/kg-biomass DAF
Mid	Parent	257	11.1	874	2.950	0.018	0.371	0.060	0.037	0.774	0.004	0.003	0.003
Mid	Parent	275	14.7	801	2.479	0.019	0.319	0.052	0.031	0.689	0.005	0.002	0.007
Torr	Torrefied	257	9.4	875	3.076	0.020	0.498	0.057	0.028	0.671	0.004	0.002	0.003
Torr	Torrefied	275	15.4	801	2.090	0.017	0.320	0.045	0.018	0.509	0.004	0.001	0.005
Carb	Carbonized	257	7.3	875	4.392	0.024	0.738	0.019	0.008	0.767	0.002	0.000	0.000
Carb	Carbonized	275	12.2	800	2.884	0.019	0.444	0.019	0.006	0.578	0.002	0.000	0.000

Fuel	Airflow	Feed rate	Average Bed T.	Water (Gross)	Water (Net)	GC Tar + Benzene	Grav. Tar	Char	ER	HHV (gas)	MW (gas)	Gas density [12]	Carbon conversion [13]	Carbon conversion [14]	Cold Gas Efficiency
	sLpm	kg/h	°C	kg/kg-biomass DAF	kg/kg-biomass DAF	kg/kg-biomass DAF	kg/kg-biomass DAF	kg/kg-biomass DAF	mol/mol	MJ/kg	g/mol	kg/m^3	kg/kg	kg/kg	MJ/MJ
Parent	257	11.1	874	0.386	0.221	0.050	0.021	0.065	0.34	4.09	28.02	1.25	0.874	96.3%	58.0%
Parent	275	14.7	801	0.371	0.206	0.045	0.044	0.123	0.28	4.45	27.72	1.24	0.772	84.9%	53.1%
Torrefied	257	9.4	875	0.178	0.145	0.036	0.019	0.197	0.31	4.20	27.46	1.22	0.766	81.9%	54.9%
Torrefied	275	15.4	801	0.197	0.164	0.024	0.022	0.213	0.20	4.55	27.23	1.21	0.544	57.9%	40.4%
Carbonized	257	7.3	875	0.127	0.058	0.002	0.004	0.329	0.39	2.82	27.73	1.24	0.714	71.6%	42.7%
Carbonized	275	12.2	800	0.127	0.058	0.002	0.001	0.394	0.25	2.99	27.53	1.23	0.480	48.2%	29.7%

[12] at 0°C, 1 atm

[13] Carbon conversion to gas only

[14] Carbon conversion to gas and any measured organic liquids

Table 4.9: Comparison of the performance of the traditional and CHO mass balancing strategies.

					Traditional method			C-H-O method				
Run Code	Fuel	Airflow	Feed rate	Average Bed T.	Carbon closure	Hydrogen closure	Oxygen closure	Nitrogen closure	Measured water	Predicted water	Measured char recovery	Predicted char recovery
		sLpm	kg/h	°C					g/m^3	g/m^3	kg/h DAF	kg/h DAF
Mid	Parent	257	11.1	874	104%	110%	105%	102%	163.7	129.1	0.36	0.09
Mid	Parent	275	14.7	801	91%	105%	105%	96%	185.1	185.1	0.36	1.19
Torr	Torrefied	257	9.4	875	108%	111%	104%	103%	70.9	42.2	1.35	0.82
Torr	Torrefied	275	15.4	801	87%	100%	103%	92%	114.4	140.7	2.51	4.04
Carb	Carbonized	257	7.3	875	96%	102%	101%	99%	35.9	34.1	1.01	1.21
Carb	Carbonized	275	12.2	800	78%	90%	101%	91%	54.1	86.2	2.06	3.94
Average					94%	103%	103%	97%				
Minimum					78%	90%	101%	91%				
Maximum					108%	111%	105%	103%				
Std. Dev.					11.1%	7.6%	1.7%	5.0%				

Table 4.10: Relative difference between the values predicted by the CHO and the traditional method.

Run Code	Fuel	Airflow	Feed rate	Average Bed T.	Gas yields	Water yield (Gross)	Char yield	Carbon conversion	Cold Gas Efficiency
Mid	Parent	257	11.1	874	1.9%	-19.7%	-74.9%	1.9%	1.9%
Mid	Parent	275	14.7	801	-4.4%	-4.4%	70.2%	-4.4%	-4.4%
Torr	Torrefied	257	9.4	875	3.1%	-38.6%	-39.5%	3.1%	3.1%
Torr	Torrefied	275	15.4	801	-7.8%	11.8%	38.1%	-7.8%	-7.8%
Carb	Carbonized	257	7.3	875	-0.5%	-5.5%	16.5%	-0.5%	-0.5%
Carb	Carbonized	275	12.2	800	-8.8%	31.2%	47.6%	-8.8%	-8.8%

4.5.2 Effect on Gas Composition and Yield

The level of thermal pre-treatment was found to have an effect on the dry gas composition of producer gas from gasification of these materials at both bed temperature levels tested. A gas with a greater heating value was produced at the 800°C bed temperature compared to the 875°C condition for all thermal pre-treatment levels. This difference can be attributed to the higher equivalence ratio (lower feed rate at a constant fluidizing velocity) that was required in order to achieve a bed temperature of 875°C. The higher equivalence ratio results in a more oxidized gas that is more diluted with nitrogen. This was somewhat offset by the higher carbon conversion observed at higher temperatures. The carbonized material produced a gas with a substantially lower heating value compared to the torrefied and parent material. Although the carbonized material produced a gas with high carbon monoxide concentration, lower carbon dioxide, and only slightly lower hydrogen concentration, the great reduction in the concentration of hydrocarbons in the producer gas from the gasification of carbonized material had an impact on the heating value. Figure 4.7 shows how the heating value of the producer gas and how the H_2/CO varied with the applied thermal pre-treatment and with the average bed temperature.

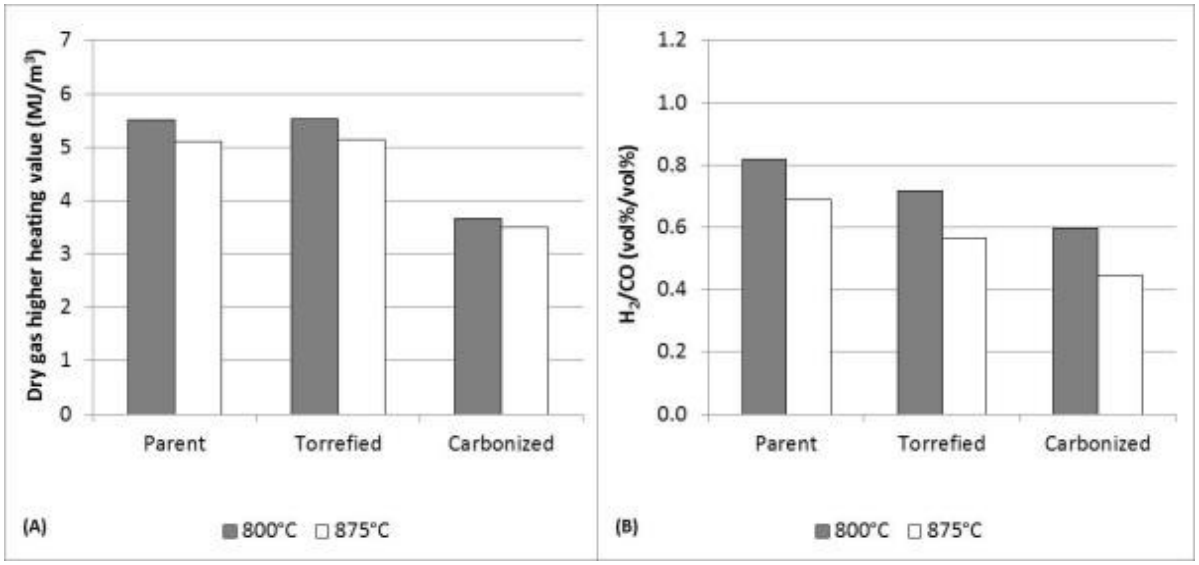

Figure 4.7: Comparison of gas properties from gasification of parent, torrefied and carbonized materials. (A) Dry gas heating value and (B) H_2/CO ratio.

The results from the mass balances show how the yield of gas species was impacted by the thermal pre-treatment of the material. This is not always immediately apparent from the

gas composition data. Despite a lower average concentration of hydrogen in the producer gas for the carbonized material compared to the parent material (9.0 vol% vs. 10.4 vol% at 800°C and 7.6 vol% vs. 8.6 vol% at 875°C), when converted to a yield basis (the amount of hydrogen gas produced per kilogram of dry, ash-free material) the carbonized material yielded a similar amount of hydrogen gas at 800°C and a greater amount at 875°C than the parent material. This is especially surprising since there was far less moisture present in the carbonized material and there was less elemental hydrogen present in the material itself compared to the parent material. The primary difference is that most of the elemental hydrogen that went into the gasifier with the carbonized material was converted to either water vapour or to hydrogen gas. With the parent material, a lot of the elemental hydrogen that went into the gasifier is contained in hydrocarbon gases and tar components (such as methane, ethylene and naphthalene). Figure 4.8 shows how the yield of hydrogen and hydrocarbon gases (methane, ethylene, acetylene, ethane, and propylene) varied with the severity of thermal pre-treatment and with average bed temperature. The figure also shows that the yield of both hydrocarbons and hydrogen gas is increased with temperature.

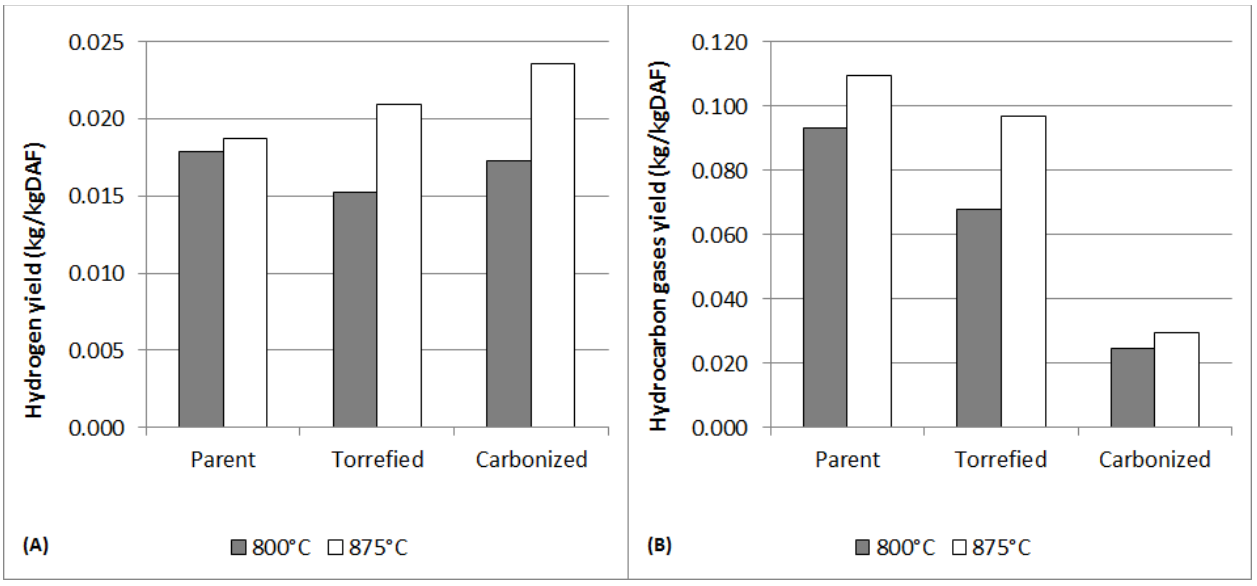

Figure 4.8: Yield of select of gaseous species in product gas from parent, torrefied, and carbonized material at 800°C and 875°C. (A) Hydrogen yield. (B) Hydrocarbon gases yield.

4.5.3 Effect on Tar

The concentration of the tar in the producer gas was affected by both the average bed temperature and by thermal pre-treatment level. The torrefied and carbonized material produced gas that contained a lower concentration of tar measured gravimetrically and measured by GC/MS. This was also true for the amount of benzene that was detected in the tar sampling isopropanol solution (Benzene is a condensable organic product that is produced in levels comparable to tar but is normally excluded from the definition of tar). The severity of the thermal pre-treatment had a very strong impact on level of reduction observed in the concentration and yield of tar. Whereas torrefaction reduced the yield of GC tar by 45% and 20% compared to the parent material at an average bed temperature of 800 and 875°C, respectively, carbonization reduced the yield of GC tar by 96% and 97% at average bed temperature of 800°C and 875°C, respectively. Similar trends can be observed with the gravimetric tar and benzene.

An increase in the average bed temperature decreased the amount of gravimetric tar that was measured for the parent and torrefied material. The same result was not observed for the carbonized material although there is strong indication that this was an experimental error[16]. Although the concentration of GC tar in the producer gas decreased with increased bed temperature for the parent, torrefied, and carbonized materials, the reduction was small and the yield of GC tar was actually increased for the parent and torrefied material at 875°C compared to 800°C. The tar concentration and tar yield numbers can be very different based on how much of the material was converted to producer gas and the ER used. The tar yield can be high even though the tar concentration was not, because the gas yield is relatively high. (The gas yield is the yield of gas from the sum of the air and the biomass. Thus it is defined in this thesis by including the oxygen and nitrogen from air and ranges from 1.5 – 4.5 $kg_{dry\ producer\ gas}/kg_{daf,biomass}$). The benzene yield also increases when the temperature is increased. Figure 4.9 compares the tar and benzene results from the parent, torrefied, and carbonized materials at 800°C and 875°C.

[16] The gravimetric tar data point at 875°C for the carbonized material is a large overestimation. The GC/MS confirmed the presence of contamination in the sample (the contamination was identified as n-heptadecane - the absence of other peaks around it also indicate a pure source of heptadecane).

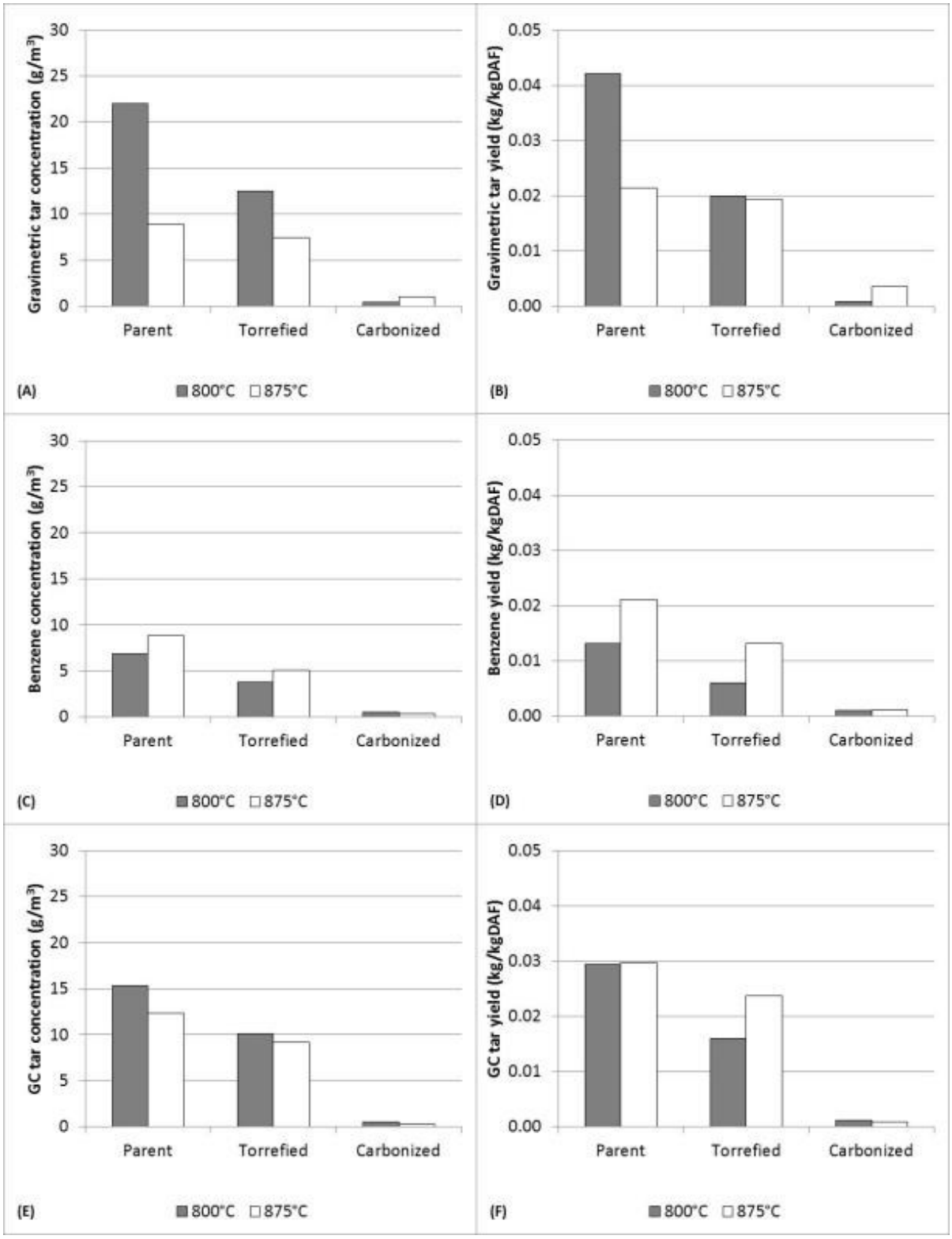

Figure 4.9: Tar production from the gasification of thermally pre-treated materials. (A) Gravimetric tar concentration, (B) gravimetric tar yield, (C) benzene concentration, (D) benzene yield, (E) GC tar concentration and (F) GC tar yield.

In addition to differences in the amount of tar present in the producer gas from the parent, torrefied and carbonized material there were also differences in the composition of the tar as determined by GC/MS. Figure 4.10 shows a comparison of the concentration of tar measured by GC/MS grouped according to their classification. The torrefied material produced a tar that had a higher concentration of class 2 tar (oxygenated tar) than the parent material. At 800°C the GC tar from the torrefied material contained 31% class 2 tars compared to 17% and 8% for the parent and carbonized material, respectively. At 875°C, the GC tar from the torrefied material contained 15% class 2 tar compared to 6% and 2% for the parent and torrefied material, respectively. The tar from the carbonized material was predominantly class 3 tars (single ring, substituted aromatics such as toluene and styrene). Of all the tar classes, class 3 tars are the most volatile which often means they are the least problematic.

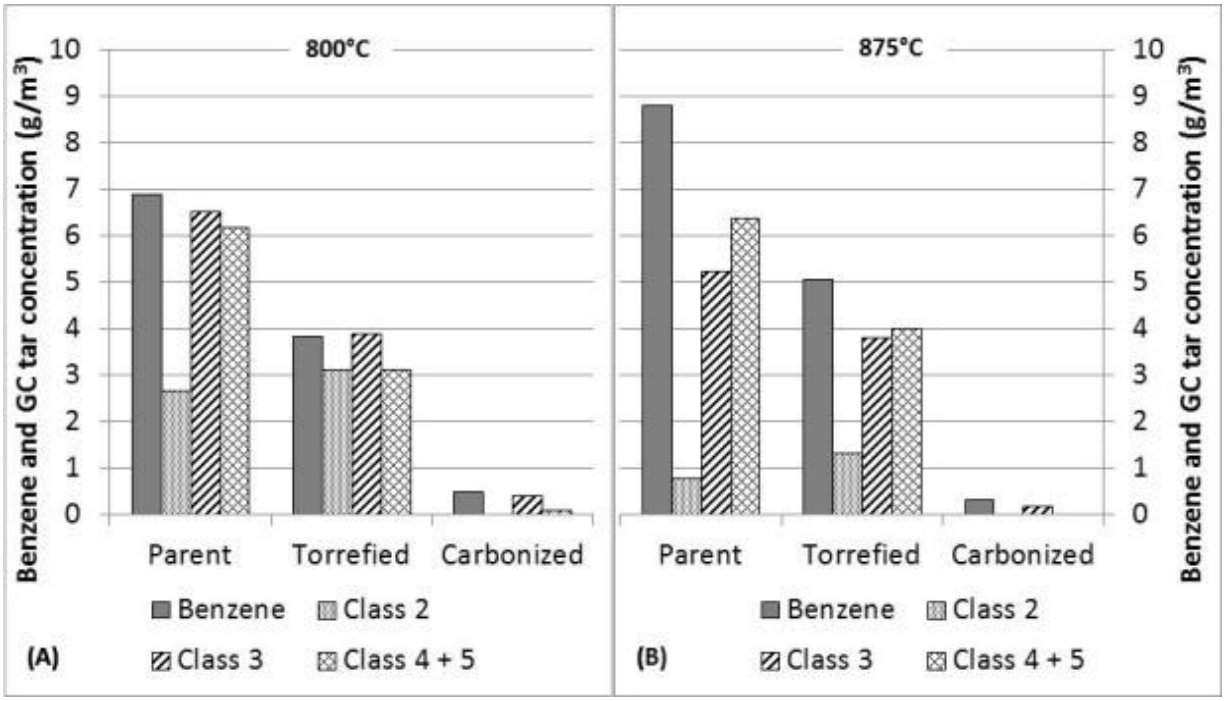

Figure 4.10: Comparison of the tar composition from parent, torrefied, and carbonized material. (A) Gasification at 800°C and (B) gasification at 875°C.

4.5.4 Effect on Carbon Conversion and Cold Gas Efficiency

The percentage of carbon converted to gas and the cold gas efficiency are shown in Figure 4.11. The severity of thermal pre-treatment impacted the fraction of carbon that was

converted to gas and largely due to those conversion differences there were corresponding differences in the cold gas efficiency that was achieved during the gasification. The carbon conversion to gas was also strongly influenced by bed temperature, and this effect was especially noticeable with the thermally pre-treated materials. Between 800°C and 875°C, the percentage of carbon converted to gases increased from 74% to 89% for the parent material (a 15% increase) compared to an increase from 50% to 79% for the torrefied material (a 29% increase) and from 44% to 71% for the carbonized material (a 27% increase). The cold gas efficiency followed similar trends.

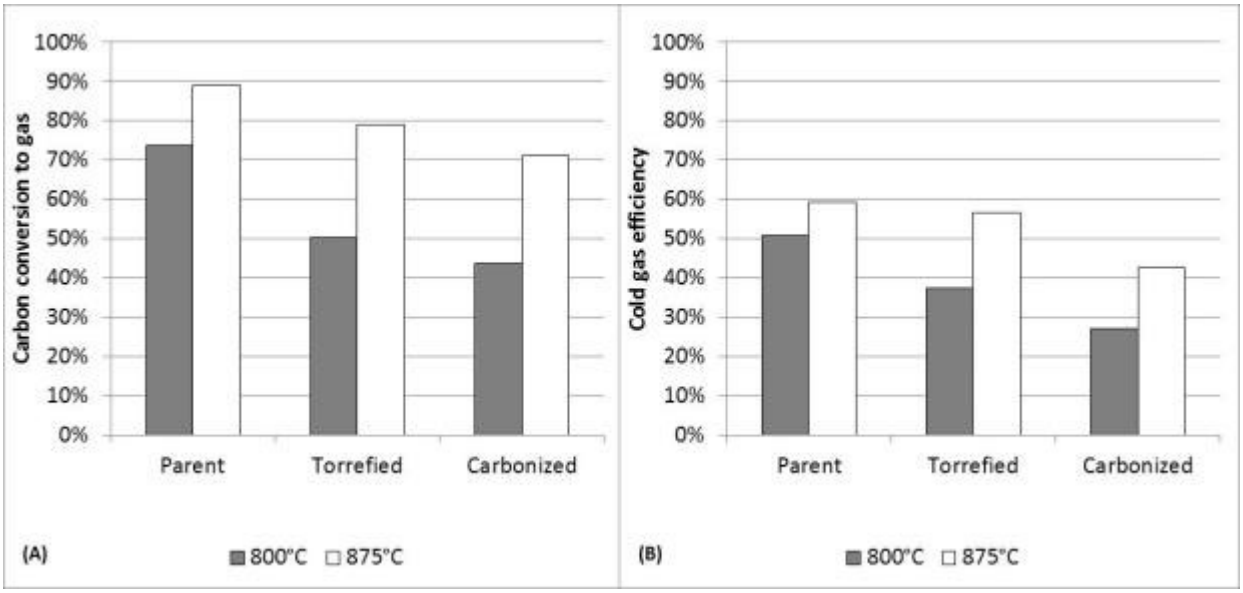

Figure 4.11: Comparison of the conversion and efficiency levels obtained from the parent, torrefied, and carbonized materials. (A) The percentage of carbon converted to gases and (B) cold gas efficiency.

The observed carbon conversion from parent, torrefaction, and carbonization shows a potential weakness of traditional approaches to modelling the gasification process. It has been remarked that wood is poor fuel for gasification due to presence of a substantial level of oxygen which means that the carbon boundary temperature (the temperature above which solid carbon is not predicted by thermodynamic equilibrium) is quite low, normally below 700°C. The carbon boundary temperature would be theoretically the most efficient temperature to operate a gasifier at. Since wood is typically gasified at temperatures in excess of 700°C the result is an over-oxidized gas. Thus, it is suggested that by using a fuel

with oxygen removed through thermal pre-treatment that removes oxygen such as torrefaction, the carbon boundary temperature can be increased and then so can the gasification efficiency (Prins et al., 2006). A key issue with this approach is that full carbon conversion is not reached even at temperatures well above 800°C for the forestry residue tested. The incomplete conversion was even more pronounced for the torrefied and carbonized material. So, although more efficient gasification may be theoretically possible through thermal pre-treatment, this concept must be balanced by the realization that the carbon conversion is practically limited by the reaction kinetics at the temperature range typically used by fluidized bed gasifiers. For fluidized bed gasifiers, especially those operating on torrefied or carbonized feedstocks, having a secondary market for the char, recycling the char or adjusting gasifier design to achieve more complete carbon conversion is a requirement.

4.5.5 Comparison with Chapter 3 Results

The parent material used for the generation of this chapter's results was identical to the mid material that was reported in chapter 3. Comparing the fuel analysis results of the mid material presented in Table 3.3 and the parent material from Table 4.1 confirms that on the basis of carbon, hydrogen, oxygen, ash content and proximate analysis that the materials were indeed very similar compositionally. Although it was the objective to replicate the conditions used in chapter 3 work, the gas composition results showed some differences that might be outside of the natural variability of the data. Table 4.11 shows a comparison of the producer gas composition obtained in the chapter 3 work at a bed temperature of 800°C and Table 4.12 shows the same comparison at 875°C. At 800°C, compared to the two mid gasification trials from chapter 3, the parent material in this chapter gave a producer gas with more nitrogen, tar, and water at the expense of hydrocarbon gases. The increase level of tar measured was particularly surprising since tar measurements from the parent material gasification resembled the characteristics of the fines gasification from chapter 3 more than it did the mid gasification. In other measures however, the producer gas from the mid material in chapter 3 and the parent material from this chapter had the same compositional "signature".

Table 4.11: Comparison of gas produced from all feed materials at 800°C in the small pilot-scale gasifier.

Run Code	Fuel	Avg. Bed T. °C	CO %vol	CO_2 %vol	H_2 %vol	CH_4 %vol	N_2 %vol	C2 gases %vol	Grav. Tar g/m^3 [10]	Water g/m^3 [10]
F1	Fines	799	13.0	17.7	5.8	3.7	57.9	1.56	17.9	151
F2	Fines	801	14.8	17.4	6.9	4.0	54.8	1.68	27.9	182
D2	Coarse	800	12.7	18.3	11.7	3.8	51.6	1.46	7.3	125
G2	Pellets	801	12.3	18.4	12.1	4.0	51.6	1.35	13.3	126
G3	Pellets	801	12.7	18.1	13.0	3.9	50.5	1.31	9.1	119
G1	Pellets	800	12.9	17.7	12.6	3.6	52.0	1.12	8.1	93
E2	Mid	801	14.4	17.6	10.8	4.2	51.1	1.65	11.9	134
E1	Mid	801	14.2	17.7	10.6	4.2	51.3	1.68	11.9	140
Mid	Parent (mid)	801	12.7	17.5	10.4	3.6	54.1	1.52	22.0	185
Torr	Torrefied	801	14.9	15.1	10.7	3.7	54.5	1.07	12.5	114
Carb	Carbonized	800	15.1	12.5	9.0	1.1	61.9	0.27	0.4	54

[10] **One m^3 is standardized to 0°C, 1 atm on a dry basis.**

Table 4.12: Comparison of gas produced from all feed materials at 875°C in the small pilot-scale gasifier

Run Code	Fuel	Avg. Bed T. °C	CO %vol	CO_2 %vol	H_2 %vol	CH_4 %vol	N_2 %vol	C2 gases %vol	Grav. Tar g/m^3 [10]	Water g/m^3 [10]
F3	Fines	871	9.5	17.8	3.8	2.5	65.0	1.17	8.9	125
F2	Fines	862	10.3	17.2	3.8	2.8	64.2	1.26	7.4	156
D2	Coarse	875	11.6	17.7	9.8	3.2	56.2	1.25	2.0	112
G2	Pellets	875	12.9	16.7	11.6	3.1	54.7	0.88	3.2	88
E2	Mid	875	13.0	17.4	9.8	3.8	54.4	1.45	6.9	112
Mid	Parent (mid)	874	12.6	16.7	8.6	3.6	57.0	1.56	8.9	164
Torr	Torrefied	875	15.9	13.6	9.0	3.2	57.2	1.12	7.5	71
Carb	Carbonized	875	16.6	11.0	7.4	0.8	63.9	0.23	1.0 [11]	36

[10] **One m^3 is standardized to 0°C, 1 atm on a dry basis.**

[11] **This gravimetric tar sample was contaminated. Analysis of the tar solution by GC/MS revealed that there was contamination by heptadecane (possibly from improperly cleaned glassware). Actual amount is far less than reported.**

The differences between the mid and parent gasification could be due to some factors including the new components in the feed system which may have resulted in a different delivery of feed material to the bed (and temperature history through the feed arm), the presence of an extra 5 sLpm nitrogen due to purges (this represents an extra input of approximately 2 % nitrogen). The bed media may have also aged in the natural air over the

duration (approximately 1 year) between experiments which may have changed its structure and thus activity (the bed media before use was notably different, it had started to clump together, potentially due to reactions analogous to those that occur in cement. This could have affected properties such as its pore structure). The micro-GC was also re-calibrated and serviced in between the experimental campaigns. At the level of error deemed tolerable (+/- 5% relative error) for the micro-GC, some of the differences could be based on measurement differences from the instrument.

Despite the differences between the mid (chapter 3) and parent (this chapter) gas results, the gas results from the torrefied and carbonized feedstocks are sufficiently different that many conclusions can still be drawn between the effect of torrefaction or carbonization relative to other pre-treatments such as pelletization.

Figure 4.12 shows a comparison of the chapter 3 and chapter 4 gas composition results at an average bed temperature of 800°C on the basis of the H_2/CO ratio. In chapter 3 it was observed that smaller particle sizes led to a decreased H_2/CO ratio. This was true not only for the finest particles, where entrainment was possible, but this was observed even between the mid and coarse particles. Since the torrefied, and especially the carbonized material, had a significant fraction of small particles compared to the parent material it would be expected that there would be a tendency towards a decreased H_2/CO ratio. The torrefied and the carbonized material also contained less moisture, which based on the comparison of moisture levels presented in chapter 3 would also expected to lower the H_2/CO ratio of the producer gas from the torrefied and carbonized material. When this is coupled with the feedstock characterization that confirms a large reduction in the H/C ratio of the torrefied and carbonized materials, it would be expected to see very low H_2/CO ratios in the product gas. The observed H_2/CO for the torrefied and carbonized materials were indeed lower, but based on the impact of moisture, particle size and elemental composition, the magnitude of the reduction was surprisingly small.

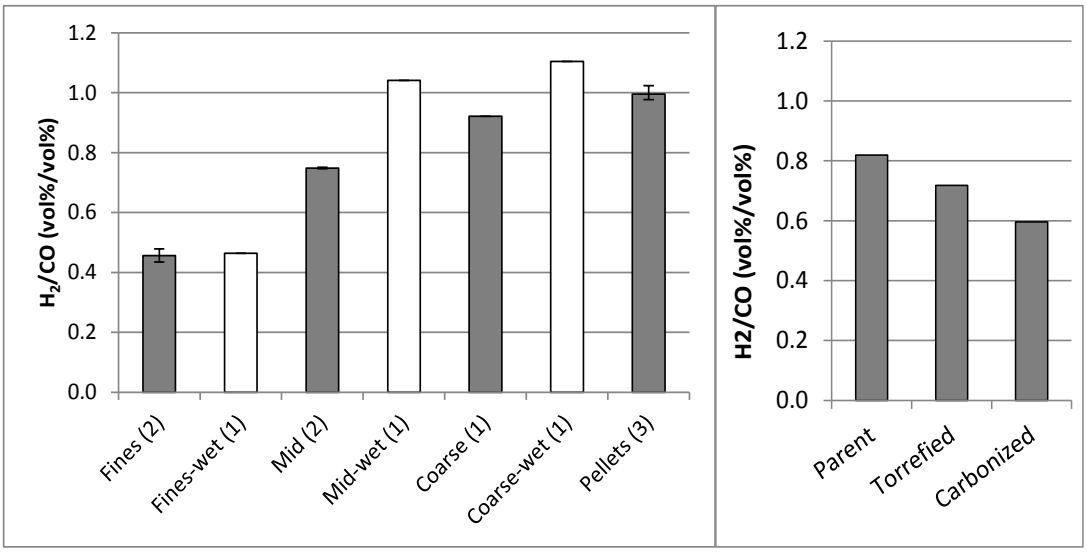

Figure 4.12: Comparison of the H_2/CO ratio of the producer gas from chapter 3 and chapter 4 data at 800°C.

Thus, although the H_2/CO in chapter 4 data was adjusted in the expected direction, it was not adjusted by the expected magnitude based on pre-treatment. A different way of looking at the gas composition difference is to compare the hydrogen yield instead of the H_2/CO as a way to understand exactly what is happening. In chapter 3, the mid feedstock yielded about 18 g H_2/kg_{DAF} at 800°C and 21 g H_2/kg_{DAF} at 875°C. The parent feedstock yielded similar amounts (18 and 19 g H_2/kg_{DAF} at 800 and 875°C, respectively). The fines from chapter 3 yielded less than 10 g H_2/kg_{DAF} across all temperature levels. Despite the strong influence that particle size has on hydrogen yield (in addition to the effect of moisture and elemental composition), the torrefied and carbonized material yielded between 15 – 24 g H_2/kg_{DAF}. This is a strong indication that very little of the hydrogen gas actually results from gas phase reforming reactions of volatiles (implying that the gas phase reactions are slow in comparison to the residence time of the gases), rather most of the hydrogen gas can probably be attributed to reactions between the char and water vapour. Since the moisture had only a small influence on the yield of hydrogen, it also means that the partial pressure of steam in the reactor also only has a small effect on the reaction rate between the char and steam. This is significant since it means that the most important factor in determining the gas composition is not what happens in the gas phase after gases are formed, but the

conditions at which the particle devolatilizes and thus how much char was formed and what the gas composition from devolatilization was.

The results from this chapter offer a potential explanation for the results from chapter 3. A model is presented that describes some key, simplified reactions during the gasification as:

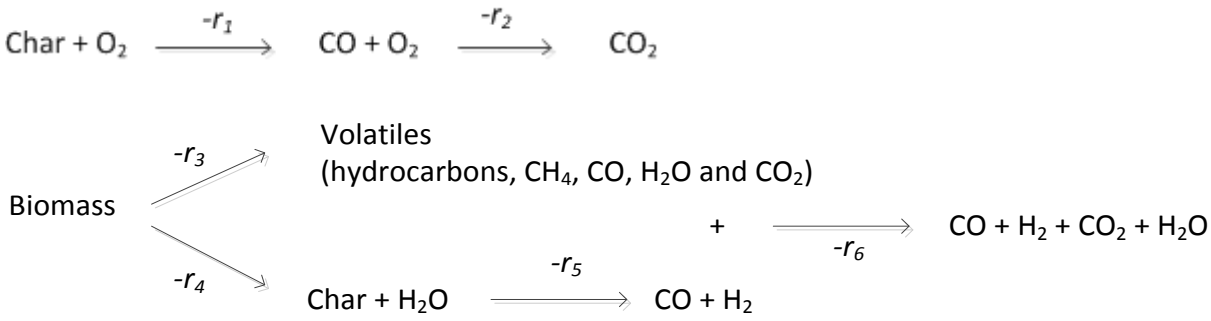

If we consider that the reactions 1 and 2 are very fast and will only occur near the bottom of the bed where oxygen is available, then all the oxygen will be consumed before it has a chance to reach the upper portions of the bed where devolatilization is occurring. Reactions 3 and 4 are very fast, however the extent to which each can occur is determined by the composition of the biomass and the heating rate at which the biomass is subjected to. How much char forms determines the amount of char available for reaction 5. The evidence is that from the devolatilization of biomass below 900°C very little hydrogen gas is formed (Fu et al., 2011; Zanzi et al., 1996). It may even be the case that much of the hydrogen formed from higher temperature pyrolysis is from the contribution of reaction 5 or 6. If we assume that reaction 6 is slow, then the hydrogen production will be determined primarily by the original distribution of char vs. volatiles, the amount of intimate contact between steam and char, and the residence time of the char. If we consider why pellets led to a high yield of hydrogen relative to the other material, the following points are considered:

- Pellets are big enough to be in the thermally thick regime. Devolatilization will be limited by the rate of heat conduction through the particle. The larger the particle, the lower the heating rate will be. A lower heating rate typically leads to a slightly enhanced production of char relative to the amount of volatiles. This is likely to only have a small effect, since if this was a major effect, a lower yield of hydrocarbon gases would be expected from the pellets.

- Compared to smaller, less dense particles, each pellet will contain a greater mass of water (since the mass of the pellet is greater than smaller, less dense particles). The pellets also stay fairly well intact even after it is converted to char. This allows for more intraparticle contact between moisture and char while the core of the particle continues to devolatilize while the outer layer is char.
- The char from the pellets was retained in the bed. The increased concentration of char in the bed would have meant that more material is available to react by reaction 5. It appears that the concentration of steam has a small positive influence of the rate of reaction 5 (comparison of the moist feed materials to the dry materials from chapter 3 shows that the hydrogen gas yield increased by about 14% on average between dry to moist fuels), but even with very dry materials (such as the torrefied and carbonized materials) it is possible to yield high amounts of hydrogen as long as they produce a relatively large portion of char compared to volatiles.

The torrefied and carbonized materials show that even with a hydrogen deficient material (less water and less hydrogen in the organic portion of the feed) that larger hydrogen gas yields are still possible. If we assume that the model presented above where the formation of hydrogen from gas phase reactions is slow in comparison to the formation of hydrogen gas from the steam gasification of char then the observation that the carbonized materials yielded the most hydrogen of any of the materials makes sense.

4.6 **Conclusions**

Thermal pre-treatments were found to have an effect on the composition of the gas from a small pilot-scale fluidized bed gasifier. The thermal pre-treatments also affected the operating behaviour of the system, the tar loading in the producer gas, and the efficiency of the process. If thermal pre-treatment is to be applied to the biomass feedstock for a gasification process, these changes in gasifier performance need to be expected.

The effect of the chemical alterations to the feedstock through torrefaction and carbonization were far more dominant than the effect from the size reduction that happened due to the thermal pre-treatment. Despite the fact that the torrefied material contained more fine material than the parent material, it still yielded less tar, and at 875°C

also yielded more hydrogen gas. The carbonized material contained even more fine material (for comparison, >70% of the carbonized material passed through a 1.18 mm screen, whereas the "fines" made for chapter 3 was the fraction passing through a 3.175 mm screen). Despite this, the carbonized material yielded by far the least amount of tar and also yielded the greatest amount of hydrogen of any of the fuels tested in chapter 3 or this chapter.

Torrefaction pre-treatment may be able to reduce the tar loading in producer gas from biomass gasification. The severity of torrefaction may have a key influence on the level of tar reduction possible. The torrefied material tested was on the severe side of what is normally considered torrefaction, but by going to a more severe thermal pre-treatment, carbonization, the tar content of the gas was reduced by more than 95% according to GC tar measurements. This observation of course needs to be weighted with the vast drop in solid fuel yield from a thermal pre-treatment as severity increases. The results do show that tar production is undoubtedly related the devolatilization products during the gasification.

The producer gas from the torrefied and parent material had a similar heating value. Although there was a reduction in the concentration of the C2 gases in the producer gas from the torrefied material, this was balanced by a higher concentration of carbon monoxide with a lower concentration of CO_2. On the other hand, the carbonized material yielded a gas with a far lower heating value than the torrefied and parent material (33% and 32% less compared to the torrefied and parent material at 800 and 875°C, respectively) which is largely due to the four-fold reduction of hydrocarbon gases in the producer gas from the carbonized material.

The incomplete conversion of char is a central issue observed with the torrefied and carbonized materials. The thermal pre-treatment of the feed material led to a lower level of carbon conversion to gas (in other words, the gasification of thermally pre-treated materials yielded more solid by-product char). This was largely expected based on the amount of fixed carbon that is reported in the proximate analysis (which also indicates that proximate analyses, based on ASTM methods, do have utility in predicting the gasification performance of different feed materials). This emphasizes that for a fluidized bed gasifier operating on thermally pre-treated materials there needs to be either a secondary market

for the by-product char or the char needs to be recycled back into the gasifier in order to achieve reasonable process efficiency.

References

Fu, P., W. Yi, X. Bai, Z. Li, S. Hong, J. Xiang. "Effect of temperature on gas composition and char structural features of pyrolyzed agricultural residues," Bioresour. Tech. **102,** 8211-8219 (2011).

Prins, M.J., K.J. Ptasinski and F.J.J.G. Janssen, "More efficient biomass gasification via torrefaction," Energy. **31**, 3458-3470 (2006).

Robinson, T., "Measurement of tar in biomass producer gas and the development of a new sampling device," undergraduate thesis submitted to the University of Ottawa, Dept. of Chemical and Biological Engineering. Ottawa, ON (2012).

Zanzi, R., K. Sjöström, and E. Björnborn, "Rapid high-temperature pyrolysis of biomass in a free-fall reactor," Fuel. **75,** 545-550 (1996).

Chapter 5. Evaluation of the Effect of Biomass Comminution at the Pilot Scale

This chapter describes the experimental equipment, methods, and results from a study of the steam-oxygen gasification of various forestry residues at the large pilot-scale gasifier. This experimental campaign satisfied many objectives. The experimental campaign produced data on trace contaminant concentrations in producer gas from a large scale gasifier using representative forestry feedstocks that are available to the Canadian paper and pulp industry. Testing of a catalytic gas cleaning system based on a precious metal catalyst was carried out. In addition, the differences between biomass feeding locations was investigated. Evaluating all of these aspects of the work is well beyond the scope of this thesis.

In this thesis, the objective of the analysis and interpretation of the data was to determine whether the effects of particle size differences that were observed in the small pilot-scale gasifier under controlled conditions can be observed in a large pilot-scale system with feed materials that have many differences other than just particle size distribution. Understanding whether the particle size differences are significant enough that they can or cannot be observed despite a number of uncontrolled factors is important in determining the applicability of data generated in the earlier chapters of this work. The influence of feed position is also discussed since it likely interacts with the gasification of small particles.

5.1 Experimental

5.1.1 Feed Materials

Five forestry residues were obtained from various locations across Canada in order to represent various available residues and opportunity fuels that could be suitable for conversion to producer gas in a fluidized bed gasifier. However, due to feeding difficulties, only four of the feed materials could be processed under similar gasification conditions. The four materials are as follows:

- Interior BC Softwood Hog (ISH)
- Mountain Pine Beetle Killed chips (PBK)

- Salt-Laden Hog (SLH)
- White Birch Chips (WBC)

The proximate, ultimate, calorific, and halogen analysis of the feed materials is presented in Table 5.1. The analysis of the ash composition is given in Table 5.2.

Table 5.1: Feed material characterization.

Parameter	Method	ISH	PBK	SLH	WBC
Moisture TGA (wb wt%)	ASTM D7582	13.89	7.91	13.52	13.04
Ash TGA (db wt%)	ASTM D7582	3.67	0.67	10.31	0.64
Volatile (db wt%)	ISO 562	76.91	83.55	66.51	85.59
Fixed Carbon (db wt%)	ASTM D7582	19.42	15.78	23.17	13.76
Carbon (db wt%)	ASTM D5373	51	51	48.8	51.5
Hydrogen (db wt%)	ASTM D5373	5.61	6.17	5.13	5.85
Nitrogen (db wt%)	ASTM D5373	0.24	0.2	0.32	0.17
Total Sulfur (db wt%)	ASTM D4239	BDL	<0.05	0.15	BDL
Oxygen by Difference (db wt%)	in-house	39.48	41.92	35.22	41.79
Gross Calorific Value (MJ/kg dry)	ISO 1928	20.5	20.4	19.4	19.2
Chlorine (mg/kg db)	in-house (pyrohydrolysis)	550	92	5070	78
Fluorine (mg/kg db)	in-house (pyrohydrolysis)	<10	<10	24	<10
Bromine (mg/kg db)	in-house (pyrohydrolysis)	<10	<10	20	<10

*BDL: Below detection limits

Table 5.2: Ash analysis of the feed materials by X-Ray Fluorescence.

Component	Method	ISH	PBK	SLH	WBC
SiO2 (wt%)	ASTM D4326	13.85	11.39	14.54	6.38
Al2O3 (wt%)	ASTM D4326	3.35	3.45	3.78	2.17
Fe2O3 (wt%)	ASTM D4326	2.27	2.65	3.07	1.86
TiO2 (wt%)	ASTM D4326	0.11	0.1	0.15	0.04
P2O5 (wt%)	ASTM D4326	9.78	11.69	7.41	8.55
CaO (wt%)	ASTM D4326	29.7	24.34	28.56	30.14
MgO (wt%)	ASTM D4326	11.11	11.25	13.24	10.2
SO3 (wt%)	ASTM D4326	3.81	2.12	3.86	2.97
Na2O (wt%)	ASTM D4326	1.31	0.77	7.08	0.7
K2O (wt%)	ASTM D4326	9.52	15.59	5.2	15.16
Barium (ppm)	ASTM D4326	1519	659	<250	3269
Strontium (ppm)	ASTM D4326	754	585	871	1038
Vanadium (ppm)	ASTM D4326	<50	<50	<50	<50
Nickel (ppm)	ASTM D4326	102	161	56	140
Manganese (ppm)	ASTM D4326	6993	15181	4781	7254
Chromium (ppm)	ASTM D4326	175	436	200	402
Copper (ppm)	ASTM D4326	94	182	95	227
Zinc (ppm)	ASTM D4326	1299	1761	345	3983
Loss on Fusion (wt%)	ASTM D4326	14.11	14.76	12.46	20.2
Sum (wt%)	ASTM D4326	100	100	99.98	100

There are some differences that were detected in the analyses carried out, some of the most notable differences between the fuels were:

- The pine beetle killed material was drier than the other feed materials.
- The chipped materials (PBK and WBC) have lower ash than the interior BC hog fuel, which has considerably less ash than the hog fuel from salt-laden logs (logs that have been floated through salt water).
- The salt laden hog has considerably more sodium in the ash (in addition to having more total ash) and has much higher levels of chlorine, as would be expected for a material that has spent considerable time in salt water.
- On an ash-free basis, the white birch chips have a noticeably lower calorific value.
- The fixed carbon fraction of the feed materials varies from a low of 13.8 wt% db to a high of 23.2 wt% db.

The difference between these feed materials that is the focus of this chapter is their particle size distribution. Figure 5.1 shows the size distribution of the feed materials. The "hog" materials contained substantially more fine material than the "chip" materials. The chip fuels contained less than 10 wt% material passing through a sieve with an 8 mesh screen-size (2.38 mm) while the hog fuels contained greater than 30 wt%.

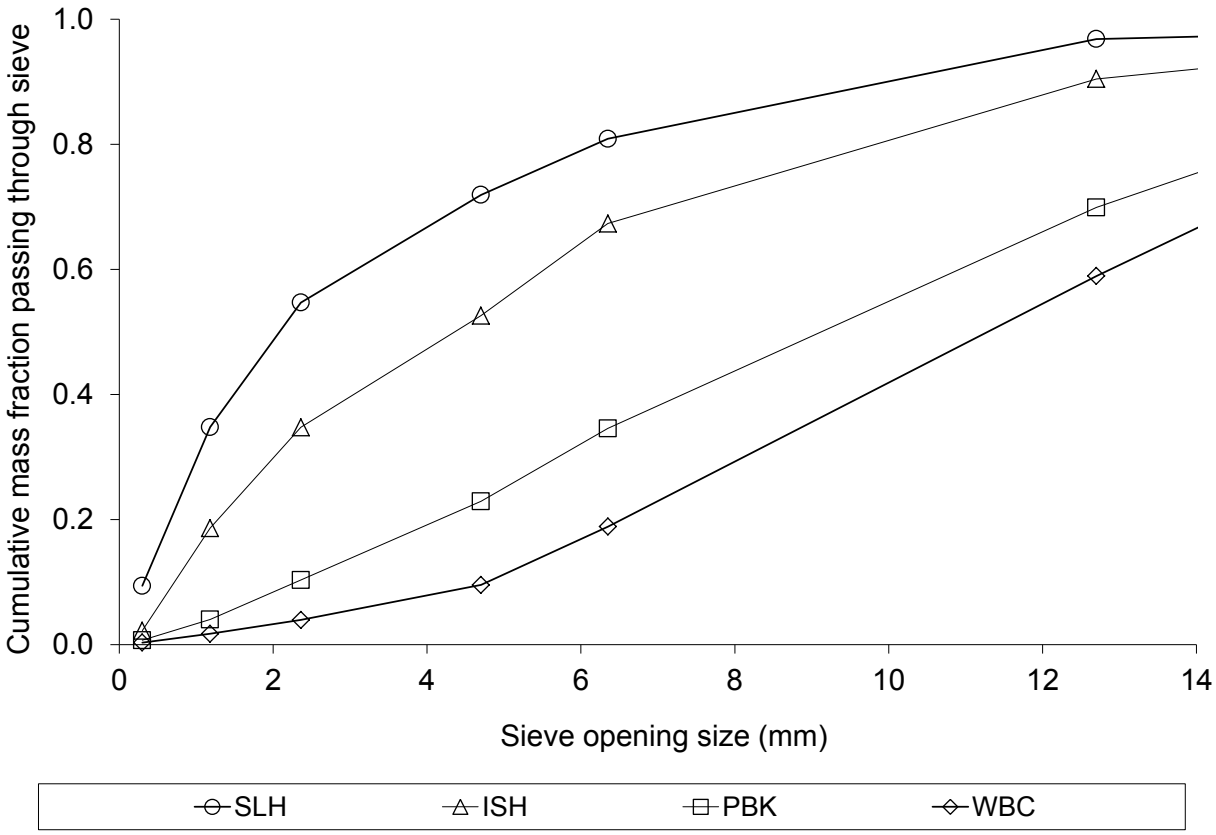

Figure 5.1: Sieve analysis of the gasified feed materials.

5.1.2 Large Pilot-scale Bubbling Fluidized Bed Gasifier

The bubbling fluidized bed (BFB) gasifier used for the comparison of these forestry residues was an atmospheric pressure unit capable of gasifying up to 500 kg/h biomass with steam located at CanmetENERGY (Ottawa, ON), steam-oxygen or air. The steam, if required, was provided via a 180 kPa_{abs} boiler with maximum steam capacity of 1360 kg/h. The boiler was attached to a fired-heater where the steam was superheated up to 650°C. Normal delivery temperature to the fluidized bed was approximately 550°C (the 100°C temperature drop is mostly due to heat loss in the delivery network from superheater to gasifier). The

gasification took place in a 1 m (40”) internal diameter (ID) BFB with the bed and freeboard total height to be 6.5 m. The gasifier was lined with 0.305 m (12”) of refractory material (a 0.1 m layer of hardened refractory, followed by a second 0.2 m layer of insulating refractory). Figure 5.2 shows some of the key dimensions of the BFB and the instrumentation locations. The locations labeled as “TEW” show the location of the thermocouples. Pressure transmitters were also installed at the same locations as the thermocouples.

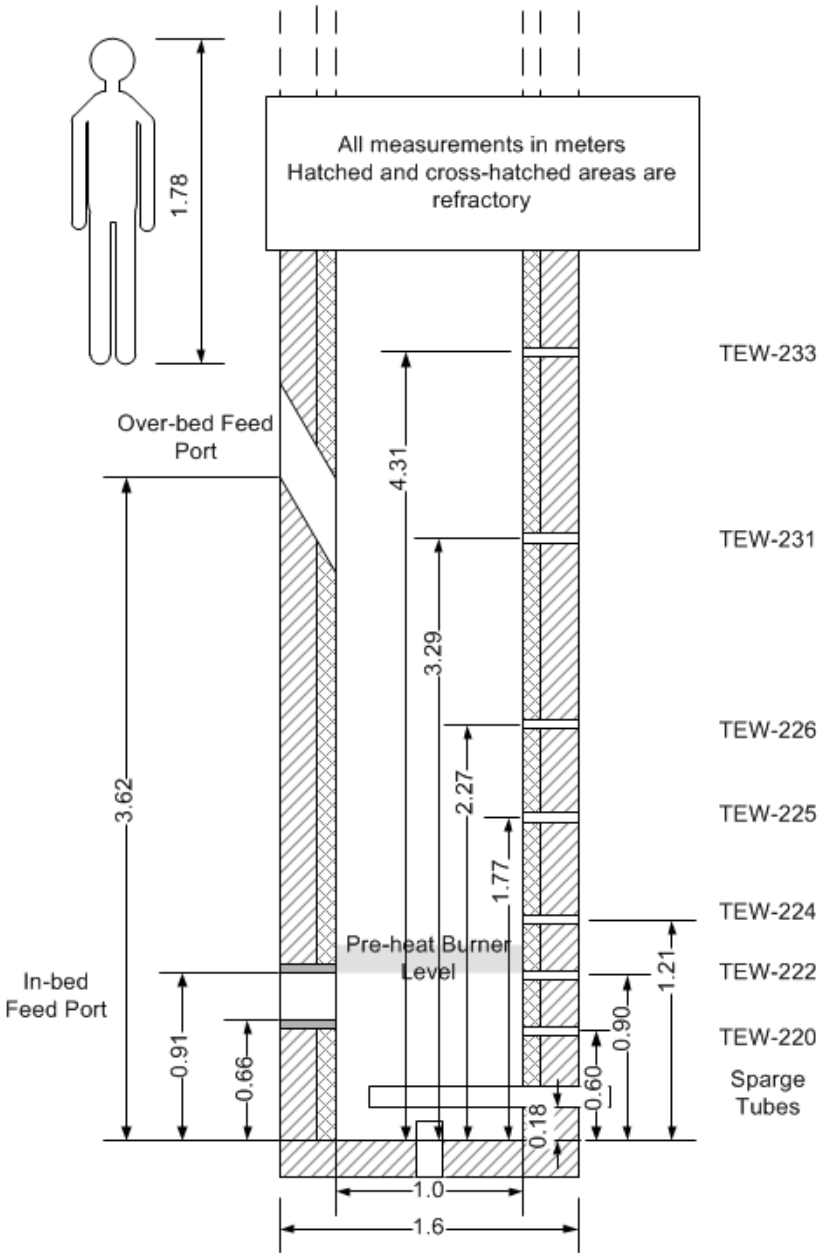

Figure 5.2: Important dimensions of large pilot-scale BFB gasifier.

The biomass feedstock was loaded into a 5 m^3 covered moving floor trailer located outside the facility. From the trailer, the feed material was pneumatically transported to the roof of the facility where the feed material fell by gravity into a fuel bin hopper within the building. A metering screw transported the feed into a set of two knife gates which provide an airlock in the feed system. Two feed augers were available for either injecting the feed material on to the top of the bed (over-bed) or beneath the surface of the bed (in-bed). In order to select a feed position, the unselected feed auger was "blinded off" so that short-circuiting of gas through the feed system was not possible.

The producer gas stream left the bed at 750 to 850°C and subsequently passed through a cyclone at roughly 600°C which removed the coarse particulate from the gas stream. After the cyclone, a small sampling port allowed for the continuous withdrawal of producer gas for analysis and to complete parallel experiments on the catalytic elimination of tar. The producer gas subsequently moved into a condenser where a portion of the steam is condensed from the producer gas stream. The level of cooling achieved in the heat exchanger was dependent on the mode of operation. Although the steam-laden producer gas facilitates a much greater heat transfer (high heat transfer coefficient due to condensing steam), the amount of heat that needed to be removed for the condensation of water was substantially larger compared to when the system was operated as an air-blown gasifier. As a steam-oxygen gasifier, the producer gas left the condenser at >65°C. As an air-blown gasifier, the condenser exit temperatures were below 50°C. The producer gas was then piped to a blower. The piping had a 6 kW (20 000 btu/h) reheat pilot installed to raise the temperature of the producer gas by 5 – 10°C in order to elevate the gas above its dewpoint (the blower was not designed to operate under condensing conditions). The producer gas was then piped to an afterburner where excess air was added and a natural gas pilot was used to ignite and combust the producer gas. Figure 5.3 captures many of the primary components of the pilot-scale gasifier. Figure 5.4 shows a photograph of the dual fluidized bed research facility in which the bubbling fluidized bed gasifier is located.

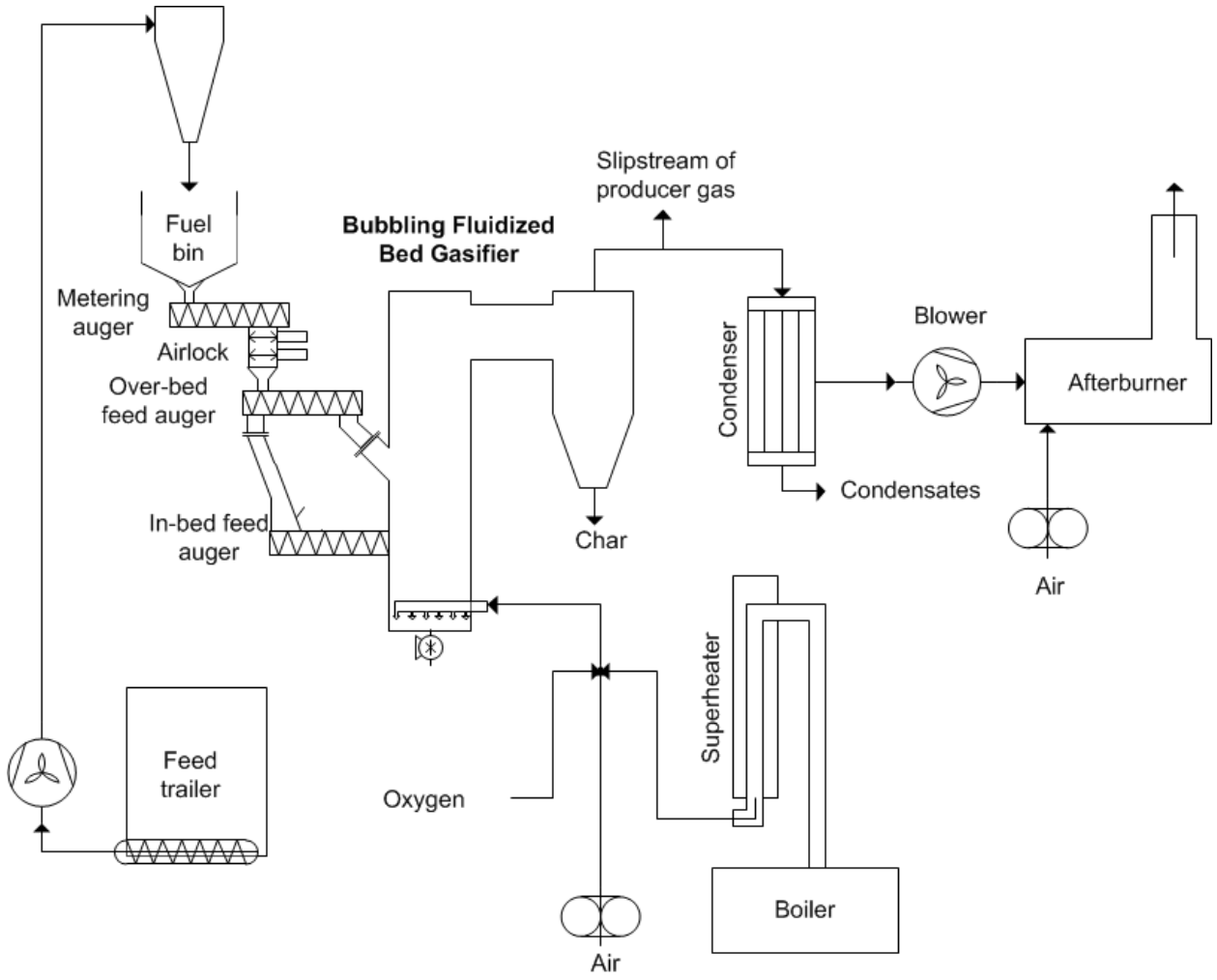

Figure 5.3: Key components of the large pilot-scale BFB.

Figure 5.4: Picture of the BFB laboratory. (A) Indoor feed bin, (B) location of the reactor and (C) Location of the cyclone.

5.1.3 Experimental Procedures

Due to the amount of refractory and the thermal mass of the bed material, the unit was preheated overnight (minimum 12 hours) to approximately 750°C prior to a run to ensure all components of the system had reached elevated temperatures. A 350 kW (1.2 mmbtu/h) preheat natural gas burner system was installed on the BFB gasifier that was used for this purpose.

Bed material was loaded into the system once at the beginning of the experimental campaign. Roughly 1500 kg of bed material (sixty 25 kg bags) was loaded into the system for the tests. Occasionally, one or two bags of sand (bed material) would need to be added to make-up for elutriated bed material. Bed sand was added during natural gas warm-up.

After the preheating period, biomass feed was initiated, and the system was operated as a combustor in order to begin introducing carbon into the bed and warming up components that do not get heated up with the gas burner (such as the bottom of the cyclone which only warms up with some solids in the gas stream). During the solid feed combustion warm up period, the boiler and superheater were also started (if steam was used as gasification medium). During warm-up, the steam was vented through steam supply system in order to warm up the pipes transporting the steam to the BFB. If a different feed position needed to be used, (i.e. the system was set-up for over-bed feeding but in-bed feeding was needed for the day), the bed was temporarily "slumped" (feed and fluidizing air shut off) while flange inserts were switched around to open up the required feed path. Once the appropriate feed position was selected, combustion feed rates and fluidizing air were restarted in order to continue the warm up and regain any lost temperature during the feed position switch.

If air-blown gasification was completed, the feed rate was tripled or quadrupled while simultaneously the amount of fluidization air was reduced by 20 – 50% in order to flip the system from combustion into gasification. Operating parameters were then gradually adjusted in order to meet desired bed temperature and feed rates for the day.

If steam-oxygen gasification was to be completed, the feed would be first stopped and then the fluidization medium would be switched from air to steam. The feeding would then be re-

started and the pure oxygen was mixed into the superheated steam prior to sparge tubes (the fuel feed rate used must be high enough that all the oxygen gets consumed).

Nitrogen was used to purge knife gate valve seats, maintain fluidization in the bed sampling port and to purge out pressure taps. Due to a relatively large amount of nitrogen used, especially for the knife gate purges, a measureable amount of nitrogen is found in the producer gas even from steam-oxygen trials.

In order to carry out the gas analysis and tar analysis, the same procedures as those outlined in chapter 3 were used. The data was analyzed using the CHO mass balancing technique outlined in chapter 3 (since calculation of the mass balances through the traditional method was not possible based on inadequate knowledge of the amount of nitrogen input).

5.1.4 Run Conditions

There were a large number of conditions tested on the large pilot-scale gasifier in the winter and spring of 2012. However, they covered a large range of temperatures and conditions. Unfortunately, due to a variety of reasons including equipment failures, many of the conditions only yielded a partial data set. Other operational issues also caused premature shutdown of the system, especially during attempted second or third run conditions. In the appendices, Figure E.6 and Figure E.7 show examples of the major operational issues observed such as plugging due to char and tar. In order to carry out the mass balances a certain minimum of information is required: knowledge of the inputs (composition and mass flow), the compositional knowledge of the outputs (tar, char, and gas), and the concentration of tar. The number of run conditions that meet these minimum mass balancing conditions are two run conditions at 750-800°C, one at <750°C, and 8 conditions at >800°C. It was elected that for the purposes of this thesis the data set of runs >800°C which have complete information to be evaluated in order to avoid the confounding effect of using data from vastly different operating conditions (especially bed temperature). Table 5.3 and Table 5.4 show the operating parameters for the conditions that are analyzed within this thesis.

The column labelled "Bed T." (Bed Temperature) in the tables represents the average temperature recorded at the thermocouple tagged TEW-222 (refer to Figure 5.2). The "Freeboard T." is the average temperature recorded at 3.1 m (122-1/4") from the bottom of the sparge tubes. The feed location refers to which type of feeding was used and the positions of the feed ports are provided in Figure 5.2. The feed rate was controlled by altering the speed of the metering auger shown in Figure 5.3. The measurement provided is based off a linear correlation between the auger speed and the actual feed rate. The parameters for the correlation were unique for each fuel and were determined by feeding each of the used materials through the feed system. The air flow is calculated from an orifice plate measurement on the air supply network. The steam flow is determined also by orifice plate. The oxygen flow was determined by a venturi meter.

Table 5.3: Operational parameters for air gasification conditions.

Date	Fuel	Bed T. (TEW-222) °C	Freeboard T. (TEW-231) °C	Feed location	Feed rate kg/h	Air flow kg/h
2012-03-07	PBK	831	699	Over-bed	221	319
2012-04-04	SLH	843	719	Over-bed	228	411
2012-04-05	SLH	825	771	In-bed	218	425

Table 5.4: Operational parameters for steam-oxygen gasification conditions.

Date	Fuel	Bed T. (TEW-222) °C	Freeboard T. (TEW-231) °C	Feed location	Feed rate kg/h	Steam flow kg/h	Oxygen flow kg/h
2012-03-14	PBK	852	755	Over-bed	200	200	76
2012-03-22	WBC	854	777	Over-bed	245	200	84
2012-03-29	ISH	855	735	Over-bed	236	200	79
2012-04-23	SLH	836	729	Over-bed	223	200	82
2012-04-26	WBC	826	786	In-bed	245	200	84

Table 5.3 and Table 5.4 show that none of the tests can be considered identical. Without repeats, it cannot be ascertained how much irreproducibility is found in the data.

In order to simplify the reporting of various experimental runs, a set of "run codes" have been developed. These are 7 digit alphabetic codes in the form *AA-BB-CCC*:

- The *AA* digits are either *OB* for Over-Bed feeding or *IB* for In-Bed feeding
- The *BB* digits are either *AG* for Air Gasification or *SG* for Steam-oxygen gasification
- The *CCC* digits are the three letter code that corresponds to the feed material used.

Based on the runs completed, each code is unique and corresponds to the runs reported in Table 5.3 and Table 5.4. As mentioned earlier, for reasons of data completeness, only the first condition's data is compared.

5.2 **Results**

5.2.1 Operational Observations

The runs were completed at neither a constant ER nor at a constant bed temperature, rather a compromise between the two measures were attempted to be achieved. As the ER (the amount of oxygen supplied relative to the feed rate) increases for a given fuel, the temperature of the bed increases. ER and bed temperature are both known to affect the tar yields, efficiency, carbon conversion, and gas composition. Since the fuels were different, it was elected that the most appropriate approach would be to try and run the fuels at a compromise between ER and bed temperature in order to be as similar as possible to other runs. This meant that the ER position and the bed temperature position for each of the fuels were slightly unique. Figure 5.5 maps the ER position of each of the runs with respect to bed temperature.

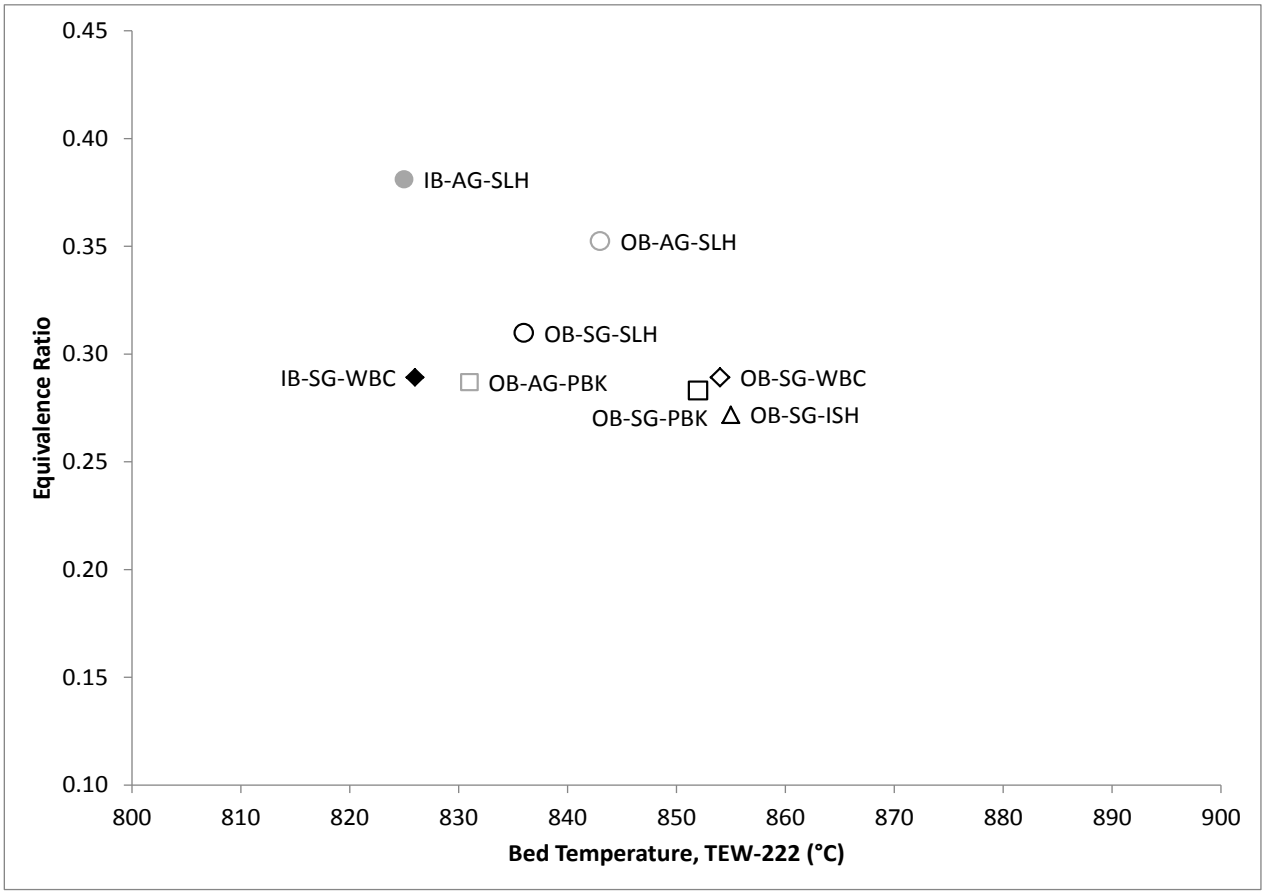

Figure 5.5: Equivalence ratio position for each run condition with respect to temperature.

From Figure 5.5 it can be observed that the runs from an in-bed feed position, the tests were carried out at lower bed temperature but at a similar or greater equivalence ratio. This indicates that there are differences in the amount of oxygen required in order to achieve a similar bed temperature between in-bed and over-bed feeding. From chapter 3, it was observed that for size fractions of the same parent material, very similar ERs were required in order to operate the system at the same bed temperature for fuels of equivalent moisture. As the chemical composition of the feed material was altered by thermal pre-treatment as shown in chapter 4, a unique ER was required in order to reach the same temperature. In the case of the large pilot-scale work, the ER required to achieve a given bed temperature depended on both the feed type and the location that the feed entered the reactor.

In chapter 3, it was presented that different fuel size distributions led to different temperature profiles. In chapter 4, evidence was presented that the chemical composition of the material also influences the temperature profile in a fluidized bed gasifier. For the large

pilot-scale experiments, in the freeboard, the temperature decreased with height more rapidly for smaller particle sizes. As can be seen from Figure 5.6 and Figure 5.7, temperature profile differences were also observed for various fuels and run conditions.

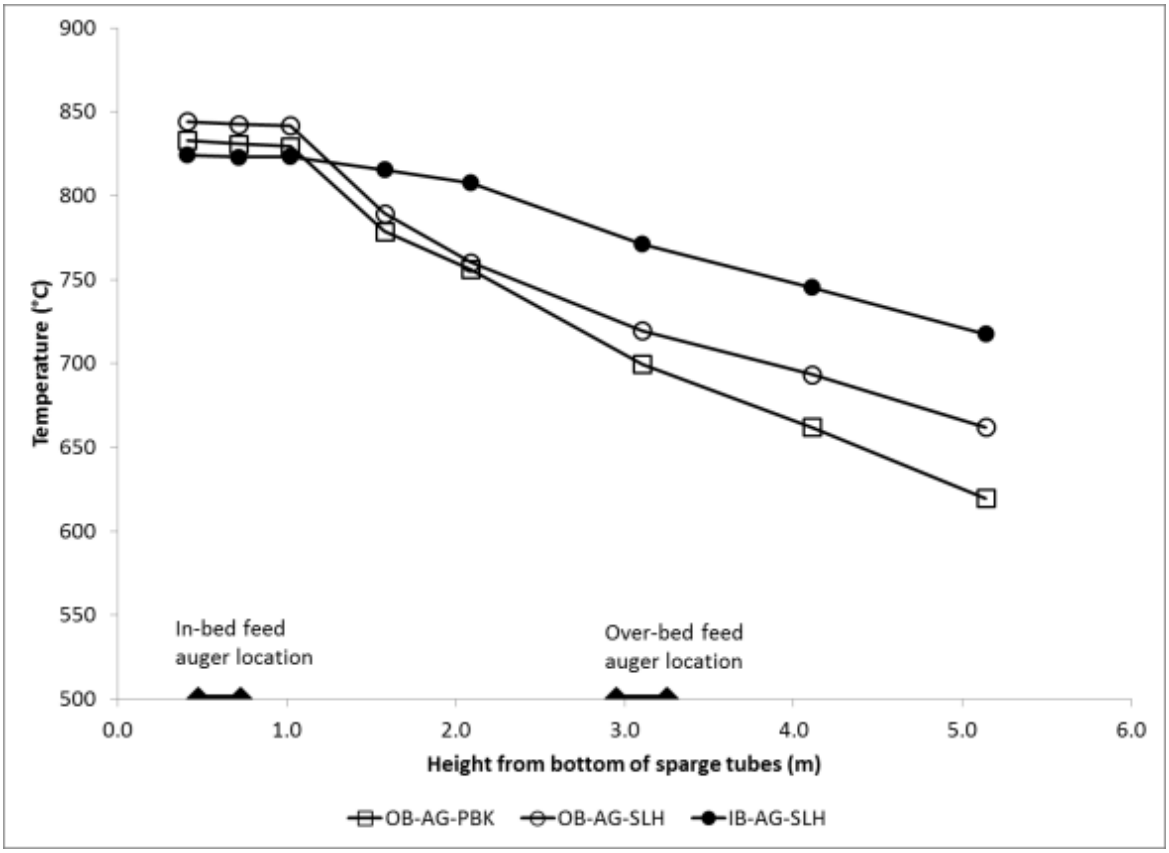

Figure 5.6: Temperature profiles observed during air gasification trials in the large pilot-scale gasifier.

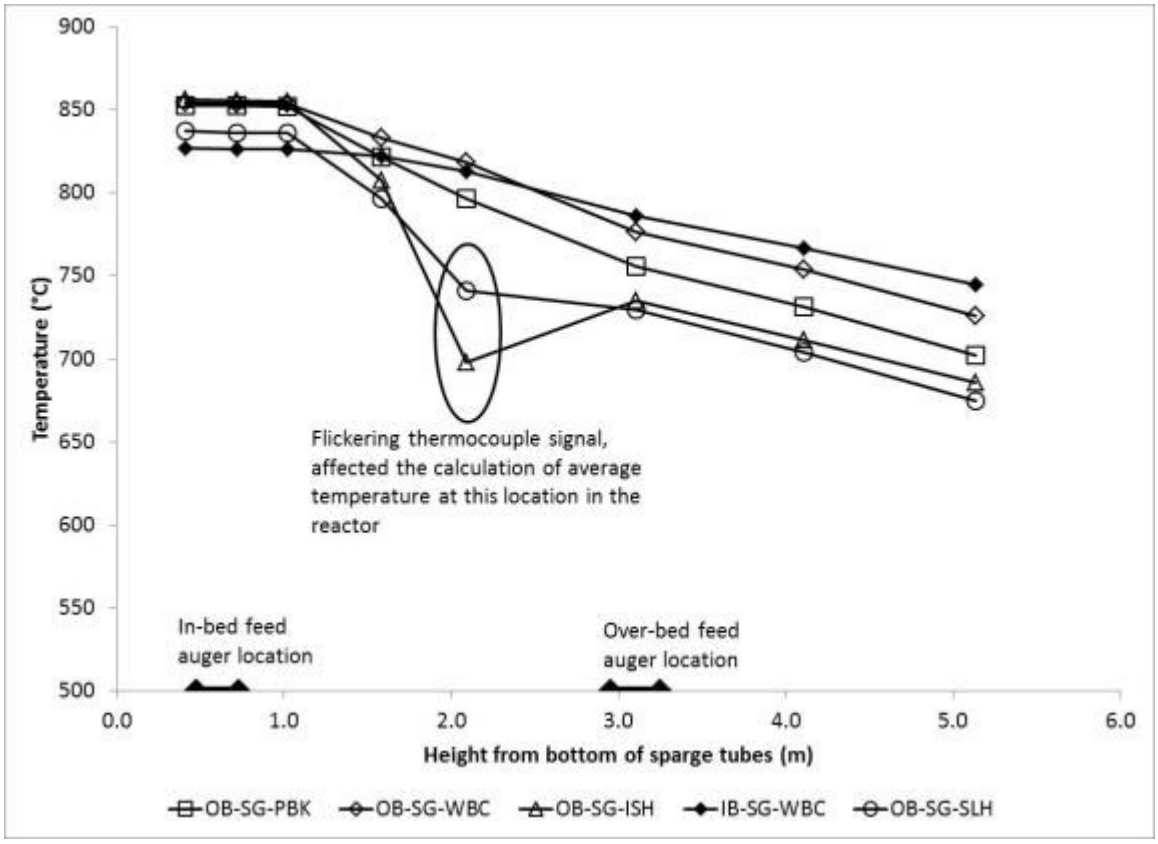

Figure 5.7: Temperature profiles observed during steam-oxy gasification trials in the large pilot-scale gasifier.

In chapter 3 it was presented that the lower freeboard temperatures were observed for smaller particle sizes. In the large pilot-scale work (Figure 5.6 and Figure 5.7), this trend might be reproduced. From the figures, the over-bed fed hog fuels (smaller size distribution) tend to display lower freeboard temperatures. A far more significant effect than particle size can be attributed to the feeding location used with the gasifier. In-bed feeding led to more gradual temperature profiles in the freeboard then over-bed feeding. At reactor heights greater than 3 m from the base of the sparge tubes, the highest temperature was always observed for experiments fed from in-bed feed position.

Detailed run charts are given in Figure C.33 - Figure C.40 which show the time resolved temperature and gas composition recorded in the system over the duration of the runs. One of the most interesting observations that can be made from the run charts is that in the case of the over-bed fed experiments, the gas composition appears to reach a stable level quickly, in the in-bed fed experiments the gas composition never appears to reach a stable

composition. Rather over the duration of the condition, for in-bed feeding, the gas composition appears to be decreasing in CO_2 and increasing in H_2 with time. This would be a strong motivation to repeat some of the tests with increased testing durations during in-bed feeding. This also shows the importance of considering the run charts when interpreting the data from this work. Although the gas composition was slowly changing (and thus hard for an operator to identify during the run) it was indeed changing. This indicates that although a thermal steady state had been achieved, a chemical steady state had not. This fact should be heavily weighed when interpreting the results from in-bed feeding.

5.2.2 Gas Composition

The measured gas composition from the large pilot-scale gasification is presented in Table 5.5 and the heating value of the dry gas is given in Figure 5.8.

Table 5.5: Gas composition measurements from the large pilot-scale gasifier.

Run Name	CO	CO_2	H_2	CH_4	N_2	C2 gases
	%vol	%vol	%vol	%vol	%vol	%vol
OB-AG-PBK	13.3	17.7	7.8	4.5	54.9	1.6
OB-AG-SLH	12.7	17.2	7.3	3.3	57.7	1.3
IB-AG-SLH	11.5	17.5	6.3	3.2	59.9	1.2
OB-SG-PBK	20.0	44.3	18.8	9.1	4.8	3.0
OB-SG-WBC	21.0	41.4	19.9	9.7	5.0	3.1
OB-SG-ISH	22.2	43.4	17.8	9.0	4.2	3.2
OB-SG-SLH	21.0	40.2	21.6	7.2	6.4	2.6
IB-SG-WBC	21.4	41.6	19.4	10.8	3.6	3.3

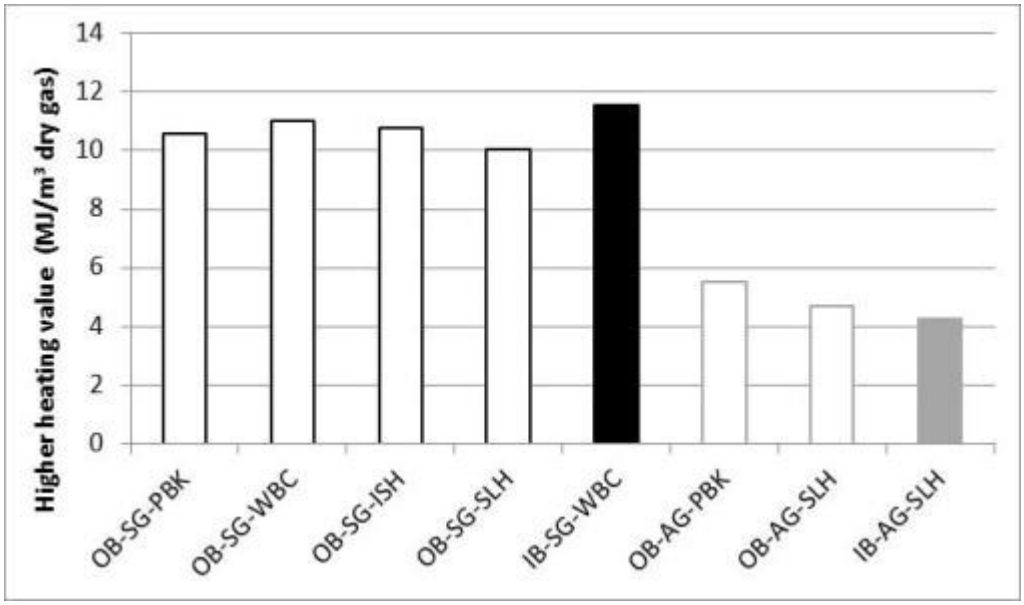

Figure 5.8: Heating value of the gases obtained from the large pilot-scale gasification of forestry residues.

Due to the large amount of nitrogen dilution, the producer gas from air blown gasification has a dry heating value that is approximately half of that of the producer gas from the steam-oxygen gasification of these materials. The salt-laden hog appears to yield a gas with a depressed heating value relative to the other forestry residues. The product gas from the salt-laden hog gasification is lower in heating value mainly due to the large reduction in the concentration of hydrocarbon gases.

The gas composition from gasification of the different forestry residues at the large pilot-sale appear quite similar This is in contrast to the differences observed in gas composition from the chapters 3 and 4 where different pre-treatments (comminution, drying, pelletization, torrefaction, and carbonization) are evaluated. From the chapter 3 data for example, at 875°C, the finest material yield a gas with 3.8 vol% H_2 compared to the pellets made from the fines which yielded a gas at the same bed temperature and fluidizing velocity of 11.6 vol% H_2. The biggest compositional difference in the large pilot-scale gasification of forestry is that the salt-laden hog (SLH) yielded a gas with a lower concentration of hydrocarbon gases (methane and C2 gases).

When the gas composition from the materials is compared on a nitrogen-free basis, the producer gas from air gasification is similar to the producer gas from steam-oxygen gasification in terms of the concentration of methane and C2 gases. On the other hand, there is a slight increase in the amount of CO from the air gasification trials relative to steam-oxygen trials and there in a slight decrease of CO_2 and H_2. This may indicate that there is some water-gas shift occurring in the gas phase, or that the large excess of steam is contributing to the heterogeneous water-gas equilibrium. Since the CO concentration is decreased for the steam-oxygen gasification trials relative to the air gasification trials (and the CO_2 is increased), a small amount water-gas shift is likely occurring. However it also seems to indicate that the gas phase kinetics of other reactions, such as the steam reformation of C2 gases and methane are not greatly affected by a large excess of steam since the methane and C2 gas concentration between the air gasification and the steam-oxygen gasification are very similar on a nitrogen free basis. Table 5.6 shows the gas composition measurements given on a nitrogen free basis.

Table 5.6: Gas composition measurements from the large pilot-scale gasifier on a nitrogen free basis.

Run Name	CO	CO_2	H_2	CH_4	C2 gases
	%vol	%vol	%vol	%vol	%vol
OB-AG-PBK	29.5	39.3	17.2	10.0	3.5
OB-AG-SLH	30.1	40.7	17.3	7.7	3.0
IB-AG-SLH	28.6	43.7	15.7	7.9	2.9
OB-SG-PBK	21.0	46.5	19.7	9.5	3.1
OB-SG-WBC	22.1	43.5	20.9	10.2	3.3
OB-SG-ISH	23.2	45.3	18.6	9.4	3.3
OB-SG-SLH	22.4	42.9	23.1	7.7	2.8
IB-SG-WBC	22.1	43.1	20.1	11.2	3.4

One of the biggest effects observed in chapter 3 due to the particle size was the impact that particle size had on the yield of hydrogen gas. Comparing the interior BC softwood hog fuel (ISH) to the two chipped fuels show that the yield of hydrogen was depressed, as expected for a fuel consisting of a greater fraction of small particles. This was not the case for the salt laden hog fuel (SLH) which had the smallest particle size distribution of the tested feed

materials. The results in chapter 4 suggested that the effects of particle size can easily be obscured by the impact of a different chemical composition (the chemical composition and size distribution of the fuel was altered in chapter 4 by thermal pre-treatments). It is possible that effect of the high level of sodium or chloride in the salt laden hog promoted the formation of hydrogen gas and that this was more pronounced than the effect of particle size. The impact of sodium and chloride is singled out because it is well recognized that sodium and chlorine can play a major role in the thermal decomposition of biomass. For example, the addition small amounts of sodium chloride to cellulose were found to greatly influence the pyrolysis products (Essig et al. 1988). For another example, the char reactivity of char from pistachio nut shell can be greatly enhanced through the addition of $NaNO_3$ (Lahijani et al., 2013).

Figure 5.9 shows the hydrogen yield that was obtained from the large pilot-scale testing. Interestingly, the yield of hydrogen gas was not greatly affected by the use of steam-oxygen gasification relative to air gasification. The hydrogen yield, for over-bed fed runs between air gasification and steam-oxygen gasification was increased from 0.013 kg/kg_{daf} to 0.017 kg/kg_{daf} for the Mountain Pine Beetle Killed (PBK) material and from 0.015 kg/kg_{daf} to 0.020 kg/kg_{daf} for the Salt Laden Hog fuel (SLH). This represents an average increase of 33% of hydrogen yield between air gasification and steam-oxygen gasification. For every run except OB-SG-SLH, more hydrogen atoms can be attributed to hydrocarbons than to hydrogen gas. For OB-SG-SLH the amount of hydrogen converted to hydrogen gas and the amount converted to hydrocarbon gases and tar is essentially equivalent. This is further indication that even with the higher freeboard temperatures present in the large pilot-scale gasifier, gas phase reactions between steam and hydrocarbons did not proceed very rapidly.

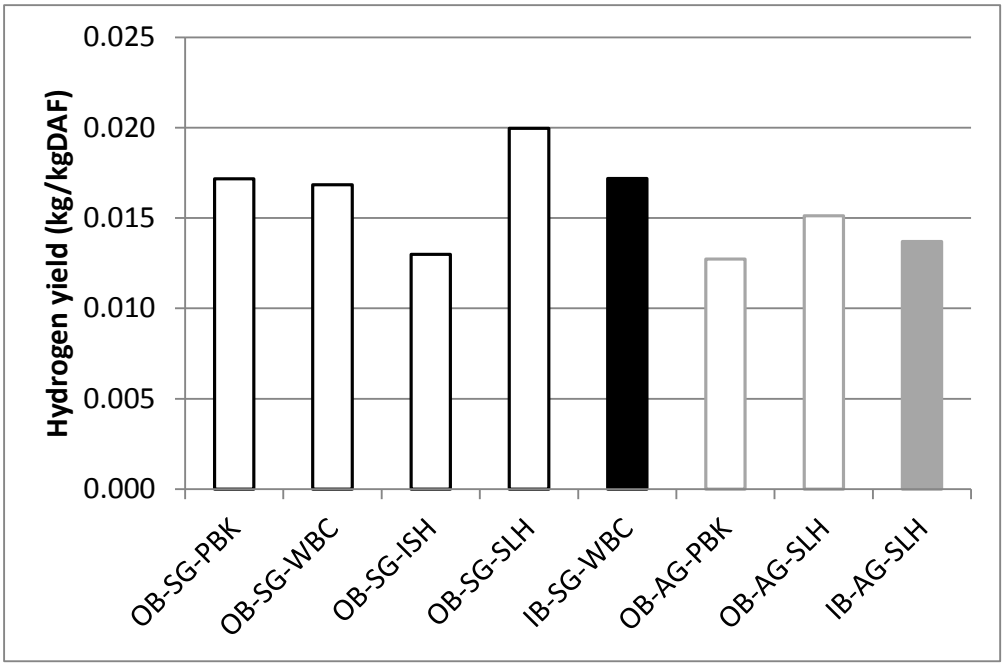

Figure 5.9: Hydrogen yield from gasification of forestry residues at the large pilot-scale

5.2.3 Water-gas Shift Position

The water-gas shift position of the product gas for the large pilot-scale gasification was once again compared to the equilibrium position of the water gas-shift reaction. Figure 5.8 shows this graphically. All of the experiments at the large pilot scale with forestry residues resulted in a gas composition that fell far below the predicted thermodynamic equilibrium of the water-gas shift reaction. This is strong evidence that even at an average bed temperature of 850°C, thermodynamic equilibrium is not reached for the water-gas shift. In other words, either kinetic or transfer limitations still play the dominant role in determining the gas phase composition.

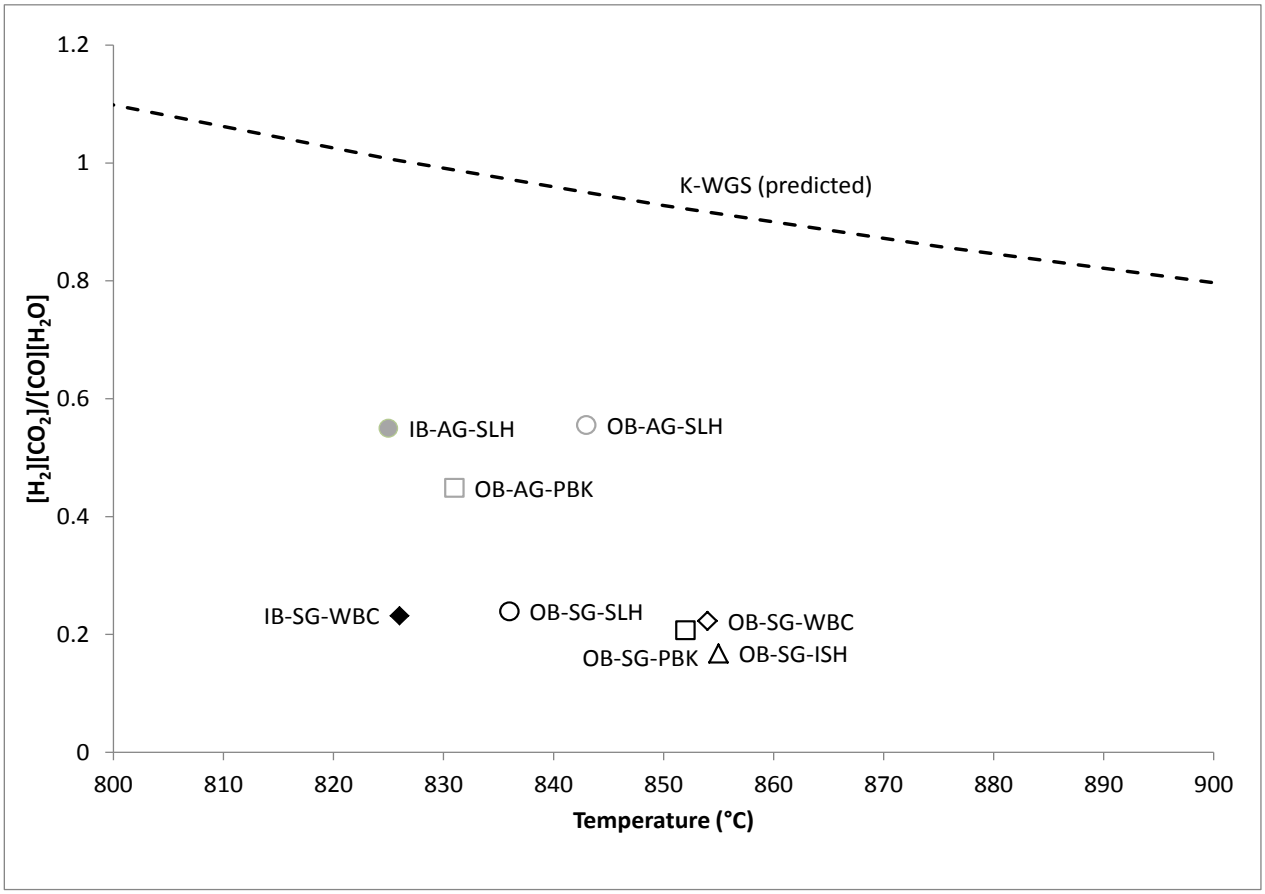

Figure 5.10: Water-gas shift position of the gasification experiments completed in the large pilot-scale gasifier.

The gas produced from the steam-oxygen gasification consistently produces a gas which lies further below the equilibrium line than the product gas from air gasification (below the equilibrium line implies the gas is richer in CO and H_2O than predicted by equilibrium). If it is accepted that the reaction rate of the water gas shift is slow compared to the gas residence time, this is obvious, adding extra steam to the system will just serve to decrease the value of the ratio: $\frac{[H_2][CO_2]}{[CO][H_2O]}$.

5.2.4 Tar Content

Based on the results of chapter 3, it is expected that the gasification of a material with a finer particle size distribution will increase the tar yield relative to larger particle sizes. It was also discussed in chapter 3 that it is possible that the high level of tars is only observed from the finer materials because the small pilot-scale gasifier uses an over-bed feed

position. Table 5.7 and Table 5.8 show the measured gravimetric and GC/MS tar content of the producer gas.

The results show that the tar concentration by GC/MS is considerably higher for the product gases from the steam-oxygen gasification trials than the air blown gasification trials. Once again, this is due in large part to the nitrogen dilution effect. The gravimetric tar results on the other hand show that they were very similar for steam-oxygen gasification versus air-blown gasification. This means that the yield of gravimetric tar is substantially lower for steam-oxygen gasification than for the air gasification. This is the case, especially when the same feed material at the same feed position is compared between over-bed and in-bed feeding. Figure 5.11 and Figure 5.12 show the gravimetric tar yield and the total of benzene plus GC tar yield from the gasification trials on the large pilot-scale gasifier. Two effects are highlighted from the figures: the hogged fuels, from an over-bed feed position, yielded more gravimetric tar than the chipped materials but similar GC tar (plus benzene) and the use of an in-bed feed yielded a greater amount of GC tar (plus benzene) but a similar amount of gravimetric tar for the salt laden hog fuel.

Table 5.7: Tar content of air blown gasification trials in the large pilot-scale facility.

Date	Fuel	Bed T. (TEW-222) °C	Freeboard T. (TEW-231) °C	Feed location	Grav. Tar g/m^3	Benzene g/m^3	Class 2 tar g/m^3	Class 3 tar g/m^3	Class 4 tar g/m^3	Class 5 tar g/m^3	Total GC/MS tar g/m^3
2012-03-07	PBK	831	699	Over-bed	7.7	8.39	0.61	3.14	3.65	0.17	7.57
2012-04-04	SLH	843	719	Over-bed	10.7	6.60	1.51	2.89	4.04	0.13	8.57
2012-04-05	SLH	825	771	In-bed	10.1	7.08	1.10	3.11	5.37	0.30	9.88

Table 5.8: Tar content of steam-oxygen gasification trials in the large pilot-scale facility.

Date	Fuel	Bed T. (TEW-222) °C	Freeboard T. (TEW-231) °C	Feed location	Grav. Tar g/m^3	Benzene g/m^3	Class 2 tar g/m^3	Class 3 tar g/m^3	Class 4 tar g/m^3	Class 5 tar g/m^3	Total GC/MS tar g/m^3
2012-03-14	PBK	852	755	Over-bed	7.6	14.91	0.64	3.70	6.43	0.49	11.26
2012-03-22	WBC	854	777	Over-bed	5.2	12.91	0.24	3.92	7.85	0.34	12.35
2012-03-29	ISH	855	735	Over-bed	17.4	20.51	2.88	6.05	14.19	1.70	24.82
2012-04-23	SLH	836	729	Over-bed	9.9	8.29	2.08	3.99	5.53	0.28	11.88
2012-04-26	WBC	826	786	In-bed	12.6	21.99	1.28	7.75	14.26	0.86	24.15

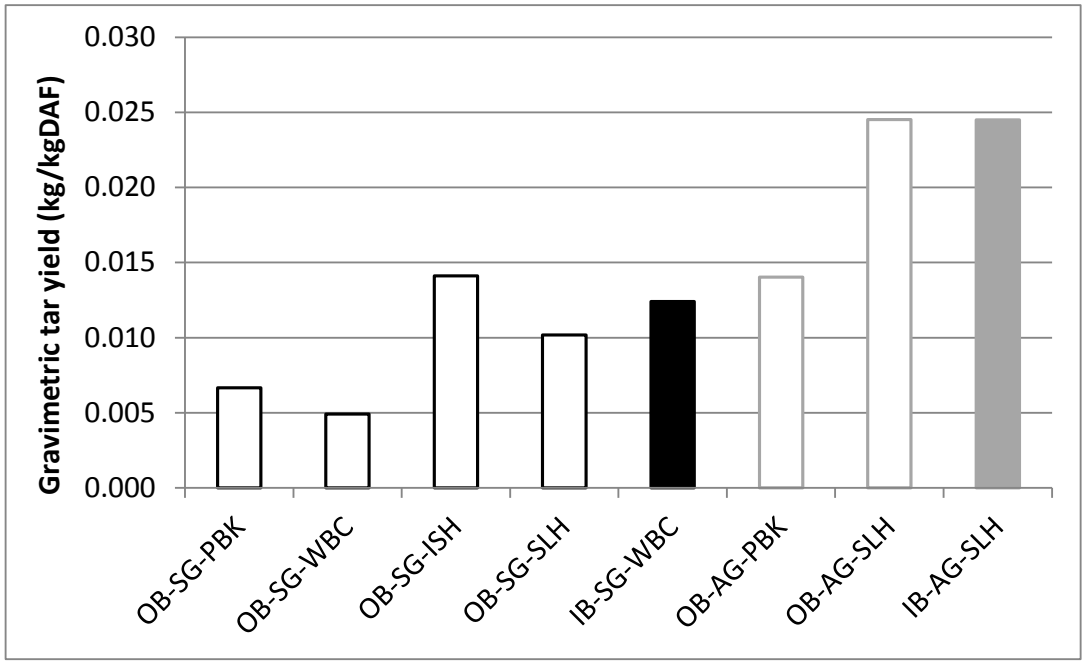

Figure 5.11: Gravimetric tar yields from the large pilot-scale gasification experiments.

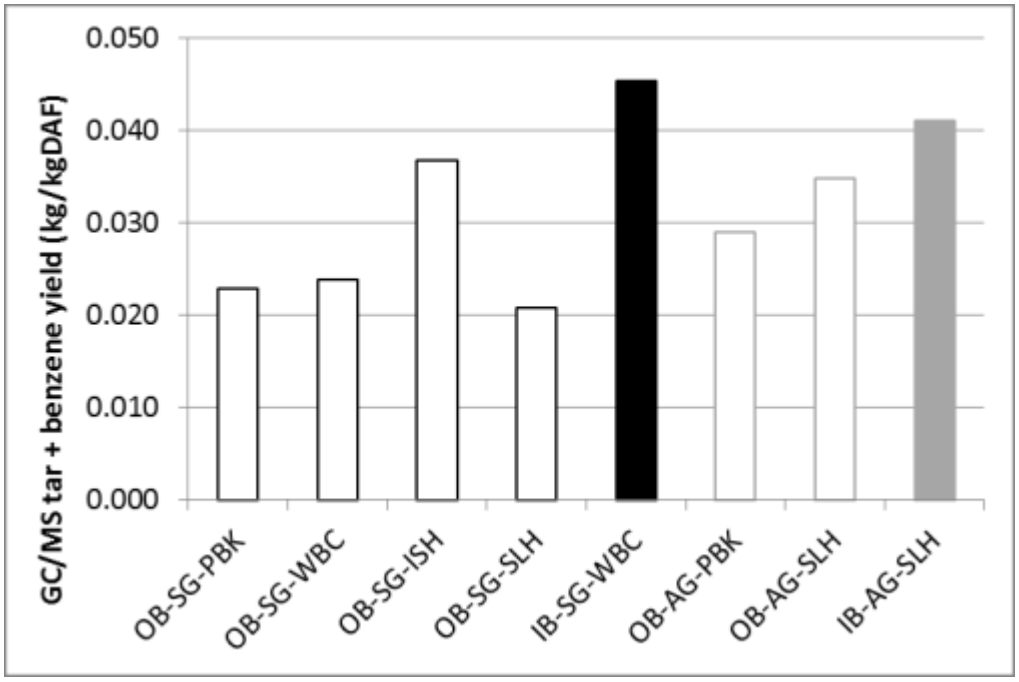

Figure 5.12: Totalized yield of GC tar and benzene from the large pilot-scale gasification experiments.

5.2.5 Carbon Conversion

Both chapter 3 and 4 indicated that an increase in the average bed temperature led to an increase in the carbon conversion. Despite the fact that the trials fed from an in-bed position were run at slightly lower temperatures, these trials led to the highest observed level of carbon conversion from the large pilot-scale gasifier. The presence of the excess steam in the steam-oxygen trials did not appear to have a large impact on the carbon conversion. From chapter 3, the indication was that for a fuel containing a significant amount of fines, a lower carbon conversion should be observed. Based on that work, it is expected that lower conversion of carbon to gases would be observed for the hog fuels relative to the chip fuels. Figure 5.13 shows the observed carbon conversion to gas from the tests. Although the interior BC softwood hog fuel showed a decreased carbon conversion relative to the other fuels, the other hog fuel, the salt laden hog fuel, did not. This may once again be due to the effect of sodium or chloride which were both present in large amounts only in the salt laden hog fuel.

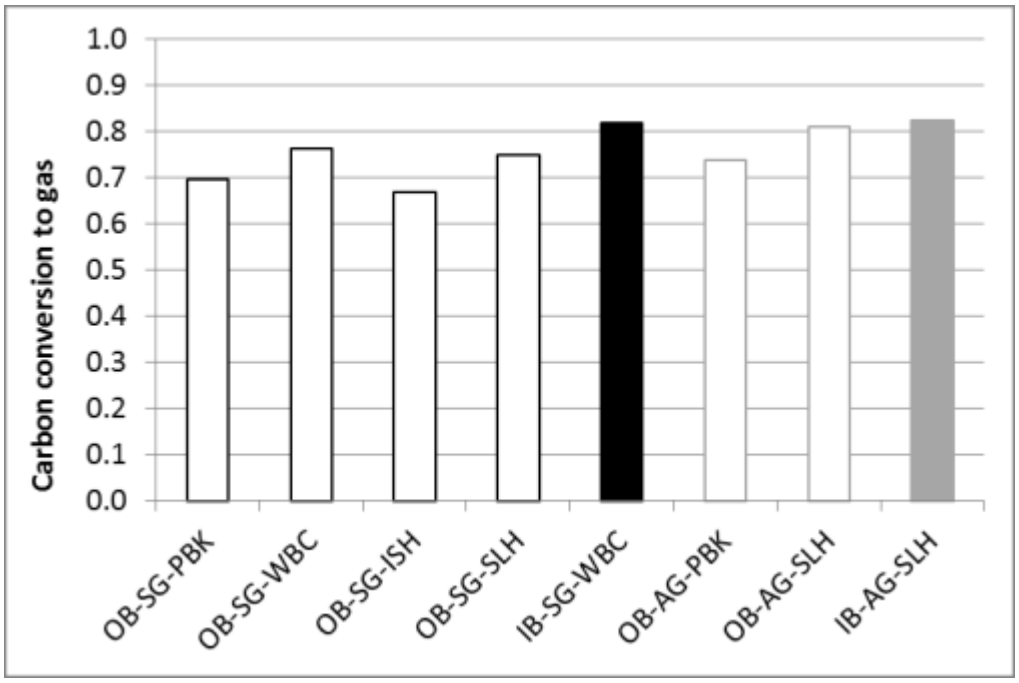

Figure 5.13: Fraction of carbon that was converted to gas during the large pilot-scale gasification work

5.3 **Conclusions**

The particle size distribution of the material affected some of the results between the gasification of four different forestry residues in a large pilot-scale gasifier. Two feed materials of a relatively coarse size distribution and two materials consisting of a significant portion of small particles were tested (small particles in this context may be considered to be particles passing through a 2.38 mm sieve). One of these materials consisting of a significant portion of small particles was atypical in the sense that it contained a high level of sodium and chloride. For the more typical forestry residue consisting of a significant portion of small particles, the trends that have been associated with fine materials were observed: low H_2/CO ratios, high tar yield, and low carbon conversion compared to the two larger fuels. On the other hand, the salt-laden hog (the atypical feed material) displayed high H_2/CO ratios, similar gravimetric tar yields, and lower GC/MS tar yields compared to the chip fuels. The effect of particle size may be weaker than the effect of salts in the feed material. In many ways this agrees with the observation from chapter 4 which was that chemical composition effects can often surpass the particle size effect during the gasification of forestry residues in a fluidized bed gasifier.

Feeding material from an in-bed feed position instead of an over-bed feed position in the large scale fluidized bed was effective in dealing with one of the issues observed with fine material. Feeding from an in-bed position, led to an increase in the fraction of carbon that was converted gases. On the other hand, a problem with feeding fine materials is that an increase of tar was observed based on the results from chapter 3. Feeding from an in-bed position led to an increase in the amount of tar that was yielded from the gasification compared to an over-bed feed position. This was much more pronounced with white birch material (larger average particle size) than the salt laden hog (material with the largest fraction of small particles). In fact, the difference observed between the in-bed and over-bed feeding of the salt laden hog is too small to conclude that the amount of tar was different. It must be cautioned that the conclusions that can be drawn from the in-bed feeding position are extremely limited by the fact that only two experimental trials were completed and that there were some important operational differences between in-bed and over-bed feeding that need to be understood.

Comparing the gas composition obtained from the steam-oxygen and the air-blown gasification on the large pilot-gasifier shows the importance of rate limitations in the gas phase. During steam-oxygen gasification there was a large excess of steam present that should have encouraged the steam reforming of methane and other hydrocarbons and the steam should have pushed the water-gas shift equilibrium towards hydrogen and carbon dioxide. At the conditions tested, the effect of the excess steam did not affect the amount of hydrocarbon gases produced significantly and only increased the hydrogen yield in the gas by about 33% which is far less than what would be expected if the gas phase was approaching water-gas shift equilibrium. This is an indication that the gas phase reactions and the conditions tested are occurring at a slow rate compared to the gaseous residence time in the gasifier. This means that the composition of the gas that is initially produced from the devolatilization of the particle, which is strongly affected by parameters that are affected by particle properties (such as heating rate which is a function of the particle size), plays a primary role in determining the composition of the producer gas.

References

Essig, M., T. Lowary, G.N. Richards and E. Schenck, “Influences of “neutral” salts on thermochemical conversion of cellulose and sucrose,” in "Research in Thermochemical Biomass Conversion," A. V. Bridgewater and J. L. Kuester, Eds. Elsevier Applied Science, London, UK (1988), pp. 384-398.

Lahijani, P., Z.A. Alimuddin, A.R. Mohamed, and M. Mohammadi, “CO_2 gasification reactivity of biomass char: Catalytic influence of alkali, alkaline earth and transition metal salts,” Bioresour. Tech. **141**, 288-295 (2013).

Chapter 6. Conclusions and Recommendations

The objectives of this thesis were to experimentally evaluate how the pre-treatment of biomass fuels affects and could be used to optimize the performance of fluidized bed gasifiers. The air-blown bubbling fluidized bed gasification of a single forestry residue that had been sieved, dried, pelletized, torrefied and carbonized was carried out in small pilot-scale system. In addition, air-blown and steam-oxygen bubbling fluidized bed gasification of four forestry residues with different size distributions were carried out in a larger scale system. This chapter summarizes the key findings of the work and highlights some remaining knowledge gaps to be addressed in future work.

6.1 Conclusions

The pre-treatment of a forestry residue through comminution, drying, pelletization, or torrefaction was found to be able to have a major impact on the fluidized bed gasification performance of a forestry residue. Different particle sizes and moisture level feedstocks were prepared from a single forestry residue and certain size fractions of that material were also subjected to pelletization, torrefaction, and carbonization. The effect of different pre-treatment levels were compared in a small pilot-scale (0.154 m diameter) bubbling fluidized bed gasifier over a range of conditions that resulted in bed temperatures between 725 to 875°C. In order to understand whether the effects observed with the particle sizes were significant enough to be observed across different forestry residues, the performance of four forestry residues were compared, operating at a bed temperature between 825 to 855°C in a large pilot-scale (1 m diameter) bubbling fluidized bed gasifier.

The effect of comminution (particle size reduction) was evaluated by studying the gasification performance of three different size fractions of the same feedstock. For the finest material (material that passed through a 3.175 mm screen), poor gasification performance was observed relative to the larger size fractions. This included increased tar production and decreased carbon conversion to gases and consequently, lower cold gas efficiency. The finest material also had a characteristic gas composition which consisted of a relatively low amount of hydrogen compared to the carbon monoxide. For the two large

particle sizes tested, it did appear that the hydrogen yield increased with particle size. It also appeared that tar production was decreased with increasing particle size.

Two moisture levels were compared in a small pilot-scale air blown fluidized bed gasifier. The “dry” feed materials had a moisture content of approximately 11 wt% while the “wet” fuels had a moisture content ranging between 24 - 31 wt%. The wet fuels were gasified at a higher equivalence ratio than the dry fuels in order to obtain the same bed temperature as the dry fuels at a constant fluidizing velocity. There was no clear change in the tar yield from the wet fuels compared to the dry fuels. A subtle change in the tar was observed in composition of the tar: the amount of class 2 tar (oxygenated species) decreased with the wet fuels. The additional moisture (or potentially the higher ER) did lead to increased carbon conversion and consequently the wet and the dry fuels gave similar cold gas efficiency. A modest improvement in the hydrogen gas yield was observed with the wet fuels. The wet fuels also yielded a gas with a lower heating value (the heating value of the gas was reduced by between 5 and 33% at a bed temperature of 800°C compared to their dry counterparts).

Pelletization was found to be an effective pre-treatment strategy to increase the H_2/CO ratio in the gas and the hydrogen gas yield from the fluidized bed gasification of a forestry residue. The gasification of pellets (6.35 mm diameter) yielded on average 19% more hydrogen gas at 725°C, 21% more hydrogen gas at 800°C, and 29% more hydrogen gas at 875°C than the fuel fraction consisting of particles retained between 3.175 and 6.35 mm screens. This was despite the fact that the pellets were slightly dryer (7 % vs. 11 % moisture).

Thermal pre-treatment can have a large impact on the gas quality from the fluidized bed gasification of biomass. This is especially true for severe thermal pre-treatment. The two thermal pre-treatment levels tested (torrefied and carbonized feedstocks) showed that a modest tar reduction is possible with torrefaction (GC tar was reduced by 45% and 20% for the torrefied materials at a bed temperature of 800 and 875°C, respectively). Almost all of the tar was eliminated by the carbonization pre-treatment: GC tar was reduced by 96% and 97% for the carbonized materials at a bed temperature of 800 and 875°C, respectively. The tar reduction is a positive impact of the thermal pre-treatment on the gasification

performance. However, there were also negative impacts on the gasifier performance. The heating value of the gas from the carbonized material was greatly reduced which was mainly due to the reduction in methane content in the gas and near complete elimination of C2 gases (ethylene, ethane, and acetylene). The torrefied and carbonized material showed that despite their lower H/C ratio, smaller particle size and lower moisture content, greater hydrogen gas yields are still possible relative to the parent material. The thermally pre-treated materials also displayed a reduction in the carbon conversion to gas during their gasification and consequently lower cold gas efficiency.

It is suggested that fine materials lead to higher tar production from an over-bed feed position because of entrainment of the particles. Although it is still expected that this is an important effect this thesis provides evidence that it is not the only effect. In the work completed with thermal pre-treatments, the torrefied and carbonized materials had substantially decreased particle size distributions relative to the parent material. The thermally pre-treated materials however produced a gas with lower tar concentration and lower tar yield. In the large pilot-scale evaluation of different forestry residues, two of the materials were compared between an over-bed and in-bed feed position. These materials had very different particle size distributions, both materials showed an increase in producer gas tar content with an in-bed feed position compared to an over-bed feed position. For a feedstock containing more than 90% of material larger than 2 mm, the concentration of tar and the yield of tar were roughly doubled by changing the feed position from over-bed feeding to in-bed feeding during steam-oxygen gasification. For a material containing approximately 50% of the material passing through a 2 mm sieve, the tar concentration and yield was roughly equivalent between over-bed and in-bed feeding. The carbon conversion to gas was enhanced using in-bed feed compared to an over-bed feed position for both forestry residues compared. When considering the in-bed results presented in this thesis, it must be respected that different “operational” performance was observed and that the evidence is based on limited trials (2 comparisons).

The work shows that the H_2/CO ratio of producer gas can certainly be adjusted by biomass feedstock pre-treatment. For applications where an elevated H_2/CO ratio is desired from a feed material that consists of a substantial portion of fines, optimization may be possible by

pelletizing the fine materials. Results on pre-treatment effects on the H_2/CO of the producer gas have been emphasized throughout this thesis for two reasons:

- In order to design a process based on syngas this ratio is going to have a profound effect on downstream process except for only the most rudimentary applications of syngas (such as directly coupled combustion to operate a boiler). For engines such as reciprocating engine and turbines, the flame speed of a gas mixture is an important design parameter. Hydrogen, owing to its high flame speed, can have a big impact on the flame speed of producer gas mixtures (Natarajan et al., 2007). For the synthesis of chemicals or liquid fuels from synthesis gas, appropriate H_2/CO ratios are essential.
- This was one of the parameters that was the most sensitive to pre-treatment factors. The sensitivity of this parameter helps to develop theories on why the differences were observed.

The hypothesis that different particle sizes may influence the approach of the gas phase to thermodynamic equilibrium was explored as a plausible explanation for observed differences in the gas composition. Ultimately the use of equilibrium to explain differences was not successful for the range of operating conditions explored (bed temperatures between 725 – 875°C). In order to understand the gas composition from fluidized bed gasifiers operating in this temperature regime, it is more important to gain an understanding of the gas phase and the solid-gas reaction kinetics of the predominant reactions and the impact of mass transfer limitations on the reactions.

6.2 **Recommendations for Future Work**

The results of the present work confirmed that the performance of the fluidized bed gasification is impacted by different feedstock pre-treatment levels applied to a forestry residue. Although understanding how pre-treatment can impact specific cases is important, in order to ensure that the findings are as widely applicable as possible, there needs to be better understanding of why these differences were observed. This thesis has presented some results that require further investigation:

- Particle entrainment is part of the issue with small particles given poor gasification performance in fluidized bed gasifiers fed from an over-bed position. However, particle entrainment could not explain all of the differences, nor did in-bed feeding lead to drastic improvements in performance in a large pilot-scale gasifier using forestry residues.
- Using thermodynamic equilibrium to predict the gas phase composition from the fluidized bed gasification of biomass was not successful. Kinetic or transfer limitations to the conversion of the char and kinetic or transfer limitations to the gas phase reactions are more important in determining the performance of a fluidized bed gasifier.

In order to better explain the results of this thesis further experimentation is needed to confirm certain hypotheses. This thesis concluded that thermodynamic equilibrium is too simplistic of a model for predicting the gas composition in fluidized bed gasifiers. Rather, an understanding of many interacting processes is needed (such as mixing and heat transfer between bed media and feed particles, reaction kinetics, diffusion of steam and carbon dioxide to char particles, heat transfer through the particles, flux of volatiles out through the particle, etc.). A few key issues that need further study include:

- Experiments should be designed in order to further understand the gasification of the finest material. Although creating a material that consists solely of small particles is expensive at the commercial scale, most biomass feedstocks will contain some fraction of small, entrainable particles. Varying gas velocities (through the bed) could be used to study the impact of particle entrainment on the observed results of the fines. Fine materials could also be tested rigorously from an in-bed feeding position and compared to other particle sizes from the same feeding position. It may still be likely that in order to properly gasify fines in a fluidized bed they must be fed in-bed, but the trials that were carried out in this thesis did not indicate this. In-bed feeding is a slightly more complicated feed arrangement for an atmospheric pressure fluidized bed. If clear advantages cannot be verified for this feed strategy then over-bed feeding may be a more appropriate design for many fluidized bed gasifiers.

- Measurement protocols need to be further improved in order to ensure reliability of the collected data and to understand all the factors that can significantly influence the performance of a fluidized bed gasifier.
- Most low value residual feedstocks are going to be a mix of particle sizes. In this thesis, relatively narrow size distributions were studied. It is possible that the particle size effects observed are not independent. For example, the data presented in thesis gives no indication whether a mix of 50% fine material and 50% coarse material can be approximated as the linear combination of the gas yield from each size fraction.
- In this work a constant fluidizing gas velocity was used for all the small pilot-scale work. The mixing of the feed particles with the bed media will depend on the fluidization number. The attrition and entrainment of the char particles will also be affected by gas velocity in the system. Thus, the impact of gas velocity could be investigated.

Modelling approaches to biomass gasifiers can also be improved based on the results of this thesis. Based on the results of the third chapter, the same fuel in different sizes and forms can have a substantial impact on the producer gas composition. A model that does not take as an input the particle size or form in order to predict gas composition is going to fail to predict the differences observed in this thesis. Simple models which consider reaction kinetics and transport limitations could be investigated and validated using particle properties as input parameters in order to understand whether the observed performance can be predicted. This would be a valuable tool in forecasting gasifier performance and would also assist in understanding the dominant mechanisms that regulate producer gas composition. As this "Recommendations" section demonstrates there are many possible experimental parameters that could be varied that are reasonably anticipated to have some interaction with the effect of pre-treatment of the gasification of biomass. A model once validated, may be very useful in screening for the most important parameters for experimental verification.

Char conversion was a limitation at the conditions tested in this work. The limitation of char conversion was especially apparent at the low temperature conditions. More efficient

gasification is theoretically possible at lower temperature (and if char and tar were considered useful products, then the efficiency from the experimental work is in fact greater at lower temperatures as expected). For some fuels there will be upper temperature limitations based on ash characteristics (generally a fluidized bed must operate below the softening point of the ash or risk the formation of agglomerations and subsequent defluidization). In order to achieve greater conversion of the char to product gases, the char can be recycled back to the gasifier. This may have other impacts on the process. For example, char is noted to have some catalytic activity for the reformation of pyrolysis products and the resultant tars. Since the char conversion was observed to be such a crucial issue, in order to understand the level of conversion that is possible with char recycling, both the small and large pilot-scale systems could install char recycling systems. It may also be useful to understand whether even more effective use of the char would be to mix it into the pellet making process. In addition to being an interesting practical application of the char, the results from such testing would also implicate from a fundamental perspective whether or not intraparticle reactions between vapours and char are effective in adjusting the producer gas composition and reducing tar.

References

Natarajan, J., T. Lieuwen, and J. Seitzman, "Laminar flame speeds of H_2/CO: Effects of CO_2 dilution, preheat temperature, and pressure" Combustion and Flame. **151,** 104-119 (2007).

Appendix A. Supplemental Characterization Information for Experimental Materials

A.1 Olivine Sand Size Distribution Data

The olivine sand was analyzed to determine it properties relevant to fluidization and fluidized bed gasification. In addition to the compositional data given, other parameters, such as its size distribution were determined. Figure A.1 shows the size distribution of the sand as measured by sieving. The Sauter mean diameter was calculated as the harmonic mean of the mass distribution data presented.

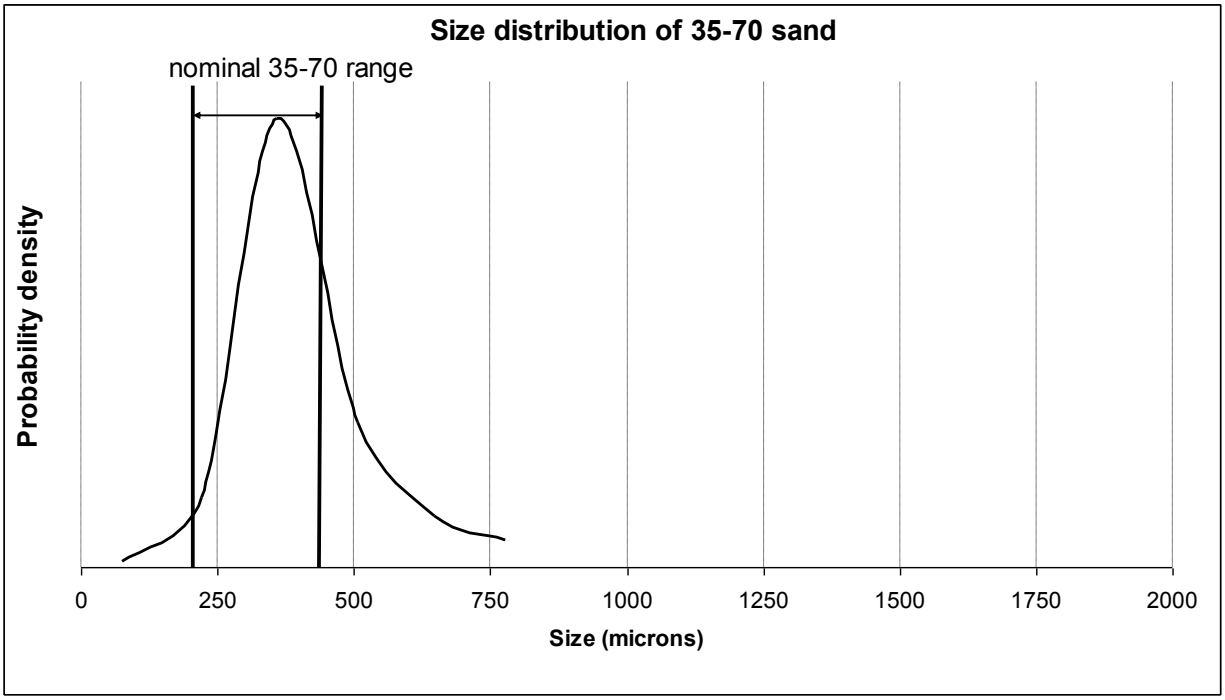

Figure A.1: Size distribution of the olivine sand used as the bed material.

A.2 Olivine Sand Composition

The bed material used for this campaign was a synthetic olivine. The sand used in these experiments is the same sand that was used for the work described in chapter 3 and 4. Periodic samples of the bed were taken during the run conditions in order to determine how the composition of the bed was changing with time.

Table A.1: Bed material composition: comparison between the beginning and end of the campaign

Component	Start of Campaign	End of Campaign
Total Chlorine by Pyrohydrolysis (ug/g db)	<15	56
Total Fluorine by Pyrohydrolysis (ug/g db)	17	21
Total Bromine by Pyrohydrolysis (ug/g db)	<10	<10
SiO2 (wt%)	43.63	43.77
Al2O3 (wt%)	2.68	3.83
Fe2O3 (wt%)	12.28	8.00
TiO2 (wt%)	<0.03	0.05
P2O5 (wt%)	0.03	0.59
CaO (wt%)	0.89	4.50
MgO (wt%)	38.91	35.60
SO3 (wt%)	<0.10	<0.10
Na2O (wt%)	<0.20	0.97
K2O (wt%)	0.45	1.49
Barium (ppm)	127	254
Strontium (ppm)	<50	164
Vanadium (ppm)	95	114
Nickel (ppm)	2513	2483
Manganese (ppm)	523	1201
Chromium (ppm)	6285	7100
Copper (ppm)	89	133
Zinc (ppm)	328	564
Loss on Fusion (wt%)	0	0
Sum (wt%)	99.87	100

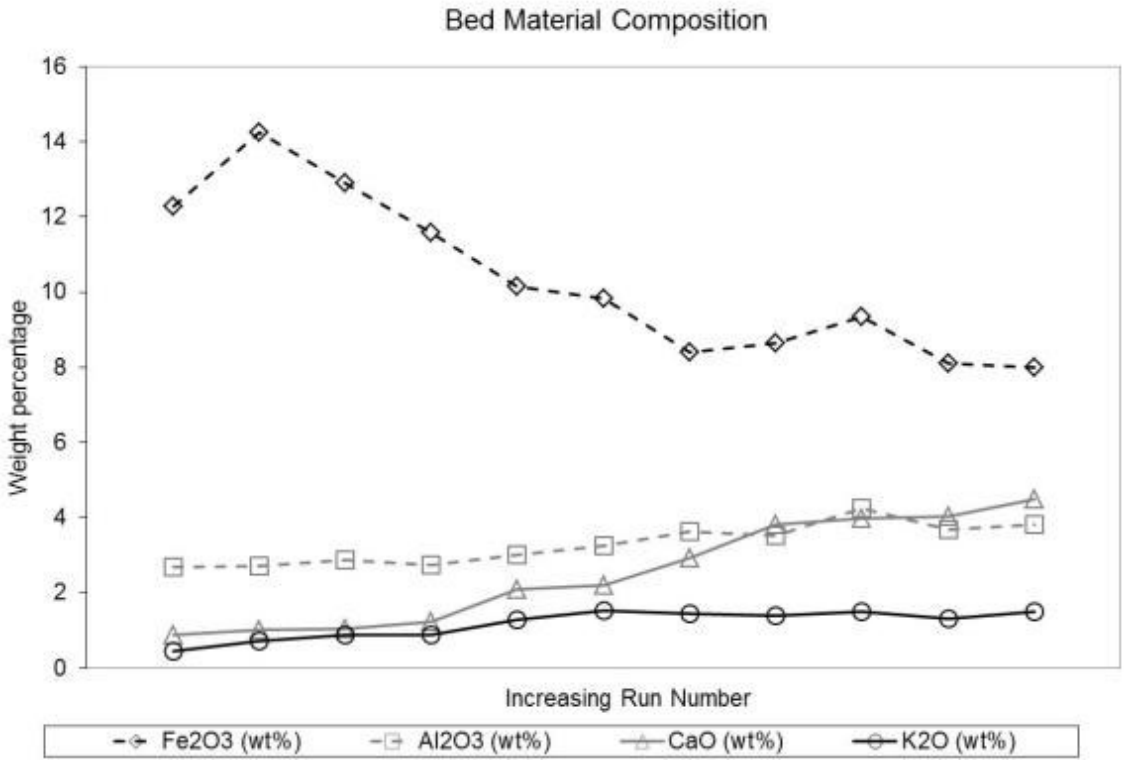

Figure A.2: Bed material composition as measured by XRF, key compositional changes with time.

A.3 **Char Analyses**

It is difficult to identify trends in the char data. This may be reflective of the difficulty of obtaining a representative sample from the collected char. Some chars even displayed negative oxygen by difference values which are likely best attributed to the relatively high amounts of ash which would have interfered with the measurement through potential oxidation, carbonation, dehydration, or calcination reactions during the char characterization. Table A.2 shows the analytical results from the char samples.

Table A.2: Proximate, ultimate, and calorific analysis of the chars obtained from the experiments.

Fuel	Avg. Bed T. °C	Ash db wt%	Volatile db wt%	Fixed Carbon db wt%	Carbon db wt%	Hydrogen db wt%	Nitrogen db wt%	Total Sulfur db wt%	Oxygen by Difference db wt%	Gross Calorific Value MJ/kg db	
Fines	871	75.08	9.86	15.05	26	0.51	0.22	0.51	-2.29	8.6	
Fines	862	73.88	15.35	10.77	24.7	0.67	0.19	0.66	0.14	8.0	
Fines	801	63.13	15.03	21.84	34.4	0.86	0.26	0.7	0.61	11.7	
Fines	799	69.47	15.33	15.2	28.9	0.7	0.22	0.65	0.01	9.5	
Fines	726	62.86	14.54	22.6	34.1	0.89	0.24	0.58	1.29	11.7	
Fines	725	51.46	14.31	34.23	44.9	1.09	0.35	0.47	1.75	16.0	
Fines-wet	800	51.34	13.5	35.16	44.1	1.1	0.58	0.33	2.58	15.3	
Fines-wet	725	44.21	14.9	40.89	49.4	1.33	0.65	0.32	4.09	17.6	
Mid	875	35.87	10.16	53.98	61.4	0.93	0.49	0.27	1.03	21.7	[6]
Mid	801	35.87	10.16	53.98	61.4	0.93	0.49	0.27	1.03	21.7	[6]
Mid	801	28.9	9.01	62.09	68.5	0.99	0.55	0.14	0.91	23.8	
Mid	725	19.92	9.21	70.87	76.2	1.45	0.57	0.1	1.8	27.3	
Mid	725	20.31	12.35	67.34	75.3	1.44	0.56	0.09	2.3	27.1	
Mid-wet	802	78.64	13.26	8.1	18.1	0.65	0.16	0.4	2.06	5.8	
Mid-wet	725	48.11	12.36	39.53	50.1	0.8	0.38	0.35	0.25	17.1	
Pellets	875	54.27	4.85	40.87	44.8	0.45	0.46	0.44	-0.41	15.8	
Pellets	801	64.74	10.91	24.36	34.3	0.58	0.36	0.59	-0.56	11.3	
Pellets	801	33.37	5.21	61.42	64.3	0.79	0.57	0.19	0.73	22.8	
Pellets	800	49.51	6.21	44.29	49.3	0.66	0.43	0.35	-0.19	17.2	
Pellets	725	31.17	7.04	61.79	65.2	1.14	0.52	0.19	1.77	23.6	
Pellets	725	32.7	6.99	60.31	63.3	1.07	0.66	0.23	2.01	22.8	
Coarse	875	55.73	12.39	31.88	45.4	0.7	0.31	0.43	-2.59	15.2	
Coarse	800	39.64	11.44	48.93	58.5	0.93	0.45	0.33	0.18	20.8	
Coarse-wet	800	60.8	13.61	25.59	38.4	0.68	0.25	0.58	-0.68	12.6	
Coarse-wet	725	39.57	14.33	46.1	57.5	1.2	0.39	0.33	1.02	20.0	

[6] Due to char plugging, it was indistinguishable to which condition the char originated, only one sample was analyzed

A.4 **Thermally Pre-treated Materials**

An analysis of the elemental composition of the ash from the thermally pre-treated materials was performed. This was completed to understand whether certain mineral could be lost during the pre-treatment which could in turn influence the gasification performance through catalytic effects. Based on expected levels of fuel heterogeneity, the results show the composition of the ash was not greatly altered in the pre-treatment process. These results also compare favorably with the ash results presented in Table 3.2.

Table A.3: Ash analysis of the parent, torrefied, and carbonized materials as determined by XRF.

Component	Units	Parent (Mid)	Torrefied	Carbonized
SiO_2	wt% ash	13.75	17.07	18.21
Al_2O_3	wt% ash	3.37	4.16	3.25
Fe_2O_3	wt% ash	2.16	3.91	2.16
TiO_2	wt% ash	0.13	0.26	0.24
P_2O_5	wt% ash	6.89	5.1	12.03
CaO	wt% ash	33.99	30.96	27.76
MgO	wt% ash	15.89	10.78	9.78
SO_3	wt% ash	4.59	3.22	3.82
Na_2O	wt% ash	0.75	1.19	2.24
K_2O	wt% ash	6.27	7.44	13.33
Barium	ppm ash	1022	1371	835
Strontium	ppm ash	772	730	519
Vanadium	ppm ash	<50	<50	<50
Nickel	ppm ash	120	445	102
Manganese	ppm ash	5200	7407	3764
Chromium	ppm ash	210	911	125
Copper	ppm ash	77	164	406
Zinc	ppm ash	978	1462	1551
Loss on Fusion	wt% ash	11.37	14.66	6.45
Sum	wt% ash	99.99	99.99	99.99

A big concern in this work was the potential that fuel heterogeneity may have played a significant role in the results. For example, because of fuel heterogeneity between and within different sacs of the same fuel, it may have been possible that the fuel fed during condition 1 was different in some important way (such as ash content) than the fuel fed

during condition 2. In order to assess this potential, each of the fuel samples from the chapter 4 work were subjected to the same test on a TA Instruments Discovery TGA. The test was as follows:

- A 250 μL alumina sample pan was weighed to generate a tare weight
- The 250 μL alumina sample pan was loaded approximately half full with ground material (parent, torrefied, or carbonized). The material had been ground using a cutting mill through a 1/16" screen.
- The 250 μL alumina sample pan was loaded into the TGA with a sample purge of 40 mL/min N_2 and a balance purge of 10 mL/min N_2.
- The TGA jumped to 105°C (heating rate not controlled) and held at that temperature for 5 minutes in order to dry the sample. The data was normalized to the dry weight of the sample at the end of the 5 minute isothermal hold at 105°C
- The sample underwent a linear heating rate of 50°C/min from 105 – 800°C. This would give some indication of the volatility of the sample (the amount of material that will volatilize under an inert environment)
- Once reaching 800°C, the temperature was held for 5 minutes while still under a N_2 environment
- The sample purge gas was switched to CO_2 at 40 mL/min and the sample was held at 800°C for another 5 minutes (this was used to assess the reactivity of the sample's char). It was never determined whether the CO_2 gasification of the char was diffusion or kinetically limited at the conditions, but future work intends to investigate this.
- The sample purge was switched to air (a synthetic mix of 21% O_2 and 79% N_2) at 40 mL/min for 30 min at 800°C in order to burn off the remaining char. The remaining weight after this step is reported as the "ash" of the sample.

Figure A.3, Figure A.4, and Figure A.5 show the results of this method ran on four samples taken from the parent, torrefied and carbonized material, respectively (each sample is denoted with a letter A, B, C, or D). This method was also used to determine the amount of ash in the char collected from the gasification (the calculated dry basis weight percentage of ash is shown on the figures for each curve). The results for the TGA

testing of the char from gasification is shown in Figure A.6 where C1 refers to condition 1 and C2 refers to condition 2.

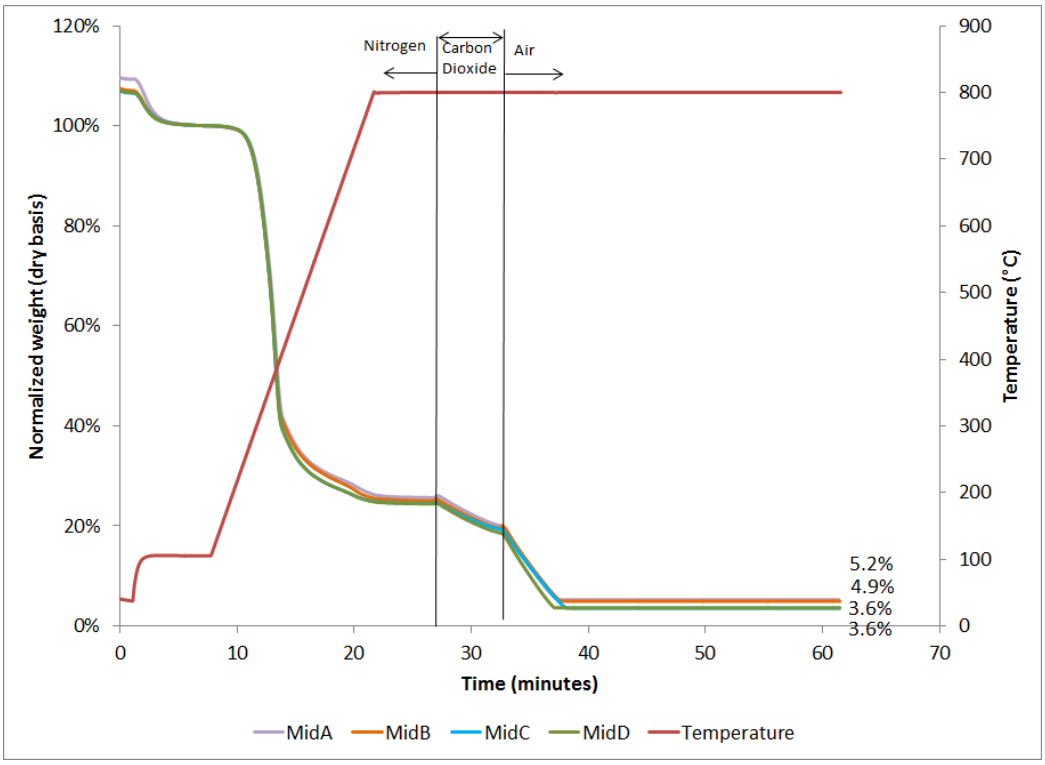

Figure A.3: Four samples of the parent material characterized by TGA

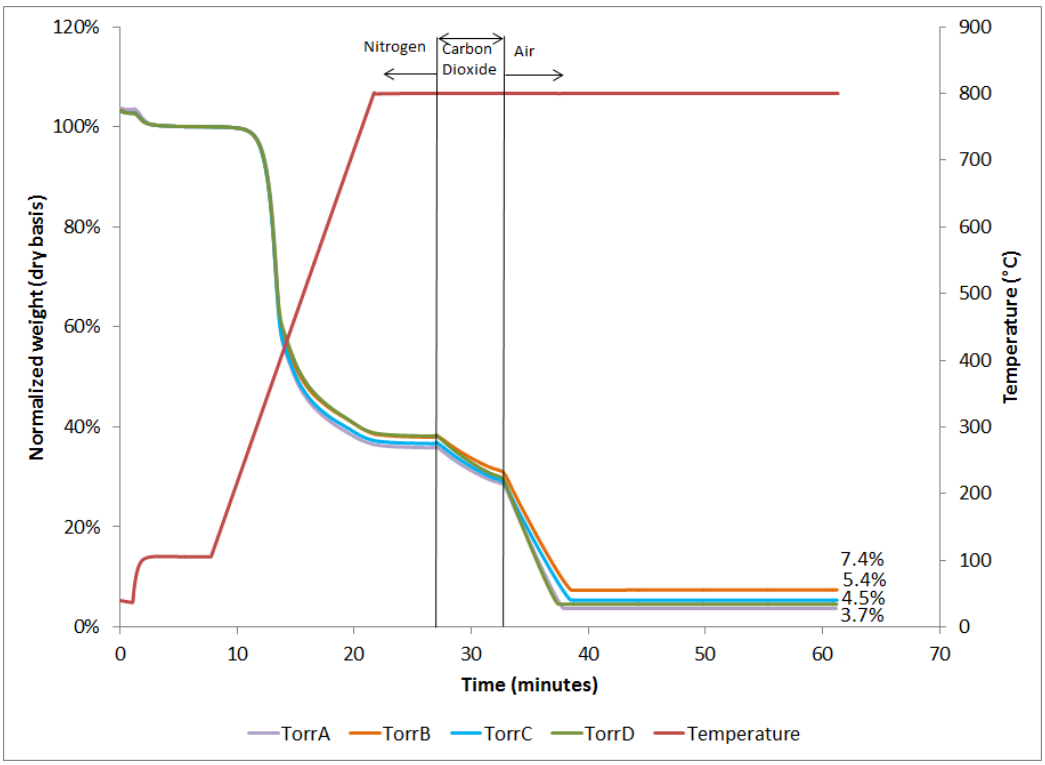

Figure A.4: Four samples of the torrefied material characterized by TGA

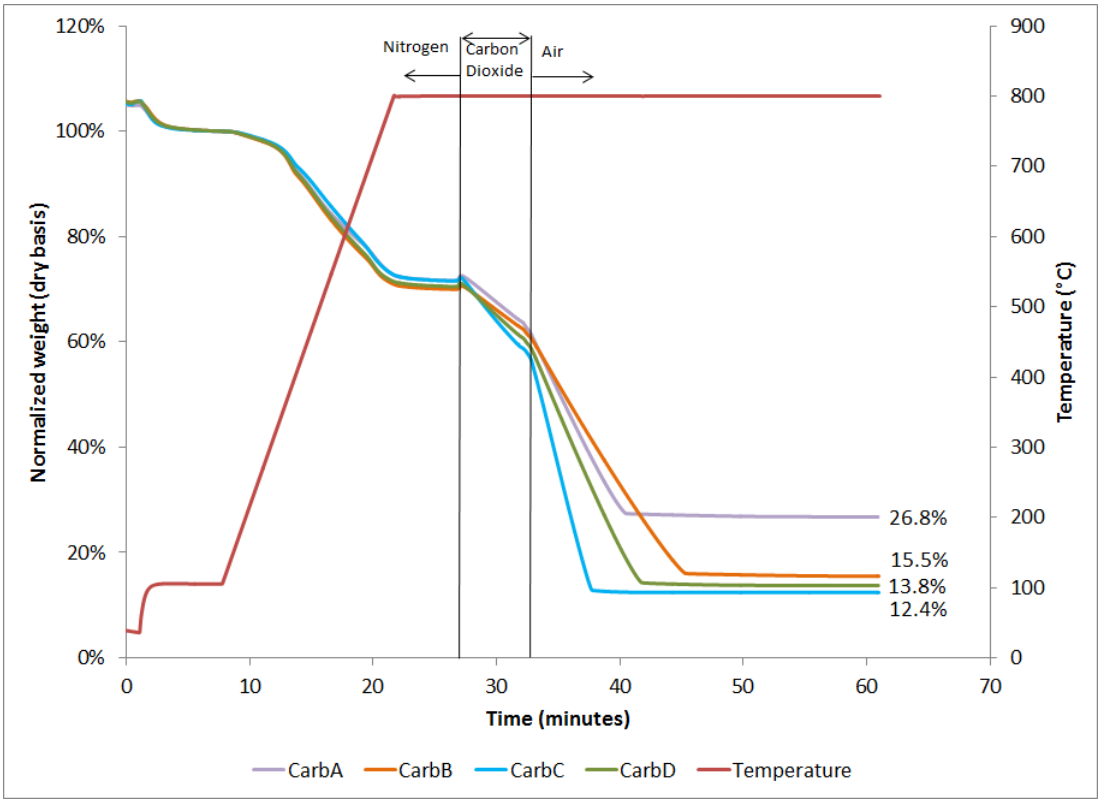

Figure A.5: Four samples of the carbonized material characterized by TGA

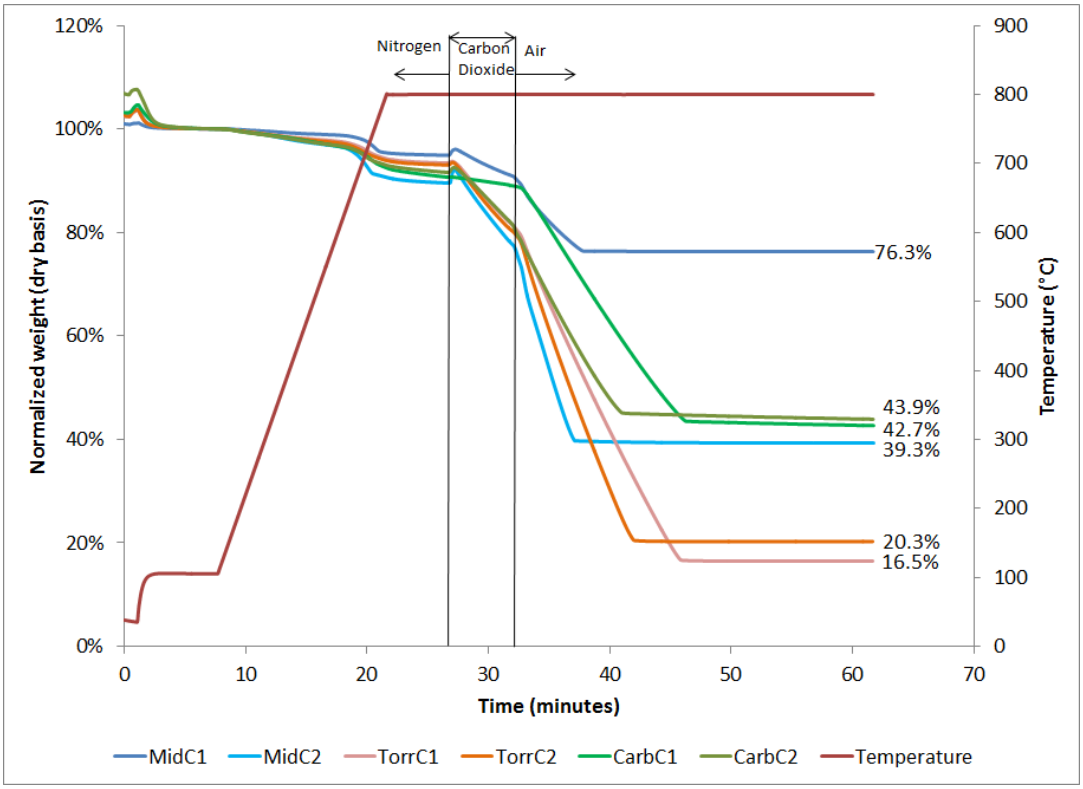

Figure A.6: Char from the gasification of parent, torrefied, and carbonized material compared by TGA

Appendix B. Mass Balancing Strategies

B.1 Traditional Mass Balance Strategy

The traditional mass balance strategy tracks 6 elemental mass balances (Carbon, Hydrogen, Oxygen, Nitrogen, Sulfur, and Argon) and the ash mass balance. The first step in such a mass balnce is to track the elemental mass flows into the system. In order to complete this all the mass inputs are lumped into three input mass flows: moisture (from the biomass), dry biomass, and air. The mass flow of total feed is measured and the average moisture results presented in Table 3.5 are used to determine the amount of moisture and dry biomass that was put into the system. The amount of air supplied to the gasifier is measured. Since water has a known molar composition, the mass input of hydrogen and oxygen due to water is determined by the following equations:

$$\dot{m}_{H_2O,in} = x_{H_2O,in}\dot{m}_{biomass} \qquad \text{Eq. B.1}$$

$$\dot{m}_H = \frac{2MW_H}{MW_{H_2O}} \dot{m}_{H_2O} \quad \text{Eq. B.2}$$

$$\dot{m}_O = \frac{MW_O}{MW_{H_2O}} \dot{m}_{H_2O} \quad \text{Eq. B.3}$$

The mass input of each of the elements and the ash due to the feed is determined from the compositional analysis of each form tested (the example given is for carbon, but also applies to H, O, N, S, Ar, and ash):

$$\dot{m}_C = x_{db,C}(1 - x_{H_2O,biomass})\dot{m}_{biomass} \quad \text{Eq. B.4}$$

The mass input of air is calculated from the standardized volumetric input:

$$\dot{m_{air}} = \frac{\dot{V}_{air}\left[\frac{\mathrm{L_{std}}}{\mathrm{min}}\right] 60 \left[\frac{\mathrm{min}}{\mathrm{h}}\right] 28.97 \left[\frac{\mathrm{g}}{\mathrm{mol}}\right]}{22.414 \left[\frac{\mathrm{L_{std}}}{\mathrm{mol}}\right] 1000 \left[\frac{\mathrm{g}}{\mathrm{kg}}\right]} \quad \text{Eq. B.5}$$

The molar composition of air is taken to be 78.08% N_2, 20.95% O_2, and 0.93% Ar. The remaining 0.04% is neglected. It assumed is that the air is perfectly dry. (This is not exactly true, but in section 3.1.3 it is shown that this is close).

The amount of dry product gas is determined by fixing the nitrogen balance. The following equation must apply:

$$\dot{n}_{N,total\ in} = \dot{n}_{N,gas\ out} + \dot{n}_{N,char\ out} \quad \text{Eq. B.6}$$

Equation B.6 can be rearranged and re-expressed where the molar flow of the dry gas ($\dot{n}_{dry\ gas}$) is the only unknown:

$$\dot{n}_{N,total\ in} = y_{N_2,dry\ gas}\dot{n}_{dry\ gas} + \frac{\dot{m}_{char,out}x_{N,char}}{MW_N} \quad \text{Eq. B.7}$$

$$\frac{\dot{n}_{N,total\ in} - \frac{\dot{m}_{char,out}x_{N,char}}{MW_N}}{y_{N_2,dry\ gas}} = \dot{n}_{dry\ gas} \quad \text{Eq. B.8}$$

Once the molar flow of dry product gas has been calculated, then the molar flow of each element is calculated based on the measured concentration of each gas species in the dry gas.

The mass output of water is determined by the measured concentration of water in the product gas:

$$\dot{m}_{H_2O,out} = \frac{c_{H_2O}\left[\frac{\mathrm{g}}{\mathrm{m}^3}\right]\dot{n}_{dry\ gas}\left[\frac{\mathrm{mol}}{\mathrm{h}}\right]22.414\left[\frac{\mathrm{L}}{\mathrm{mol}}\right]}{1000\left[\frac{\mathrm{L}}{\mathrm{m}^3}\right]1000\left[\frac{\mathrm{g}}{\mathrm{kg}}\right]} \qquad \text{Eq. B.9}$$

The mass output of tar is calculated in the same way. There are however a few subtleties with the tar. Tar for the purposes of the mass balancing does include benzene in its definition (otherwise the mass output due to benzene production in the gasifier would not be captured). Two measurement methods were used in order to determine the amount of tar. Both measurement methods likely underestimate the total amount of tar: the gravimetric method will miss the most volatile tar components and the GC/MS will miss any contribution for a tar component that is not calibrated or does not evaporate in a GC. To capture the mass balance as best as possible, the mass balance is completed with the greater measurement of the two (For example, if during a run condition the tar concentration in dry gas was measured as 8.1 g/m^3 by gravimetric methods and 11.9 g/m^3 by GC/MS, the mass balance is completed using a tar concentration of 11.9 g/m^3). In order to determine the elemental mass flow contribution due to the tar, the C-H-O composition is determined from the GC/MS results when the data is available. In the event that the tar sample was not analyzed by GC/MS (some tar measurements were completed by gravimetric method only), the tar for mass balancing purposes is assumed to have a composition equal to the average tar composition from GC/MS at that bed temperature. The average tar composition for each bed temperature level tested is given in Table B.1.

Table B.1: Average tar composition (weight percentage) measured by GC/MS for each bed temperature tested

	Bed Temperature (°C)		
	725	800	875
Carbon	86.6%	90.0%	92.0%
Hydrogen	7.4%	7.5%	7.4%
Oxygen	6.0%	2.5%	0.5%

The traditional mass balance strategy allows for a mass balance closure (recovery) of each element to be determined, where the recovery is determined as (the example given is for carbon, but also applies for H, O, N, S, Ar, and ash):

$$R_C = \frac{\dot{m}_{C,out}}{\dot{m}_{C,in}} \qquad \text{Eq. B.10}$$

It would be expected that the recovery should be a bit low in all cases due to unaccounted species such as C3 – C6 hydrocarbons and due to the fact that the tar concentration is expected to be an underestimate of liquid weight organic material in the product stream.

Due to the limited amount of measurements carried out on sulfur species, low mass balance closures are expected for sulfur. In addition, the micro-GC uses Argon as a carrier gas, thus no measurement of Argon in the product gas was possible, the Argon recovery was always 0%. By the nature of the method, the nitrogen balance is fixed to 100%, the implicit assumption is that all nitrogen goes to N_2. The input nitrogen from the feed is very small compared to the mass input of nitrogen from air.

In order to determine the yield of each product compared to the mass input of dry-ash-free (DAF) biomass from gasification, the following was applied (the example given is for H_2, but also applies for CO, CH_4, C_2H_4, CO_2, C_2H_6, C_2H_2, C_3H_6, Tar, and Char):

$$Y_{H_2} = \frac{\dot{m}_{H_2}}{\left(1 - x_{H_2O,biomass}\right)\dot{m}_{biomass} - \dot{m}_{ash,in}} \qquad \text{Eq. B.11}$$

Since the nitrogen and oxygen from air also contribute to the gas yield, the gas yield will be substantially greater than 1 kg / $kg_{biomass\ DAF}$. The water yield is split into a gross water yield and a net water yield. The net water yield is supposed to reflect how much water was

produced in the reaction as opposed to the sum of water produced from the reaction and water entering the gasifier as moisture in the feed materials. The difference is the following:

$$\Upsilon_{H_2O,gross} = \frac{\dot{m}_{H_2O,out}}{\left(1 - x_{H_2O,biomass}\right)\dot{m}_{biomass} - \dot{m}_{ash,in}} \quad \text{Eq. B.12}$$

$$\Upsilon_{H_2O,net} = \frac{\dot{m}_{H_2O,out} - \dot{m}_{H_2O,in}}{\left(1 - x_{H_2O,biomass}\right)\dot{m}_{biomass} - \dot{m}_{ash,in}} \quad \text{Eq. B.13}$$

The equivalence ratio of the gasifier is also calculated in the mass balancing spreadsheet. The equivalence ratio is the amount of oxygen supplied to the gasifier relative to the amount of air that would need to be supplied for stoichiometric combustion of the feed material. This ratio is found by equation B.14.

$$ER = \frac{\dot{n}_{O_{2,air}}}{\dot{n}_{C,feed} + \frac{1}{4}\dot{n}_{H,feed} - \frac{1}{2}\dot{n}_{O,feed}} = \frac{\frac{\dot{m}_{O_{2,air}}}{MW_{O_2}}}{\frac{\dot{m}_{C,feed}}{MW_C} + \frac{\dot{m}_{H,feed}}{4MW_H} - \frac{\dot{m}_{O,feed}}{2MW_O}} \quad \text{Eq. B.14}$$

The carbon conversion to gas (C to gas) is determined by the ratio of mass output of carbon in the product gas relative to the mass input of carbon in the biomass:

$$\chi_{C\ to\ gas} = \frac{\dot{m}_{C,dry\ gas}}{\dot{m}_{C,biomass}} \quad \text{Eq. B.15}$$

The carbon conversion to gas and tar (C to gas + tar) is determined by the ratio of the mass output of carbon in the product gas and the tar relative to the input amount of carbon in the biomass:

$$\chi_{C\ to\ gas+tar} = \frac{\dot{m}_{C,dry\ gas} + \dot{m}_{C,tar}}{\dot{m}_{C,biomass}} \quad \text{Eq. B.16}$$

The cold gas efficiency (CGE) represents the efficiency through which the gasification converts input energy into heating value in the product gas. Since the only energy input to

this gasifier was the heating value of the feed material this comparison is calculated as the following:

$$CGE = \frac{\hat{E}_{dry\ gas}\dot{m}_{dry\ gas}}{\hat{E}_{biomass,db}\dot{m}_{biomass,db}} \qquad \text{Eq. B.17}$$

B.2 **CHO Mass Balance Strategy**

Instead of fixing the nitrogen balance, the CHO mass balance strategy fixes the carbon, hydrogen and oxygen balance. In this case, the performance of the CHO mass balance strategy cannot be evaluated in terms of how closely the carbon, hydrogen, and oxygen mass balances closure approaches 100%. Rather, the performance of this method is evaluated by how closely the mass balance predictions agree with the measured values. For example, the CHO mass balance predicts water content in the producer gas and the nitrogen content in the producer gas (they do not take these as inputs). A comparison of the measured nitrogen and water content with the predicted values is a good indication of whether the mass balance is giving reasonable results.

The essential concept is that the mass balance takes an input carbon, hydrogen, and oxygen (C-H-O) composition of three input streams (dry biomass, moisture, and oxygen from air) of which to total mass flow of each is known. By using the C-H-O composition of the three output streams (dry gas + tar, water, and char) the mass output of these streams can be calculated. The following calculations replace equations B.6, B.7, and B.8.

The input to the mass balance can be written as follows:

$$\mathrm{M_{CHO}} = \begin{bmatrix} m_{C,in} \\ m_{H,in} \\ m_{O,in} \end{bmatrix} = \begin{bmatrix} m_{C,out} \\ m_{H,out} \\ m_{O,out} \end{bmatrix} \qquad \text{Eq. B.18}$$

$$\mathrm{M_{CHO,in}} = \begin{bmatrix} m_{C,in} \\ m_{H,in} \\ m_{O,in} \end{bmatrix} = \mathrm{X_{CHO,in}}\,\mathrm{M_{in}}$$

$$= \begin{bmatrix} x_{b,C} & x_{steam,C} & x_{air,C} \\ x_{b,H} & x_{steam,H} & x_{air,H} \\ x_{b,O} & x_{steam,O} & x_{air,O} \end{bmatrix} \begin{bmatrix} m_{b,in} \\ m_{steam,in} \\ m_{oxygen,in} \end{bmatrix} \qquad \text{Eq. B.19}$$

$$= \begin{bmatrix} x_{b,C} & 0 & 0 \\ x_{b,H} & 0.1119 & 0 \\ x_{b,O} & 0.8881 & 0.2314 \end{bmatrix} \begin{bmatrix} m_{b,in} \\ m_{steam,in} \\ m_{oxygen,in} \end{bmatrix}$$

The output from the mass balance can be written as in equation B.20:

$$\mathrm{M_{CHO,out}} = \begin{bmatrix} m_{C,out} \\ m_{H,out} \\ m_{O,out} \end{bmatrix} = \mathrm{X_{CHO,out}}\,\mathrm{M_{out}}$$

$$= \begin{bmatrix} x_{gt,C} & x_{steam,C} & x_{char,C} \\ x_{gt,H} & x_{steam,H} & x_{char,H} \\ x_{gt,O} & x_{steam,O} & x_{char,O} \end{bmatrix} \begin{bmatrix} m_{gt,out} \\ m_{steam,out} \\ m_{char,out} \end{bmatrix} \qquad \text{Eq. B.20}$$

$$= \begin{bmatrix} x_{b,C} & 0 & x_{char,C} \\ x_{b,H} & 0.1119 & x_{char,H} \\ x_{b,O} & 0.8881 & x_{char,O} \end{bmatrix} \begin{bmatrix} m_{gt,out} \\ m_{steam,out} \\ m_{char,out} \end{bmatrix}$$

Since one of the objectives of this mass balance is too simplify the amount of data that needs to be collected in order to carry out a reasonable gasifier mass balance, a further simplification was made in the absence of good compositional data on the char. When exact compositional data on the char was lacking it was assumed that the char is pure carbon. In this case, the mass output of char will be in ash-free terms:

$$\mathrm{M_{CHO,out}} = \begin{bmatrix} x_{b,C} & 0 & 1 \\ x_{b,H} & 0.1119 & 0 \\ x_{b,O} & 0.8881 & 0 \end{bmatrix} \begin{bmatrix} m_{gt,out} \\ m_{steam,out} \\ m_{char,in} \end{bmatrix} \qquad \text{Eq. B.21}$$

In order to solve the system for the vector $\mathrm{M_{out}}$, the following operations can be carried out:

$$\mathrm{X_{CHO,in}}\,\mathrm{M_{in}} = \mathrm{X_{CHO,out}}\,\mathrm{M_{out}}$$

$$\mathrm{X_{CHO,out}}^{-1}\left(\mathrm{X_{CHO,in}}\,\mathrm{M_{in}}\right) = \mathrm{X_{CHO,out}}^{-1}\left(\mathrm{X_{CHO,out}}\,\mathrm{M_{out}}\right) \qquad \text{Eq. B.22}$$

$$X_{CHO,out}{}^{-1}\left(X_{CHO,in}\, M_{in}\right) = M_{out}$$

B.3 **Comparison of Mass Balance Results using Chapter 3 Data**

In order to determine which mass balance strategy is more appropriate to apply, the results from both methods were compared. The comparison aimed to provide an assessment of which observed differences were independent of the uncertainties associated with the mass balance input data. One uncertainty of the data is that the fuel characterization was performed on one sample of each feed material which leads to the risk that the fuel sample analyzed was not representative. An example of this is discussed when the fuel analysis of the fines and pellets are compared in section 3.1.1. The expectation is that the fines and pellets are identical fuels in terms of carbon, hydrogen, oxygen and ash (the pellets were created from the fines and pelletization should not be affecting the chemical composition of the fuel). Also, there is a reason to believe that the amount of char underestimates the actual amount of char produced and that the measured amount of tar underestimates the actual amount of tar produced. These are examples of the uncertainties present in the mass balance input data. The two different mass balance approaches would have different levels of sensitivities to some of the input data. For example, using the traditional approach, the dry gas yield can be sensitive to the accuracy of the measured nitrogen concentration in the gas. A few case studies were carried out in order to evaluate how the uncertainty in a single parameter could affect the results of the mass balance. Table B.2 shows how the results from the two methods vary, based on a single example condition (run code: E1, condition 1). The input parameters varied in the table were:

- To assess the sensitivity of each method to the nitrogen content of the gas, this parameter was varied by ±5% relative error (The measured nitrogen value was 51.3 vol%, the cases tested were 48.7 vol% and 53.9 vol%). All the other gas concentrations were adjusted in order to normalize the gas composition to account for 100% of the gas.
- To examine the sensitivity of the methods to the concentration of producer gas components, the carbon monoxide content of the gas was adjusted by ±5% relative

error (The measured carbon monoxide content was 14.2 vol%, the cases tested were 13.5 vol% and 14.9 vol%). All the other gas concentrations were adjusted in order to normalize the gas composition to account for 100% of the gas.

- Since it is suspected that there is a high level of uncertainty in the ash content of the fuel based on the comparison of the fines and pellets fuel analysis, the initial ash content of the fuel was varied by a large amount (±50%) in order to assess the effect of uncertainty in the fuel analysis. In this case the amount of ash was varied between 2.15 wt% and 6.45 wt%.

Table B.2 shows that the actual relative difference between the methods (black column on the right hand side of the table) was in most cases larger than the response of the methods to the variations employed in these case studies. The yields from the gas mass output (such as the hydrogen yield, the tar yield, the cold gas efficiency or the carbon conversion) are different by about 7% between the two methods. The predictions on the water and char mass outputs are much more different between the methods. Fortunately, the reported parameters such as carbon conversion, tar yield, and cold gas efficiency are based on the gas yield.

For the traditional mass balance method, it is possible to assess how well it was performing by looking at how closely the carbon, hydrogen, and oxygen elemental mass balances approach 100% closure. For the CHO mass balance, how closely the nitrogen balance approaches 100% gives a similar assessment of how well the mass balance was performing. Table B.3 shows how the two mass balance techniques compare in terms of mass balance closure and in the case of the CHO method, how well the predicted water content and predicted char production agree with the measured values.

Table B.2: Sample sensitivities of each mass balance method to input parameters (Mids, 800 °C – run code E1: condition 1).

Case		Traditional Reference	C-H-O Reference	Traditional +5% N_2	Traditional -5% N_2	C-H-O +5% N_2	C-H-O -5% N_2	Traditional +5% CO	Traditional -5% CO	C-H-O +5% CO	C-H-O -5% CO	Traditional +50% Ash	Traditional -50% Ash	C-H-O +50% Ash	C-H-O -50% Ash	Relative error between methods
dry gas yield	kg/kg_{DAF}	2.322	2.169	-3.4%	2.6%	4.1%	-2.6%	0.8%	-0.8%	-2.2%	2.2%	2.3%	-2.2%	2.4%	-2.3%	6.6%
Hydrogen	kg/kg_{DAF}	0.018	0.017	-7.1%	5.3%	0.1%	0.0%	0.0%	0.0%	-3.0%	3.1%	2.3%	-2.2%	2.4%	-2.3%	6.6%
Carbon Monoxide	kg/kg_{DAF}	0.335	0.313	-7.1%	5.3%	0.1%	0.0%	5.7%	-5.6%	2.6%	-2.7%	2.3%	-2.2%	2.4%	-2.3%	6.6%
Methane	kg/kg_{DAF}	0.057	0.053	-7.1%	5.3%	0.1%	0.0%	0.0%	0.0%	-3.0%	3.1%	2.3%	-2.2%	2.4%	-2.3%	6.6%
Ethylene	kg/kg_{DAF}	0.031	0.029	-7.1%	5.3%	0.1%	0.0%	0.0%	0.0%	-3.0%	3.1%	2.3%	-2.2%	2.4%	-2.3%	6.6%
Carbon Dioxide	kg/kg_{DAF}	0.657	0.613	-7.1%	5.3%	0.1%	0.0%	0.0%	0.0%	-3.0%	3.1%	2.3%	-2.2%	2.4%	-2.3%	6.6%
Ethane	kg/kg_{DAF}	0.007	0.007	-7.1%	5.3%	0.1%	0.0%	0.0%	0.0%	-3.0%	3.1%	2.3%	-2.2%	2.4%	-2.3%	6.6%
Acetylene	kg/kg_{DAF}	0.002	0.001	-7.1%	5.3%	0.1%	0.0%	0.0%	0.0%	-3.0%	3.1%	2.3%	-2.2%	2.4%	-2.3%	6.6%
Propylene	kg/kg_{DAF}	0.007	0.006	-7.1%	5.3%	0.1%	0.0%	0.0%	0.0%	-3.0%	3.1%	2.3%	-2.2%	2.4%	-2.3%	6.6%
Water (Gross)	kg/kg_{DAF}	0.264	0.314	-4.8%	5.3%	-0.2%	0.0%	0.7%	-0.7%	3.1%	-3.2%	2.3%	-2.2%	-1.0%	1.1%	15.8%
Water (Net)	kg/kg_{DAF}	0.133	0.182	-9.5%	10.5%	-0.4%	0.0%	1.4%	-1.4%	5.3%	-5.5%	2.3%	-2.2%	-3.5%	3.6%	27.2%
GC Tar + Benzene	kg/kg_{DAF}	0.032	0.030	-4.8%	5.3%	2.7%	-0.1%	0.7%	-0.7%	-2.3%	2.3%	2.3%	-2.2%	2.4%	-2.3%	6.6%
Grav. Tar	kg/kg_{DAF}	0.022	0.021	-4.8%	5.3%	2.7%	-0.1%	0.7%	-0.7%	-2.3%	2.3%	2.3%	-2.2%	2.4%	-2.3%	6.6%
Char	kg/kg_{DAF}	0.052	0.163	0.0%	0.0%	-1.0%	0.0%	0.0%	0.0%	3.9%	-4.0%	2.3%	-2.2%	-7.9%	8.0%	67.8%
E/R	mol/mol	0.26	0.26	0.0%	0.0%	0.0%	0.0%	0.0%	0.0%	0.0%	0.0%	2.2%	-2.2%	2.2%	-2.2%	0.0%
HHV(gas)	MJ/kg	4.92	4.92	-3.9%	2.7%	-3.9%	2.7%	0.9%	-0.9%	0.9%	-0.9%	0.0%	0.0%	0.0%	0.0%	0.0%
MW(gas)	g/mol	27.61	27.61	1.4%	-2.6%	1.4%	-2.6%	0.1%	-0.1%	0.1%	-0.1%	0.0%	0.0%	0.0%	0.0%	0.0%
Gas density [6]	kg/m^3	1.23	1.23	1.4%	-2.6%	1.4%	-2.6%	0.1%	-0.1%	0.1%	-0.1%	0.0%	0.0%	0.0%	0.0%	0.0%
Carbon conversion [7]	kg/kg	0.783	0.731	-7.1%	5.3%	0.1%	0.0%	2.0%	-2.0%	-1.0%	1.0%	2.2%	-2.2%	2.2%	-2.2%	6.6%
Carbon conversion [8]	kg/kg	0.840	0.784	-7.0%	5.3%	0.3%	0.0%	1.9%	-1.9%	-1.1%	1.1%	2.2%	-2.2%	2.2%	-2.2%	6.6%
Cold Gas Efficiency	MJ/MJ	0.545	0.509	-7.1%	5.3%	0.1%	0.0%	1.7%	-1.7%	-1.3%	1.4%	2.2%	-2.2%	2.2%	-2.2%	6.6%

[6] at 0°C, 1 atm
[7] Carbon conversion to gas only
[8] Carbon conversion to gas and condensable organics (tar)

Table B.3: Mass balance closure comparison between the two methods.

					Traditional method			C-H-O method				
Run Code	Fuel	Airflow	Feed rate	Average Bed T.	Carbon closure	Hydrogen closure	Oxygen closure	Nitrogen closure	Measured water	Predicted water	Measured char recovery	Predicted char recovery
		sLpm	kg/h	°C					g/m^3	g/m^3	kg/h DAF	kg/h DAF
F3	Fines	257	9.4	871	95%	82%	95%	93%	124.9	189.5	0.22	0.68
F2	Fines	257	10.1	862	89%	89%	98%	95%	156.3	196.6	0.31	0.99
F2	Fines	275	16.9	801	86%	92%	103%	86%	182.3	257.7	0.33	2.24
F1	Fines	275	15.4	799	87%	82%	95%	89%	150.8	248.4	0.49	1.96
F3	Fines	296	24.1	726	80%	84%	97%	83%	232.5	385.5	1.37	4.82
F1	Fines	296	20.1	725	95%	94%	105%	82%	200.2	296.7	0.78	2.60
C	Fines-wet	275	14.7	800	106%	91%	99%	87%	219.3	310.9	0.58	0.95
C	Fines-wet	296	20.4	725	96%	91%	100%	83%	301.1	439.8	1.28	2.73
E2	Mid	257	10.6	875	*98%*	*103%*	*104%*	96%	111.5	112.6	*0.00*	0.26
E2	Mid	275	14.6	801	*92%*	*101%*	*103%*	95%	134.3	141.4	*0.00*	0.80
E1	Mid	275	15.7	801	91%	95%	100%	93%	140.2	178.2	0.50	1.55
E1	Mid	296	22.7	725	75%	89%	99%	87%	202.0	297.0	1.04	4.55
E3	Mid	296	21.1	725	87%	93%	99%	91%	188.5	250.1	1.43	3.35
B	Mid-wet	275	13.8	802	92%	93%	98%	97%	191.8	222.5	0.32	0.98
B	Mid-wet	296	17.9	725	86%	99%	104%	91%	260.0	302.1	0.42	1.91
D2	Coarse	257	10.8	875	92%	92%	98%	96%	111.9	143.1	0.22	0.80
D2	Coarse	275	14.6	800	93%	95%	100%	93%	125.1	164.6	0.60	1.51
A	Coarse-wet	275	12.6	800	95%	95%	100%	93%	241.9	286.6	0.20	0.70
A	Coarse-wet	296	16.8	725	92%	96%	102%	90%	308.5	373.9	0.66	1.66
G2	Pellets	257	10.1	875	*94%*	*102%*	*103%*	98%	87.7	85.8	*0.00*	0.39
G2	Pellets	275	14.8	801	*85%*	*105%*	*105%*	97%	126.3	115.2	*0.00*	1.19
G3	Pellets	275	14.6	801	103%	108%	107%	95%	119.0	110.4	1.13	1.18
G1	Pellets	275	13.7	800	101%	98%	101%	96%	93.2	110.4	0.91	1.08
G1	Pellets	296	22.5	725	106%	100%	103%	91%	158.5	197.9	3.37	3.44
G3	Pellets	296	22	725	*85%*	*54%*	*71%*	90%	*0.0*	224.6	2.09	4.28
Average					92%	93%	100%	92%				
Minimum					75%	82%	95%	82%				
Maximum					106%	108%	107%	98%				
Std. Dev.					8.0%	6.1%	3.0%	4.6%				

Underlined values are not used in the calculation of averages, minimums, maximums, or standard deviations since a key input measurement is missing (char or water)

Table B.2 shows that the CHO method is fairly effective in its goal of minimizing the impact of errors in the nitrogen content of the product gas. With the traditional approach, a relative error of 5% of the measurement of nitrogen content (with all the other gas concentrations correspondingly adjusted to normalize the total of the gas composition to 100%) leads to a relative error of -7.3 to 5.3% on the carbon conversion and the cold gas efficiency. Conversely, for the CHO method, the same error on the nitrogen concentration leads 0 – 0.3% relative error on the carbon conversion and cold gas efficiency measurements. This shows that if there is biased error in the measurement of the nitrogen content of the gas, the results from the CHO method is far less sensitive to that error based on this case study.

If there is an error in the measurement of other gas concentrations, such as the carbon monoxide, the CHO method is slightly less sensitive in terms of the output carbon conversion and cold gas efficiency. For the traditional method, a measurement error on carbon monoxide affects the carbon monoxide yield by a large margin but leaves the other gas yields relatively unaffected. On the other hand, a measurement error in the input carbon monoxide concentration of the product gas when analyzed with the CHO method has the effect of distributing the impact throughout the yields of all the gas species.

Table B.3 shows that both the mass balance techniques appear to have non-random errors (results that are consistently lower or consistently higher than expected). The traditional method may give acceptable oxygen balances, but the carbon and hydrogen balance appear to be consistently low. On the other hand the nitrogen closure for the CHO method is consistently low, the predicted water content is often higher than the measured water content, and the predicted char content is often much, much greater than the measured amount. The results suggest there may be the following errors and insufficiencies in the measurement methods:

- The measured water content might be consistently low. It is quite possible that two impingers were not sufficient to capture all of the water from the sampled gas. Impinger sampling, especially without using fritted impingers, is known to have aerosol collection issues. It is possible that the measurement differences between the measured water content and the predicted water content are partly due to aerosol slip through the sampling apparatus. The water measurement method employed was

crude since it also could not distinguish water from condensable organics. In order to use the traditional method, it may be necessary to improve the impinger sampling set-up to ensure all the water is removed and to determine the fraction of organics in the water. In some cases the amount of organics could be substantial.

- The magnitude of char "slip" that is suggested by the difference between the measured and predicted char content is much larger than previously appreciated. Cyclones are only effective at separating large char particles from the hot gas stream. It was always appreciated that there would be some collection insufficiency for the char measurements, since small char particles (<10 μm) would likely be escaping through the cyclone. Disassembly of the gasifier's components after the cyclone show evidence of particulate material that slipped through the cyclone (char and ash in the clean out ports of the gas cooler and the afterburner).
- The tar measurement used for the mass balance was the greater of the gravimetric tar or the GC/MS tar + benzene measurement. Both of those tar measurement methods probably underestimate the total tar produced. The gravimetric tar method will only account for the fraction of tar that is of suitably low volatility. Other works completed at CanmetENERGY have shown for the tar evaporation method employed in this thesis nearly all of the single ring aromatics are lost in the evaporation as well as a portion of the phenol, cresols and naphthalenes (in other words, these components are not accounted for by the gravimetric method). GC/MS tar + benzene on the other hand, will only account for compounds that are amenable to GC/MS analysis and present in large enough amounts to be reliably quantified. This is likely a more severe problem at the low temperature condition (725°C) where the tar is less mature and consists of hundreds of identifiable compounds present in small amounts. The less mature tar will also consist of more reactive components that polymerize or coke instead of vaporizing under the conditions of the GC.
- The micro-GC employed was only calibrated for H_2, N_2, O_2, CO, CH_4, CO_2, C_2H_6, C_2H_4, C_2H_2, and C_3H_6. Any gases larger than propylene were only occasionally measured by gas bags. Although these species were only detected in small amounts, the sum of all these species would have had a minor impact on the mass balances. The gas bag

measurements were taken in order to confirm the accuracy of the micro-GC and did show good agreement.

Appendix C. Run Charts

C.1 Run Charts from the Small Pilot-scale Experiments

Figure C.1 through Figure C.26 show the gas composition and operational parameters of each experimental run completed in order to elucidate the effect of particle size, moisture level, and pelletization on the fluidized bed gasification of a forestry residue. The "Gas composition" chart shows the measured concentrations of various gaseous components over the course of the run. Since the analytical equipment requires a dry gas sample, these gas compositions represent the volume % of the main gas species in dry gas. Table C.1 gives a description of each of the lines and points on the gas composition run charts.

Table C.1: Description of data points on the gas composition charts

Name	Description
Hydrogen	The amount of H_2 in the product gas as measured by Micro-GC
Oxygen	The amount of O_2 in the product gas as measured by Micro-GC
Methane	The amount of CH_4 in the product gas as measured by Micro-GC
Carbon Monoxide	The amount of CO in the product gas as measured by Micro-GC
Carbon Dioxide	The amount of CO_2 in the product gas as measured by Micro-GC
CO HI	The amount of CO in the product gas as measured by the NDIR analyzer
CO2	The amount of CO_2 in the product gas as measured by the NDIR analyzer

The “Operations summary” chart shows various key parameters over the course of each gasification experiment. Key temperatures, airflows, instantaneous feed rates, and the pressure a one location are given in the operations summary charts. Table C.2 describes each of the parameters shown in the operations summaries.

Table C.2: Description of the data points on the operations summary charts

Name	Description
ZONE 1 T. TE 02	Bed temperature, located 0.219 m from the distributor plate
ZONE 2 T. TE 03	Bed temperature, located 0.432 m from the distributor plate
ZONE 3 T. TE 04	Splash zone temperature (sometimes in the bed), located 0.679 m from the distributor plate
REACTOR T. TE 05	Freeboard temperature (sometimes in the splash zone), located 0.953 m from the distributor plate
REACTOR T. TE 06	Freeboard temperature, located xx m from the distributor plate
REACTOR T. TE 07	Freeboard temperature, located 1.267 m from the distributor plate
REACTOR T. TE 08	Freeboard temperature, located 1.604 m from the distributor plate
Pri Air Flow	Fluidizing air flow rate in standard liters per minutes
Bed P. PT 01	Bed pressure, located 0.219 m from the distributor plate in inches of water column
Feed Rate	The instantaneous feed rate approximated from the feed belt speed and weight in kg/h

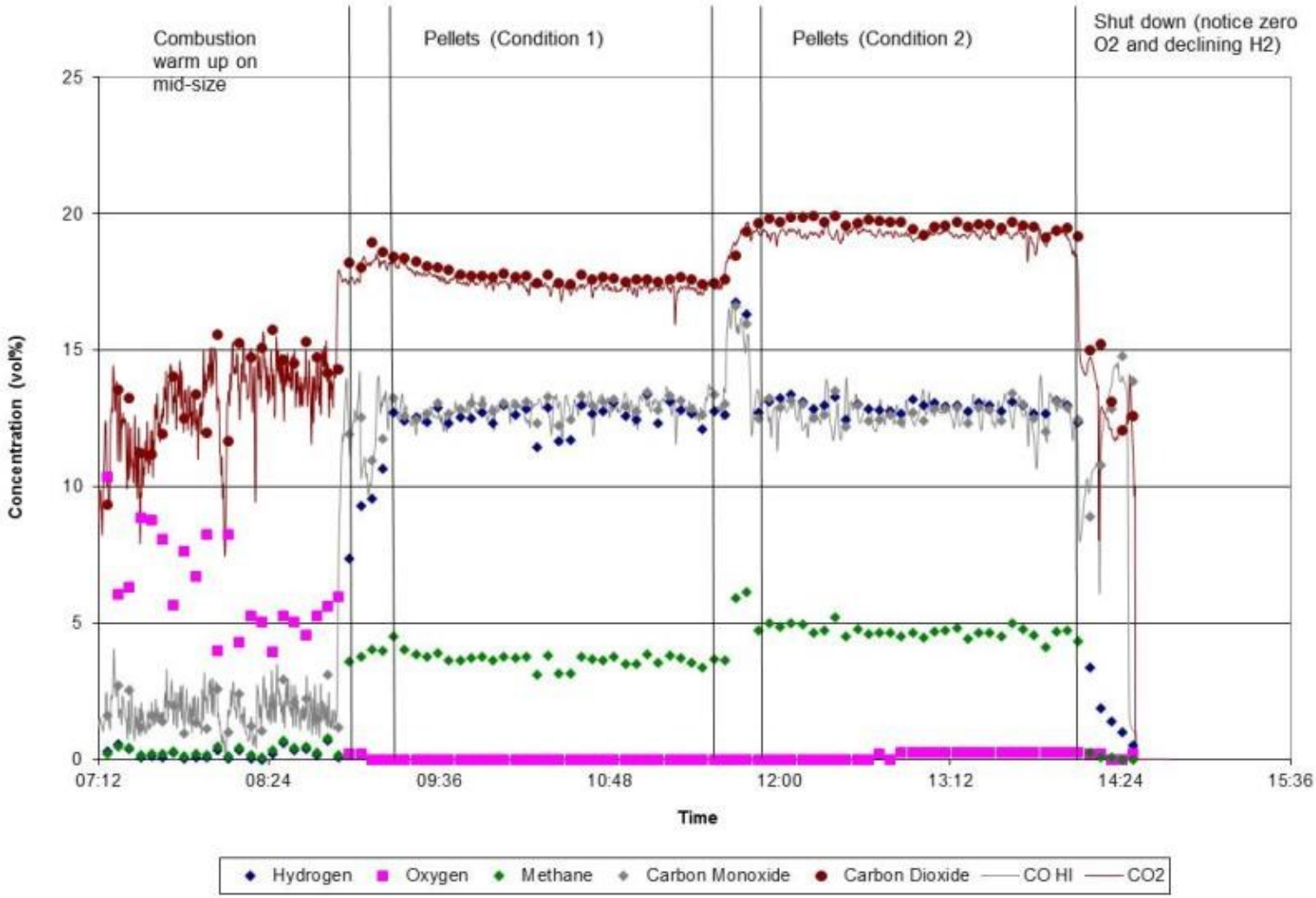

Figure C.1: Gas composition, Pellets run code G1

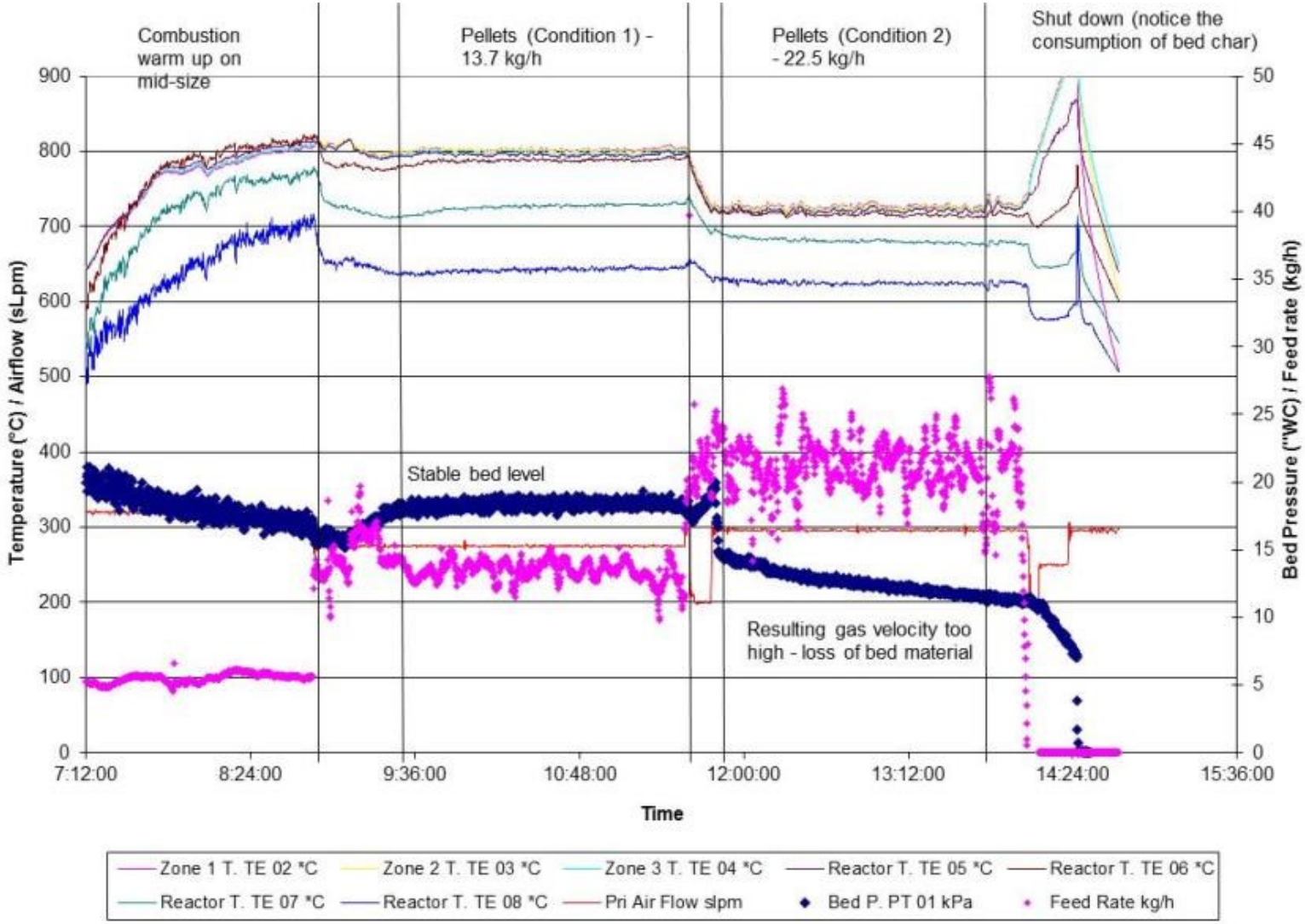

Figure C.2: Operations Summary, Pellets run code G1

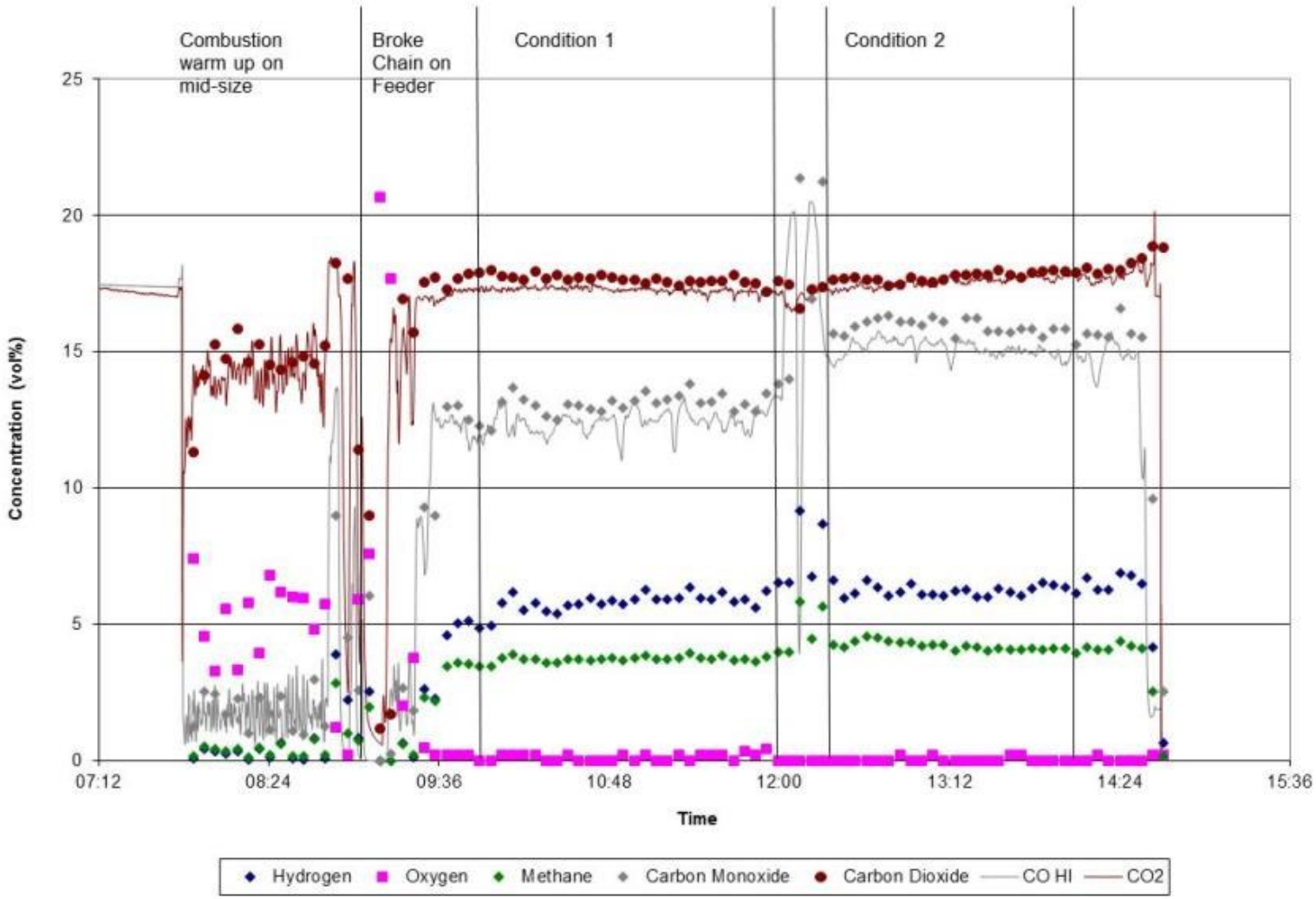

Figure C.3: Gas composition, Fines run code F1

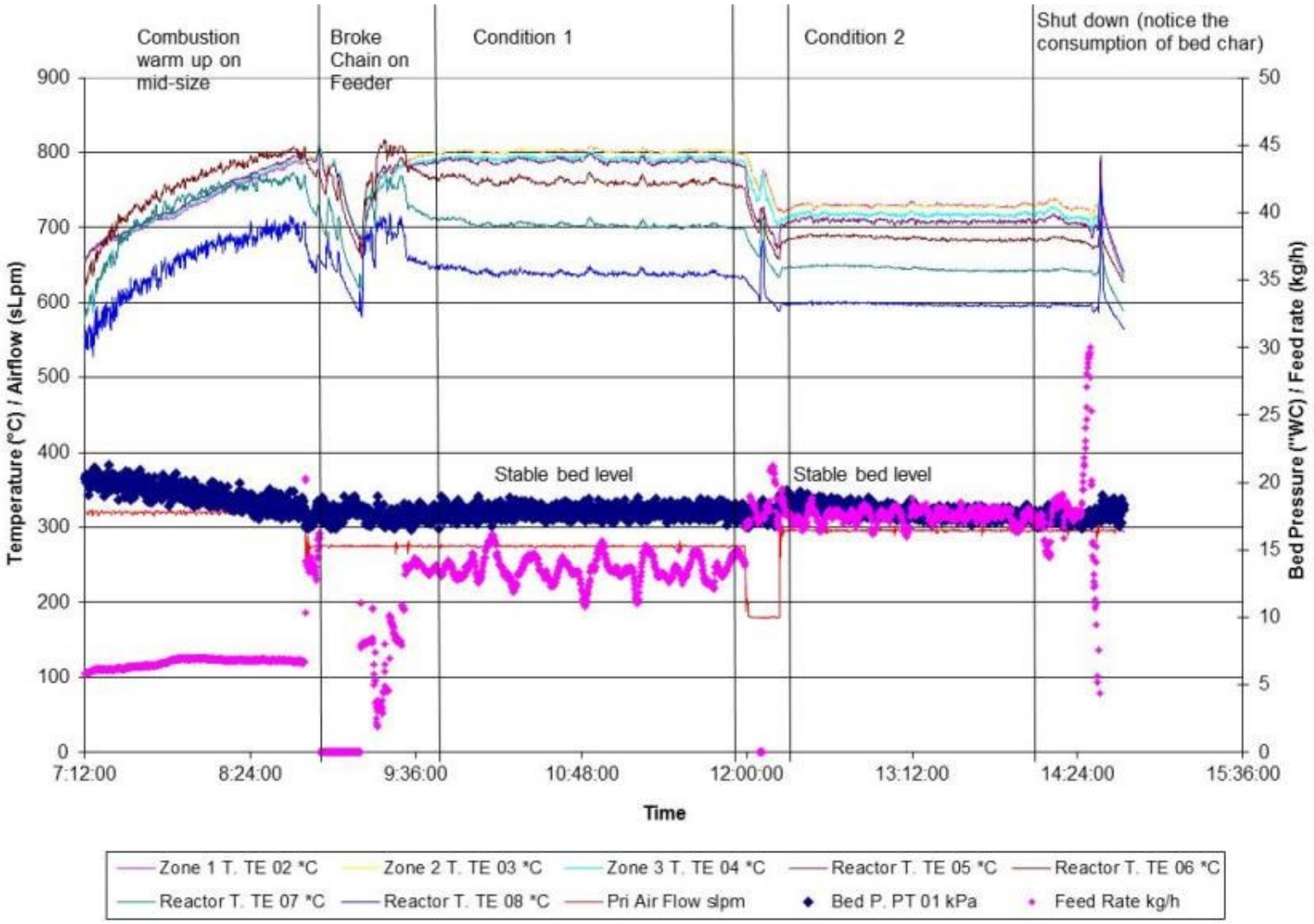

Figure C.4: Operations Summary, Fines run code F1

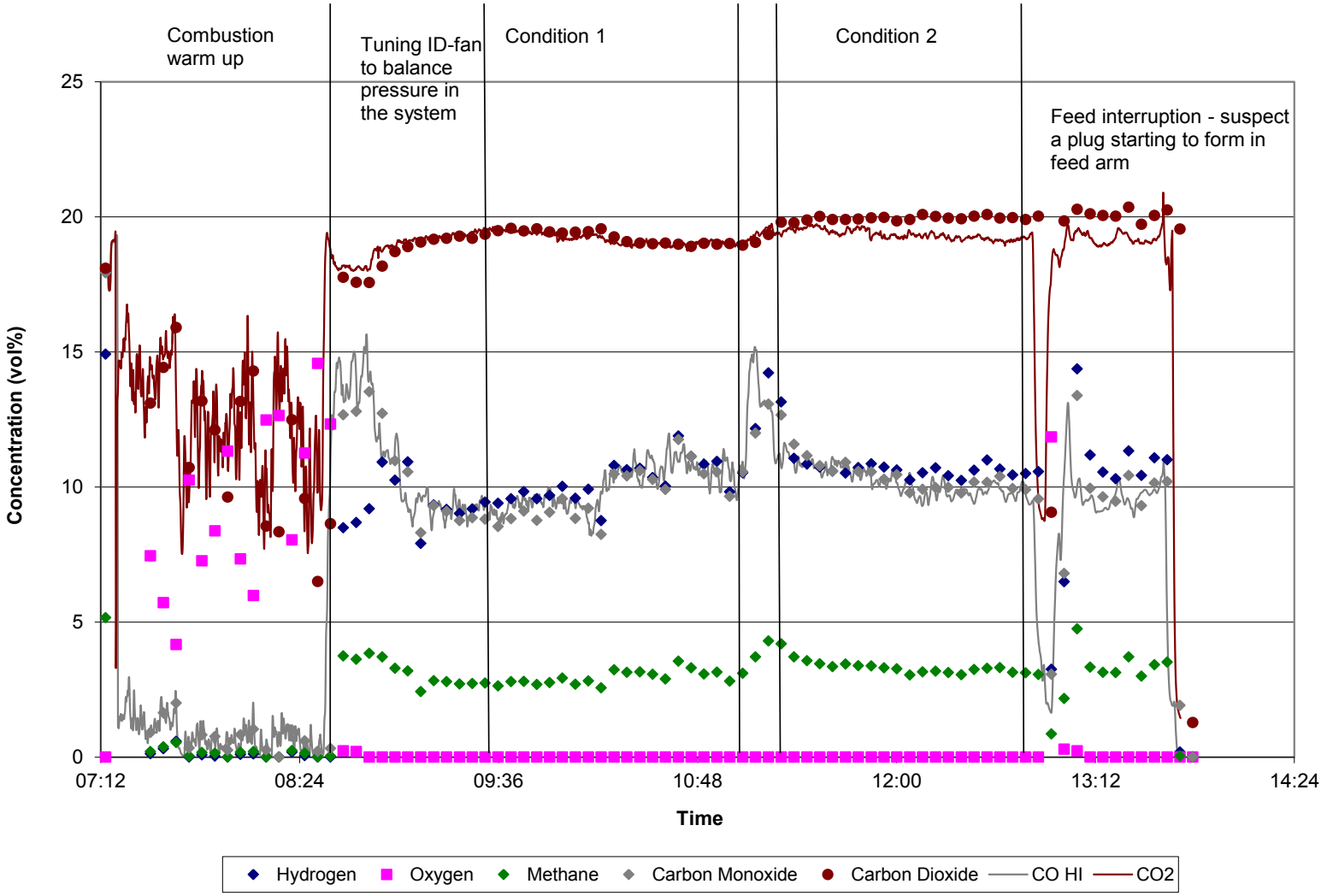

Figure C.5: Gas composition, mid-wet run code B

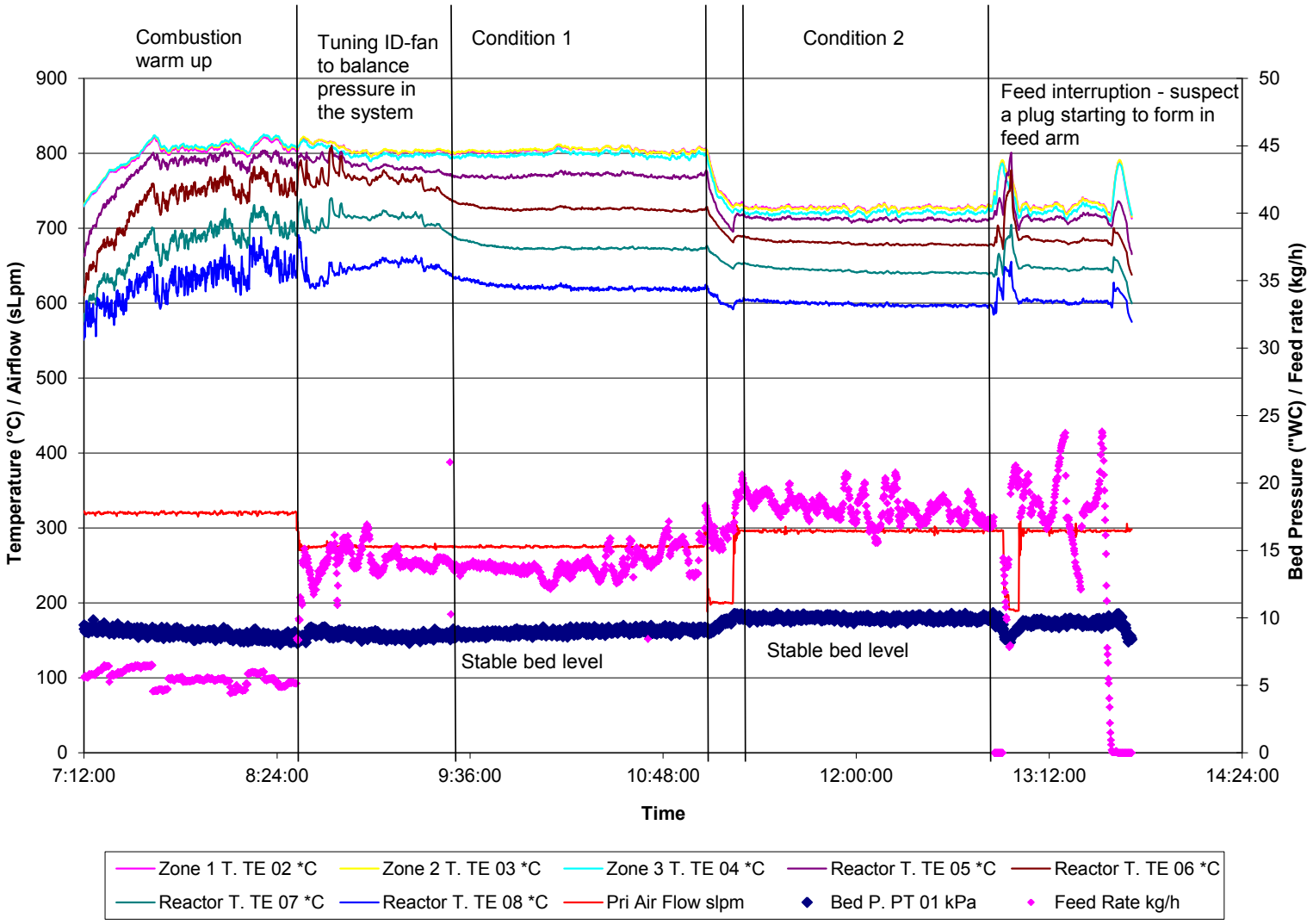

Figure C.6: Operations summary, mid-wet run code B

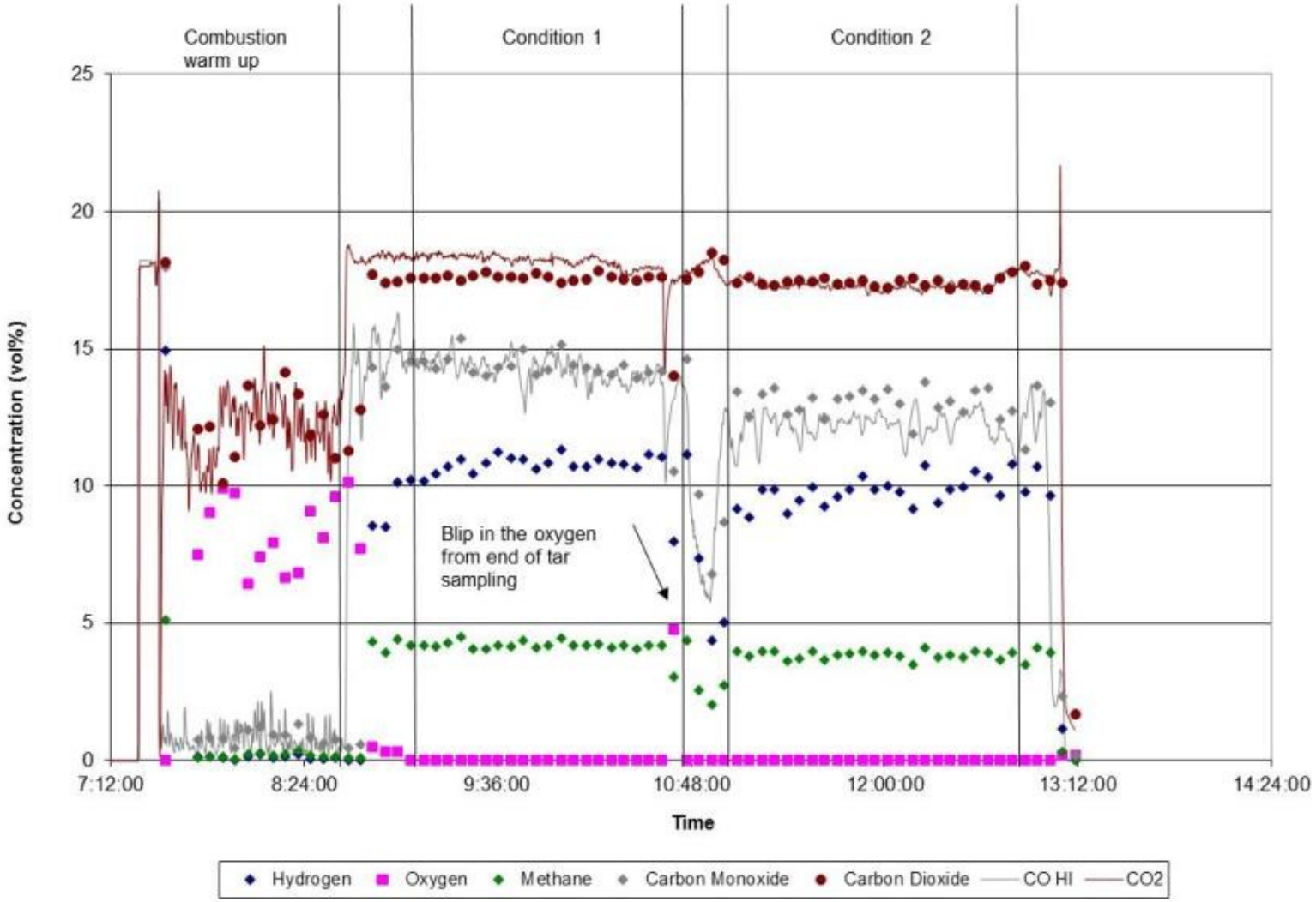

Figure C.7: Gas composition, mids run code E2

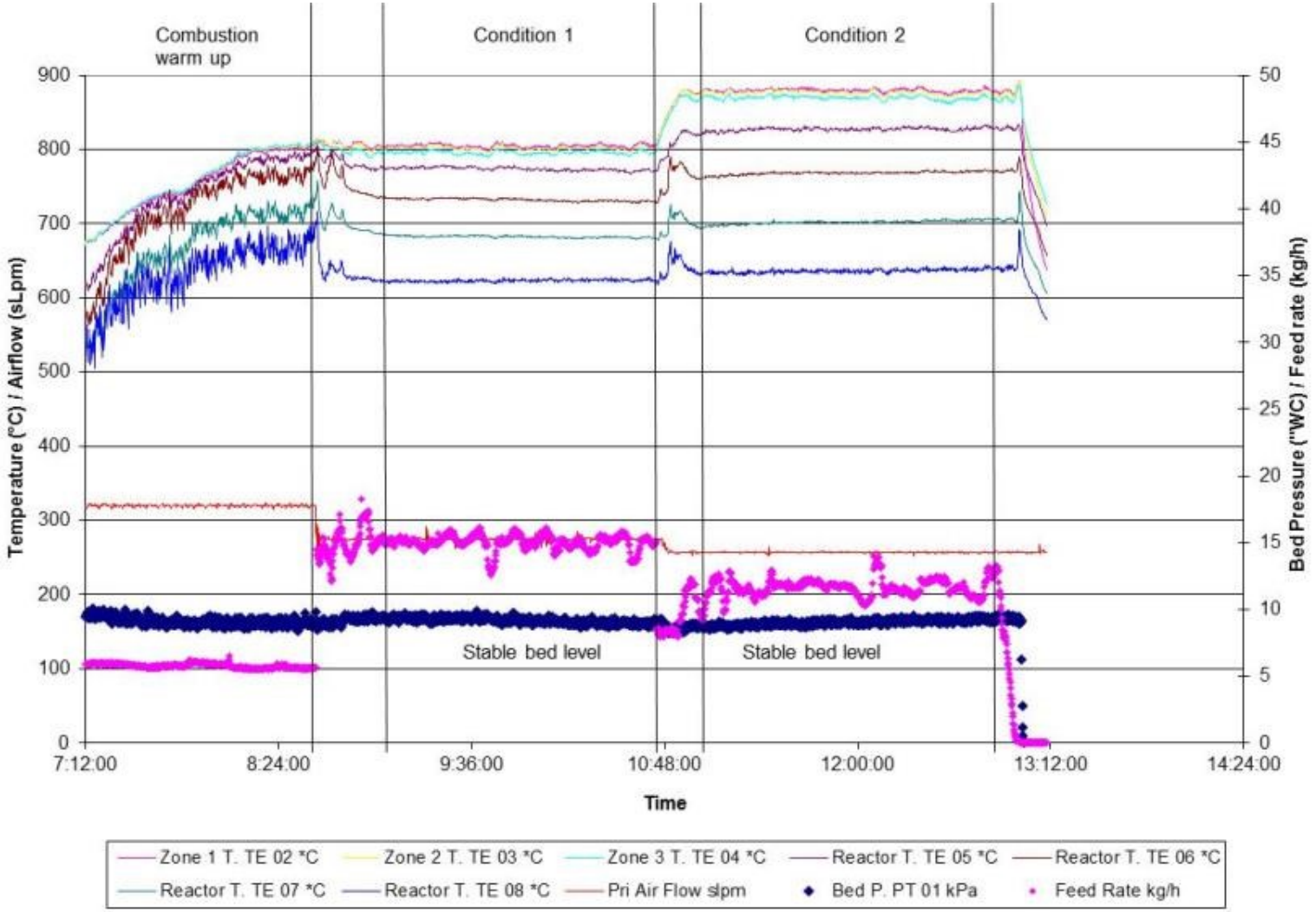

Figure C.8: Operations summary, mids run code E2

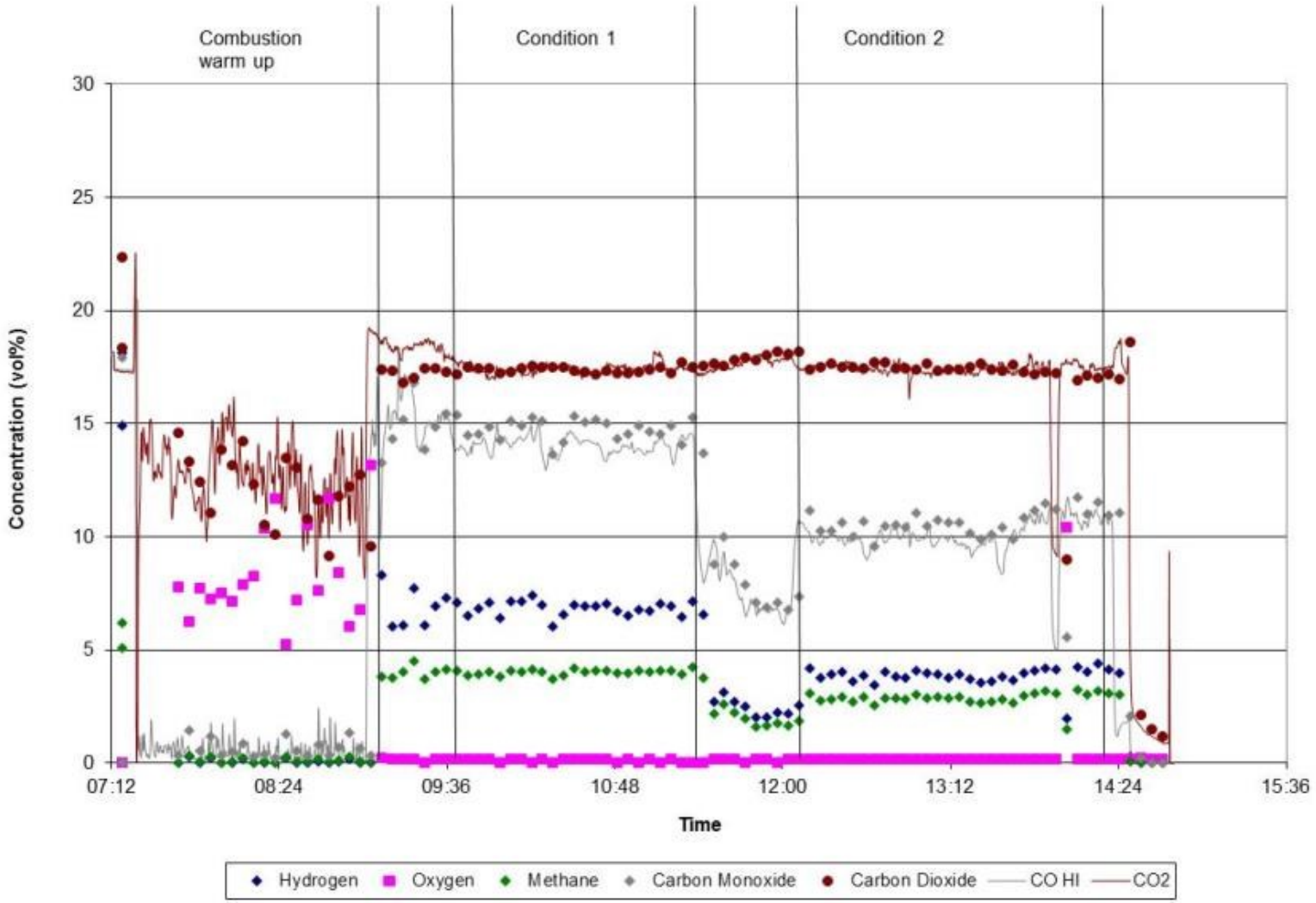

Figure C.9: Gas composition, fines run code F2

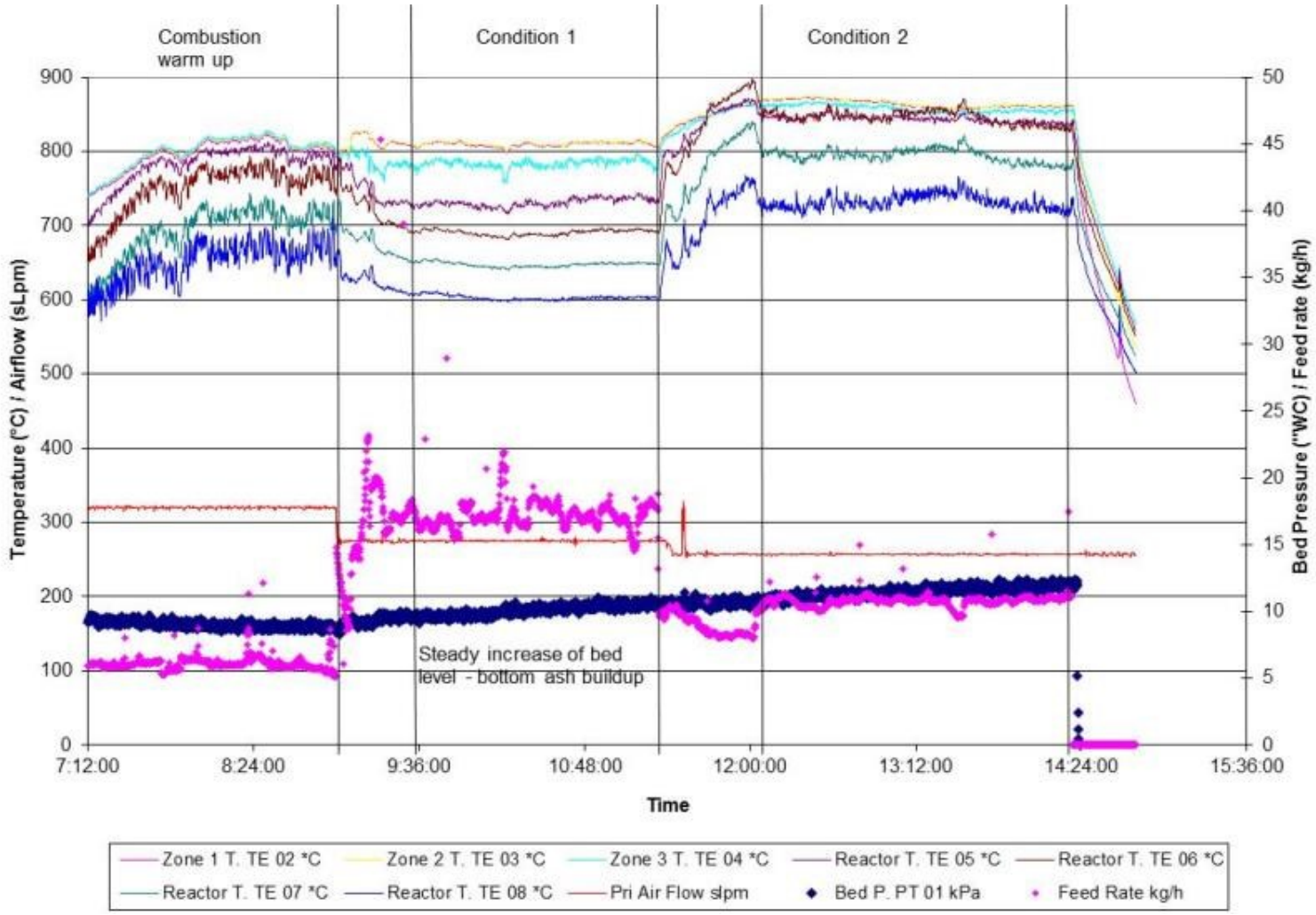

Figure C.10: Operations summary, fines run code F2

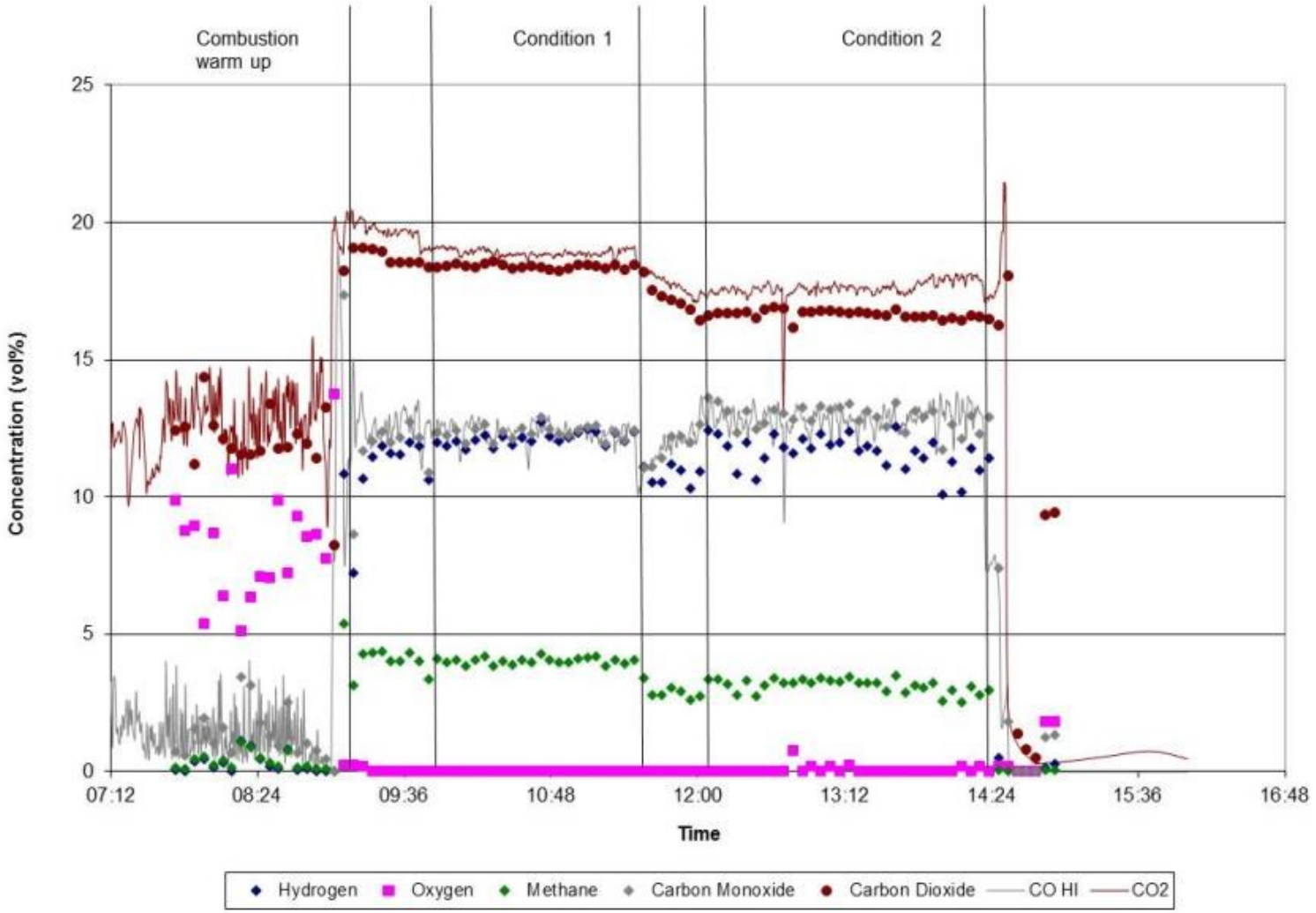

Figure C.11: Gas composition, pellets run code G2

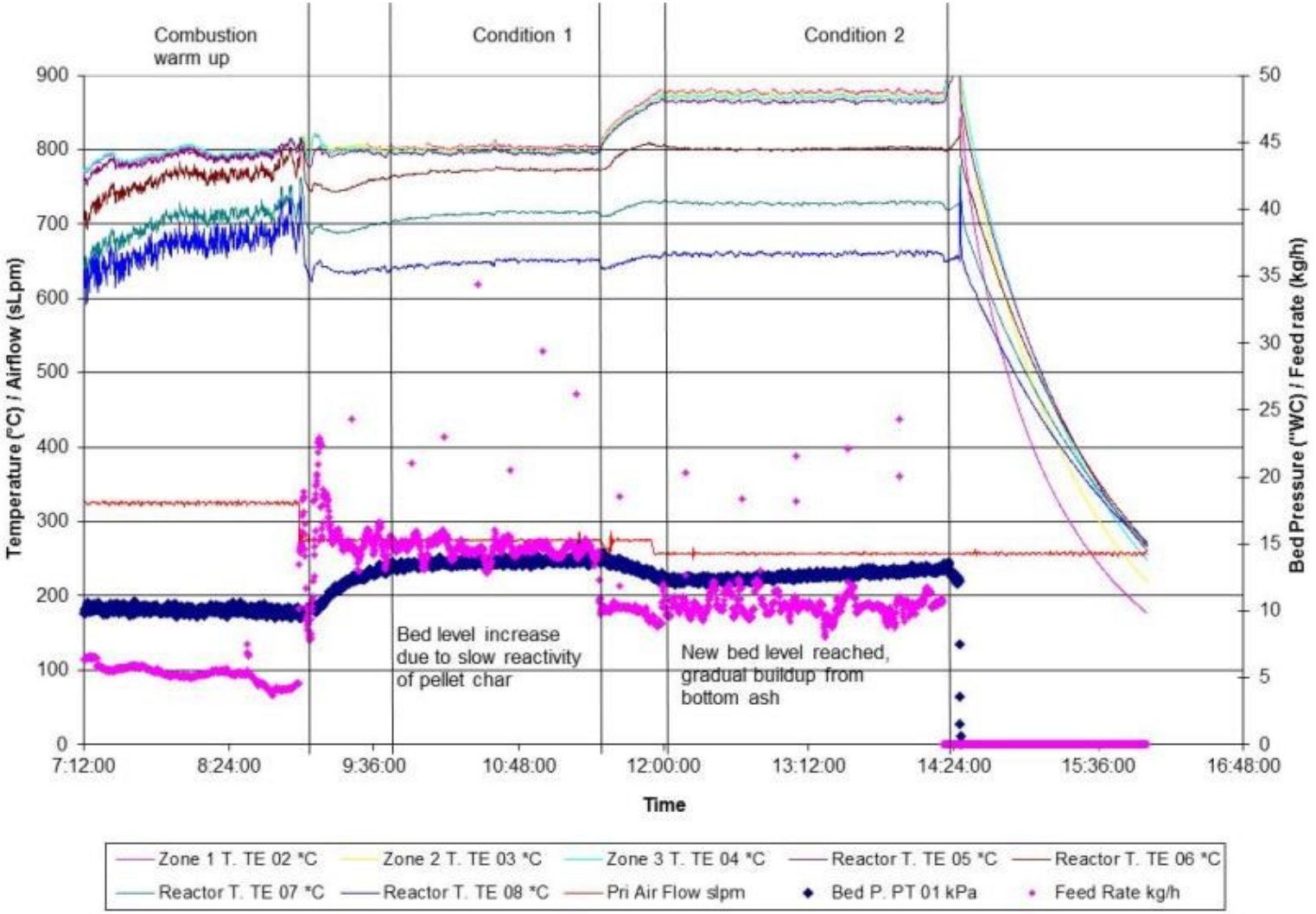

Figure C.12: Operations summary, pellets run code G2

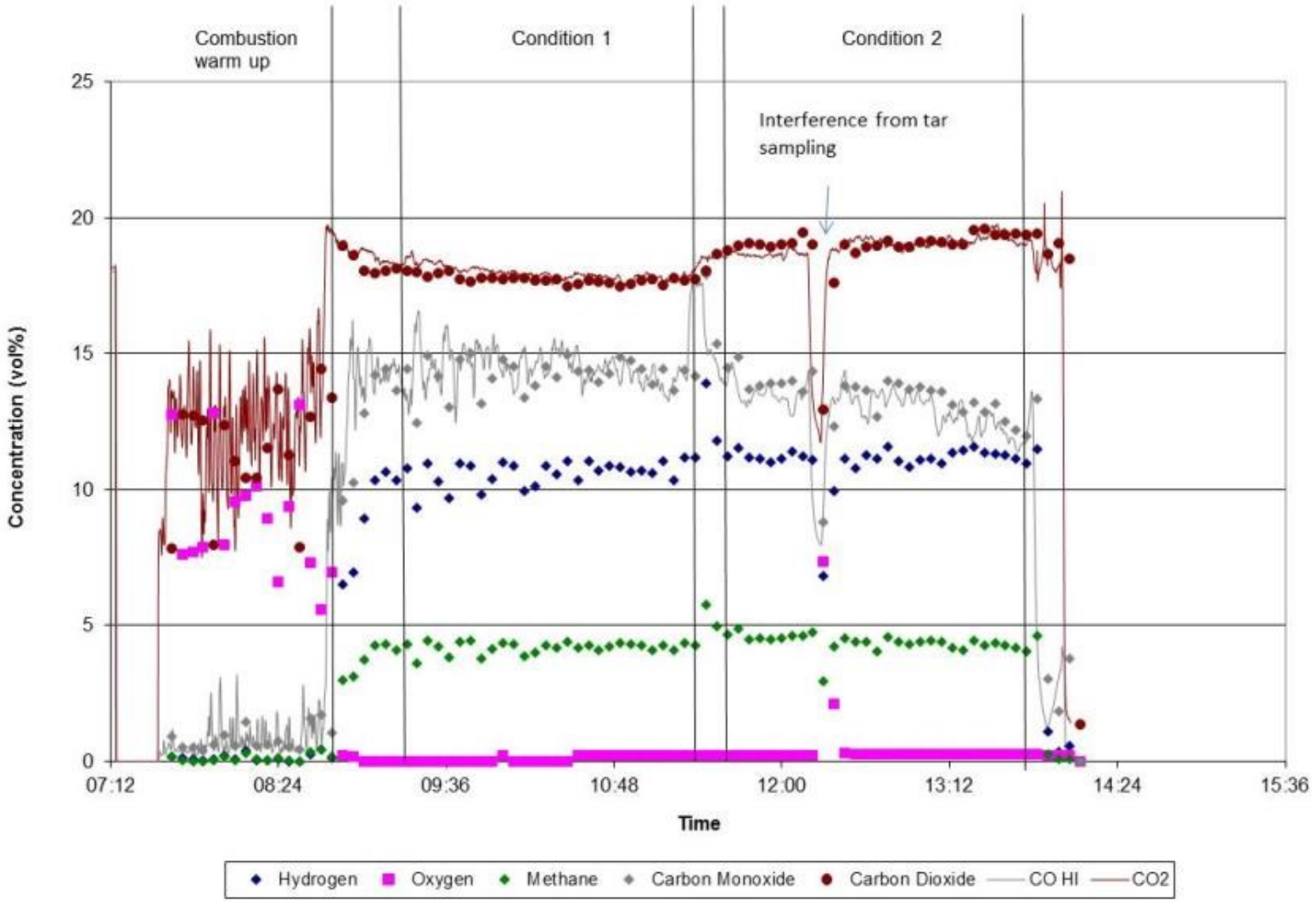

Figure C.13: Gas composition, mids run code E1

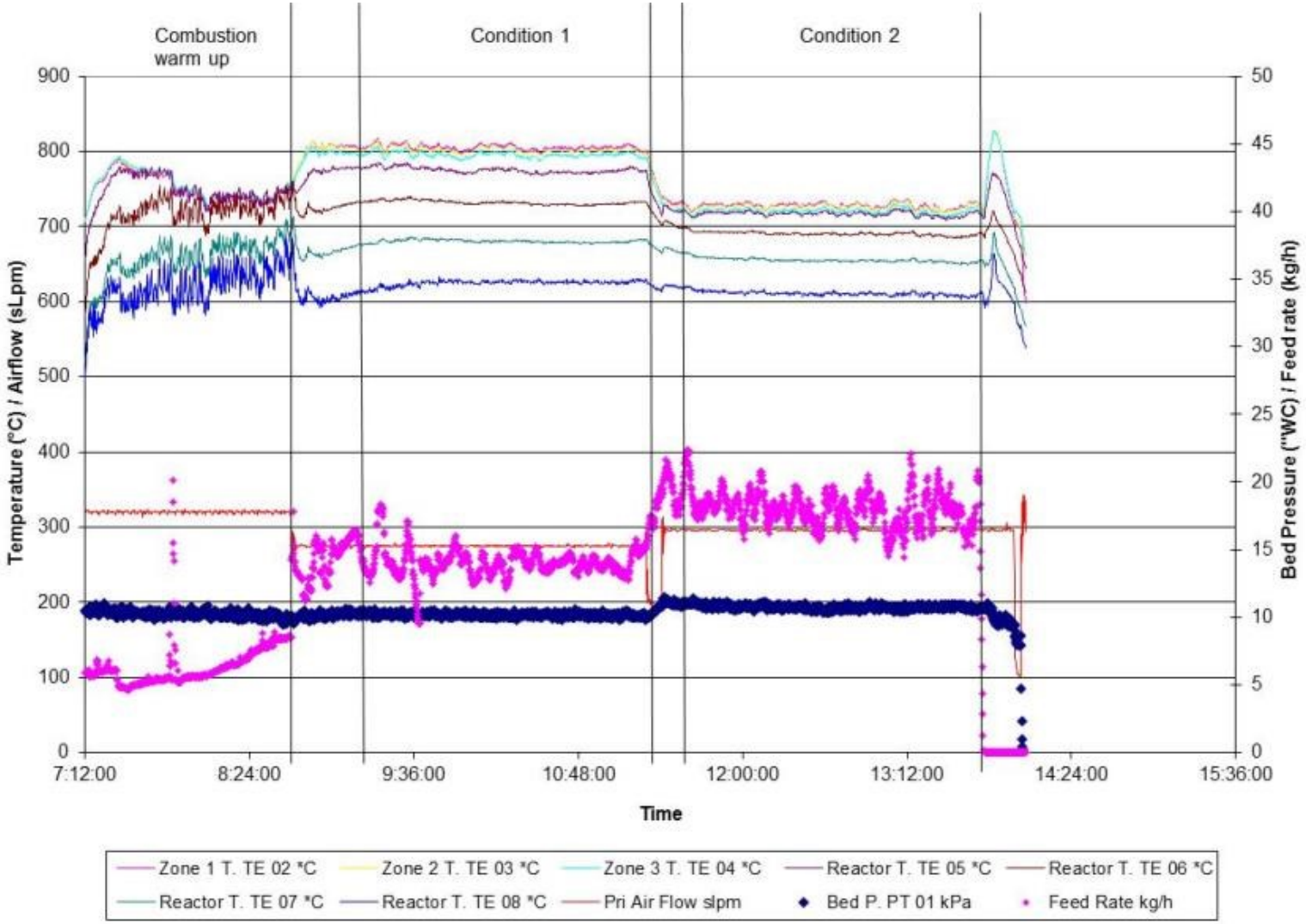

Figure C.14: Operation summary, mids run code E1

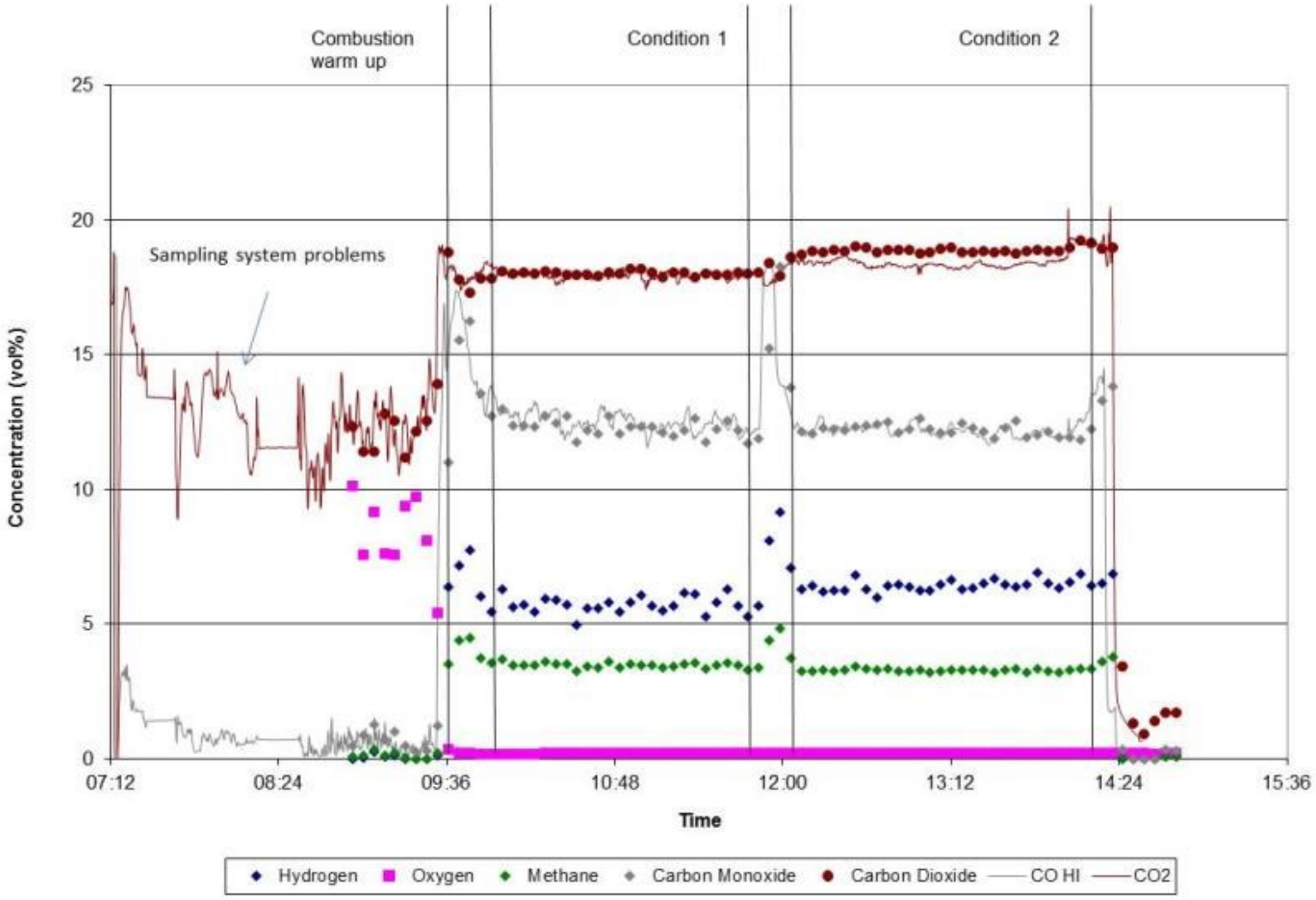

Figure C.15: Gas composition summary, fines-wet run code C

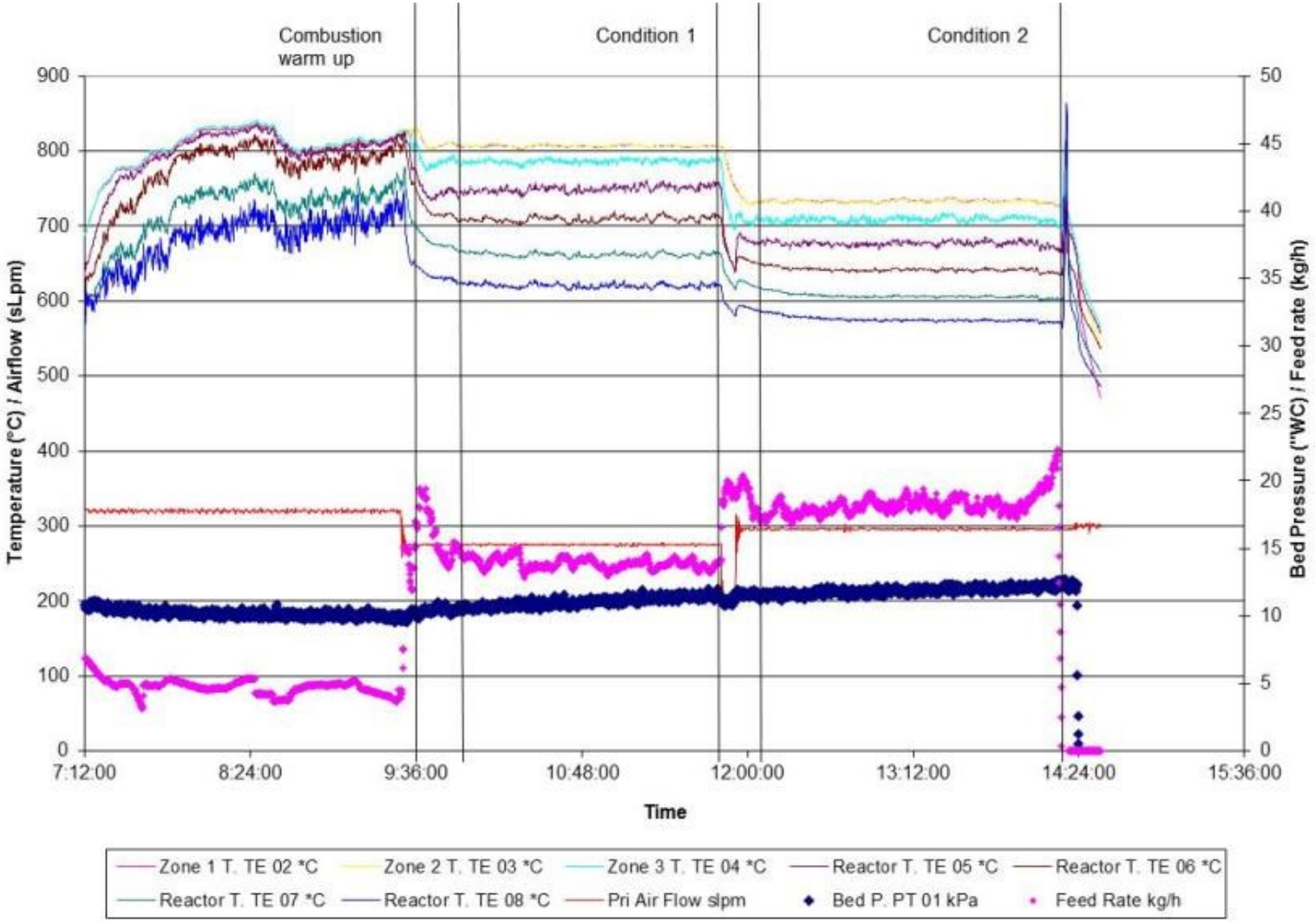

Figure C.16: Operations summary, fines-wet run code C

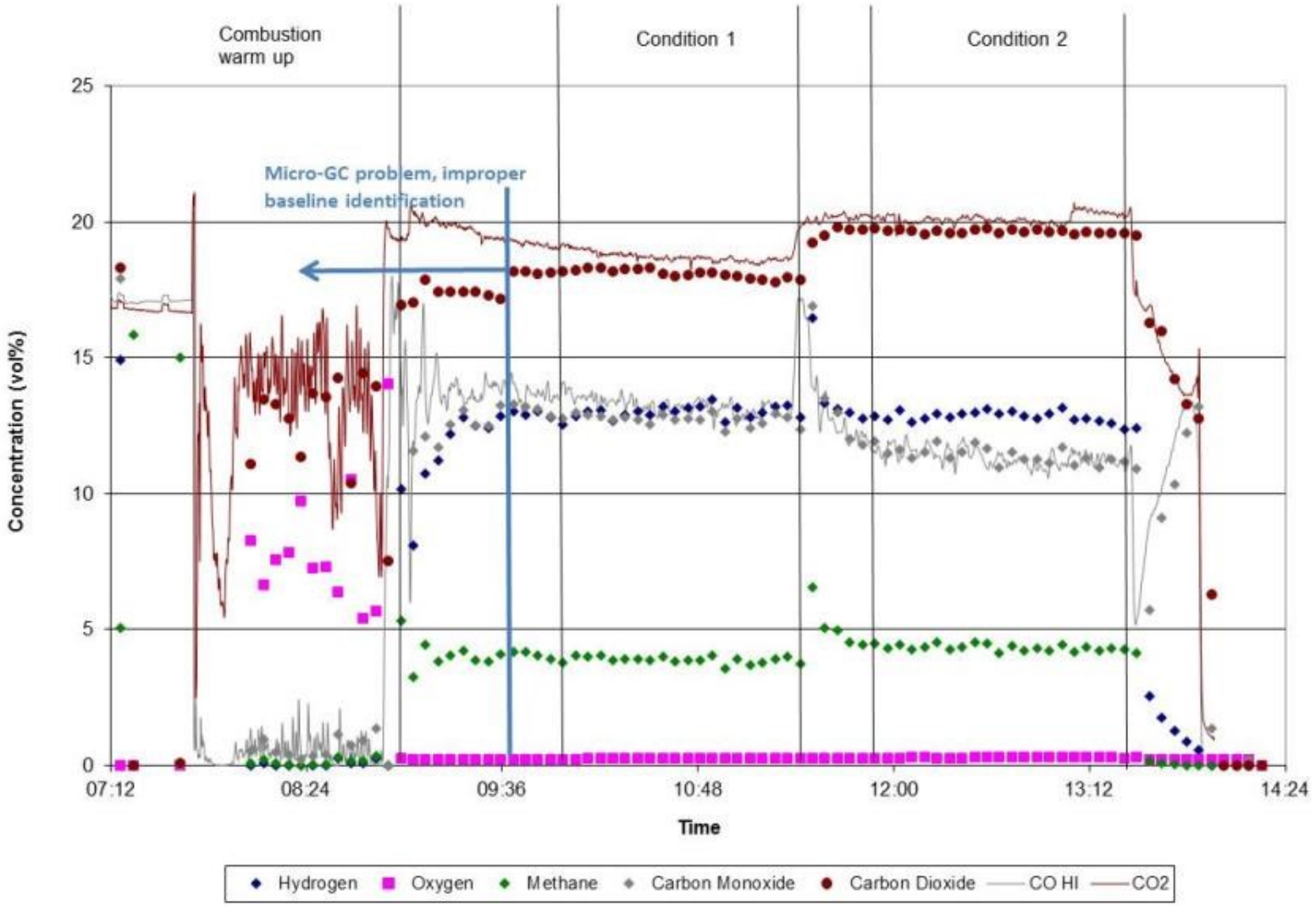

Figure C.17: Gas composition, pellets run code G3

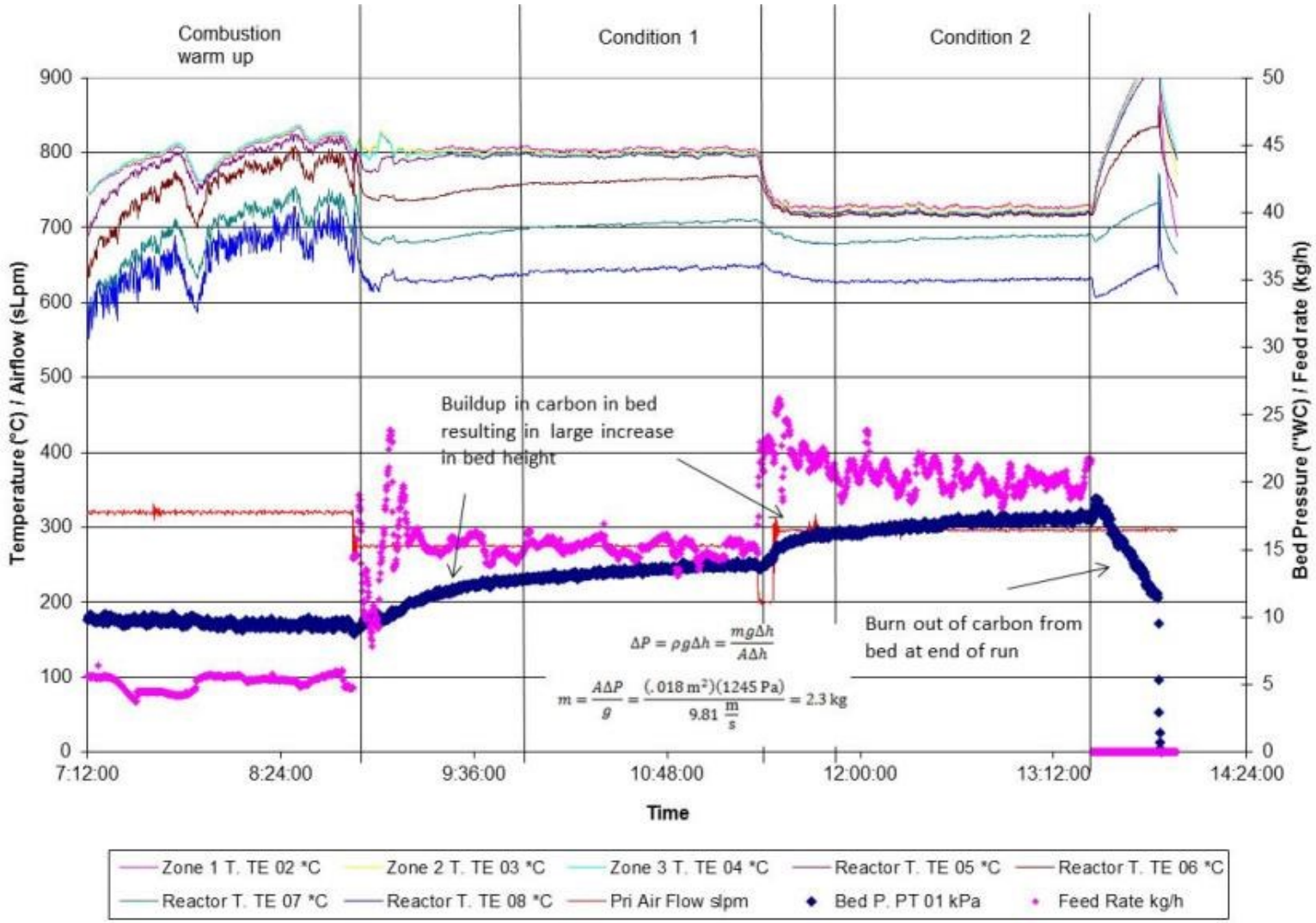

Figure C.18: Operations Summary, pellets run code G3

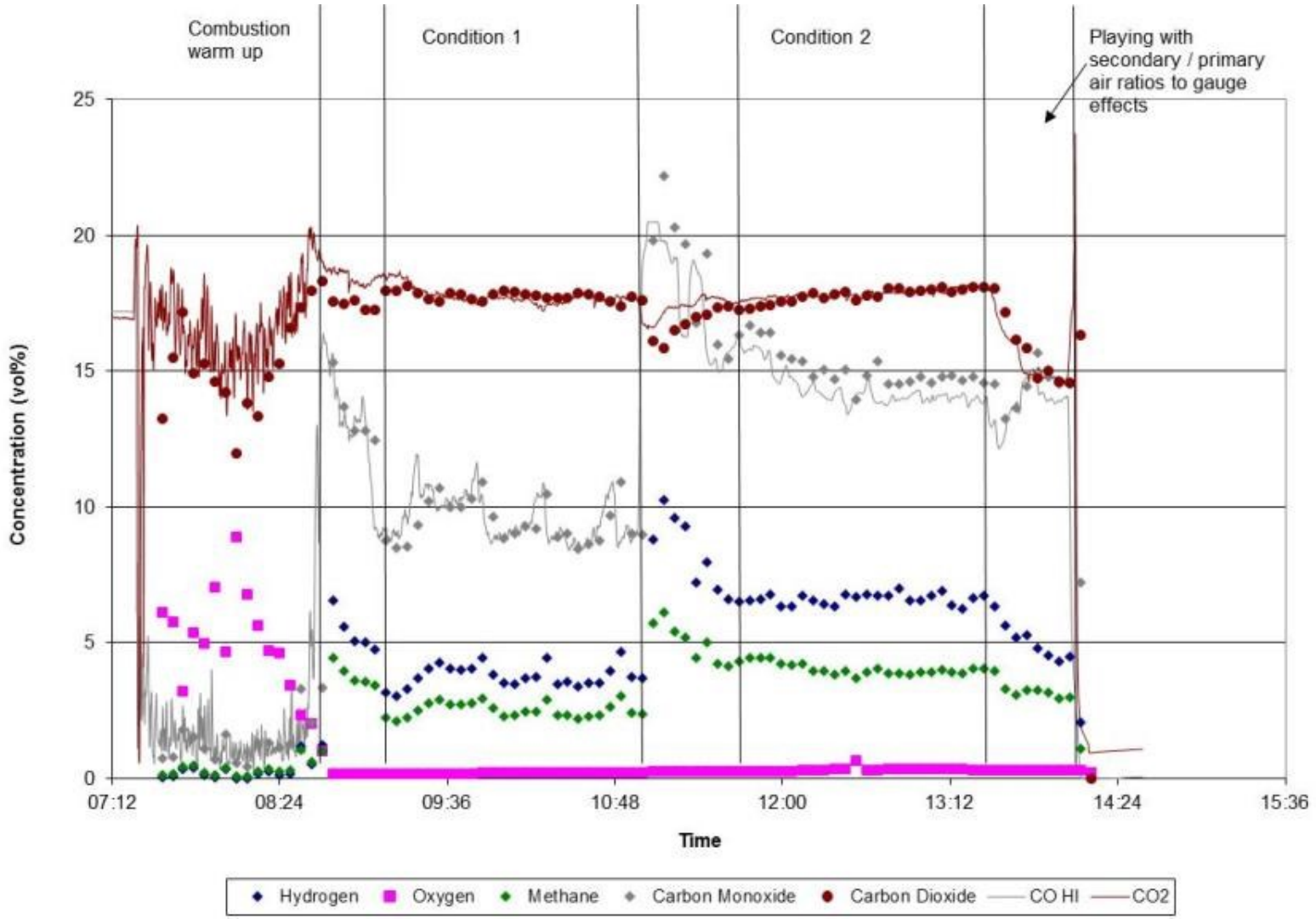

Figure C.19: Gas composition, fines run code E3

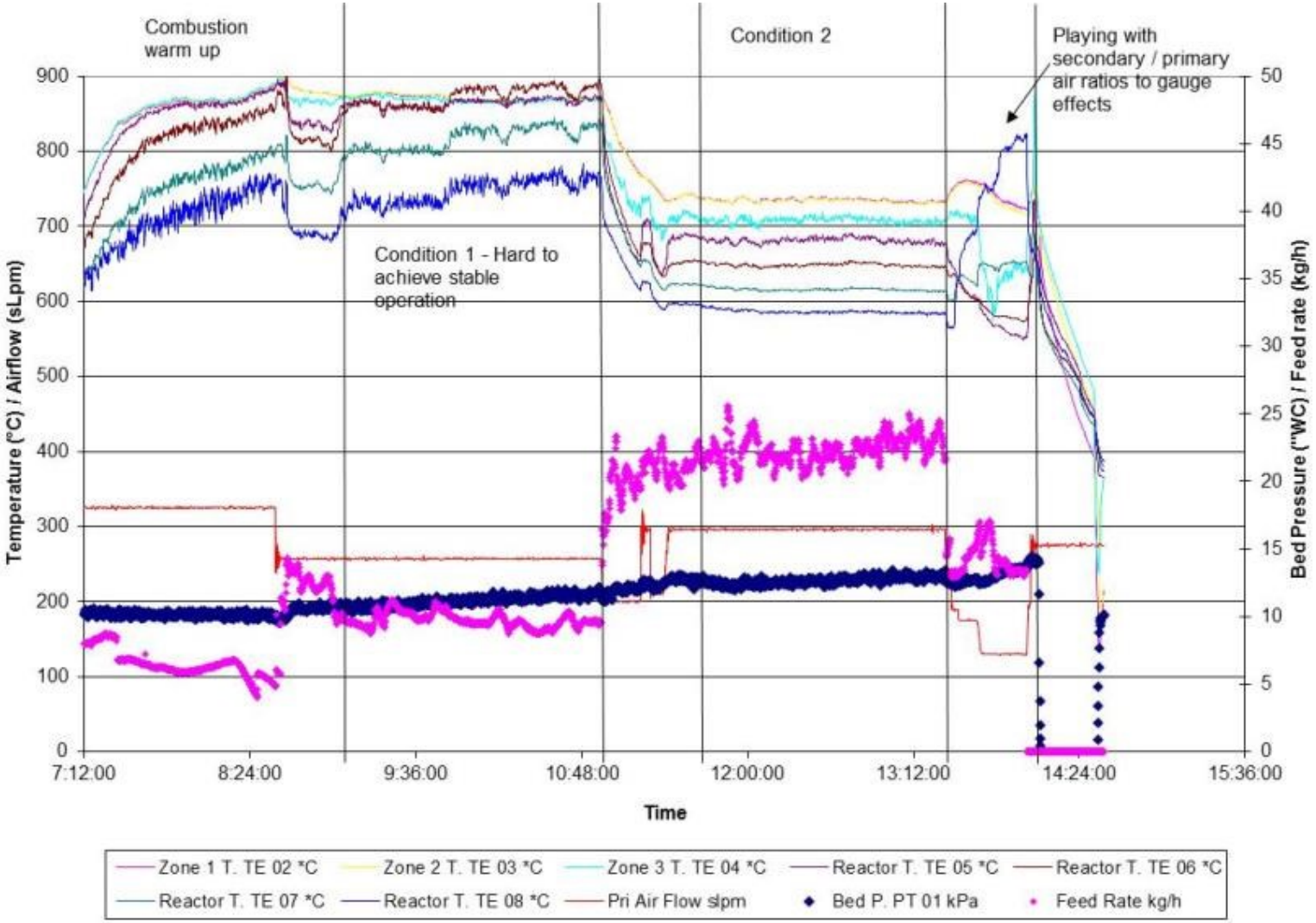

Figure C.20: Operations summary, fines run code F3

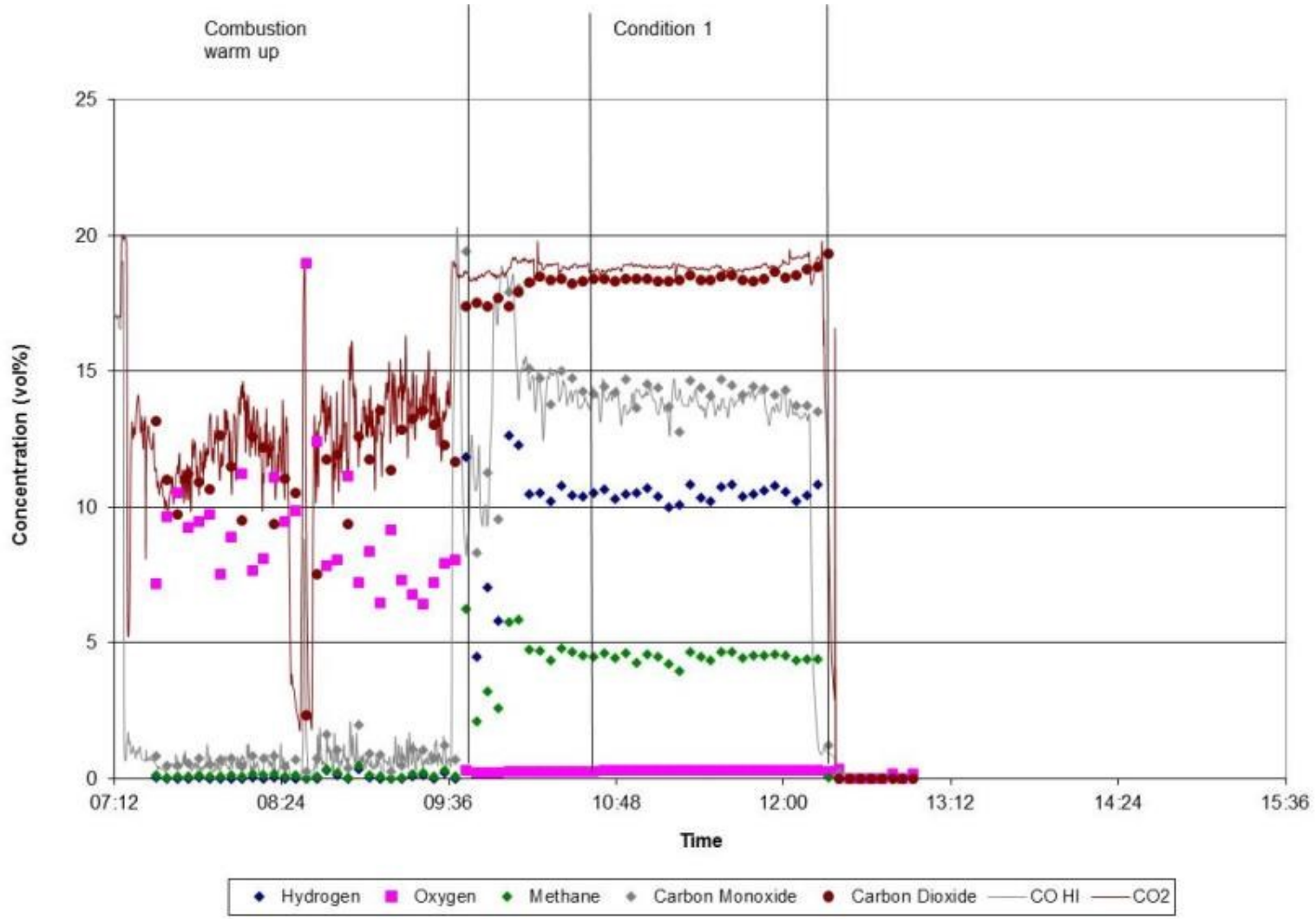

Figure C.21: Gas composition, mids run code E3

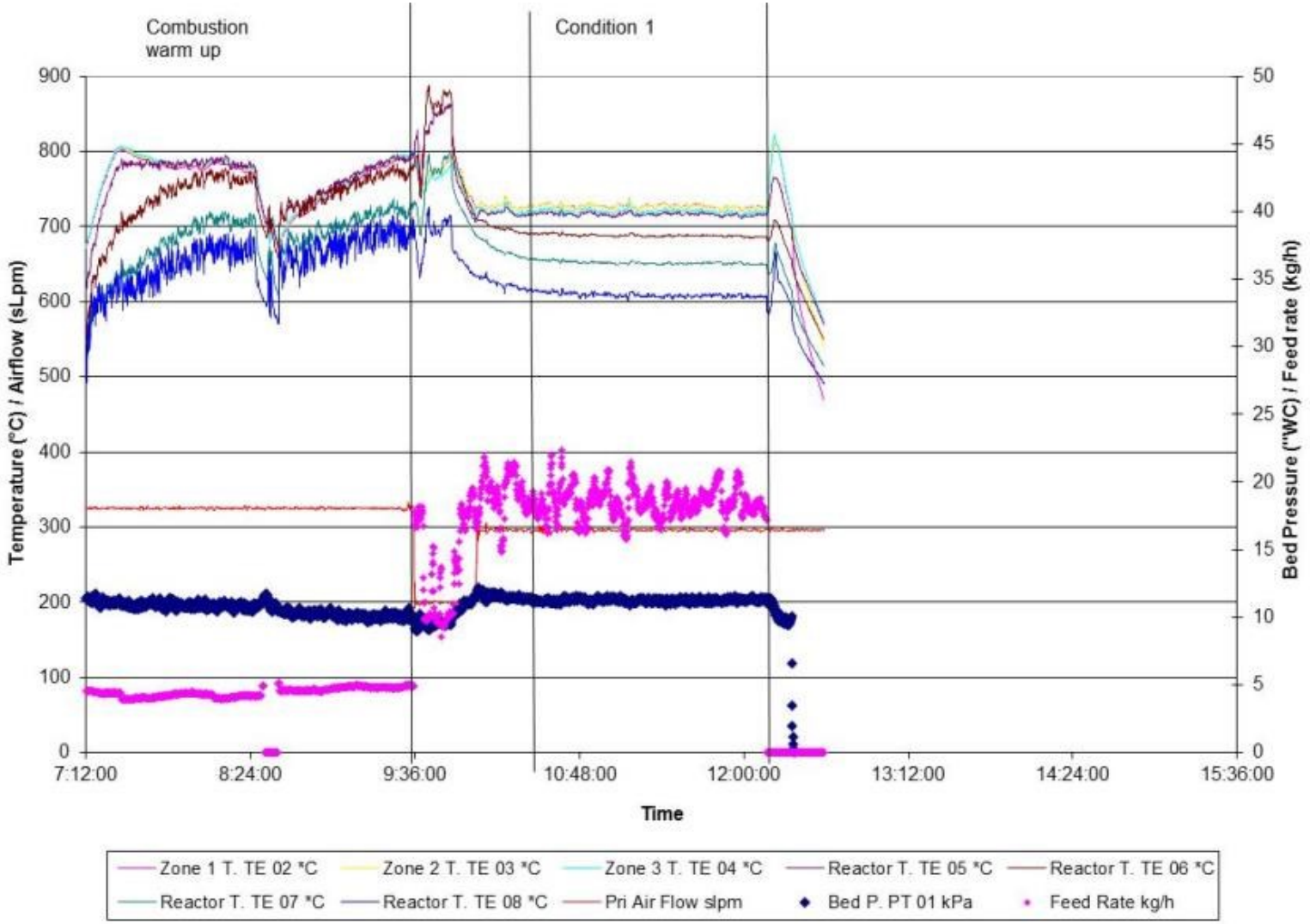

Figure C.22: Operations summary, mids run code E3

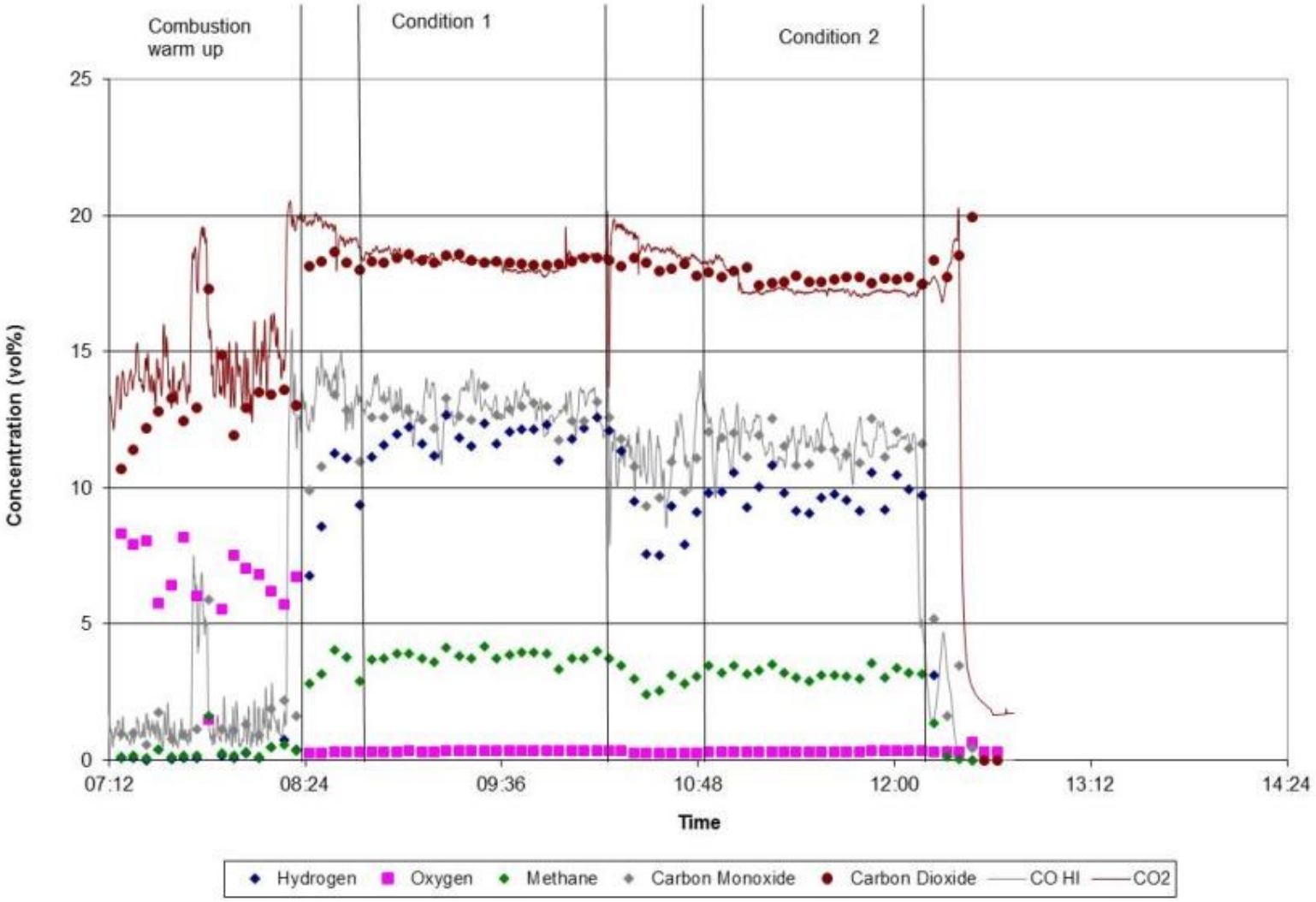

Figure C.23: Gas composition, Coarse run code D1

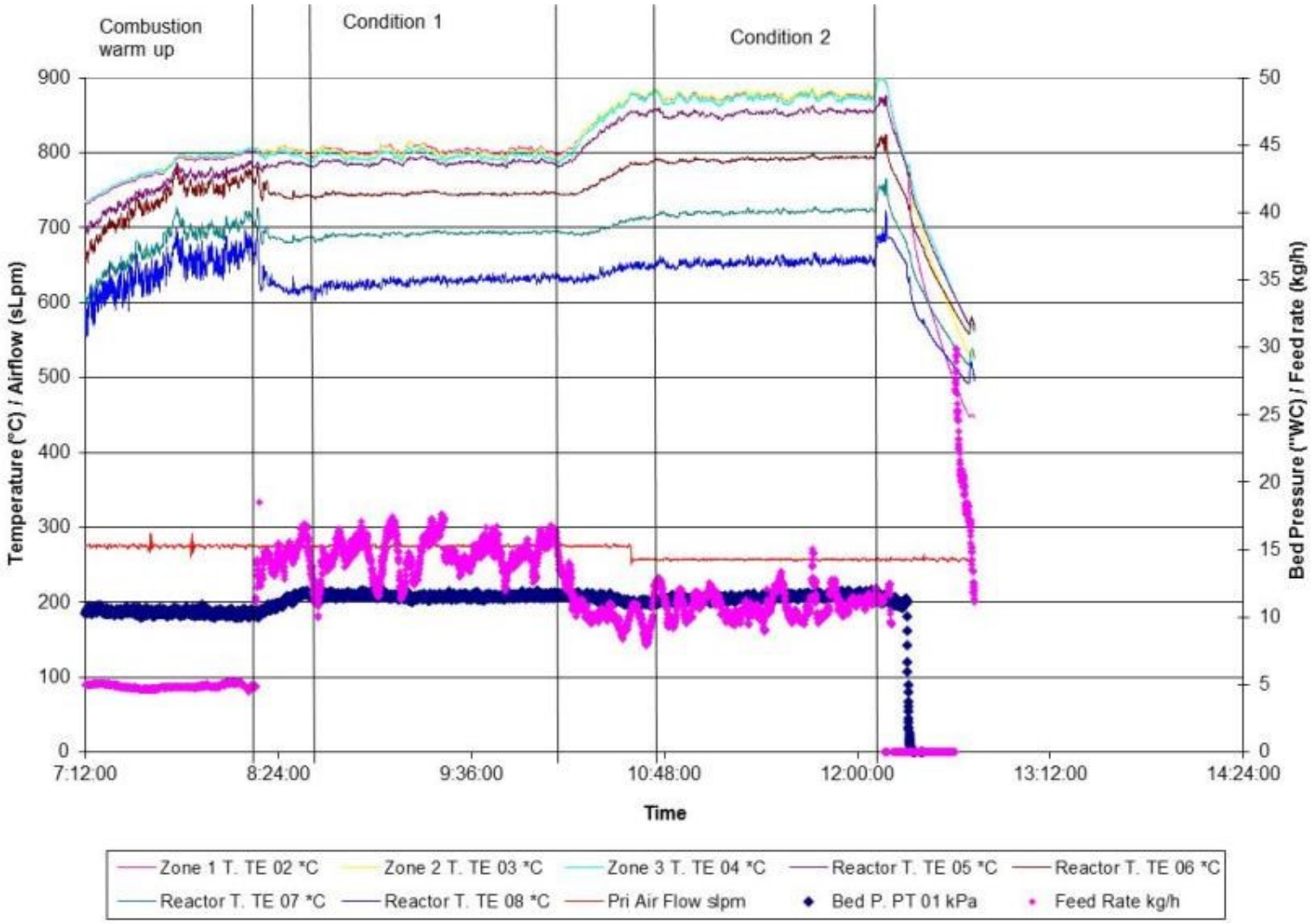

Figure C.24: Operations summary, coarse run code D1

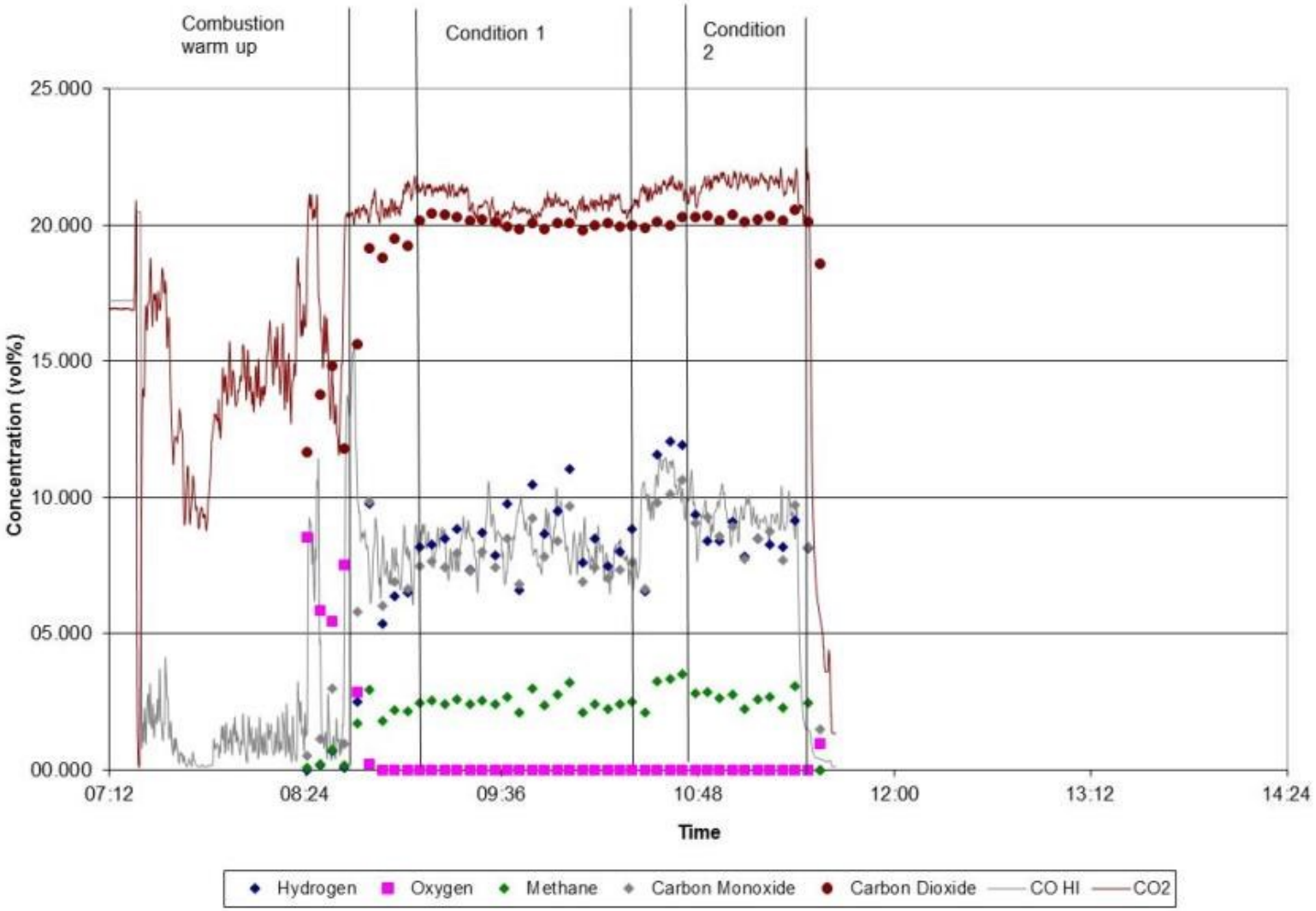

Figure C.25: Gas composition, coarse-wet run code A

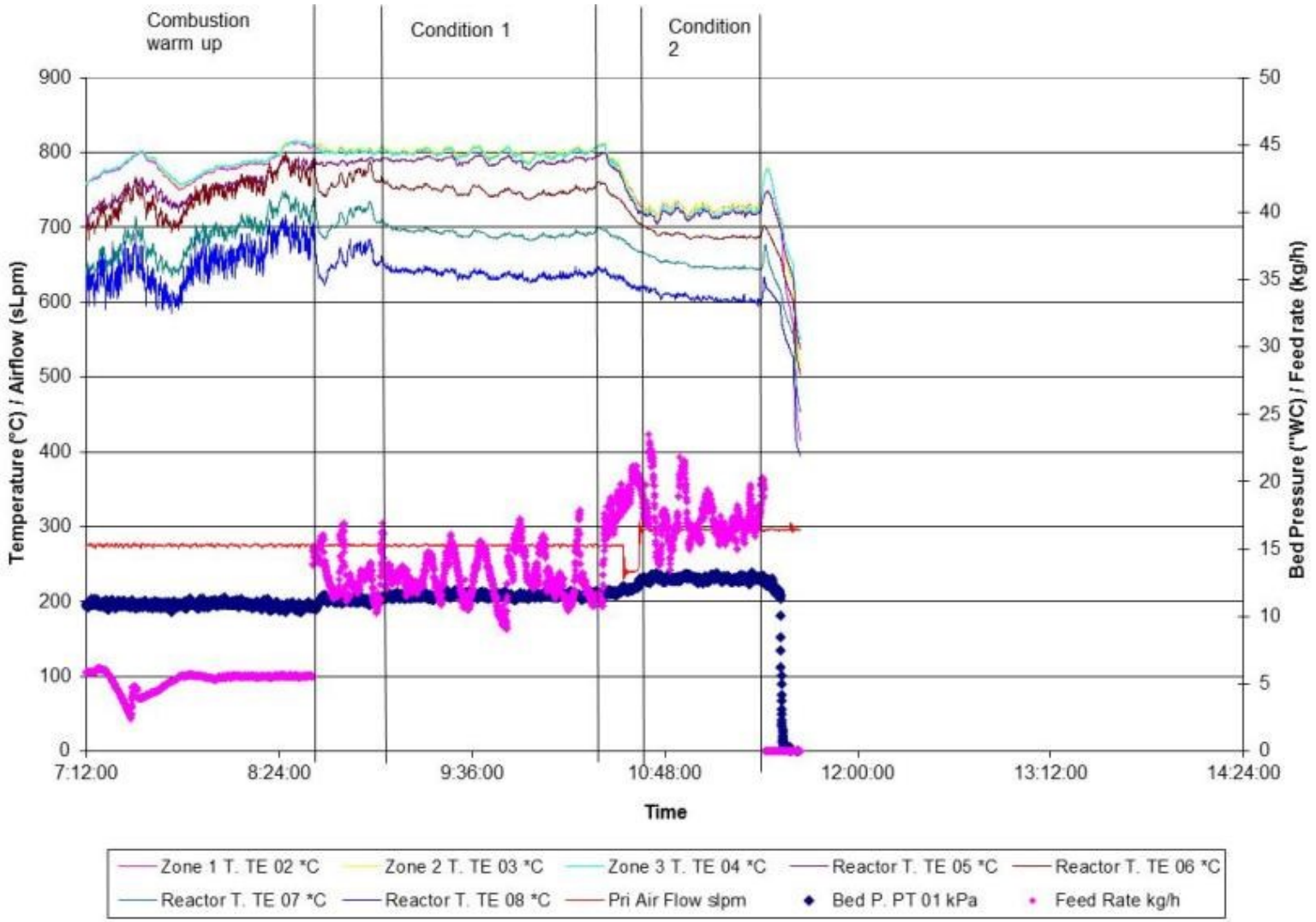

Figure C.26: Operations summary, coarse-wet run code A

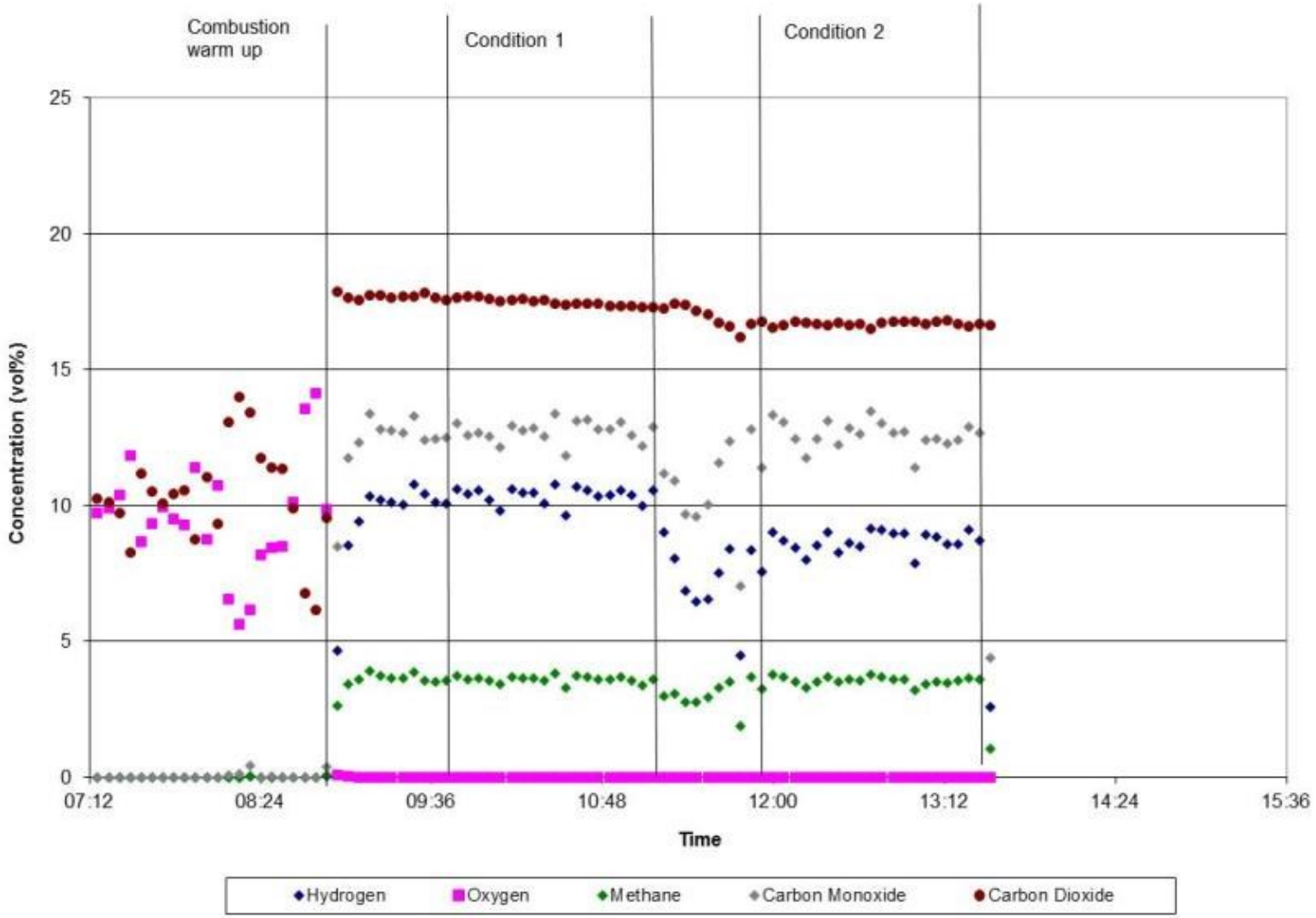

Figure C.27: Gas composition summary, run code Mid

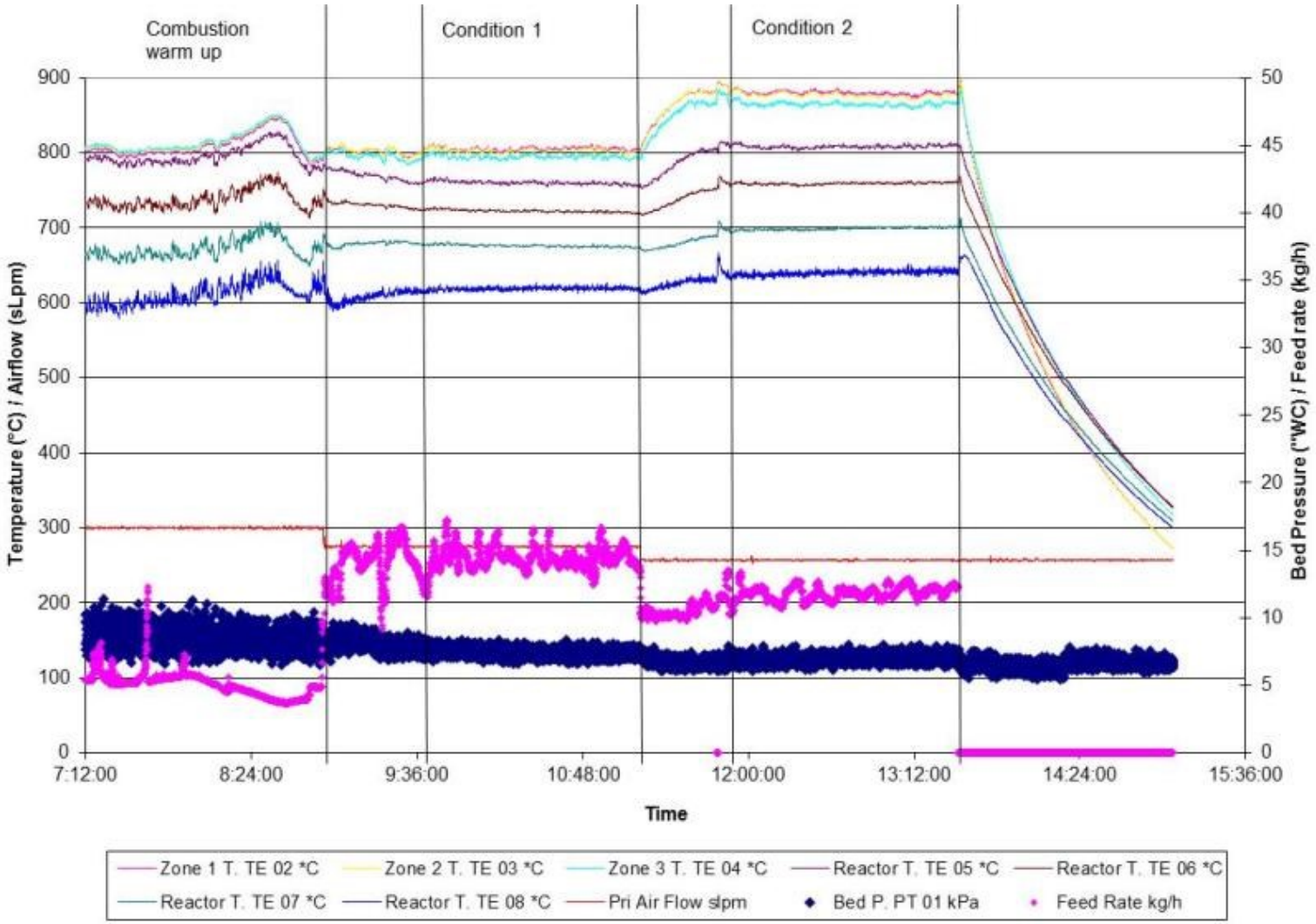

Figure C.28: Operations summary, run code Mid

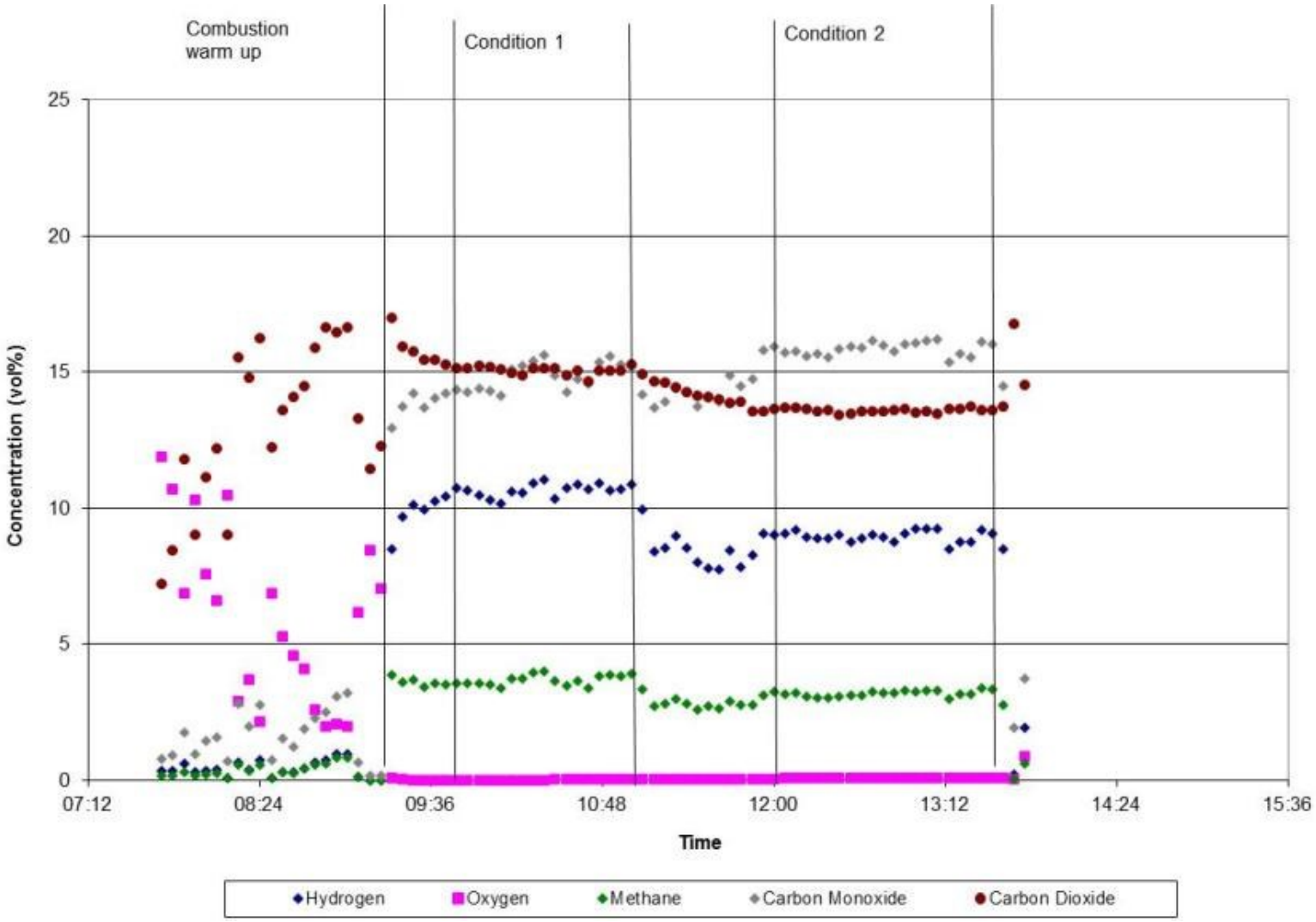

Figure C.29; Gas composition summary, run code Torr

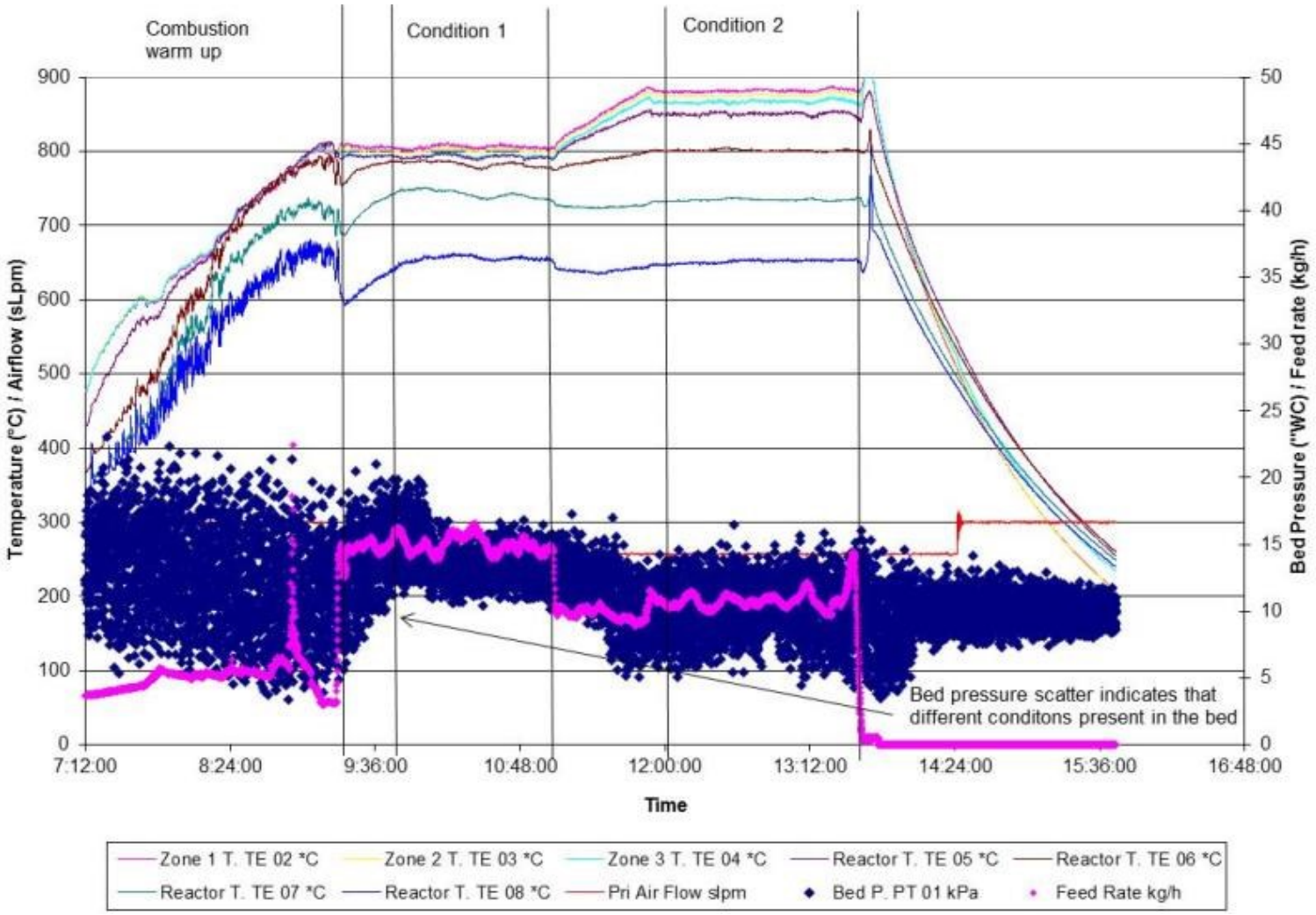

Figure C.30: Operations summary, run code Torr

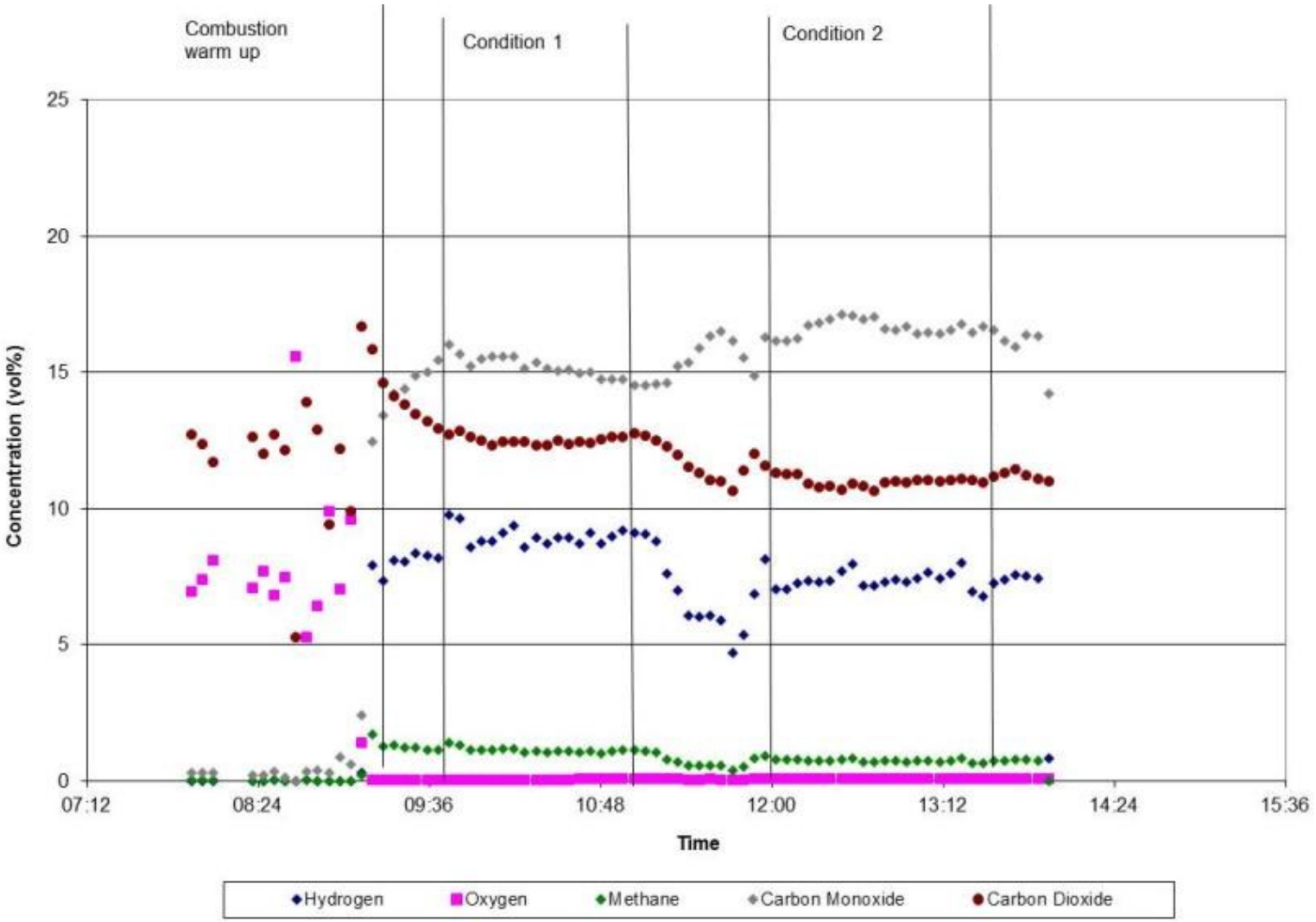

Figure C.31: Gas composition summary, run code Carb

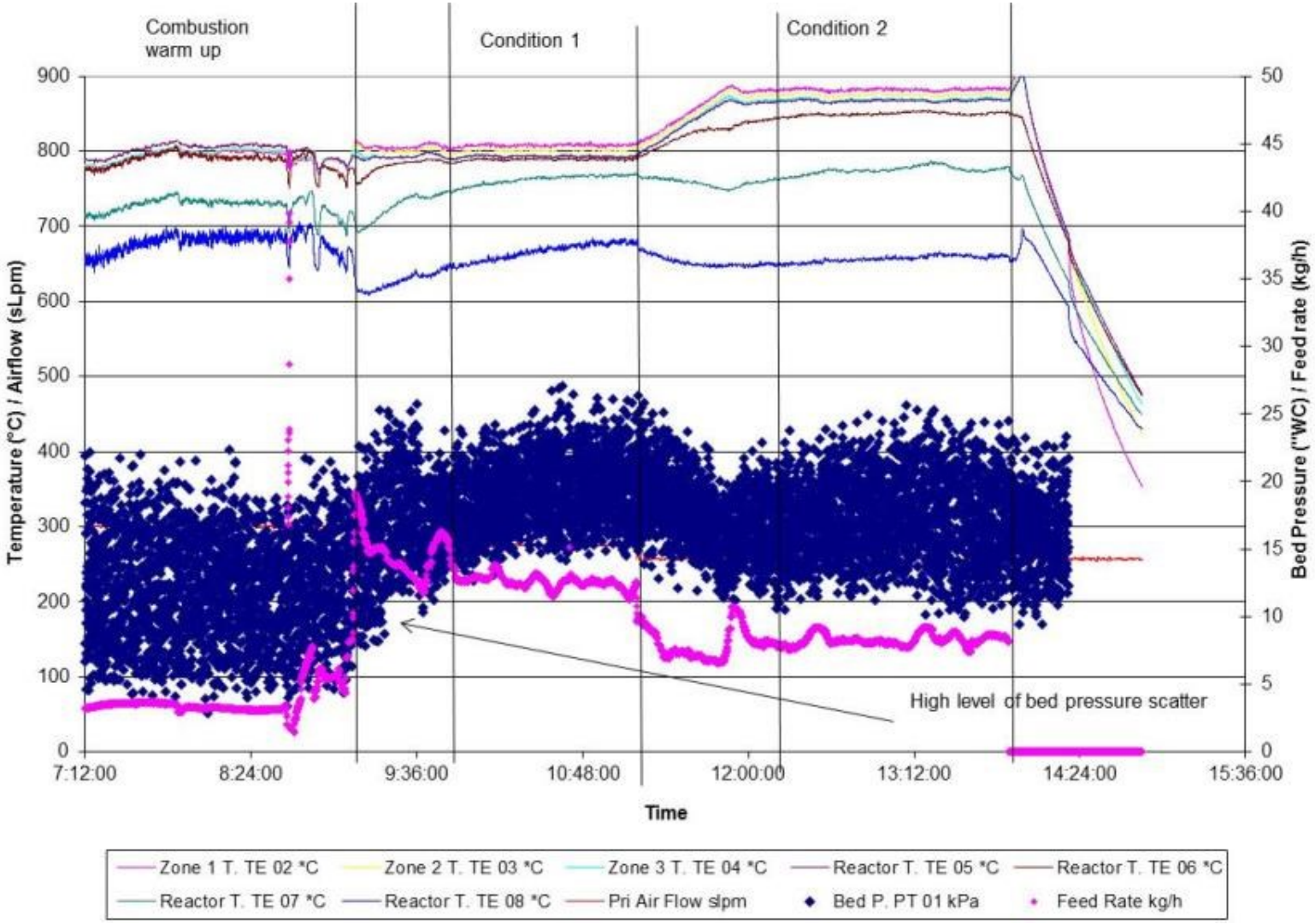

Figure C.32: Operations summary, run code Carb

C.2 **Run Charts from the Large Pilot-scale Gasifier**

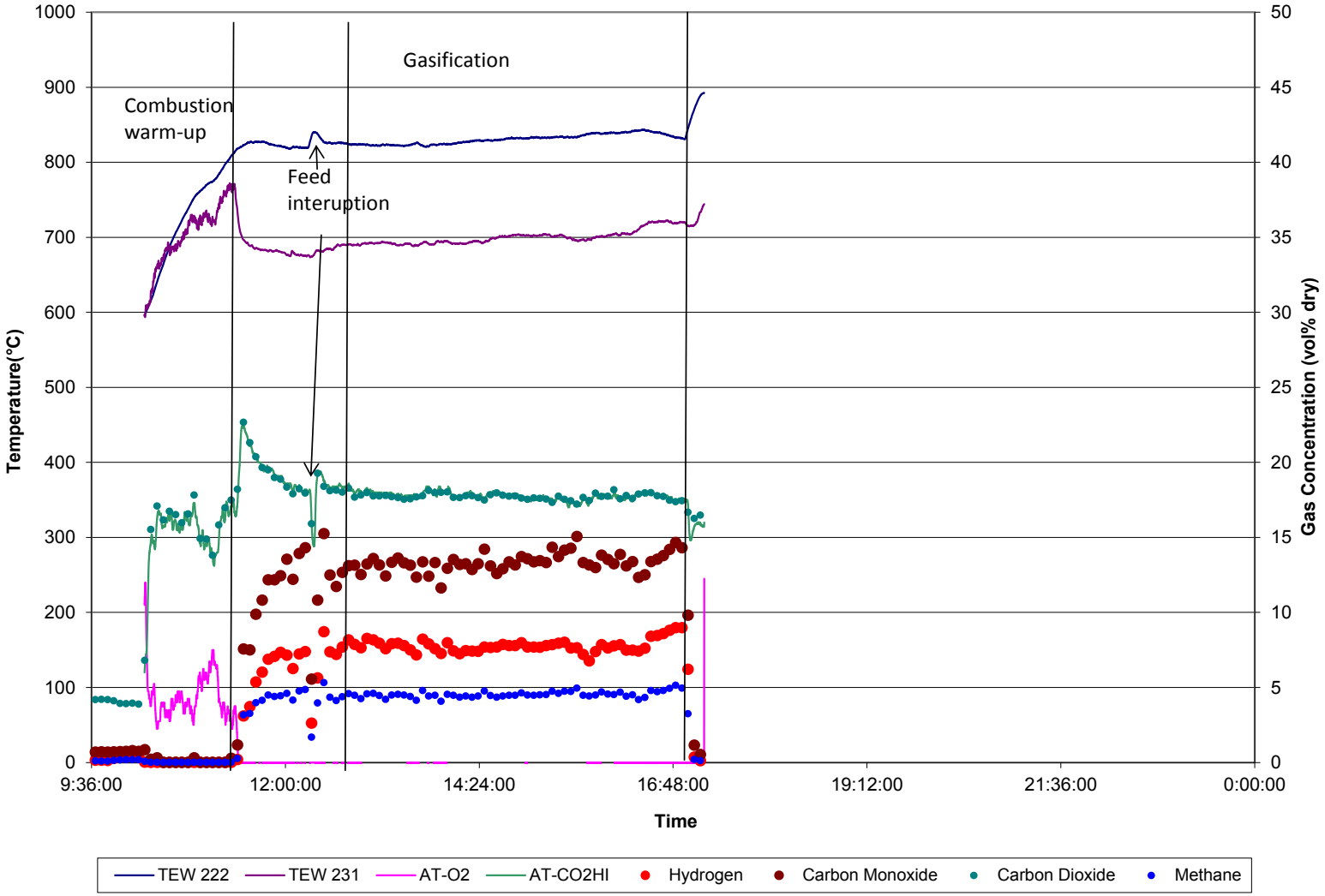

Figure C.33: Run chart from OB-AG-PBK

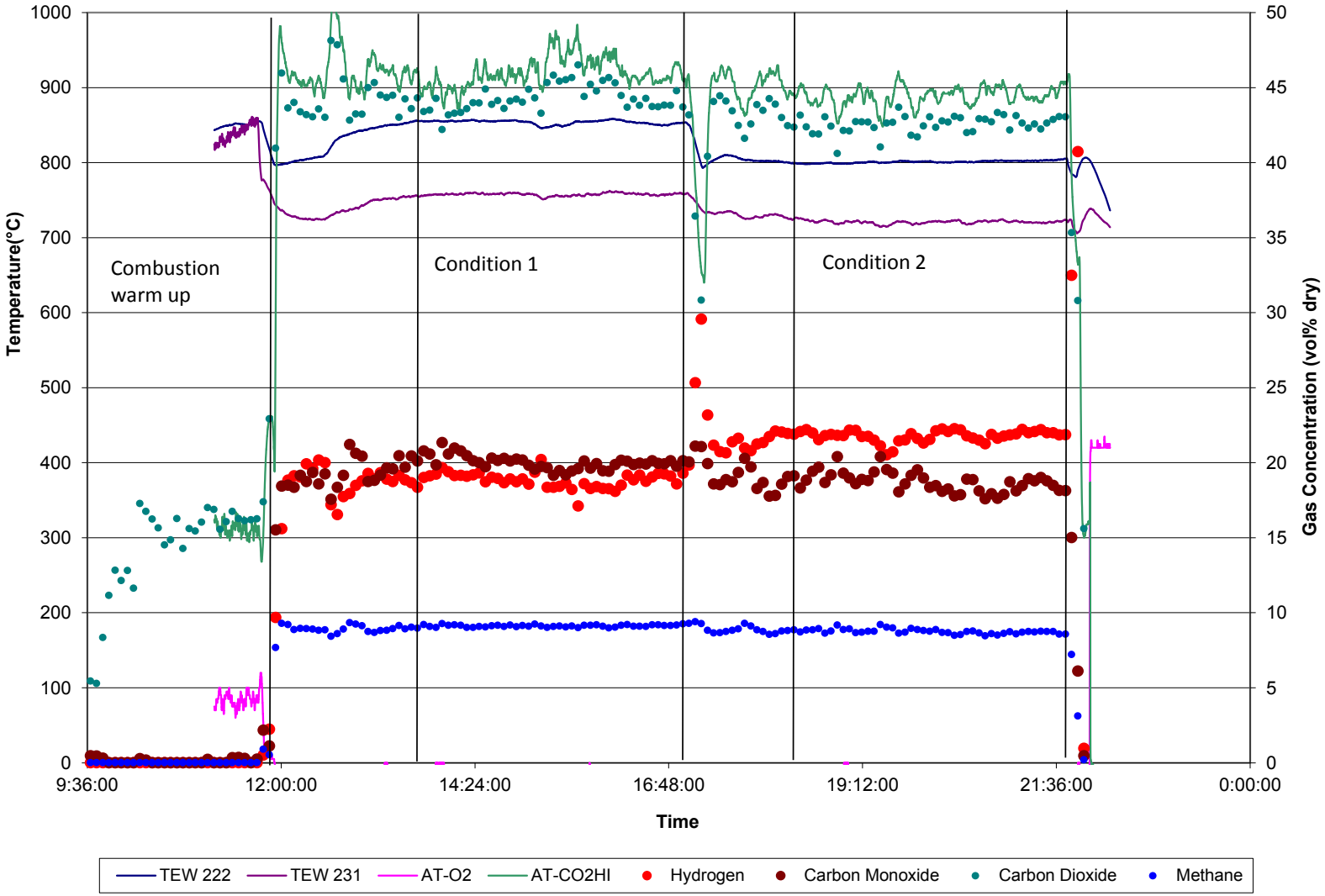

Figure C.34: Run chart from OB-SG-PBK

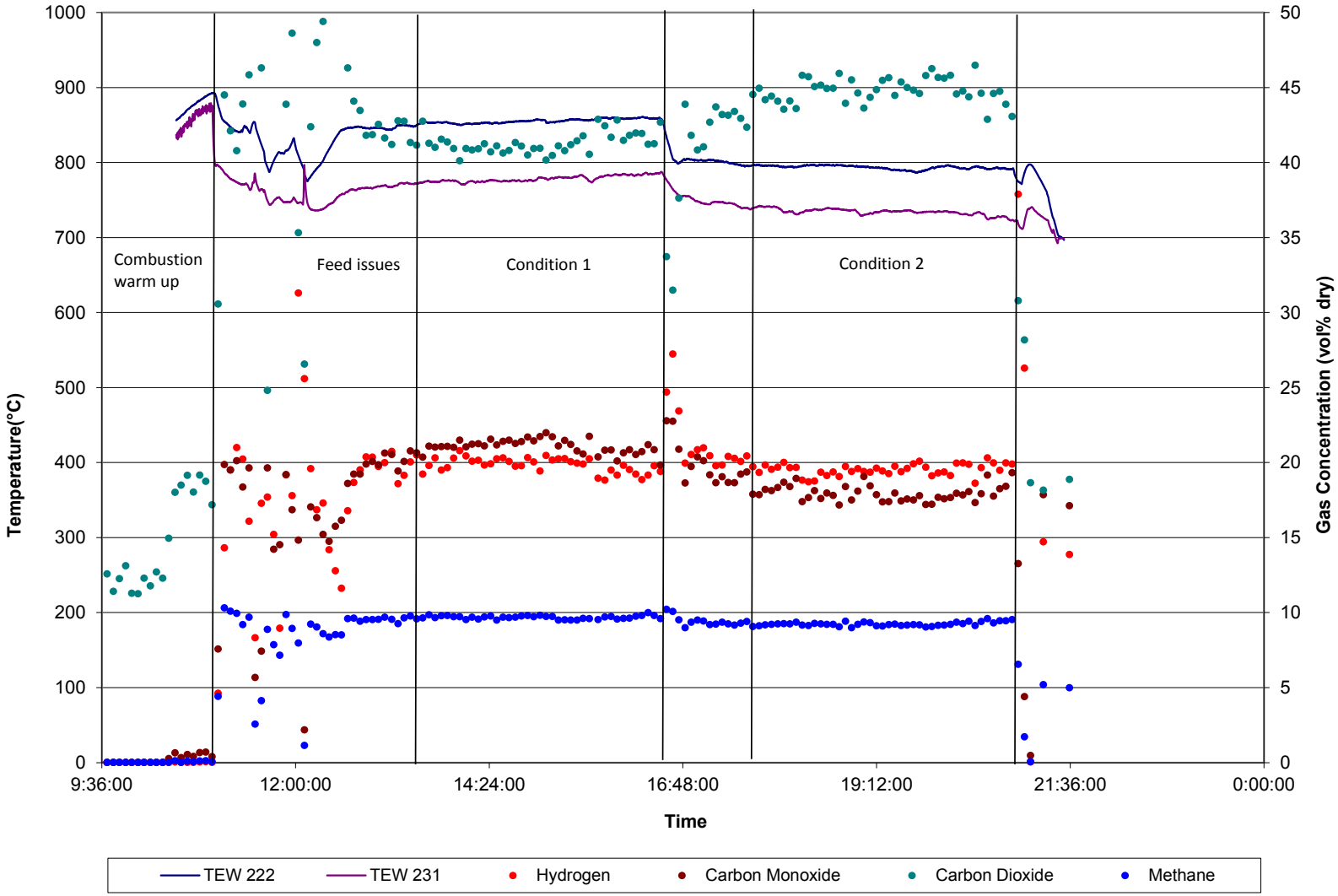

Figure C.35: Run chart from OB-SG-WBC

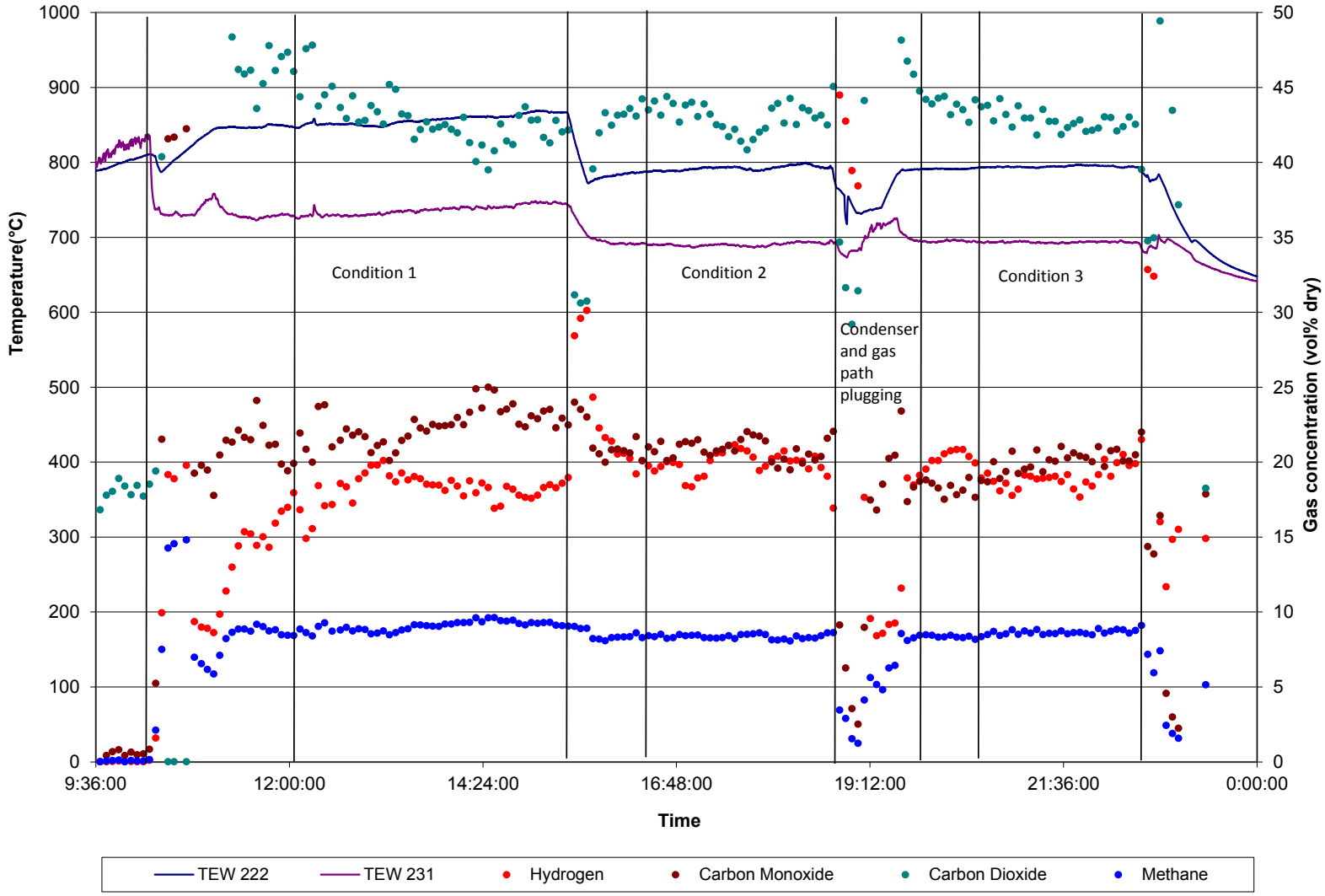

Figure C.36: Run chart from OB-SG-ISH

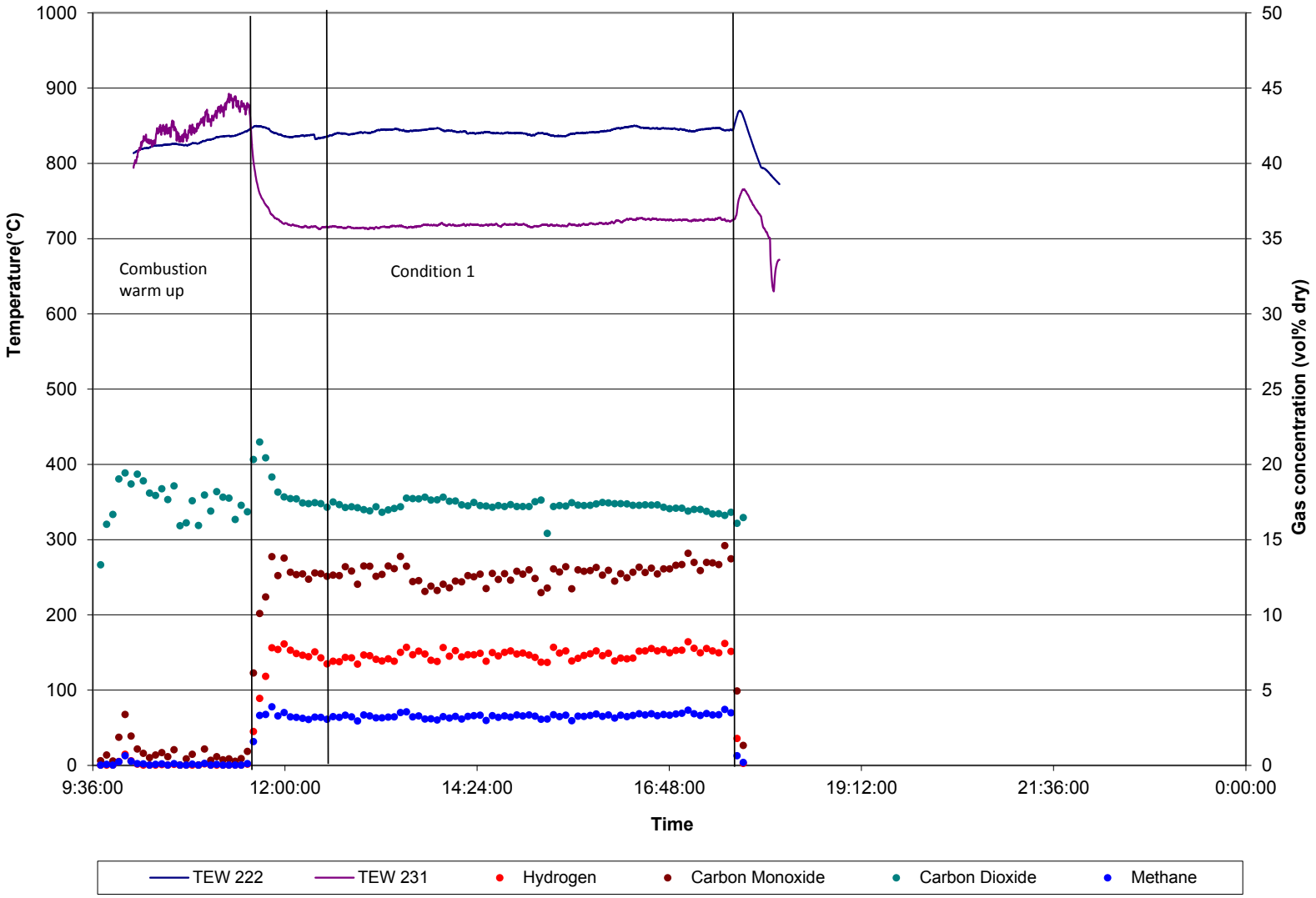

Figure C.37: Run chart from AG-OB-SLH

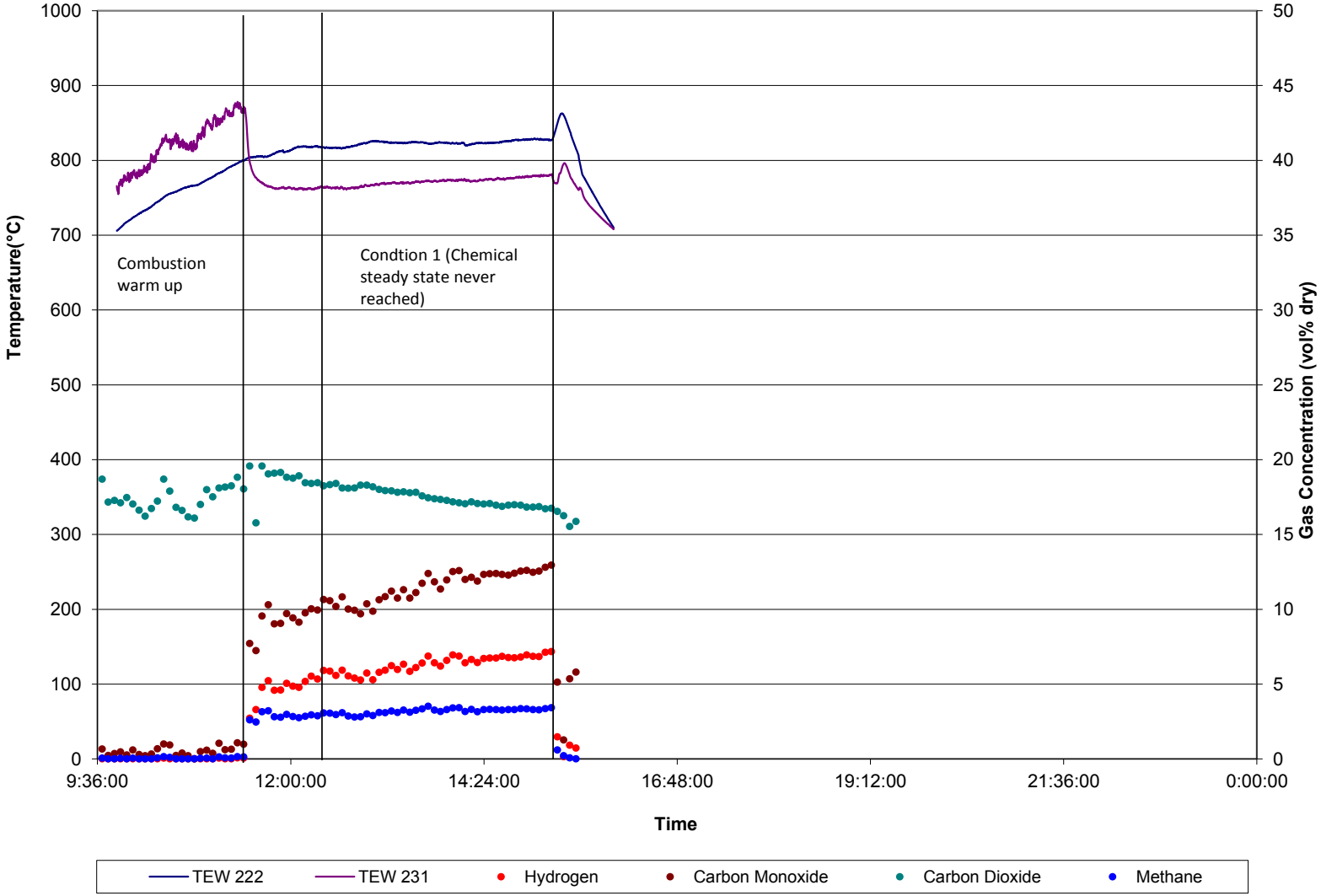

Figure C.38: Run chart from IB-AG-SLH

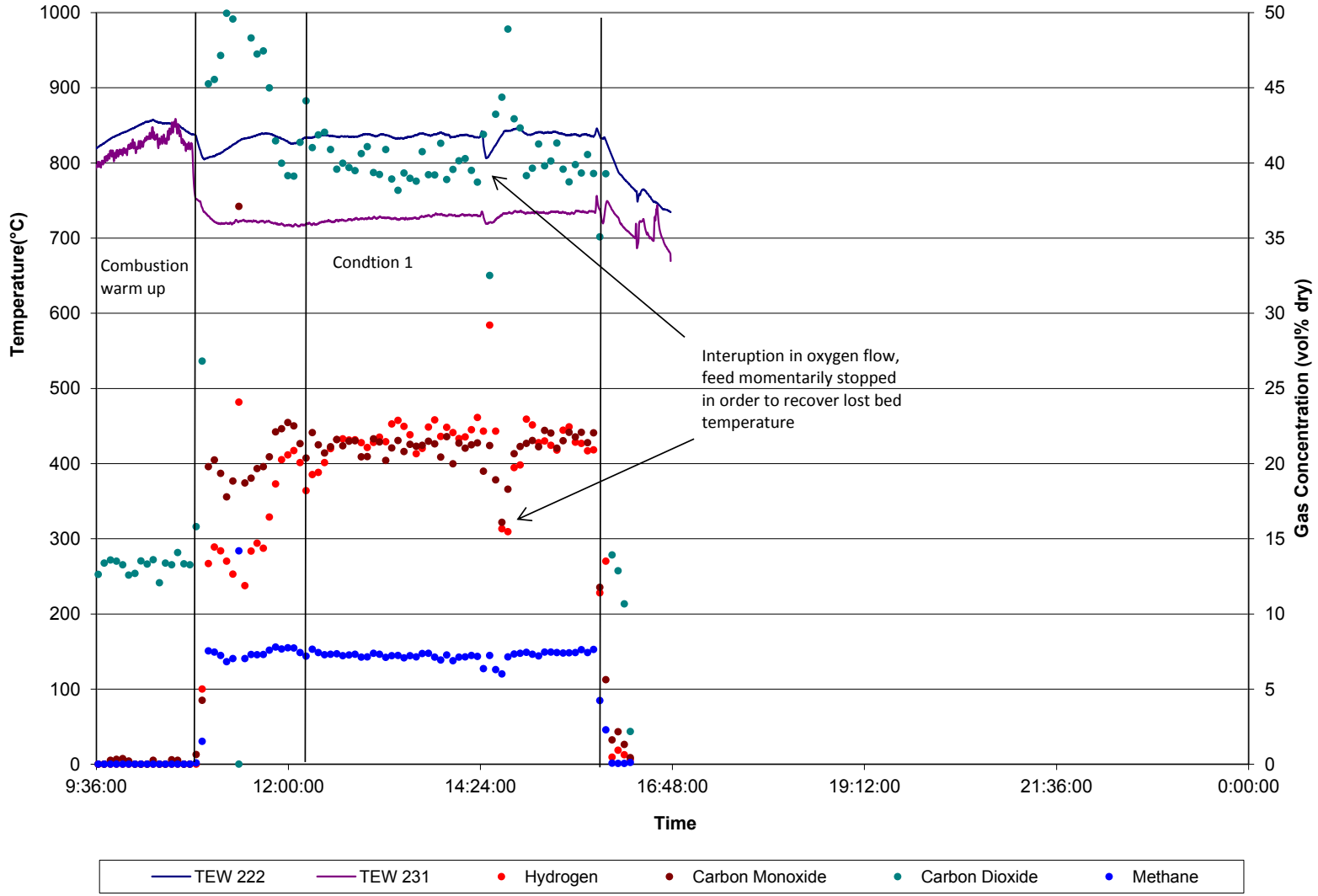

Figure C.39: Run chart from OB-SG-SLH

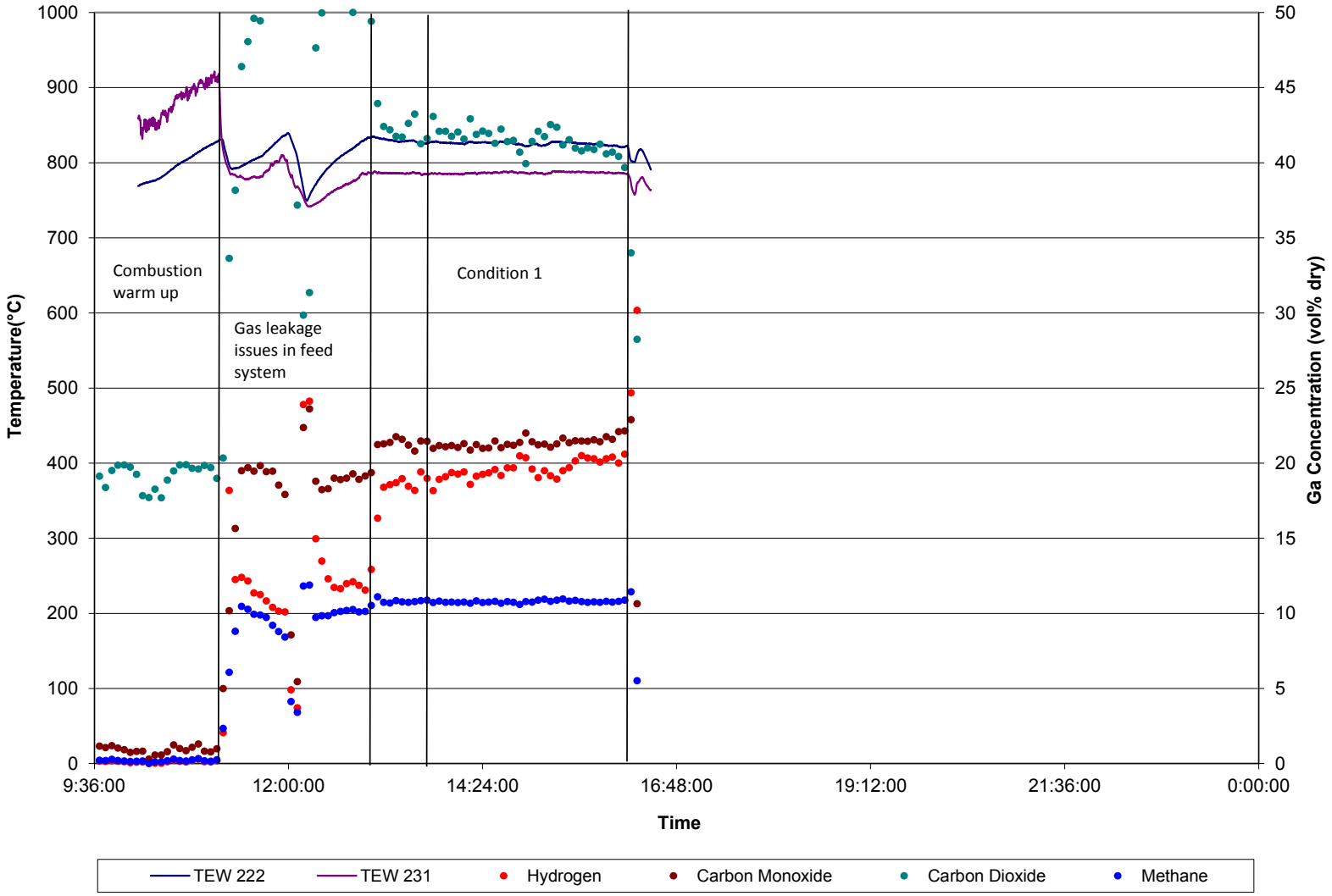

Figure C.40: Run chart from IB-SG-WBC

Appendix D. Supplemental Results

D.1 Results from Traditional Mass Balance Approach (Chapter 3 Data)

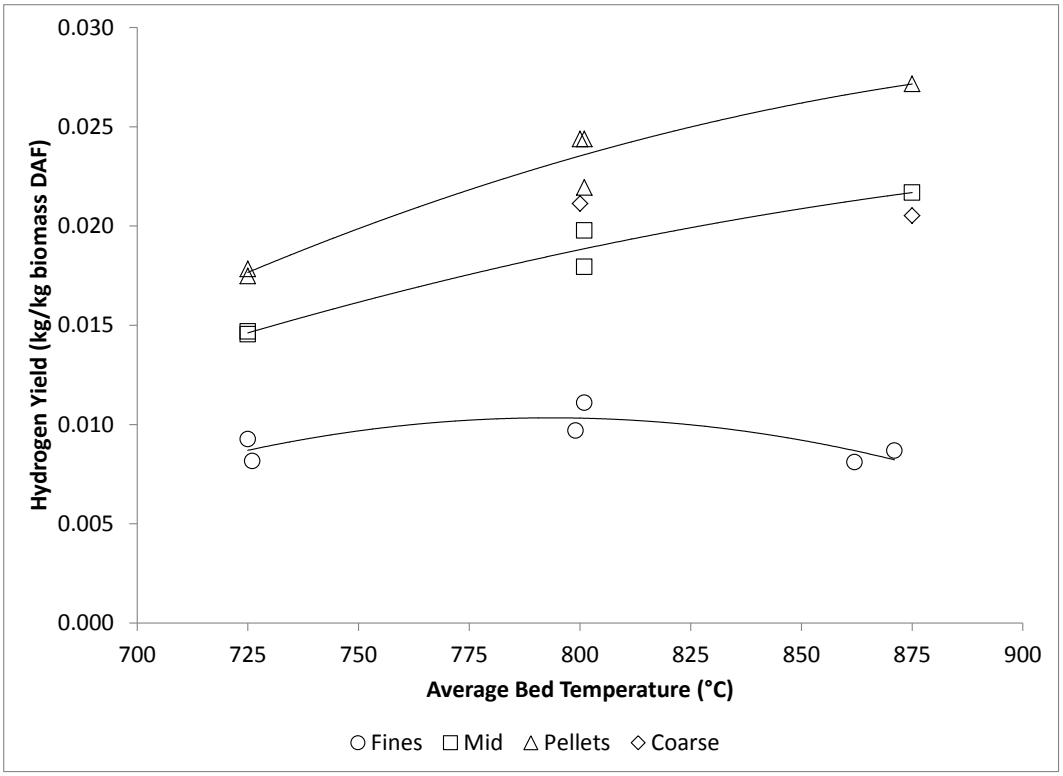

Figure D.1: Hydrogen gas yield based on the traditional mass balance approach.

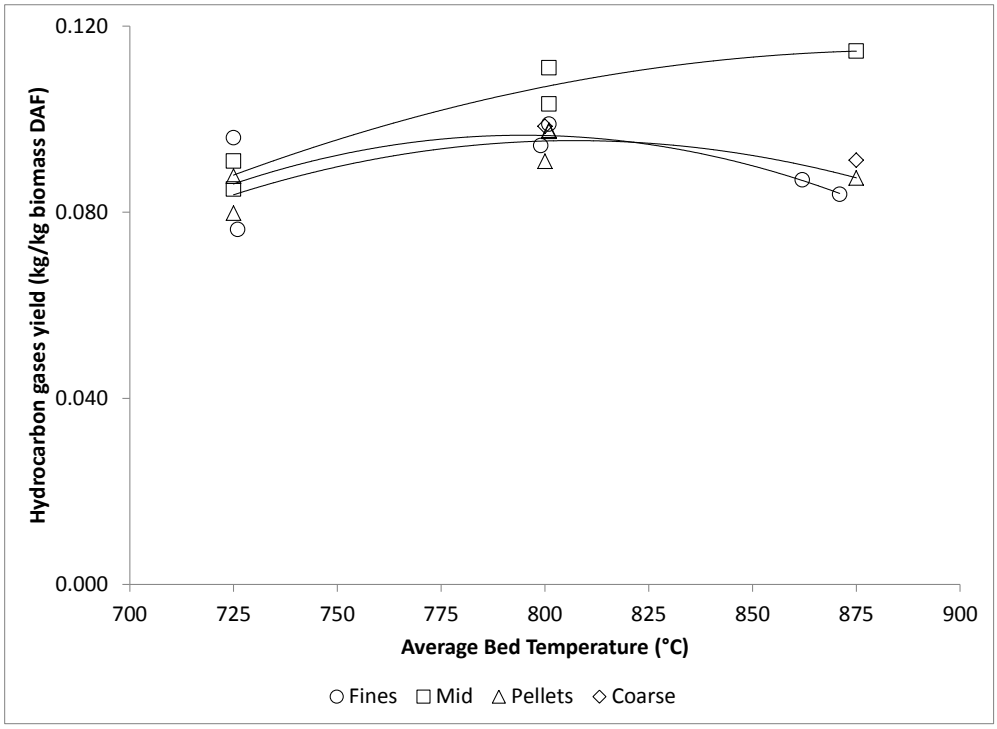

Figure D.2: Light hydrocarbon gases (C1-C3) yield based on the traditional mass balance approach.

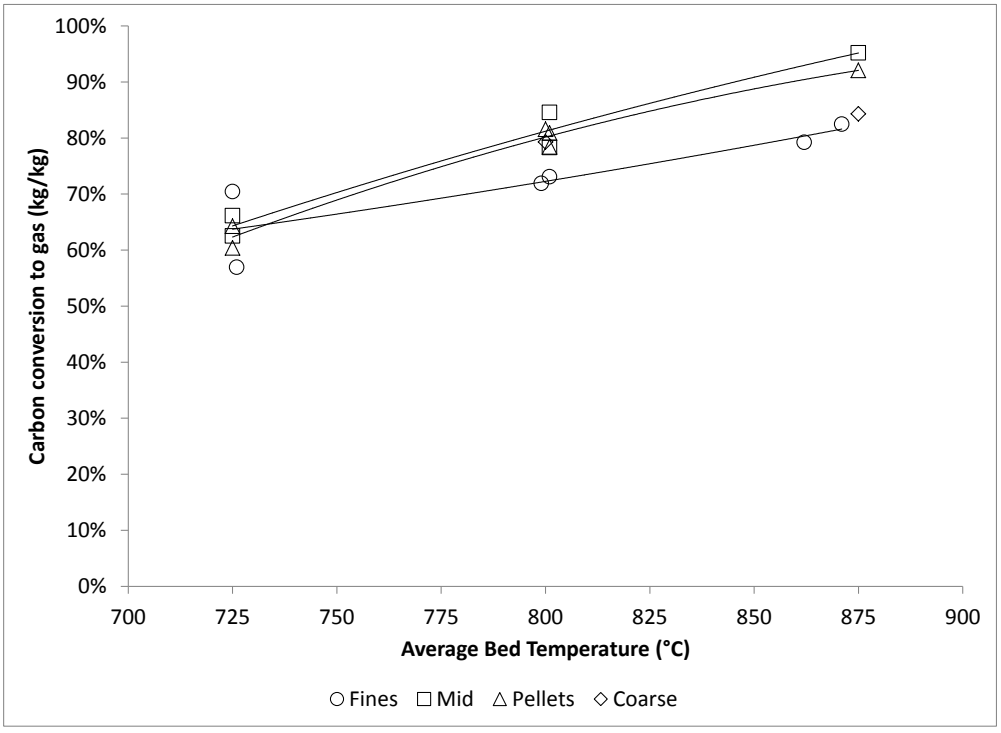

Figure D.3: Percentage of carbon converted to gases based on the traditional mass balance approach.

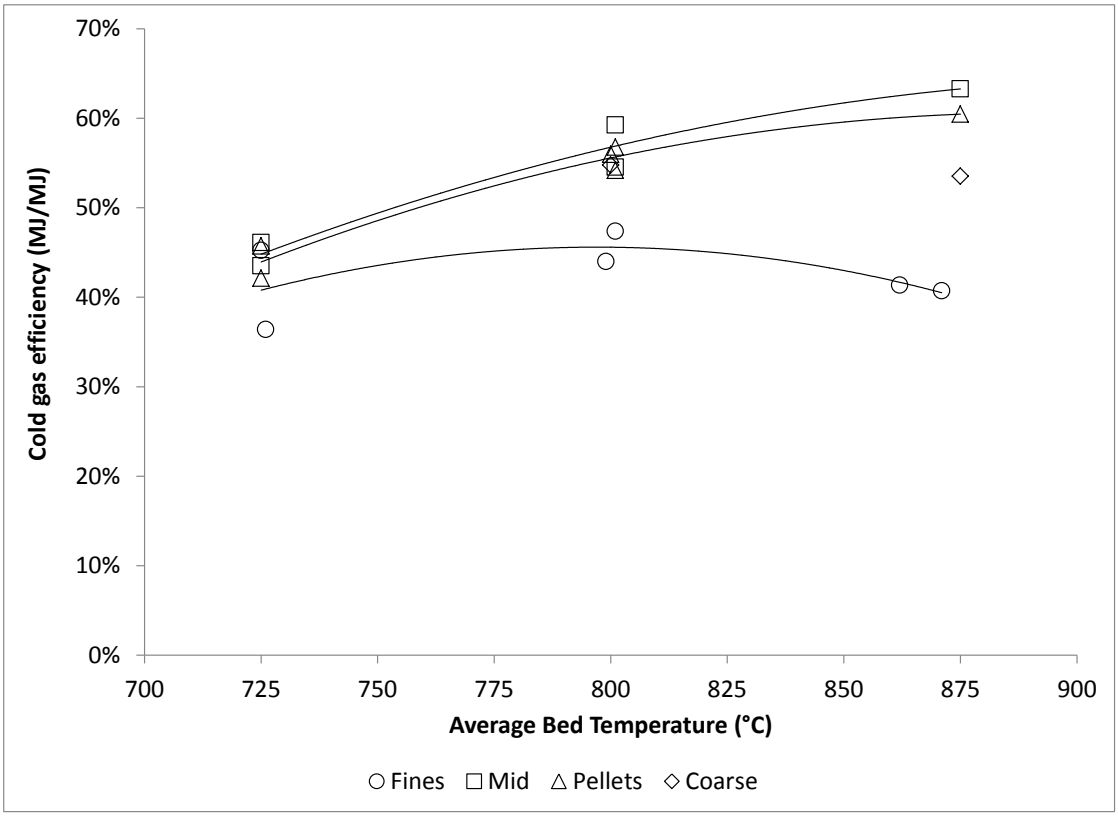

Figure D.4: Cold gas efficiency as calculated based on the traditional mass balance approach.

D.2 Gasifier Temperature Profiles (Chapter 3 Data)

Figure D.5 through Figure D.8 show the temperature profile along the height of the reactor, whereas the x-axis represents the vertical position of the thermocouple relative to the distributor plate of the gasifier. Each temperature measurement represents the average temperature (averaged over the duration of the condition) recorded by the thermocouple at that location in the reactor.

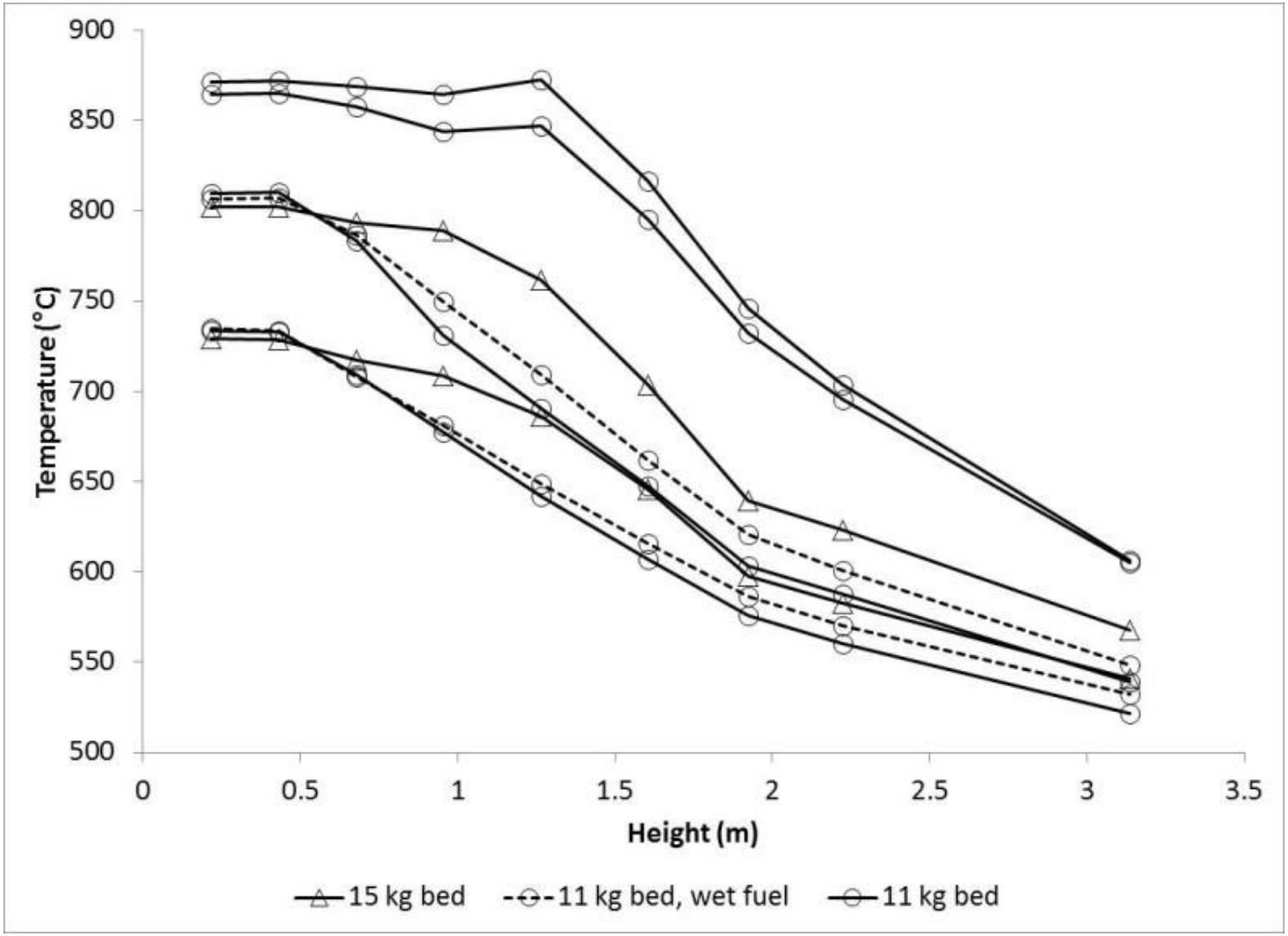

Figure D.5: Temperature profiles along the height of the gasifier for the fines experiments

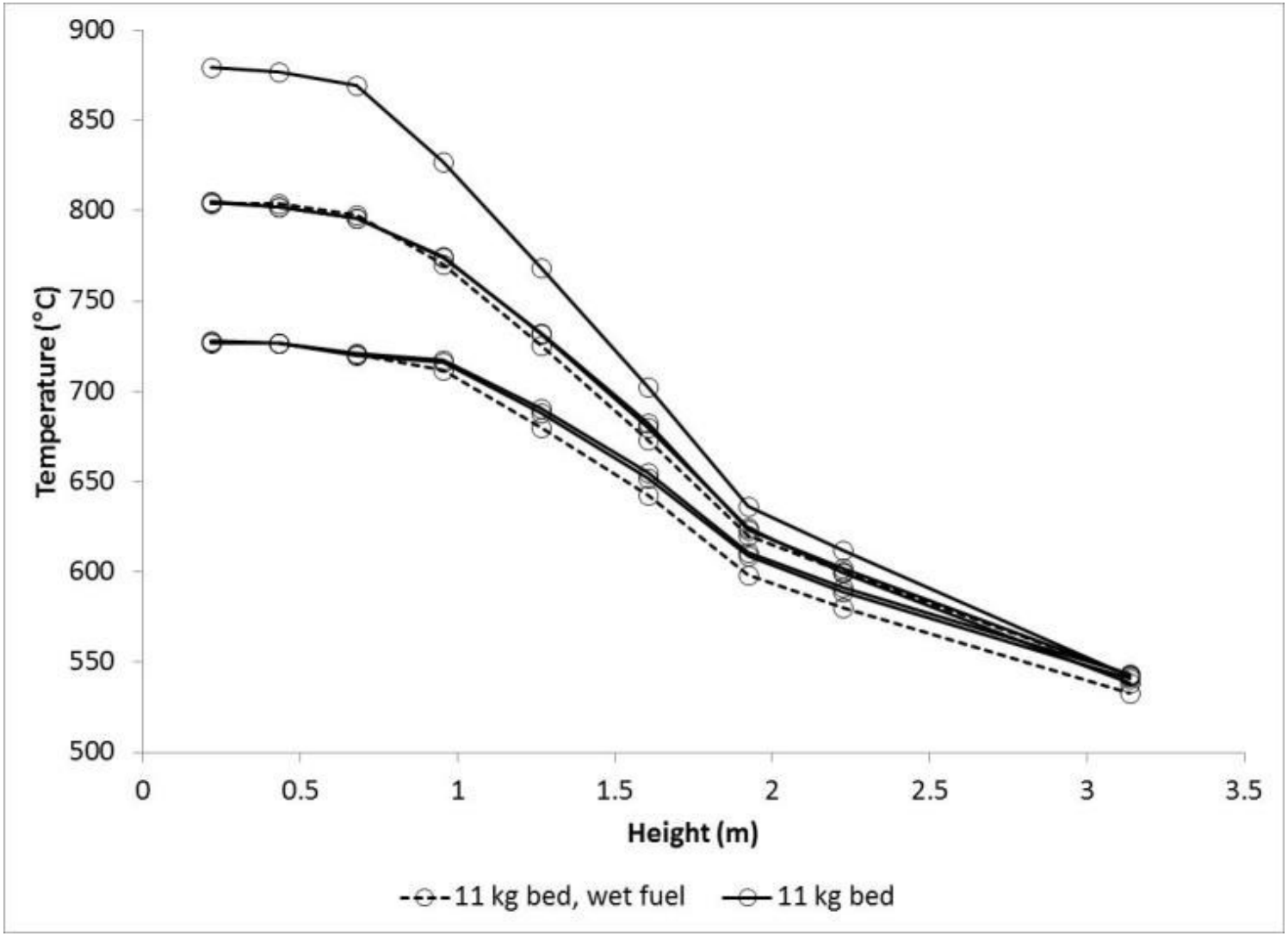

Figure D.6: Temperature profiles along the height of the gasifier for the mids experiments

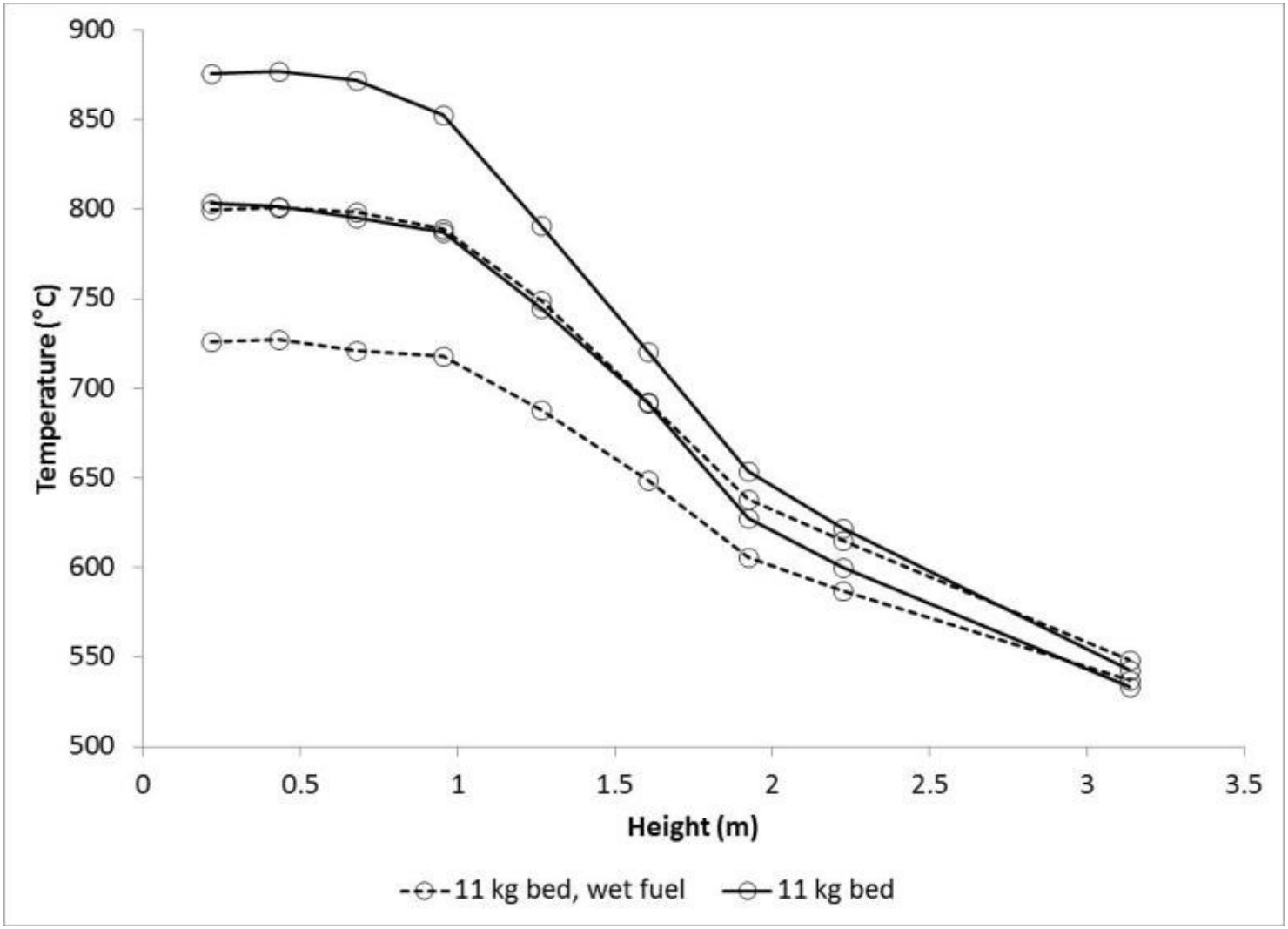

Figure D.7: Temperature profiles along the height of the gasifier for the coarse experiments

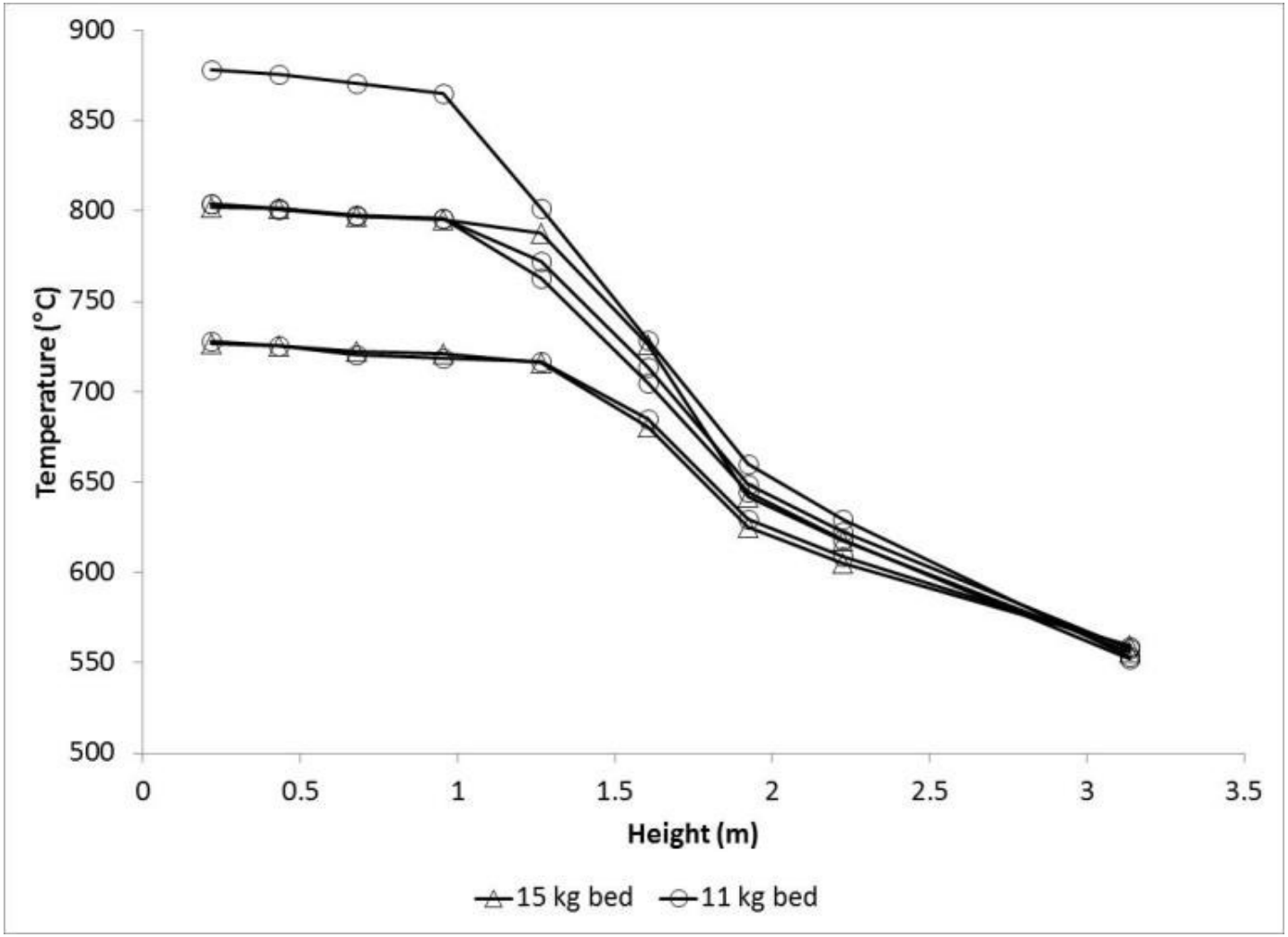

Figure D.8: Temperature profiles along the height of the gasifier for the pellets experiments

D.3 **Fluidization Velocity (Chapter 3 Data)**

The superficial fluidizing gas velocity can be calculated as follows:

$$u_s = \frac{\dot{V}}{A_c} \qquad \text{Eq. D.1}$$

Assuming ideal gas law, the volumetric flow rate of the gas is determined, by the following

$$\dot{V} = \frac{\dot{V_{air}}[\text{sLpm}]}{22.414\ \left[\frac{\text{L}_{\text{std}}}{\text{mol}}\right] 60 \left[\frac{\text{s}}{\text{min}}\right]} * \frac{RT}{P + \Delta P_{bed}} \qquad \text{Eq. D.2}$$

The pressure at the base of the bed will be equal to atmospheric pressure plus the hydrostatic pressure of the bed, where the hydrostatic pressure of the bed is:

$$\Delta P_{bed} = \rho_{bulk,olivine} g \Delta h_{bed,static} \qquad \text{Eq. D.3}$$

The height can be determined from the mass of the olivine sand loaded and the bulk density of the olivine sand:

$$\Delta h_{bed,static} = \frac{m_{olivine}}{\rho_{bulk,olivine} A_c} \qquad \text{Eq. D.4}$$

$$\Delta P_{bed} = g \frac{m_{olivine}}{A_c} \qquad \text{Eq. D.5}$$

For the fluidized bed test (6" NPS Schedule 40 pipe) and the 11 kg initial mass of sand added, the pressure drop between the bottom and the top of the bed should be:

$$\Delta P_{bed} = 9.8 \frac{\text{m}}{\text{s}^2} \frac{11\ \text{kg}}{0.01864\ \text{m}^2} = 5783\ \text{Pa} \qquad \text{Eq. D.6}$$

For the three temperature levels tested, the superficial gas velocity calculation can be used to show that all three temperature conditions were tested at the same superficial gas velocity:

$$u_s = \frac{\left(\frac{296[\text{sLpm}]}{22.414\ \left[\frac{\text{L}_{\text{std}}}{\text{mol}}\right] 60 \left[\frac{\text{s}}{\text{min}}\right]} * \frac{8.314 * (273 + 725)}{101325 + 5783} \right)}{0.01864\ \text{m}^2} = 0.91 \frac{\text{m}}{\text{s}} \qquad \text{Eq. D.7}$$

$$u_s = \frac{\left(\frac{275[\text{sLpm}]}{22.414\ \left[\frac{\text{L}_{\text{std}}}{\text{mol}}\right] 60 \left[\frac{\text{s}}{\text{min}}\right]} * \frac{8.314 * (273 + 800)}{101325 + 5783} \right)}{0.01864\ \text{m}^2} = 0.91 \frac{\text{m}}{\text{s}} \qquad \text{Eq. D.8}$$

$$u_s = \frac{\left(\frac{257[\text{sLpm}]}{22.414\ \left[\frac{\text{L}_{\text{std}}}{\text{mol}}\right] 60 \left[\frac{\text{s}}{\text{min}}\right]} * \frac{8.314 * (273 + 875)}{101325 + 5783} \right)}{0.01864\ \text{m}^2} = 0.91 \frac{\text{m}}{\text{s}} \qquad \text{Eq. D.9}$$

The superficial gas velocity at the top of the bed will depend on the amount of gas that was produced and can be assumed to take place at roughly atmospheric pressure. If it is assumed that gas production and composition does not change through the freeboard, then the following can be applied:

$$\dot{V} = (\dot{n}_{dry\ gas} + \dot{n}_{water}) * \frac{RT}{P} \qquad \text{Eq. D.10}$$

Application of the above formula to the data gives the results shown in Table D.1. The table shows that although the fluidization velocity due to air at the base of the bed is kept constant, the potential fluidization velocity at the top of the bed was not constant between temperature levels. The average fluidization velocity at the top of the bed was 1.73 m/s at 725°C, 1.61 m/s at 800°C, and 1.44 m/s 875°C. In addition to slight changes to the mixing parameters of the bed at the different temperature levels, the increased gas velocity at the lower temperature level tests could have elutriated slightly more material than would have been at the higher temperature condition. This may have contributed slightly to the enhanced carbon conversion at higher temperature, although it is expected that the temperature of the bed played a much more important role.

Table D.1: Fluidization velocities at the top of the bed

Date	Fuel	Average Bed T. °C	Superficial velocity at the top of the bed m/s
29/08/2012	Fines	871	1.34
07/08/2012	Fines	862	1.36
07/08/2012	Fines	801	1.57
30/07/2012	Fines	799	1.52
29/08/2012	Fines	726	1.71
30/07/2012	Fines	725	1.58
14/08/2012	Fines-wet	800	1.56
14/08/2012	Fines-wet	725	1.68
02/08/2012	Mid	875	1.52
02/08/2012	Mid	801	1.66
13/08/2012	Mid	801	1.68
13/08/2012	Mid	725	1.82
30/08/2012	Mid	725	1.80
01/08/2012	Mid-wet	802	1.65
01/08/2012	Mid-wet	725	1.74
08/08/2012	Pellets	875	1.49
08/08/2012	Pellets	801	1.62
20/08/2012	Pellets	801	1.62
24/07/2012	Pellets	800	1.59
24/07/2012	Pellets	725	1.78
20/08/2012	Pellets	725	1.75
26/09/2012	Coarse	875	1.51
26/09/2012	Coarse	800	1.63
27/09/2012	Coarse-wet	800	1.58
27/09/2012	Coarse-wet	725	1.69

D.4 **Energy Distributions (Chapter 3 data)**

Table D.2: Energy distribution in gas, tar, and char from CHO mass balance technique

Fuel	Avg. Bed T.	Input	H_2	CO	CH_4	C_2H_4	C_2H_6	C_2H_2	C_3H_6	*Dry gas*	Tar	Char	Total Calorific Output
	°C	MJ/h	MJ/h	MJ/h	MJ/h	MJ/h	MJ/h	MJ/h	MJ/h	MJ/h	MJ/h	MJ/h	MJ/h
Fines	871	**157**	8.4	20.7	17.4	9.4	1.7	1.7	0.2	***59.4***	11.0	21.3	**92**
Fines	862	**168**	8.5	23.0	19.7	10.5	2.0	1.6	0.5	***65.8***	5.3	29.9	**101**
Fines	801	**282**	17.8	37.9	32.4	16.3	4.4	1.1	5.0	***114.9***	22.6	71.2	**209**
Fines	799	**257**	14.6	32.7	29.3	15.0	3.7	1.0	4.2	***100.6***	19.1	61.0	**181**
Fines	726	**402**	17.9	40.6	34.1	13.8	5.5	0.6	8.6	***121.1***	38.5	152.1	**312**
Fines	725	**335**	16.9	42.6	35.4	14.6	5.8	0.6	9.0	***124.8***	50.1	85.9	**261**
Fines-wet	800	**207**	14.1	30.0	26.7	14.0	3.6	1.0	3.7	***93.1***	18.1	29.8	**141**
Fines-wet	725	**288**	16.4	30.8	26.1	10.4	4.5	0.3	6.2	***94.8***	30.7	86.0	**212**
Mid	875	**189**	26.7	35.2	32.7	16.1	3.0	0.6	0.8	***115.0***	5.9	8.9	**130**
Mid	801	**260**	33.2	43.8	40.3	19.9	4.7	0.8	4.2	***146.9***	21.4	26.9	**195**
Mid	801	**279**	31.7	42.2	39.1	19.7	4.6	1.0	4.1	***142.3***	16.2	51.7	**210**
Mid	725	**404**	35.0	42.3	43.3	16.7	6.7	0.4	8.8	***153.2***	9.9	155.3	**318**
Mid	725	**376**	33.7	45.2	44.9	17.3	6.7	0.6	9.5	***157.8***	24.3	113.8	**296**
Mid-wet	802	**210**	28.8	27.4	26.1	12.9	3.5	0.6	2.4	***101.8***	11.1	26.5	**139**
Mid-wet	725	**273**	31.5	30.4	30.3	11.8	4.8	0.3	6.2	***115.2***	15.4	63.1	**194**
Pellets	875	**180**	31.9	35.1	26.9	9.5	2.4	0.3	0.0	***106.1***	2.8	13.4	**122**
Pellets	801	**263**	37.5	37.8	38.7	15.9	4.4	0.7	3.1	***138.1***	18.5	37.7	**194**
Pellets	801	**260**	40.4	39.1	37.6	15.3	4.2	0.7	2.9	***140.3***	14.6	40.5	**195**
Pellets	800	**244**	38.2	38.9	34.3	12.8	3.8	0.6	2.4	***130.9***	11.3	36.7	**179**
Pellets	725	**400**	43.5	42.4	49.3	15.6	7.0	0.5	8.2	***166.3***	38.6	118.3	**323**
Pellets	725	**391**	41.4	36.4	43.5	13.5	6.1	0.3	7.6	***148.9***	16.1	145.2	**310**
Coarse	875	**192**	25.6	30.0	26.3	13.2	2.4	0.6	0.4	***98.5***	6.3	25.8	**131**
Coarse	800	**260**	34.4	37.0	34.8	16.8	4.4	0.5	3.8	***131.7***	11.3	51.9	**195**
Coarse-wet	800	**174**	21.4	19.4	19.8	10.1	2.6	0.5	1.6	***75.5***	7.6	22.3	**105**
Coarse-wet	725	**232**	23.1	23.0	22.1	9.5	3.7	0.4	4.7	***86.5***	14.1	55.2	**156**

D.5 **Information on the Thermodynamic Simulation**

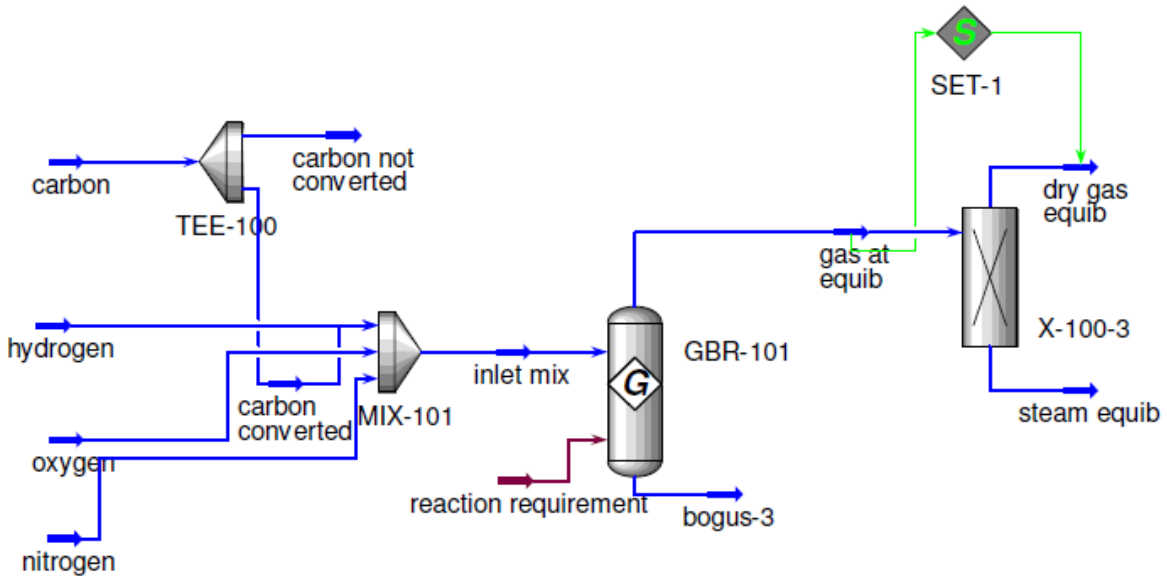

Figure D.9: UniSim flowsheet used for the simulation.

The components that were tracked in the Gibbs reactor were:

- Methane
- Ethane
- Propane
- Ethylene
- Acetylene
- Hydrogen
- Carbon Monoxide
- Water
- Nitrogen
- Benzene
- Naphthalene
- Propylene
- Carbon Dioxide

- Oxygen
- Carbon
- Hydrogen Cyanide
- Ammonia
- Nitric Oxide
- Nitrogen Dioxide
- Methylamine

Separately from the UniSim simulation the equilibrium position of water-gas shift position was also evaluated. The following approximation was used:

$$\mathrm{Log}_{10}\left(K_{equil}\right) = \frac{2408.1}{T + 273.15} + 1.5350\mathrm{Log}_{10}(T + 273.15) - 7.452(10^{-5})(T + 273.15) - 6.7753 \qquad \text{Eq. D.11}$$

Appendix E. Supplemental Pictures

Figure E.1: Gas sampling system in the small pilot scale gasification laboratory (open heated filter cabinet, heated head sampling pumps and micro-GC are visible)

Figure E.2: "Tar Trap" from the gas sampling system installed in the small pilot-scale gasification facility

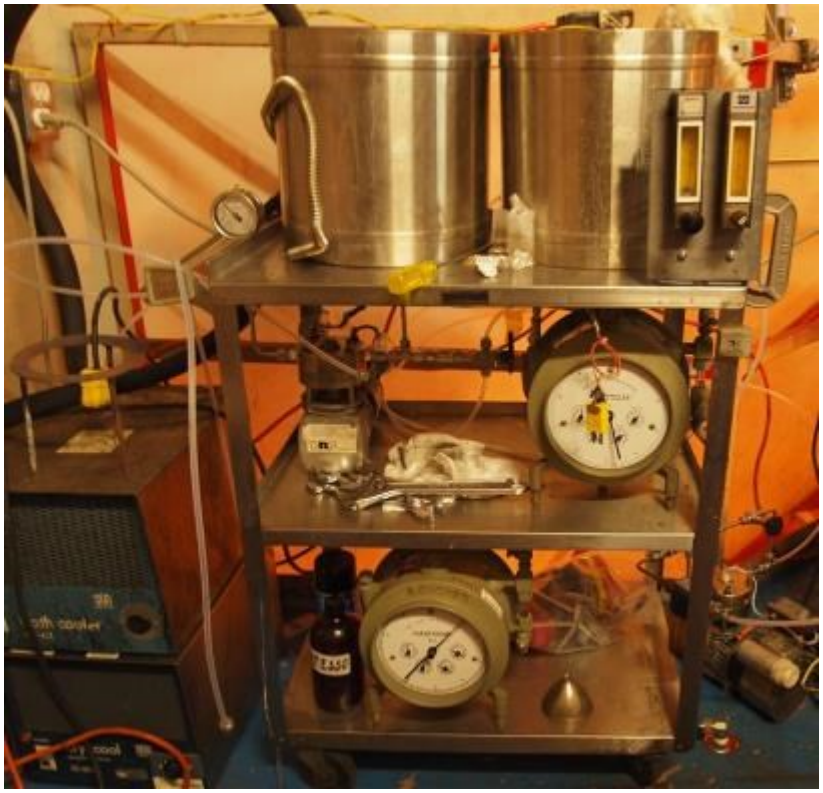

Figure E.3: Tar sampling equipment (impingers not present) in the small pilot scale gasification facility

Figure E.4: One of the rotary evaporators used to determine the amount of gravimetric tar

Figure E.5: Bed material samples taken during operation of the large pilot-scale gasifier

Figure E.6: Char / tar accumulation in the condenser from the large pilot-scale gasifier

Figure E.7: Char / tar fouling found in the gas blower housing from the large pilot-scale gasifier